



Best Value Granular Material for Road Foundations

Minnesota
Department of
Transportation

**RESEARCH
SERVICES**

Office of
Policy Analysis,
Research &
Innovation

Erol Tutumluer, Principal Investigator
Department of Civil & Environmental Engineering
University of Illinois at Urbana-Champaign

January 2012

Research Project
Final Report 2012-01

Your Destination... Our Priority



All agencies, departments, divisions and units that develop, use and/or purchase written materials for distribution to the public must ensure that each document contain a statement indicating that the information is available in alternative formats to individuals with disabilities upon request. Include the following statement on each document that is distributed:

To request this document in an alternative format, call Bruce Lattu at 651-366-4718 or 1-800-657-3774 (Greater Minnesota); 711 or 1-800-627-3529 (Minnesota Relay). You may also send an e-mail to bruce.lattu@state.mn.us. (Please request at least one week in advance).

Technical Report Documentation Page

1. Report No. MN/RC 2012-01	2.	3. Recipients Accession No.	
4. Title and Subtitle Best Value Granular Material for Road Foundations		5. Report Date January 2012	
		6.	
7. Author(s) Yuanjie Xiao and Erol Tutumluer		8. Performing Organization Report No.	
9. Performing Organization Name and Address University of Illinois at Urbana-Champaign Department of Civil & Environmental Engineering 205 N Mathews Avenue Urbana, IL 61801		10. Project/Task/Work Unit No.	
		11. Contract (C) or Grant (G) No. (c) 89260 (wo) 1	
12. Sponsoring Organization Name and Address Minnesota Department of Transportation Research Services Section 395 John Ireland Blvd., MS 330 St. Paul, MN 55155		13. Type of Report and Period Covered Final Report	
		14. Sponsoring Agency Code	
15. Supplementary Notes http://www.lrrb.org/pdf/201201.pdf			
16. Abstract (Limit: 250 words) <p>Aggregate base materials are becoming increasingly expensive in many parts of Minnesota because gravel mines and rock quarries are being lost to other land uses. These aggregate materials are classified for use and placed in quantities based on design procedures and testing techniques that are several decades old. To optimize material use and reduce waste, new mechanistic-based design procedures and testing techniques need to be implemented to achieve better value during road construction.</p> <p>This research study is aimed at evaluating pavement base/subbase performances of locally available aggregate materials (with gradations still falling within the MnDOT specified gradation bands) in Minnesota through mechanistic pavement analysis and design. The main objective of this study is to demonstrate that locally available aggregate materials can be economically efficient in the implementation of the available mechanistic-based design procedures in Minnesota through the MnPAVE mechanistic-empirical flexible pavement design method. The goal is to develop the components of a new granular material best value software module to be added to the MnPAVE program.</p> <p>This report summarizes the detailed research findings from which the following conclusions can be drawn: (1) locally available aggregate materials with varying levels of quality can still properly serve traffic-level and environment-related loading from a mechanistic-empirical pavement design perspective provided that important aggregate properties, such as gradation and particle shape, are optimized; (2) potential shear failure in base and especially subbase need to be properly addressed as non-unique modulus-strength relationships were observed; and (3) the proper use of local materials can be quite cost-effective.</p>			
17. Document Analysis/Descriptors Aggregates, Granular bases, Mechanistic design, Modulus, Modulus of resilience, Shear strength, Quality control, Best Value, MnPAVE, Aggregate gradation, Shape, Aggregates by shape and surface texture		18. Availability Statement No restrictions. Document available from: National Technical Information Services, Alexandria, Virginia 22312	
19. Security Class (this report) Unclassified	20. Security Class (this page) Unclassified	21. No. of Pages 167	22. Price

Best Value Granular Material for Road Foundations

Final Report

Prepared by:

Yuanjie Xiao
Erol Tutemluer

Department of Civil & Environmental Engineering
University of Illinois at Urbana-Champaign

January 2012

Published by:

Minnesota Department of Transportation
Research Services Section
395 John Ireland Boulevard, MS 330
St. Paul, Minnesota 55155

This report represents the results of research conducted by the authors and does not necessarily represent the views or policies of the Local Road Research Board, the Minnesota Department of Transportation, or the University of Illinois at Urbana-Champaign. This report does not contain a standard or specified technique.

The authors, the Local Road Research Board, the Minnesota Department of Transportation, and the University of Illinois at Urbana-Champaign do not endorse products or manufacturers. Any trade or manufacturers' names that may appear herein do so solely because they are considered essential to this report.

Acknowledgments

The authors gratefully acknowledge the funding support of the Minnesota Department of Transportation (MnDOT) and all the database support of MnDOT Office of Materials and Road Research during the conduct of this study. The authors would also like to acknowledge the members of the technical advisory panel (TAP) for their technical advice and feedback. Finally, the authors are appreciative of Mr. John Siekmeier, the technical liaison and TAP chair of this research project, for all the constructive help and support he provided; Dr. Shongtao Dai for his help with modulus and strength data collection; and Mr. Bruce Tanquist for facilitating the MnPAVE implementation work.

Table of Contents

Chapter 1	Introduction.....	1
1.1	Problem Statement	1
1.2	Research Objectives	1
1.3	Research Methodology and Tasks.....	2
1.3.1	Task 1 Establish Aggregate Index Properties	2
1.3.2	Task 2 Collect Aggregate Strength and Modulus Data.....	2
1.3.3	Task 3 Establish Linkages between Aggregate Properties and Design Inputs	2
1.3.4	Task 4 Conduct Sensitivity Analyses.....	3
1.3.5	Task 5 Validate Sensitivity Analysis Results Using Additional Aggregate Strength Data.....	3
1.3.6	Task 6 Develop Best Value Granular Material Selection Tool Components	3
1.4	Report Organization	3
Chapter 2	Literature Review.....	5
2.1	Current Classification Systems for Unbound Aggregate Materials	5
2.1.1	Traditional “Recipe-based” Classification System	5
2.1.2	Mechanistic Classification System	7
2.2	Factors Affecting Modulus, Strength, and Rutting Behavior of Unbound Aggregate Materials	9
2.2.1	Moisture (Suction) and Density Conditions.....	9
2.2.2	Gradation.....	10
2.2.3	Fines Content	12
2.2.4	Aggregate Shape Properties	13
2.3	Review of Existing M_R Predictive Models	13
2.4	Summary	17
Chapter 3	Establishment of Aggregate Index Properties.....	18
3.1	Introduction	18
3.2	Brief Description of ASIS Database	18
3.3	Locations of Locally Available Aggregate Sources in Minnesota.....	20
3.4	Compiled Aggregate Cost Information on Local Materials.....	20
3.5	Summary	20
Chapter 4	Collection of Aggregate Strength and Modulus Data.....	23
4.1	Introduction	23

4.2	Description of MnDOT Aggregate Databases	23
4.2.1	Aggregate Resilient Modulus Database	23
4.2.2	Additional Aggregate Strength Database.....	27
4.3	Preliminary Analyses of Aggregate Source Properties Affecting Modulus and Strength Behavior.....	31
4.4	Summary	38
Chapter 5	Establishment of Linkages between Aggregate Properties and Design Inputs.....	39
5.1	Introduction	39
5.2	Description of Study Data	39
5.3	Importance of Aggregate Shape Properties.....	40
5.4	Regression Analysis Methodology.....	42
5.5	Regression Model Development	43
5.5.1	Selection and Diagnostics of Predictor Variables.....	43
5.5.2	First-order Model	44
5.5.3	Examine and Test for Normality and Constant Variance	48
5.5.4	Model Validation Using 15% Data.....	48
5.5.5	Model Development with Combined Data Sets.....	51
5.6	Monte Carlo Simulation of Resilient Modulus	52
5.6.1	Development of M_R Predictive Model	52
5.6.2	Simulation Results	53
5.7	Reliability-Based Evaluation of Aggregate Source Properties Affecting Resilient Modulus Behavior	54
5.7.1	Limit State Function Used	54
5.7.2	Variables and Distributions.....	57
5.7.3	Form Analysis.....	57
5.7.4	Sensitivity of Variables to the Reliability Index.....	59
5.8	Summary	62
Chapter 6	MnPAVE Sensitivity Analyses of Design Inputs to Pavement Life Expectancies	63
6.1	Introduction	63
6.2	Representative Aggregate Quality Levels.....	63
6.3	Sensitivity Analysis Matrix.....	66
6.4	GT-PAVE Structural FE Modeling.....	67

6.5	Sensitivity Analysis Results and Discussion.....	69
6.5.1	Effect of Aggregate Quality on Fatigue Life Performance.....	70
6.5.2	Effect of Aggregate Quality on Rutting Life Performance.....	73
6.6	Summary	77
Chapter 7	Validation of Sensitivity Analysis Results Using Additional Aggregate Strength Data	79
7.1	Introduction	79
7.2	Modulus-Strength Relationships Observed for Different MnDOT Aggregate Classes.....	79
7.2.1	Aggregate Base Materials (Class 5/6).....	80
7.2.2	Granular Subbase Materials (Class 3/4).....	83
7.2.3	Salvaged Materials (Class 7).....	86
7.2.4	Important Implications	87
7.3	Preliminary Gradation Refinement Guidelines for Optimized Strength Behavior	89
7.3.1	Motivation.....	89
7.3.2	Critical Gradation Parameter(s) Governing Shear Strength Behavior.....	90
7.3.3	Interpretation of the Gravel-to-Sand Ratio	91
7.3.4	Analyses of Other Aggregate Databases Collected	94
7.3.5	Preliminary Performance-based Gradation Guidelines.....	97
7.4	Recommendations for Aggregate Strength Input in MnPAVE Analysis.....	97
7.5	Summary	98
7.5.1	Observed Modulus-Strength Relationships	98
7.5.2	Validation of MnPAVE Sensitivity Analysis Results.....	99
7.5.3	Preliminary Performance-based Gradation Selection Guidelines.....	99
Chapter 8	Development of Best Value Granular Material Selection Tool Components.....	100
8.1	Introduction	100
8.1.1	GIS Based Aggregate Source Management Component	100
8.1.2	Aggregate Property Selection Component for Pavement Design.....	103
8.1.3	Aggregate Source Selection/Utilization Component	106
8.2	Aggregate Property Selection Component for Pavement Design	106
8.2.1	Implementation Plan	106
8.2.2	Literature Review.....	108
8.2.3	Constitutive Relationship.....	111

8.2.4	Iterative Framework	112
8.3	Summary	118
Chapter 9	Conclusions and Recommendations	120
9.1	Major Research Findings	120
9.1.1	Linkages Established between Aggregate Source Properties and Mechanistic Design Inputs	120
9.1.2	Sensitivity Analyses of Mechanistic Design Inputs on Pavement Life Expectancy	120
9.1.3	Validation of Sensitivity Analyses Using MnDOT Aggregate Strength Data.....	121
9.2	Recommendations for Future Research	122
References	123
Appendix A: University of Illinois Laboratory Databases of Aggregate Modulus and Strength Test Results		
Appendix B: Determination of MnPAVE Equivalent Single Modulus Input from GT-PAVE Finite Element (FE) Modeling		
Appendix C: Review of Gradation Quantification Methods		
Appendix D: List of Symbols and Abbreviations		

List of Tables

Table 2.1. Examples of Using Non-standard Materials in Low-Volume Sealed Roads (Cook and Gourley, 2002).....	6
Table 2.2. Various M_R Prediction Models/ Equations Reviewed	14
Table 2.3. Important Properties for M_R Prediction (Yau and Von Quintus, 2002).....	16
Table 2.4. Commonly-used Soil Properties for Predicting M_R (George, 2004).....	17
Table 3.1. Illustrative Examples of Aggregate Source Properties Stored in ASIS Database	19
Table 3.2. Aggregate Cost Information Recorded in the ASIS Database.....	21
Table 4.1. Description of M_R Samples Used for UIAIA Image Analyses	26
Table 4.2. Analysis Results of 9 MnDOT M_R Samples Processed Using UIAIA	26
Table 4.3. Details of the Aggregate Strength Data Compiled	27
Table 4.4. Details of the Aggregate Materials Compiled in the MnDOT Strength Database	31
Table 5.1. Summary of the Variables Used in the Regression Analyses.....	41
Table 5.2. Summary of Regression Results for 9 MnDOT Aggregate Samples	42
Table 5.3. Significant Aggregate Index Properties identified by ANOVA Analysis* ($\alpha=0.05$).....	44
Table 5.4. Significant Aggregate Index Properties Identified by ANOVA Analysis.....	45
Table 5.5. Summary of Multiple Linear Regression (MLR) Analysis Results for Identifying Properties Used to Predict $\log k_1$ of M_R Constitutive Equation.....	47
Table 5.6. Summary of MLR Analysis Results for Identifying Properties Used to Predict k_2 Parameter of M_R Constitutive Equation	47
Table 5.7. Summary of MLR Analysis Results for Identifying Properties Used to Predict k_3 Parameter of M_R Constitutive Equation	48
Table 5.8. Comparisons between MSPR and MSE Values for the Three k Parameters.....	49
Table 5.9. Representative Stress Levels in Typical MnDOT Pavement Layers*.....	53
Table 5.10. Input Parameters and Distributions.....	53
Table 5.11. Monte Carlo Simulation Results for M_R (Unit: ksi; 1 ksi=6.9 MPa)	54
Table 5.12. Representative Stress Level and Design Modulus for Aggregate Base Layer in a Typical Conventional Pavement Structure	56
Table 5.13. Abbreviations and Brief Descriptions of Significant Variables Influencing Resilient Modulus Behavior	56
Table 5.14. Basic Statistics of Aggregate Source Properties Used.....	57
Table 5.15. Correlation Coefficients of Variables	58
Table 5.16. Importance Vector of Variables Obtained from FERUM Program.....	60

Table 5.17. Sensitivity of Variables Studied with the Reliability Index	61
Table 6.1. Characterization of Representative Aggregate Base and Granular Subbase Materials	65
Table 6.2. Input Values for All the Variables Used in the Sensitivity Analysis.....	66
Table 7.1. Representative Stress Levels in Typical MnDOT Pavement Layers.....	80
Table 8.1. Recommendations for Determining the Number of Sublayers.....	115
Table 8.2. Proposed Stress Points Locations within Each Sublayer.....	116

List of Figures

Figure 2.1. Non-standard Material Groups and Their Likely Problems (Cook and Gourley, 2002).....	5
Figure 2.2. Physical (Left) Versus Mechanical (Right) Classification for Various Unbound Granular Materials (Paute et al., 1994)	7
Figure 2.3. Stress (σ_1) Levels at Which $\epsilon_p = 1\%$, 5% , and 10% at $N=10^6$, 10^6 , and $50,000$, Respectively, at $DOC = 97\%$, 100% , 103% , and 105% (Van Niekerk, 2002).....	10
Figure 2.4. Effect of Grading and Compaction on Plastic Strain (Thom and Brown, 1988)	11
Figure 2.5. MnDOT Specified Gradation Bands for Different Aggregate Classes	12
Figure 3.1. A Snapshot of the ASIS Excel Spreadsheet	19
Figure 3.2. Geographical Locations of 87 Prospect Pits Selected for this Study	20
Figure 3.3. ArcGIS Based Database Management Interfaces for (a) Searching and Graphically Displaying (b) % Passing No.200 Sieve and (c) Material Cost Features	21
Figure 3.4. Typical Aggregate Costs Obtained from MnDOT	22
Figure 4.1. 12 MnDOT Aggregate Samples Received at the University of Illinois ATREL	25
Figure 4.2. Gradations of Traditional Base/Subbase Materials in MnDOT Database: (a) Select Granular; (b) Granite; (c) Pit-run Gravel; and (d) Limestone	29
Figure 4.3. Gradations of Non-traditional Waste Base/Subbase Materials in MnDOT Database: (a) Taconite Tailings; (b) Reclaimed Concrete (Class 7C); (c) Reclaimed Bituminous (Class 7B); and (d) Full-depth Reclamation (FDR).....	30
Figure 4.4. Factors Affecting Resilient Modulus and Peak Deviator Stress Results – Class 5	33
Figure 4.5. Factors Affecting Resilient Modulus and Peak Deviator Stress Results – Class 6	34
Figure 4.6. Factors Affecting Resilient Modulus and Peak Deviator Stress Results, Class 3/4	35
Figure 4.7. Factors Affecting Resilient Modulus and Peak Deviator Stress Results – Select Granular (4-psi Confining Pressure for σ_{df})	36
Figure 4.8. Factors Affecting Resilient Modulus and Peak Deviator Stress Results – Select Granular (8-psi Confining Pressure for σ_{df})	37
Figure 5.1. Measured vs. Predicted Values for $\log k_1$	49
Figure 5.2. Measured vs. Predicted Values for k_2	50
Figure 5.3. Measured vs. Predicted Values for k_3	50
Figure 5.4. Sensitivity Charts for M_R	55
Figure 5.5. FORM Approximations (Haukaas and Kiureghian, 1999).....	59

Figure 5.6. Relative Contributions of Various Variables to Resilient Modulus (M_R)	60
Figure 5.7. The Relative Contribution of Each Variable to Resilient Modulus (M_R)	61
Figure 6.1. Computed Resilient Moduli for Different Unbound (a) Aggregate Base and (b) Granular Subbase Materials (1 psi = 6.89 kPa)	64
Figure 6.2. Gradations of Representative Aggregate Base and Granular Subbase Materials.....	65
Figure 6.3. Illustrations of GT-PAVE (a) Finite Element Mesh and (b) Modeling Results.....	68
Figure 6.4. Equivalent M_R Values Linked to Aggregate Quality for (a) 4-in., (b) 6-in., (c) 8-in. Asphalt Surface Thicknesses and (d) Current Default MnPAVE Fall Design Moduli (1 in. = 25.4 mm; 1 ksi = 6.89 MPa)	69
Figure 6.5. Fatigue Life Predictions for Different Base-Subbase Qualities in (a) Beltrami and (b) Olmsted Counties (M-L Stands for Medium Quality Base and Low Quality Subbase)	71
Figure 6.6. Effects of Unbound Granular Material Quality on Fatigue Life for Beltrami County: (a) 0.6 Million ESALs; (b) 1.5 Million ESALs; and (c) 6 Million ESALs (H- L Stands for High Quality Base and Low Quality Subbase).....	72
Figure 6.7. Rutting Life Predictions for Different Base-Subbase Qualities in (a) Beltrami and (b) Olmsted Counties (M-L Stands for Medium Quality Base and Low Quality Subbase)	74
Figure 6.8. Effects of Unbound Granular Material Quality on Rutting Life for Beltrami County: (a) 0.6 Million ESALs; (b) 1.5 Million ESALs; and (c) 6 Million ESALs (H- L Stands for High Quality Base and Low Quality Subbase).....	75
Figure 6.9. Pavement Service Life Comparison for Different Base and Subbase Quality Combinations (H-L Stands for High Quality Base and Low Quality Subbase).....	76
Figure 7.1. Resilient Modulus and Peak Deviator Stress ($\sigma_{df@4psi}$) Results – Class 6 Aggregates (NMPS16-30, for Example, Denotes the 30th Sample with NMPS of 16 in.).....	81
Figure 7.2. Resilient Modulus and Peak Deviator Stress ($\sigma_{df@4psi}$) Results – Class 5 Aggregates.....	82
Figure 7.3. Resilient Modulus and Peak Deviator Stress ($\sigma_{df@4psi}$) Results for Combined Class 3 and 4 Granular Subbase Materials	84
Figure 7.4. Resilient Modulus and Peak Deviator Stress (σ_{df}) Results for Select Granular (Granular Subbase) Materials.....	85
Figure 7.5. Resilient Modulus and Peak Deviator Stress (σ_{df}) Results for Class 7 Salvaged Materials	87
Figure 7.6. Resilient Modulus-Shear Strength Relationships for “Standard” (a) Aggregate Base and (b) Granular Subbase Materials at Near Optimum Moisture Conditions [1 psi = 6.89 kPa]	88

Figure 7.7. Peak Deviator Stress at Failure (σ_{df}) vs Gravel-to-Sand (G/S) Ratio for Various Aggregates: (a) 4-psi, (b) 5-psi, (c) 8-psi, and (d) 10-psi Confining Pressure [1 psi = 6.89kPa; 1 pcf = 16.02 kg/m ³]	91
Figure 7.8. Different Packing States of Gravel-Sand-Fines Mixture with Different Gravel/Sand Ratios (Small Black Dots Represent Fines Fraction)	92
Figure 7.9. Maximum Dry Density (γ_{dmax}) and Optimum Moisture Content (ω_{opt}) vs Gravel-to-Sand Ratio (G/S) at (a) 4-psi and (b) 8-psi Confining Pressure [1 psi = 6.89kPa; 1 pcf = 16.02 kg/m ³]	93
Figure 7.10. The Gravel-to-Sand Ratio Effects Observed in Other Databases Collected from: (a) Garg and Thompson (1997); (b) Tian et al. (1998); and (c) Tutumluer et al. (2009) [1 psi = 6.89kPa; 1 pcf = 16.02 kg/m ³]	96
Figure 8.1. Overview of the Proposed/Envisioned MnPAVE Best Value Granular Material Components	100
Figure 8.2. Design Concepts for the Aggregate Source Management Component	101
Figure 8.3. Conceptual Windows Proposed for the Aggregate Source Management Component	102
Figure 8.4. Conceptual Windows Proposed for the Aggregate Property Selection Component	105
Figure 8.5. Conceptual Windows Proposed for the Aggregate Source Selection/Utilization Component	107
Figure 8.6. Pavement System and Evaluation Points Used for Stress State Analysis (Khazanovich et al., 2006)	110
Figure 8.7. The Iterative Procedure Adopted by MEPDG for Obtaining One Single Modulus (Khazanovich et al., 2006)	111
Figure 8.8. The Iterative Procedure of (a) Subdividing Each Nonlinear Granular Layer into a Number of “Imaginary” Sublayers and (b) Transforming “Imaginary” Sublayers into Single Equivalent (subscript “e”) Layers Using the Odemark Method	113
Figure 8.9. The Conceptual Window Showing the Proposed Nonlinear Mode in MnPAVE	114
Figure 8.10. Mohr-Coulomb Representation of Shear Strength and the Failure Envelope	118

Executive Summary

Background

Unbound aggregate materials used for constructing flexible pavement foundations are becoming increasingly scarce and expensive in many parts of Minnesota because gravel mines and rock quarries are being lost to other land uses thus hindering road construction and maintenance both financially and logistically. Under such circumstances, the optimized selection and utilization of locally available aggregates having gradations still within MnDOT-specified bands has become a major concern. The aggregate type and quality, in addition to traffic load-related factors, are important ones for determining required thicknesses of unbound aggregate layers for which the primary function is load distribution through aggregate interlock and protect weak subgrade underneath. “Quality” here refers exclusively to structural support (or bearing capacity), not to other non-trivial aspects of quality such as freeze-thaw or wet-dry durability. To ensure the design and performance of unbound aggregate layers and eventually the whole pavement structure, individual aggregate properties influencing quality need to be examined and properly selected. These properties may include aggregate shape, texture and angularity, gradation, fines content (percentage passing No. 200 sieve), plasticity index, moisture and density conditions related to compaction, and their interactions.

Currently, aggregate materials, preferably dense-graded, are classified for use and placed in quantities based on testing techniques, material specifications, and design procedures that are several decades old and/or intended for “standard” materials with proven performance record. These testing techniques, material specifications, and design procedures may not be always linked to the application of the aggregate resource, nor do they specify the acceptable limits for aggregate quality aspects or evaluate the potential impact of these quality aspects. As Minnesota’s flexible pavement design procedures are gradually making the transition from use of the Hveem R-value and Soil Factor to the use of resilient modulus-based MnPAVE structural analysis and design, an awareness of optimizing aggregate type, quality, and layer thicknesses from mechanistic-based pavement design according to performance requirements of locally available materials would be useful for selecting aggregate, reducing waste, better utilizing construction dollars, and even more importantly, achieving better values. For the sake of promoting sustainability, more adaptable design methods and performance-based specifications also need to be developed to accommodate aggregates with a wider range of physical characteristics.

Research Objectives

This research has focused on developing sustainable, best value design solutions to adequately address the following concerns:

- How do individual aggregate properties and changes in these properties quantitatively impact aggregate quality aspects characterized by resilient modulus and shear strength?
- Where in pavements should locally available materials, often of marginal quality, be placed?

- What pavement types and critical traffic design levels should be considered beyond which no satisfactory pavement performance may be achieved by using marginal materials in a cost-effective manner?
- What would be the optimum combination of high-quality and marginal-quality aggregate material uses considering certain design features and site factors?
- How should one specify individual aggregate material properties on the basis of their end use performance as required by site-specific traffic and environmental conditions?

This research study is aimed at evaluating pavement base/subbase performances of locally available aggregate materials (with gradations still falling within the MnDOT specified gradation bands) in Minnesota through mechanistic-based pavement analysis and design. The main objective of this study is to demonstrate that locally available aggregate materials can be economically efficient in the implementation of the available mechanistic-based design procedures in Minnesota through the MnPAVE mechanistic-empirical flexible pavement design method. The goal is to develop the components of a new granular material best value software module to be added to the MnPAVE program.

Research Scope and Methodology

The study first linked the aforementioned aggregate index properties to the collected field and laboratory aggregate strength and resilient modulus (M_R) data in order to identify mechanistic design input ranges. Specifically, available aggregate index property databases were utilized to obtain aggregate properties for categorizing locally available aggregate base and granular subbase materials from quarries and borrow pits around Minnesota. Furthermore, existing laboratory and in situ strength and M_R test data were also collected from MnDOT sponsored research studies. Multiple linear regression models were then developed for the M_R data as a function of the various aggregate properties, followed by the study of corresponding M_R sensitivities using both the Monte Carlo type simulation and the First-order Reliability Method (FORM).

For the various aggregate types and properties identified/used throughout Minnesota for different MnDOT aggregate classes, two mechanistic design inputs—resilient modulus and peak deviator stress at failure (shear strength indicator)—were used to uniquely classify those aggregates into three representative quality ranges (i.e., high, medium, and low). A comprehensive mechanistic analysis matrix was then carefully designed with various scenarios considering pavement structure and climatic effects. MnPAVE analyses were conducted to investigate the effects of unbound aggregate layer characteristics (i.e., material quality affecting modulus input and layer thickness) on conventional flexible pavement life expectancies predicted. To further validate sensitivity analysis results obtained, aggregate strength data obtained from previous MnDOT laboratory and field studies were collected in the form of peak deviator stresses at failure. The established trends in the M_R database were evaluated and modulus-strength relationships were developed for the different MnDOT aggregate classes. Additionally, linkages between quantitative gradation parameters and the mechanical behavior of aggregate base/granular subbase materials were also explored from MnDOT aggregate strength database analysis with certain preliminary guidelines proposed for performance-based gradation requirements. Finally, in an effort to synthesize all the research findings, the best value granular material selection components are proposed for implementation into the MnPAVE pavement

analysis and design program to facilitate GIS-based aggregate source management, aggregate property determination for design, and cost-effective aggregate source selection/utilization.

Summary of Research Outcomes

The results of statistical analyses for establishing M_R correlations with aggregate properties identified the importance of aggregate shape properties. The addition of aggregate shape properties into regression analyses significantly improved the M_R model parameter correlations. Among the three imaging-based shape indices examined (F&E Ratio, AI and ST), based on the regression results obtained, surface texture (ST) was statistically the most significant influencing k_1 predictions; whereas angularity index (AI) was the most significant influencing k_2 and k_3 predictions. Other significant aggregate index properties affecting M_R were also identified and summarized.

The findings from the MnPAVE sensitivity analyses indicated that use of locally available and somewhat marginal quality materials may be quite cost-effective for low-volume roads, provided that the 20-year design traffic level does not exceed 1.5 million equivalent single-axle loads (ESALs). The quality of base layer was found to directly impact fatigue life expectancy. With low quality materials used in the base, increasing base layer thickness did not seem to improve fatigue life. Whereas, increasing base thickness significantly improved subgrade rutting performance. As expected, a stronger engineered subgrade contributes significantly to improved rutting performance. Interestingly, subbase material quality, again linked to modulus characteristics only here, seemed to much more significantly impact rutting performance than the quality standards of base materials. According to the results, a high quality, stiff subbase exhibits a bridging effect to better protect the subgrade and offset detrimental effects of low base stiffness.

As revealed from data analyses on the laboratory M_R and peak deviator stress at failure (σ_{df}) for a given confining pressure, it appears that modulus and strength relationships for most aggregate base and especially granular subbase materials are non-unique, suggesting the necessity of incorporating a limiting working shear stress to strength ratio to avoid catastrophic shear failure in base and especially subbase courses. It may also be insufficient to establish the quality of aggregate base/granular subbase materials based solely on resilient modulus, as certain aggregate materials exhibiting similar resilient moduli were observed to show considerable differences in shear resistance, i.e. shear strength. Both Mn/DOT aggregate database and additional aggregate test results collected from the literature revealed that a Gravel-to-Sand (G/S) ratio was an important gradation parameter governing aggregate shear strength behavior. It was then postulated that within the current Mn/DOT specified gradation bands, those with the same G/S value of around 1.5 would exhibit similar shear strength behavior regardless of their maximum particle size provided that other properties such as fines content, moisture and density conditions (AASHTO T99) and aggregate shape were not dramatically different from each other.

Recommendations for Future Research

Testing more aggregate materials from other aggregate sources for shape/morphological and mechanical properties would definitely improve the developed correlations that are useful for estimating M_R inputs at basic and intermediate design levels in MnPAVE. Permanent strain (or deformation) test results, or simply data from preconditioning cycles of laboratory repeated load triaxial M_R tests, if available in the future, should also be analyzed to confirm the observed

aggregate quality aspects. The conclusions, which are subject to further validation with extensive field performance data before being implemented, pertain to aggregate base and granular subbase materials used in Minnesota and the local climatic conditions. Further, nonlinear cross-anisotropic aggregate base and granular subbase modeling in the mechanistic analysis could generate more accurate pavement responses predicted; however, such advanced analyses would also require distress models to be calibrated with the new response predictions.

Chapter 1 Introduction

1.1 Problem Statement

Aggregate materials that are widely used in road construction and maintenance applications to replace unsuitable soil, prepare pavement working platform, or construct flexible pavement foundation layers are becoming increasingly scarce and expensive in many parts of Minnesota, particularly in urban areas. Such local shortages or depletions of aggregates, especially “standard” or traditional high quality crushed ones, around those areas result from multifaceted obstacles. Firstly, geographical distribution of natural deposits of high-quality aggregates needed for road construction is uneven in nature and not found in some areas; secondly, in areas where high-quality aggregates exist, gravel mines and rock quarries are being either lost to other land uses or restricted from mining due to public perception and conservation efforts; thirdly, higher quality standards may further reduce the amount of usable aggregates mined from specific sources. As a result, road construction/maintenance applications have been hindered in certain regions both financially and logistically.

The aggregate type and quality are important factors for determining required thicknesses of unbound aggregate layers whether the application is in the pavement working platform construction or in low to medium volume pavement design applications. Dense-graded aggregates are usually preferred for constructing such a layer with the primary function to serve load distribution. It has been well recognized that aggregates with high fines (minus No. 200 sieve size) contents and/or excessive Plasticity Index (PI) values may exhibit increased or high moisture sensitivity to negatively impact performance, and that when fines are low in percentage and non-plastic in nature, it is often the aggregate shape, angularity (crushed or uncrushed) and texture properties that impact the rutting potential of the unbound layer. The traditional testing procedures/techniques and current “recipe-based” specifications used for classifying aggregate materials, which either match design with performance based on field experiences or are intended for building roads with high traffic levels, have been adequate and have generally produced long lasting roads for “standard” materials with well-proved performance in the past. However, those testing techniques and specifications are not always linked to the application of the aggregate resource, nor do they specify the acceptable limits for aggregate quality aspects or evaluate the impact of these quality aspects on the design and performance of unbound aggregate layers and eventually the whole pavement structures.

Minnesota’s flexible pavement design procedures are gradually transitioning from R-value and Soil Factor to the MnPAVE structural analysis and design. This is similar to what is occurring nationally with the Mechanistic-Empirical Pavement Design Guide (MEPDG software can be found at <http://www.trb.org/mepdg/>). Those new mechanistic design procedures and testing techniques available need to be implemented so that road construction can better optimize material use and reduce waste. More adaptable design methods and performance-based specifications can be developed to accommodate aggregates with a wider range of aggregate physical characteristics.

1.2 Research Objectives

Unbound aggregate base and granular subbase layers are major pavement structural components for distributing wheel loads and providing adequate protection of subgrade to ensure longevity or proper performance of flexible pavements. This research study is aimed at

evaluating the pavement base/subbase performances of locally available aggregate materials (of which the gradations are still within the MnDOT specified bands) within Minnesota through mechanistic-based pavement analysis and design. The main objective of this study is to demonstrate that such locally available aggregate materials can be economically efficient in the implementation of the available mechanistic-based design procedures in Minnesota through MnPAVE Mechanistic-Empirical Flexible Pavement Design Method. This goal is to develop the components of a new granular material best value software module to be added to the MnPAVE program. Specific objectives are as follows:

- Develop proper material selection and utilization according to aggregate properties;
- Optimize aggregate layer thickness during the design process based on cost and mechanistic material properties related to performance, and as a result;
- Promote more economical use of the locally available aggregate materials in Minnesota.

1.3 Research Methodology and Tasks

The original work plan for this study involved five different tasks. However, modifications were made later on the original scope to include additional research tasks. Brief descriptions on the scopes of individual tasks are presented below according to the modified work plan.

1.3.1 Task 1 Establish Aggregate Index Properties

The objectives of this task were to gather information on the types, sources and properties of locally available aggregates in Minnesota and obtain typical costs. Information on gravel pits, rock quarries, and commercial aggregate sources in Minnesota were collected from the Aggregate Source Information System (ASIS); whereas MnDOT's aggregate index property database, i.e., the Laboratory Information Management System (LIMS), was used to collect individual aggregate test results in electronic data tables.

1.3.2 Task 2 Collect Aggregate Strength and Modulus Data

Under this task, mechanistic pavement analysis and design inputs were collected as the strength and resilient modulus (M_R) data for unbound aggregate pavement base and subbase applications. Existing laboratory and in situ test data for Minnesota's aggregates were obtained from related research studies performed under MnDOT supervision. In addition, as part of a comprehensive literature search, strength and M_R data were also collected from other relevant research efforts, such as a large database of laboratory M_R test results compiled by the Principal Investigator (PI) for over a decade at the University of Illinois and the current Illinois Department of Transportation research project laboratory data on three different types and qualities of aggregate materials. Aggregate index properties of those aforementioned databases were collected and archived accordingly.

1.3.3 Task 3 Establish Linkages between Aggregate Properties and Design Inputs

The objective of this task is to develop methods to optimize the use of unbound aggregates with wide ranges of physical characteristics in pavement base and subbase layers. Under this task, the aggregate index properties were linked to the collected field and laboratory aggregate strength and M_R data and the aggregate properties, such as gradation, shape, texture

and angularity, moisture and density state in relation to optimum condition, and fines content for identifying mechanistic design moduli ranges.

1.3.4 Task 4 Conduct Sensitivity Analyses

For the various aggregate types and properties identified/used throughout Minnesota for different MnDOT aggregate classes, a comprehensive matrix of mechanistic design moduli were established. Using these inputs, MnPAVE analyses were conducted to identify the sensitivity of the design inputs to pavement life expectancies. The findings included a set of guidelines for best value aggregate materials intended to provide engineers, designers, and aggregate producers with proper aggregate index properties and improved specifications linked to field application requirements.

1.3.5 Task 5 Validate Sensitivity Analysis Results Using Additional Aggregate Strength Data

This task verified the Task 4 sensitivity analysis results, which primarily assumed different M_R levels could be linked to various material quality standards in relation to strength properties. Aggregate strength data from the available M_R tests, in the form of peak deviator stresses at failure, and other previous MnDOT laboratory and field (MnROAD) studies were collected to evaluate the established trends in the M_R database. Modulus-strength relationships were developed for the different MnDOT aggregate classes and studied together with the field data from MnROAD studies to validate the sensitivity results. This task is essentially needed for accurately interpreting Task 4 results in relation to the strength properties of the established material quality standards.

1.3.6 Task 6 Develop Best Value Granular Material Selection Tool Components

This task dealt with the development of the best value granular material tool components to incorporate into the MnPAVE program and to implement mechanistic pavement design concepts in aggregate selection/utilization. With the proposed developments, the current version of the MnPAVE program is targeted for a major improvement for aggregate design property selection. The final coding and packaging of MnPAVE software with the developed components, however, is not an intended goal but rather that task is left to software developers who work for MnDOT.

1.4 Report Organization

Chapter 2 of this report reviews major aggregate properties affecting strength, modulus and deformation characteristics of constructed aggregate base and granular subbase layers and important findings are highlighted from previous research studies. Chapter 3 presents essential aggregate index properties established from aggregate source information while Chapter 4 describes the collection of aggregate strength and modulus data from relevant research studies sponsored by MnDOT as well as those completed recently at the University of Illinois. Chapter 5 describes the scientific approach adopted in this research effort to develop regression based correlations for predicting mechanistic pavement design inputs, i.e., strength and modulus, from different aggregate source properties and studying the sensitivities of those design inputs to identified aggregate properties. MnPAVE sensitivity analysis results are described in detail in Chapter 6. Chapter 7 presents the results from the verification of sensitivity analysis results, which employs additional shear strength test results conducted on Minnesota aggregate materials.

Modulus-strength relationships are developed for aggregate materials of different Classes at different conditions. Also presented in Chapter 7 are the preliminary performance-based gradation refinements identified and established from the robust linkages between critical gradation parameters and shear strength behavior of aggregate base and granular subbase materials. Finally, based on the major findings of this research study, the best value granular material selection components are recommended in Chapter 8 for implementation into the MnPAVE pavement analysis and design program. Major research study findings as conclusions and recommended future research needs are summarized in Chapter 9.

Chapter 2 Literature Review

2.1 Current Classification Systems for Unbound Aggregate Materials

2.1.1 Traditional “Recipe-based” Classification System

Pavement engineers commonly use aggregate quality to describe the suitability of an aggregate for use in road construction; however, a number of ways rather than one single formalized procedure exist for classifying aggregate materials and rating the quality of an aggregate. These “recipe-based” physical and mechanical classification systems are currently used for judging the performance of an aggregate. By using a variety of aggregate tests and specifications developed by ASTM, AASHTO, and certain state and local agency procedures, the former system considers the intrinsic physical properties of the material that are related to basic geologic origin, mineralogy, and other properties such as hardness and durability. One major disadvantage associated with such physical classification systems is that it could possibly accept unsuitable materials in some cases and reject desired materials in other cases, as summarized by Cook and Gourley (2002). Under such physical classification framework, naturally occurring materials could be excluded for use due to any combination of grading, plasticity, particle hardness, strength, etc. lying outside the specification-demanded requirements, as outlined in Figure 2.1.

		Non-Standard Material Groups																					
		Strong Rock	Weak Rock								Natural Granular Materials						Pedogenic Materials						
		Foliated Metamorphic Rocks	Basic Igneous Rocks	Recent Coral Deposits	Marls and weak Limestones	Weak Volcanic Breccias/Agglomerates	Weak Conglomerates	Weak Sandstones	Weak Volcanic Tuffs	Fractured/Weathered Limestones	Shales/Mudstones	Weathered Strong Rocks	Alluvial Sands	Alluvial Clayey Sand Deposits	Aeolian Sand Deposits	Colluvial Deposits	Alluvial Gravel Deposits	Volcanic Pyroclastics	Residual Clayey Sand Deposits	Residual Gravel Deposits	Laterite Deposits	Calcrete Deposits	Silcrete Deposits
Primary Specification Criteria	High PI Fines																						
	Low Particle Strength																						
	Poor Grading																						
	Poor Durability																						
	Poor Particle Shape																						
Additional Impacting Criteria	High Mica Content																						
	High Water Absorption																						
	High Variability																						
	In-service Deterioration																						
	Low PI Fines																						

Potential Problem Characteristics

Figure 2.1. Non-standard Material Groups and Their Likely Problems (Cook and Gourley, 2002)

In many areas shortage of “standard” or traditional aggregate materials satisfying normal requirements for road paving, non-standard local aggregate sources have been successfully applied in low volume road constructions of which several typical examples are documented in

Table 2.1. Besides, an early field trial constructed by the Transport Research Laboratory (TRL) in 1978 where three marls (local calcareous materials) outside the recommended gradation envelope were substituted for the crushed stone base indicated that the use of a much wider range of marls, if properly stabilized, is viable both technically and economically, as justified by the low values of rut depth and deflection and the high strength of the base (Woodbridge, 1999). Bullen (2003) also showed that the use of local aggregate materials in Australia, with appropriate design, can not only provide the desired pavement performance, but can also promote sustainability in terms of significant cost saving, natural resource conservation, and even environment protection.

Table 2.1. Examples of Using Non-standard Materials in Low-Volume Sealed Roads (Cook and Gourley, 2002)

Material & Reference	Location	Climatic Environment	Material Characteristics	Utilisation
Calcrete Lionjanga et al (1987) Greening and Rolt (1997)	Botswana	Semi-arid	Low particle strength Low compacted strength Poor grading High plasticity	Roadbase: <u>Revised specifications</u> developed for both sealed and unsealed shoulder designs. Successfully used as roadbase with acceptable performance (0.3×10^6 esa) for materials with soaked CBR >35% and PI <30 if shoulders are sealed.
Laterite Grace and Toll (1987) Gourley and Greening (1997) CIRIA (1988)	Malawi	Seasonally wet tropical	Low particle strength Low compacted strength Poor grading High plasticity	Roadbase: <u>Construction procedure</u> modified to allow traffic to run on roadbase for one rainy season before proof rolling, shaping and sealing in the following dry season. All sites well drained and with crown-height at least over 1m.
Marl Woodbridge et al (1987)	Belize	Wet humid tropical	Low particle strength Poor grading	Roadbase and sub-base: Embankment construction (600-750mm of fill) used throughout due to seasonally high water-table. Only non-plastic or slightly plastic materials selected. Controlled heavy compaction used to lock material and achieve >98% MDD. Good maintenance regime adopted including regular clearing of drains and unsealed shoulder maintenance.
Basalt Pinard & Jakalas, (1987).	Botswana	Sub-tropical	Crushed material (with added fines) passed specification criteria; but had demonstrably poor in-service durability.	Roadbase. Addition of plastic (active) fines to improve the grading along with modification using too low a percentage (below ICL) of lime (lime also suspect i.e. inactive) led to early failure due to moisture interaction/volumetric change in the road base material. Unsealed shoulder design.
Weathered Basalt Gourley and Greening (1999)	Botswana	Sub-tropical	Ripped weathered (Grade III+) basalt selected. Grading out of recommended specification; PI <12 and soaked CBR >55.	Roadbase: Normal construction methodology adopted. 1m embankment and sealed shoulders.
Coral Cardno & Davies (1994) Beavan (1971)	Papua New Guinea	Wet humid tropical	Low particle strength Poor grading (including oversize) High plasticity	Roadbase: <u>Modified specification</u> based on the requirement of high compaction giving dense layers (max. 150mm). Selection of appropriate compaction plant vital (a function of grading and PI)
Cinder Gravels Newill et al (1987)	Ethiopia	Semi Arid	Low particle strength and high porosity Poor grading	Roadbase: Procedures developed to control selection; <u>mechanical stabilisation</u> with ash fines and selection of appropriate compaction plant vital.
Schist/Phyllite Fookes & Marsh 1981)	Nepal	Monsoonal sub-tropical	Poor aggregate shape	Modified <u>processing procedure</u> to ensure better shape

In United States, for instance, the taconite aggregate resources in Minnesota, the industrial by-products from iron ore mining, have very recently been demonstrated in MnROAD low volume test section studies as a promising supply of high quality, low cost aggregates for roadway use (Clyne et al., 2010). In Texas, locally available materials (mostly Grade 4), sometimes even with high amount of fines, have been used (with or without stabilization) not only for low volume roads but also for major roads in some districts.

In spite of all the potential benefits and documented successful applications of local aggregate sources, one major obstacle to their widespread use is the significant engineering

uncertainty (or risk) inherent with their long-term performance which cannot be addressed by current physical classification systems and then considered properly in pavement design; moreover, many state transportation agencies are currently reluctant to relax the traditionally conservative standard specifications.

2.1.2 Mechanistic Classification System

Separate from the physical classification presented above, the mechanistic classification discerns different qualities of unbound aggregates from mechanical properties that are required as input to the constitutive relationships incorporated into mechanistic-empirical pavement design procedures, as illustrated in Figure 2.2. It is expected that such mechanistic classification systems, in combination with certain levels of local experiences, should have direct relevance or even robust linkage to the actual performance of materials used in pavement layers. The mechanistic nature of the responses of unbound aggregate materials can be characterized by resilient modulus (stiffness) while permanent deformation linked to shear strength often relates to rutting damage accumulation.

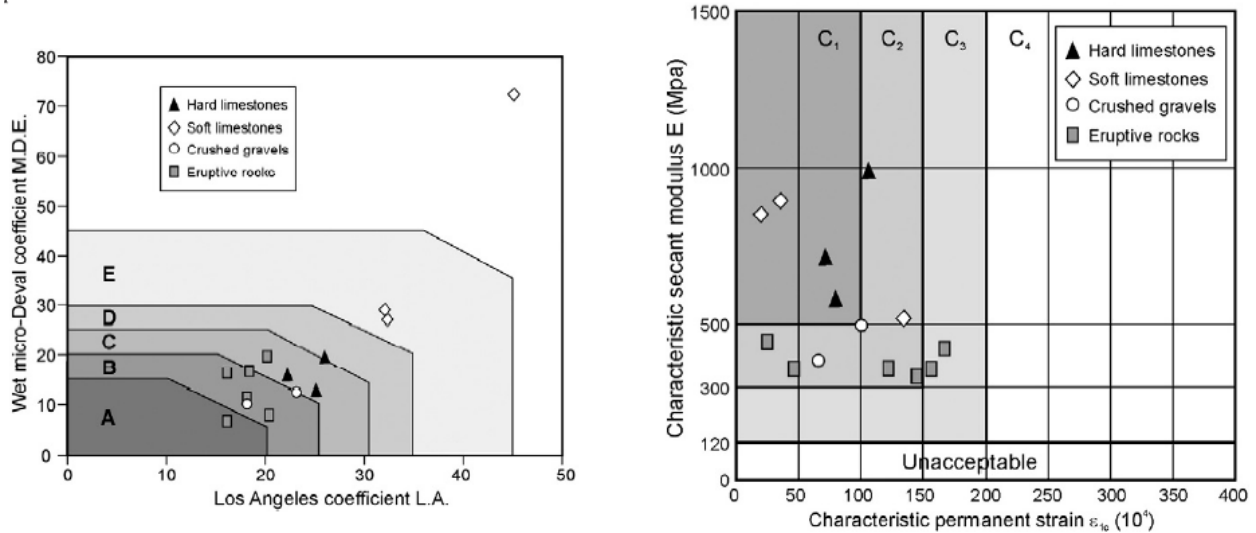


Figure 2.2. Physical (Left) Versus Mechanical (Right) Classification for Various Unbound Granular Materials (Paute et al., 1994)

The resilient modulus (M_R) is a key mechanistic pavement analysis and design input for measuring the elastic response of pavement geomaterials under the repeated application of traffic loads. To characterize the resilient behavior of unbound granular materials in terms of M_R , a variety of mechanistic response models have been proposed to express the modulus as a function of applied stress states including confinement and shear effects (Uzan, 1985; Witczak and Uzan, 1988; NCHRP 1-37A). As part of the research activities undertaken for the NCHRP 4-23 project, entitled, “Performance Related Tests of Aggregates for Use in Unbound Pavement Layers”, a total of thirteen good and poor performing base/subbase aggregates with varying material properties obtained from eight different States in the U.S. were studied by Seyhan and Tutumluer (2002) for potential linkages between anisotropic resilient modular ratios at various stress states and the quality and strength properties. Detailed analyses of the test results indicated that those supposedly “good performing” materials usually have low to moderate amount of fines and/or

average particle size (D_{50} corresponding to 50% passing) greater than 4.75 mm (No. 4 sieve size); whereas the “poor performing” ones in general have high fines of possibly plastic nature.

As both the resilient (recoverable) and permanent deformation/strain components should be considered simultaneously for mechanistic-empirical evaluation of unbound aggregate behavior, the resistance to permanent deformation under repeated traffic loading relates to rutting damage accumulation in unbound aggregate materials. For example, Australian Road Association determines both resilient modulus and permanent deformation from repeated load triaxial tests to characterize unbound aggregates as well as marginal materials (AUSTROADS, 2003). Khogali and Mohamed (2007) developed a mechanistic aggregate classification system based on a test procedure for combined determination of the resilient modulus and permanent deformation potential involving both elastic and plastic responses. Recently, Tao et al. (2010) introduced a mechanistic-based design approach to characterize and compare the behavior of traditional and recycled pavement base materials which employed dissipated energy concept to explain different shakedown responses of materials obtained from laboratory repeated load triaxial tests and full-scaled accelerated loading tests. It was implied that permanent deformation characteristics of pavement materials provided a better measure for evaluating recycled and marginal materials against traditional unbound aggregates.

Shear strength is an important mechanistic property of unbound aggregate materials. The shear resistance of the material mainly contributes to developing a load resistance quality that greatly reduces the stresses transmitted to the underlying layers (Garg and Thompson, 1997). Saeed et al. (2001) found under NCHRP Project 4-23 study that shear strength of unbound aggregates under repeated loading had the most significant influence on pavement performance. Seyhan and Tutumluer (2002) suggested that a limiting value of the shear stress ratio (the level of applied shear stress as a fraction of the shear strength of the material) controlled the permanent deformation behavior of aggregates; and that “good” quality aggregates typically had low shear stress ratios in the range of 0.2 to 0.5.

To better assess performance and rank different sources of aggregate materials, coupling mechanistic characteristics including moduli, strength, and permanent strains under representative ranges of operating environmental conditions is of essential importance from the Mechanistic-Empirical Pavement Design perspective. Without utilizing performance-based material specifications to be developed, optimized material use with reduced waste, and eventually better utilized construction dollars cannot be achieved extensively.

From a mechanistic-empirical pavement design perspective, it may be challenging how to best utilize different qualities of locally available aggregate materials in road bases/subbases. For example, Lukanen (1980) found early on that certain Minnesota DOT (MnDOT) Class 3 aggregates were even stronger than Class 6 aggregates when placed in pavement granular layers. This was a surprising field evaluation considering the fact that as MnDOT aggregate classes increase, usually better materials, such as a Class 6 high quality, are designated. During Mn/ROAD study, similar contradictory trends were also observed in backcalculated base layer moduli from falling weight deflectometer (FWD) testing of flexible pavements (Ovik et al., 2000). For both thin (< 15 cm) and thick (> 15 cm) asphalt concrete surfacing, the backcalculated base moduli of Class 3sp materials were often found to be greater than those of higher material classes, i.e. 4sp, 5sp, and 6sp (Ovik et al., 2000). In the light of these findings several issues may need to be addressed, such as, how to specify material properties based on their end-use performances; where in pavements to place locally available materials of marginal quality (either natural or recycled); what type of pavements and critical traffic design levels

should be determined beyond which no satisfactory pavement performance can be cost-effectively maintained by using marginal materials; and finally, what would be the optimum combination of high and marginal quality aggregate uses considering certain design features and site factors so that aggregate base and granular subbase materials can be optimized for satisfactory pavement performance.

2.2 Factors Affecting Modulus, Strength, and Rutting Behavior of Unbound Aggregate Materials

While resilient modulus (M_R) is a key design input for mechanistic pavement response analysis, permanent deformation of unbound base/subbase and subgrade layers dictate the long term behavior linked to rutting performances of pavements (Puppala, 2008). Factors affecting mechanical behavior (modulus, strength and permanent deformation) of unbound granular materials can be classified into two main categories, i.e., (i) primary load related factors including applied stress level, stress path, stress history, the number of load applications, etc., and (ii) secondary factors related to material properties. As for load related factors, it has been well recognized that permanent deformations rapidly accumulate with an increase in applied deviator stress and diminish when confining pressure increases (Morgan, 1966; Wood, 1982), and that as the stress ratio defined as the magnitude of dynamic axial stress divided by the peak static stress (confining pressure) increases, the permanent axial strain increases at each confining pressure tested (Pumphrey and Lentz, 1986). On the other hand, various granular material properties, such as moisture content/degree of saturation, density, gradation, and aggregate particle shape, also affect mechanical behavior under repeated loading applications. With no intention to be exhaustive, the secondary factor related material properties, more complicated and less understood than load related ones, are discussed in detail next.

2.2.1 Moisture (Suction) and Density Conditions

Depending on the magnitude of the load or applied stress state in relation to the strength, modulus and permanent deformation properties vary considerably with moisture/suction and temperature, which in turn depend on the weather conditions. Seasonal variations mainly due to variations in moisture/suction are among the important factors influencing unbound pavement material moduli and eventually contributing to decreased load carrying capacity and possibly pavement failure. Increased moisture content develops pore water pressure and thus increases permanent deformation accumulation (Barksdale, 1972; Dawson et al, 1996). The increase in moisture content in excess of initial compaction value, primarily due to capillary rise from the water table, was indicated to be more critical in the long term than the seasonal variation in the layer moduli (AASHTO 2004 Appendix DD). Increased moisture makes unbound materials and soil weaker by reducing suction due to increasing pore water pressure, and thus decreasing the M_R and the strength, especially for uniformly graded dense aggregates with higher fines contents (Thompson and Robnett, 1970; Dempsey, 1982). Noticeable pore water pressure usually starts to develop at saturation levels in excess of 85%, resulting in dramatically decreased rutting resistance (Thom and Brown, 1987). Minnesota is currently among few lead states in U.S. to include field moisture measurement in their construction quality assurance specifications, and has recently implemented mechanistic pavement design built upon unsaturated soil mechanics principles (Gupta et al., 2007).

Density has long been used as a quality control measure for determining the compaction of subgrade and base/subbase applications, although the development of field stiffness/modulus based construction specification for compaction of earthwork and unbound aggregate is currently underway (NCHRP 10-84 project). Barksdale (1972) reported that the degree of compaction was inversely related to the permanent strain development, as indicated by the significant decrease in permanent deformation accumulation for samples compacted at 100% instead of at 95% AASHTO T-180 modified Proctor compaction. The degree of compaction (DOC) was reported as the most important factor controlling permanent deformation development by Van Niekerk (2002) who observed that 50% to 70% higher axial stresses were needed to cause similar magnitude of permanent deformation when the degree of compaction increased from 97% to 103% for the investigated gradations (see Figure 2.3).

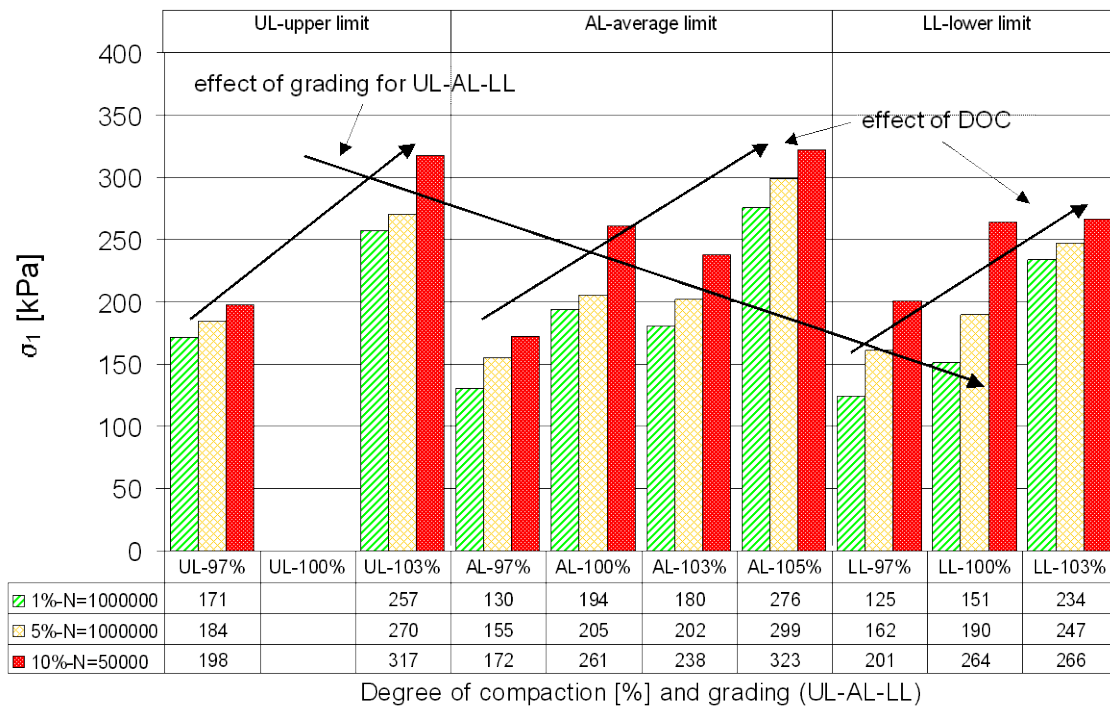


Figure 2.3. Stress (σ_1) Levels at Which $\epsilon_p = 1\%$, 5% , and 10% at $N=10^6$, 10^6 , and $50,000$, Respectively, at DOC = 97% , 100% , 103% , and 105% (Van Niekerk, 2002)

The impact of density seems to be ambiguous on the resilient modulus behavior as contrary to the permanent deformation behavior: both little change (Knutson and Thompson, 1977; Elliott and Thornton, 1988; Lekarp et al., 2000) and a general increase (Rowshanzamir, 1995; Tutumluer and Seyhan, 1998) in the resilient modulus were reported by researchers for increasing density. Holubec (1969) found that increased density improves properties of unbound aggregates with angular particles more than for aggregates with rounded particles, provided there is no increase in the transient pore pressure during repetitive loading.

2.2.2 Gradation

When compared to aggregate type and mineralogy, properties such as aggregate gradation (a.k.a, particle size distribution) and its interactions with others are not well understood.

Gradation itself is a key factor influencing not only the mechanical response behavior characterized by resilient modulus (M_R), shear strength and permanent deformation, but also permeability, frost susceptibility, erosion susceptibility, etc. (Bilodeau, 2007; Bilodeau, 2008). Figure 2.4 shows that open graded aggregate samples, when uncompacted, were less deformed than the dense graded one (Thom and Brown, 1988); whereas for heavily and lightly compacted samples, no relevance was found between grading and compaction effort. It is worth mentioning that the grading parameter n in Figure 2.4 is given by the Talbot's equation as follows:

$$P = 100 * \left(\frac{d}{D} \right)^n \quad (2.1)$$

where D is the maximum particle size and d is the particle size corresponding to percent passing certain sieve size.

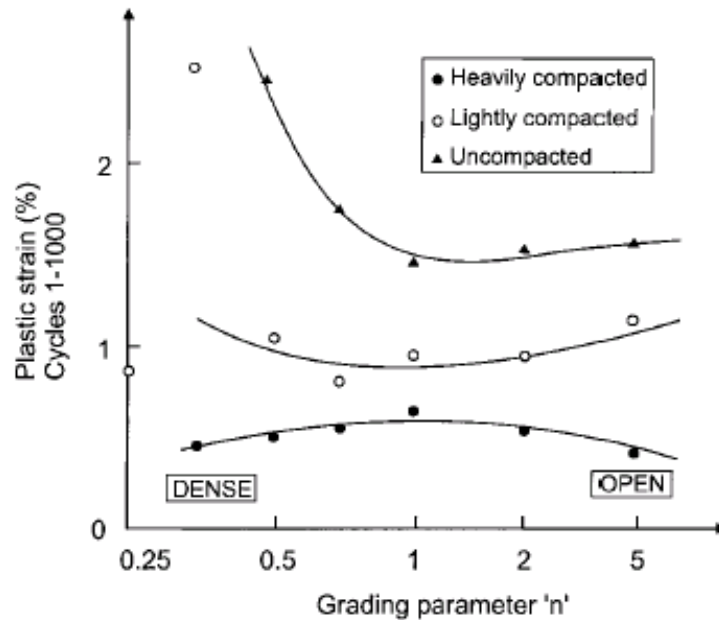


Figure 2.4. Effect of Grading and Compaction on Plastic Strain (Thom and Brown, 1988)

In Van Niekerk's study (2002), the gradation effect was also observed at different degrees of compaction (DOC). As shown in Figure 2.5, at a given DOC level, the axial stresses needed to cause similar magnitude of permanent deformation descended from the upper limit (UL) to the average limit (AL), and then to the lower limit (LL), implying improved permanent deformation resistance for coarser gradations studied.

With an expectation to ensure adequate pavement performance, MnDOT, among many other state highway agencies, currently employs different empirical gradation bands for unbound aggregates of classes from 1 to 7 used in road base/subbase construction, as illustrated in Figure 2.5.

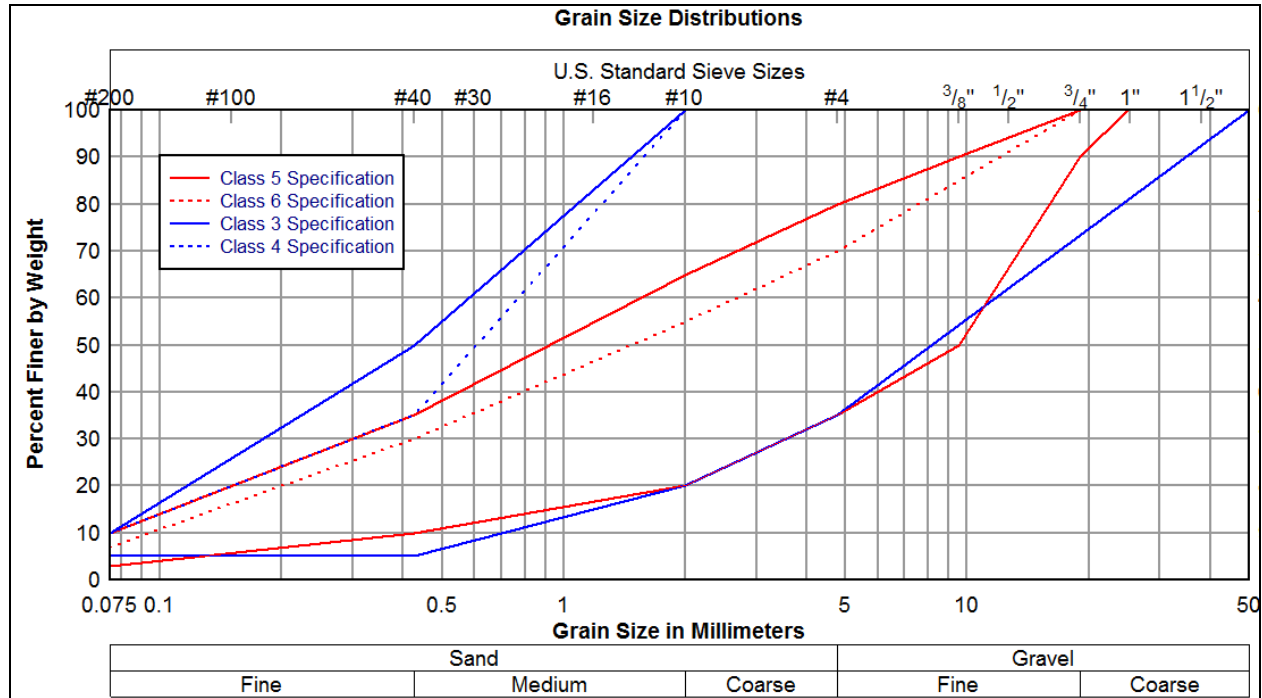


Figure 2.5. MnDOT Specified Gradation Bands for Different Aggregate Classes

2.2.3 Fines Content

Excessive fines content (percent passing the No. 200 sieve), especially in combination with high moisture content (or saturation level) and/or high deviator stress level, was reported to detrimentally affect both the resilient response and the permanent deformation (rutting) potential of unbound aggregate materials by making them moisture sensitive and frost susceptible (Thom and Brown, 1988; Barksdale, 1972; Tutumluer and Seyhan, 2000). Fines content is often interconnected with gradation to exert influences on strength and resilient and permanent deformation characteristics of unbound granular materials in a sense that more than optimum amount of fines will fill up all the voids between coarser particles and further reduce inter-particle interactions by separating them apart. An optimum fines content of around 8% was recommended by Gray's (1962) to achieve maximum strength for 25-mm (1-in.) top sized dense-graded crushed aggregate base materials, with such an optimum amount decreasing with increasing maximum aggregate size. The maximum allowable fines content in an aggregate gradation was also investigated by Tutumluer and Seyhan (2000) from another perspective of anisotropic modular ratios and attainable aggregate moduli, which determined an optimum 7% non-plastic fines content for the Illinois Department of Transportation (IDOT) CA-6 dense-graded crushed aggregate base material tested. Bilodeau et al. (2009) identified, from a laboratory study conducted on the performance of unbound granular materials with six gradations and three aggregate sources commonly used in Canada, one fines-related volumetric parameter (termed fine fraction porosity) that described satisfactorily not only the mechanical performance but also the environmental stresses sensitivity of materials tested. Also identified from their study were the adapted (or optimized) gradation zones that ensured adequate overall performance of those three aggregate sources.

2.2.4 Aggregate Shape Properties

The impact of aggregate particle shape on the resilient modulus, shear strength, and permanent deformation behavior of unbound base/subbase layers in a pavement structure has long been realized. Allen (1973) reported that angular particles had better permanent deformation resistance due to improved particle interlock and higher angle of shear resistance between particles, as compared to rounded solid particles. Barksdale and Itani (1989) also concluded that blade shaped crushed particles are slightly more susceptible to rutting than other types of crushed aggregate and that cube-shaped, rounded river gravel with smooth surfaces is more susceptible than crushed aggregates. Aggregates made with uncrushed or partially crushed particles were reported to have a lower resilient modulus and higher Poisson's ratio than those with angular crushed particles (Hicks and Monismith, 1971; Allen and Thompson, 1974; Thom, 1988; Thom and Brown, 1988; Barksdale and Itani, 1989), as attributed to the higher number of contact points in crushed aggregates which distribute loads better and create more friction between particles (Lekarp et al., 2000).

With the aid of imaging technology, capturing aggregate shape profiles and quantifying aggregate morphology can be accomplished in an accurate and objective way. Imaging-based particle morphological/shape indices were developed, linked to performances of aggregate materials, and found to contribute mainly to the resilient behavior, strength and stability. Rao et al. (2002) conducted laboratory rapid shear triaxial tests on rounded uncrushed gravel, angular crushed stone, and a 50-50 blend of the two aggregates for which aggregate angularity index variations were quantified by imaging based techniques. It was observed that an increase in crushed materials beyond 50% significantly increased friction angle as well as the resistance to permanent deformation accumulation. Later on, Pan et al. (2005) found that increased surface texture and particle angularity as quantified from imaging increased the resilient modulus of asphalt concrete indicating that surface characteristics directly relate to permanent deformation resistance. Investigating effects of aggregate shape properties was also one of the subjects of the recent Illinois Center for Transportation (ICT) R27-1 research project conducted at the University of Illinois, which focused on characterizing strength, stiffness and deformation behavior of three aggregate materials i.e., limestone, dolomite and uncrushed gravel, commonly used in Illinois for subgrade replacement and subbase (Tutumluer and Mishra, 2009).

2.3 Review of Existing M_R Predictive Models

A common method to develop M_R prediction models/equations is to directly relate resilient modulus values with various aggregate or soil properties, applied stress states, and/or in-situ test results using statistical regression tools. As examples, several typical prediction models and their predictor variables are summarized in Table 2.2. It can be clearly seen that the predictor variables are routinely used soil properties and their combinations. Yau and Von Quintus (2002) summarized in the final report of the FHWA-RD-02-051 project the physical properties that are believed to be the most important for predicting resilient modulus for each material and soil type, as listed in Table 2.2. Table 2.2 also presents selected variables for predicting M_R values of both coarse and fine-grained soils according to George (2004). Reviewing these previous M_R predictive models for coarse-grained soils, it is clear that the Proctor compaction data, i.e., both achieved and optimum moisture contents and dry density, and the percent passing No. 200 sieve are very important predictor variables used in almost all predictive models reported.

Table 2.2. Various M_R Prediction Models/ Equations Reviewed

References	Index Properties	Prediction Models
Carmichael & Stuart (1985)	ω_c , SM & GR, PI, P_{200} , CH & MH	$\text{Log } M_R = 0.523 - 0.025(\omega_c) + 0.544(\log \theta) + 0.173(\text{SM}) + 0.197(\text{GR})$ $M_R = 37.431 - 0.4566(\text{PI}) - 0.6179(\omega_c) - 0.1424(P_{200}) + 0.1791(\sigma_3) - 0.3248(\sigma_d) + 36.722$ $(\text{CH}) + 17.097 (\text{MH}).$
Drumm et al. (1990)	% Clay, PI, γ_s , S, P_{200} , LL	$M_R (\text{ksi}) = \frac{a' + b' \sigma_d}{\sigma_d}$ for $\sigma_d > 0$ $a' = 318.2 + 0.337 (q_u) + 0.73(\% \text{Clay}) + 2.26(\text{PI}) - 0.915(\gamma_s) - 2.19(\text{S})$ $- 0.304(P_{200});$ $b' = 2.10 + 0.00039(1/a) + 0.104(q_u) + 0.09(\text{LL}) - 0.10 (P_{200});$
Ashraf & George (2004)	$\text{LL}/\omega_c \gamma_{dr}$, P_{200} , γ_{dr}/ω_c , $P_{200}/\log C_u$	$M_R (\text{MPa}) = 16.75((\text{LL}/\omega_c \gamma_{dr})^{2.06} + (P_{200}/100)^{-0.59})$ $M_R (\text{MPa}) = 307.4 (\gamma_{dr}/\omega_c)^{0.86} (P_{200}/\log c_u)^{-0.46}$
LTPP-FHWA Study (2002)	$P_{3/8}$, P_4 , % Clay, LL, ω_{opt} , γ_s , % Silt, γ_s/γ_{opt} , ω_c/ω_{opt} , PI	coarse-grained sand soils $k_1 = 3.2868 - 0.0412 P_{3/8} + 0.0267 P_4 + 0.0137 (\% \text{Clay}) + 0.0083 \text{LL} - 0.0379 \omega_{opt} - 0.0004 \gamma_s$ $k_2 = 0.5670 + 0.0045 P_{3/8} - 2.98 \times 10^{-5} P_4 - 0.0043 (\% \text{Silt}) - 0.0102 (\% \text{Clay}) - 0.0041 \text{LL} + 0.0014 \omega_{opt} - 3.41 \times 10^{-5} \gamma_s - 0.4582 (\gamma_s / \gamma_{opt}) + 0.1779 (\omega_c / \omega_{opt})$ $k_3 = -3.5677 + 0.1142 P_{3/8} - 0.0839 P_4 - 0.1249 P_{200} + 0.1030 (\% \text{Silt}) + 0.1191 (\% \text{Clay}) - 0.0069 \text{LL} - 0.0103 \omega_{opt} - 0.0017 \gamma_s + 4.3177 (\gamma_s / \gamma_{opt}) - 1.1095 (\omega_c / \omega_{opt}).$ Fine-grain silt soils: $k_1 = 1.0480 + 0.0177 (\% \text{Clay}) + 0.0279 \text{PI} - 0.0370 \omega_c$ $k_2 = 0.5097 - 0.0286 \text{PI}$ $k_3 = -0.2218 + 0.0047 (\% \text{Silt}) + 0.0849 \text{PI} - 0.1399 \omega_c$ Fine-grain clay soils: $k_1 = 1.3577 + 0.0106 (\% \text{Clay}) - 0.0437 \omega_c$ $k_2 = 0.5193 - 0.0073 P_4 + 0.0095 P_{40} - 0.0027 P_{200} - 0.003 \text{LL} - 0.0049 \omega_{opt}$ $k_3 = 1.4258 - 0.0288 P_4 + 0.0303 P_{40} - 0.0521 P_{200} + 0.0251 (\% \text{Silt}) + 0.0535 \text{LL} - 0.0672 \omega_{opt} - 0.0026 \gamma_{opt} + 0.0025 \gamma_s - 0.6055 (\omega_c / \omega_{opt})$
Santha (1994)	ω_c , ω_c ratio, COMP, % Silt, % Clay, γ_s , $\text{SW}^2/\% \text{Clay}$, γ_s^2/P_{40} , ω_{opt} , SATU, SW, SH, CBR, $(\text{SW}+\text{SH})/\% \text{Clay}$, SATU^2/SH , $\text{CBR} * \text{SH}$, LL, PI, $P_{40} * \text{SATU}$, P_{40}	For granular soils: $M_R = k_1 P_a (\theta / P_a)^{k_2} (\sigma_d / P_a)^{k_3}$ where, $\text{Log } k_1 = 3.479 - 0.07 \omega_c + 0.24 \omega_c \text{ratio} + 3.681 \text{COMP} + 0.011 \% \text{Silt} + 0.006 \% \text{Clay} + 0.025 \text{SW} - 0.039 \gamma_s + 0.004 (\text{SW}^2 / \% \text{Clay}) + 0.003 (\gamma_s^2 / P_{40});$ $k_2 = 6.044 - 0.053 \omega_{opt} - 2.076 \text{COMP} + 0.0053 \text{SATU} - 0.0056 \% \text{Clay} + 0.0088 \text{SW} - 0.0069 \text{SH} - 0.027 \gamma_s + 0.012 \text{CBR} + 0.003 (\text{SW}^2 / \% \text{Clay} - 0.31 (\text{SW} + \text{SH}) / \% \text{Clay});$ and $k_3 = 3.752 - 0.068 \omega_c + 0.309 \omega_c \text{ratio} - 0.006 \% \text{Silt} + 0.0053 \% \text{Clay} + 0.026 \text{SH} - 0.033 \gamma_s - 0.0009 (\text{SW}^2 / \% \text{Clay}) + 0.00004 (\text{SATU}^2 / \text{SH}) - 0.0026 (\text{CBR} * \text{SH}).$ For cohesive soils: $M_R = k_1 P_a (\sigma_d / P_a)^{k_3}$ where, $\text{Log } k_1 = 19.813 - 0.045 \omega_{opt} - 0.131 \omega_c - 9.171 \text{COMP} + 0.0337 \% \text{Silt} + 0.011 - 0.016 \text{PI} - 0.021 \text{SW} - 0.052 \gamma_s + 0.00001 (P_{40} * \text{SATU});$ $k_3 = 10.274 - 0.097 \omega_{opt} - 1.06 \omega_c \text{ratio} - 3.471 \text{COMP} + 0.0088 P_{40} - 0.0087 \text{PI} + 0.014 \text{SH} - 0.046 \gamma_s;$
Dai et al. (2002)	ω_c , γ_s , PI, LL, P_{200} , S	$M_R = k_1 \theta^{k_2} \sigma_d^{k_3}$ where, $k_1 = 5770.8 - 520.98 (\gamma_s)^{0.5} - 3941.8 (\omega_c)^{0.5} + 33.1 \text{PI} - 36.62 \text{LL} - 17.93 P_{200}$ $k_2 = -5.334 + 0.000316 (\gamma_s)^3 + 9.686 (\omega_c) - 0.054 \text{PI} + 0.046 \text{LL} + 0.022 P_{200}$ $k_3 = 409.9 - 306.18 (\gamma_s)^{0.1} - 82.63 (\omega_c) + 0.033 \text{PI} + 0.138 \text{S} - 0.041 \text{LL}$
Mohammad et al. (1999)	ω_c , γ_s , γ_s/γ_{opt} , ω_c ratio, LL, PL, % Sand, % Silt	$M_R = k_1 P_a (\sigma_{oct} / P_a)^{k_2} (\tau_{oct} / P_a)^{k_3}$ $\text{Log } k_1 = -0.679 + 0.0922 \omega_c + 0.00559 \gamma_s + 3.54 (\gamma_s / \gamma_{opt}) + 2.47 \omega_c \text{ratio} + 0.00676 \text{LL} + 0.0116 \text{PL} + 0.022 (\% \text{sand}) + 0.0182 (\% \text{silt})$ $\text{Log } k_2 = -0.887 + 0.0044 \omega_c + 0.00934 \gamma_s + 0.264 (\gamma_s / \gamma_{opt}) + 0.305 \omega_c \text{ratio} + 0.00877 \text{LL} + 0.00665 \text{PL} + 0.0116 (\% \text{sand}) + 0.00429 (\% \text{silt})$ $\text{Log } k_3 = -0.638 + 0.00252 \omega_c + 0.00207 \gamma_s + 0.61 (\gamma_s / \gamma_{opt}) + 0.152 \omega_c \text{ratio} + 0.00049 \text{LL} + 0.00416 \text{PL} + 0.00311 (\% \text{sand}) + 0.00143 (\% \text{silt}).$

(Continued)

References	Index Properties	Prediction Models
Yau and Von Quitus (2004)	$P_{3/8}$, P_4 , P_{40} , P_{200} , % Silt, % Clay, LL, PI, ω_{opt} , $\gamma_{d,opt}$, ω_s , γ_s , $\gamma_s/\gamma_{d,opt}$, $\omega_s/\omega_{d,opt}$, $(\gamma_{d,opt})^2/P_{40}$	<p><u>Crushed Stone Materials – LTPP Material Code 303</u></p> $M_R = [0.7632 + 0.0084(P_{3/8}) + 0.0088LL - 0.0371W_{opt} - 0.0001\gamma_{opt}] P_a^*$ $\left[\frac{\theta}{P_a} \right]^{2.2159 - 0.0016P_{3/8} + 0.0008LL - 0.038W_{opt} - 0.0006\gamma_{opt} + 2.4 \times 10^{-7} \left[\frac{\gamma_{opt}^2}{P_{40}} \right]}$ $\left[\frac{\tau_{oct}}{P_a} + 1 \right]^{-1.1720 - 0.0082LL - 0.0014W_{opt} + 0.0005\gamma_{opt}}$ <p><u>Crushed Gravel – LTPP Material Code 304</u></p> $M_R = \left[-0.8282 - 0.0065(P_{3/8}) + 0.0114LL + 0.0004PI - 0.0187W_{opt} + 0.0036W_s + 0.0013\gamma_s - 2.6 \times 10^{-6} \left(\frac{\gamma_{opt}^2}{P_{40}} \right) \right]$ $P_a \left[\frac{\theta}{P_a} \right]^{4.9555 - 0.0057LL - 0.0075PI - 0.0470W_s - 0.0022\gamma_{opt} + 2.8 \times 10^{-6} \left[\frac{\gamma_{opt}^2}{P_{40}} \right]} \left[\frac{\tau_{oct}}{P_a} + 1 \right]^{-3.514 + 0.0016\gamma_s}$ <p><u>Uncrushed Gravel – LTPP Material Code 302</u></p> $M_R = \left[-1.8961 + 0.0014(\gamma_s) - 0.1184 \left(\frac{W_s}{W_{opt}} \right) \right] P_a \left[\frac{\theta}{P_a} \right]^{0.8860 - 0.0074P_{200} - 0.0007\gamma_s + 1.4971 \left(\frac{\gamma_s}{\gamma_{opt}} \right) + 0.1399 \left(\frac{W_s}{W_{opt}} \right)}$ $\left[\frac{\tau_{oct}}{P_a} + 1 \right]^{-0.5979 + 0.0348W_{opt} + 0.0004\gamma_{opt} - 0.5166 \left(\frac{W_s}{W_{opt}} \right)}$ <p><u>Coarse-Grained Soil-Aggregate Mixture – LTPP Material Code 308</u></p> $M_R = \left[-0.5856 + 0.0130P_{3/8} - 0.0174P_4 + 0.0027P_{200} + 0.0149PI + 1.6 \times 10^{-4}(\gamma_{opt}) - 0.0426W_s + 1.6456 \left(\frac{\gamma_s}{\gamma_{opt}} \right) + 0.3932 \left(\frac{W_s}{W_{opt}} \right) - 8.2 \times 10^{-7} \left(\frac{\gamma_{opt}^2}{P_{40}} \right) \right] P_a^*$ $\left[\frac{\theta}{P_a} \right]^{0.7833 - 0.0060P_{200} - 0.0081PI + 0.0001\gamma_{opt} - 0.1481 \left(\frac{W_s}{W_{opt}} \right) - 2.7 \times 10^{-7} \left(\frac{\gamma_{opt}^2}{P_{40}} \right)} \left[\frac{\tau_{oct}}{P_a} + 1 \right]^{-0.1906 - 0.0026P_{200} + 8.1 \times 10^{-7} \left(\frac{\gamma_{opt}^2}{P_{40}} \right)}$
Titi et al. (2006)	ω , $\omega - \omega_{opt}$, γ_d , PI, P_{200} , γ_d/γ_{dmax} , ω/ω_{opt} , $\gamma_d/\gamma_{dmax} * \omega/\omega_{opt}$, P_{200}/ω , $\gamma_d/\gamma_{dmax} * (\omega - \omega_{opt})/\omega_{opt}$	<p><i>Coarse-grained soil:</i></p> $k_1 = 8642.873 + 132.643P_{No.200} - 428.067(\%Silt) - 254.685PI + 197.230\gamma_d - 381.400 \left(\frac{W}{W_{opt}} \right) \quad (R^2 = 0.83)$ $k_2 = 2.3250 - 0.00853P_{No.200} + 0.02579LL - 0.06224PI - 1.73380 \left(\frac{\gamma_d}{\gamma_{dmax}} \right) + 0.20911 \left(\frac{W}{W_{opt}} \right) \quad (R^2 = 0.58)$ $k_3 = -32.5449 + 0.7691P_{No.200} - 1.1370(\%Silt) + 31.5542 \left(\frac{\gamma_d}{\gamma_{dmax}} \right) - 0.4128(W - W_{opt}) \quad (R^2 = 0.82)$
Rahim (2005)	γ_d , ω_c , $P_{200}/\log C_u$	<p><i>Coarse-grained (sandy) soil:</i></p> $M_R = 324.14 \left(\frac{\gamma_d}{w_c + 1} \right)^{0.8998} \left(\frac{\#200}{\log C_u} \right)^{-0.4652}$ $R^2 = 0.75, (S_e/S_y = 0.163) \quad RMSE = 12.6$

(Continued)

References	Index Properties	Prediction Models
Malla & Joshi (2008)	MC, OMC, MC/OMC, DD, MAXDD, DD/MAXDD, LL, PI, CU, CC, S3, S2, S1_HALF, S1, S3_4, S1_2, S3_8, SN4, SN10, SN40, SN80, SN200, CSAND, FSAND, SILT, CLAY	<p><i>Coarse-grained samples with CU < 600</i></p> $\log k_1 = -0.64428 - 0.00773 \times MC - 0.62335 \times DDR + 0.02531 \times S3 - 0.01504 \times S1_HALF - 0.00694 \times SN200 + 0.00469 \times SILT + 0.00033564 \times CU - 0.00432 \times CC \quad (R^2 = 0.60; \text{Adj. } R^2 = 0.51),$ $k_2 = -0.74167 + 0.00804 \times MC + 0.00035328 \times DD + 0.00713 \times S1_HALF - 0.00401 \times SN40 + 0.00459 \times FSAND - 0.000156 \times CU + 0.00166 \times CC \quad (R^2 = 0.32; \text{Adj. } R^2 = 0.26),$ $k_3 = -0.90585 - 0.00186 \times MC + 0.00021603 \times MAXDD + 0.01777 \times S2 - 0.01830 \times S1 + 0.00528 \times SN10 - 0.00531 \times SN200 \quad (R^2 = 0.62; \text{Adj. } R^2 = 0.59).$ <p><i>Coarse-grained samples with CU < 20</i></p> $\log k_1 = 0.50635 - 0.00945 \times OMC - 0.70408 \times DDR - 0.00784 \times SN200 + 0.00716 \times SILT + 0.00775 \times CLAY - 0.00470 \times CU - 0.01280 \times CC \quad (R^2 = 0.53; \text{Adj. } R^2 = 0.46),$ $k_2 = 0.39366 + 0.00769 \times OMC + 0.00036161 \times DD - 0.00026109 \times MAXDD - 0.00352 \times SN40 + 0.00414 \times FSAND - 0.01338 \times CLAY + 0.01099 \times CU \quad (R^2 = 0.41; \text{Adj. } R^2 = 0.32),$ $k_3 = 1.06845 - 0.00356 \times MC - 0.57787 \times DDR - 0.01942 \times S3 + 0.01379 \times S1_HALF - 0.00073415 \times SN80 - 0.00359 \times CU \quad (R^2 = 0.44; \text{Adj. } R^2 = 0.37).$

Table 2.3. Important Properties for M_R Prediction (Yau and Von Quintus, 2002)

Independent Variable	Base/Subbase Material							Soils			
	303, Crushed Stone	304, Crushed Gravel	302, Uncrushed Gravel	306, Sand	308, Coarse-Grained Soil-Aggr. Mixture	307, Fine-Grained Soil-Aggr. Mixture	309, Fine-Grained Soil	Gravel	Sand	Silt	Clay
Percent passing 3/8-in sieve, $P_{3/8}$	✓	✓		✓	✓	✓		✓	✓		
Percent passing No. 4 sieve, P_4					✓	✓			✓		✓
Percent passing No. 40 sieve, P_{40}	✓	✓		✓	✓		✓				✓
Percent passing No. 200 sieve, P_{200}			✓		✓	✓			✓		✓
Percent Clay, %Clay								✓	✓	✓	✓
Percent Silt, %Silt									✓	✓	✓
Liquid Limit, LL	✓	✓		✓		✓		✓	✓		✓
Plasticity Index, PI		✓		✓	✓		✓	✓		✓	
Water content of test specimen, W_p		✓	✓		✓			✓	✓	✓	✓
Dry density of test specimen, γ_d		✓	✓		✓	✓			✓		✓
Optimum water content, W_{opt}	✓	✓	✓		✓	✓			✓		✓
Maximum dry unit weight, γ_{dmax}	✓	✓	✓	✓	✓	✓			✓		✓
Number of M_R Tests	109	49	81	66	187	32	92	122	509	108	512

1 in = 25.4 mm

Table 2.4. Commonly-used Soil Properties for Predicting M_R (George, 2004)

Model	Soil Texture	List of Variables	Selected Variables
LTTP	Coarse-grain	$P_{3/8}$, P_4 , %Clay, LL, w_{opt} , γ_s , %Silt, γ_{opt} , w_c , P_{200}	%Clay, LL, w_{opt} , %Silt, γ_{opt} , P_{200}
	Fine-grain	% Clay, PI, w_c , % Silt	% Clay, PI, w_c , % Silt
	Fine-grain clay	% Clay, w_c , P_4 , P_{40} , P_{200} , LL, w_{opt} , % Silt, LL, γ_{opt} , γ_s	% Clay, w_c , P_{40} , P_{200} , LL, w_{opt} , % Silt, LL,
Georgia	Coarse-grain	w_{opt} , w_c , COMP, %Silt, LL, PI, SW, SH, P_{40} , γ_s , S	w_c , %Silt, PI, S
Minnesota	Fine-grain	γ_s , w_c , PI, LL, P_{200} , S	γ_s , w_c , PI, LL, P_{200} , S
Carmichael	Coarse-grain	w_c , Soil Class	w_c ,
	Fine-grain	PI, w_c , P_{200} , Soil Class	PI, w_c , P_{200}
Drumm	Fine-grain	q_u , % Clay, PI, γ_s , S, w_c , P_{200} , LL	q_u , % Clay, PI, S, w_c , P_{200} , LL
Wyoming	Fine-grain	PI, S, P_{200}	PI, S, P_{200}
Mississippi	Coarse-grain	w_c , γ_d , P_{200} , C_u	w_c , γ_d , P_{200}
	Fine-grain	LL, w_c , γ_d , γ_{opt} , P_{200}	LL, w_c , γ_d , γ_{opt} , P_{200}

2.4 Summary

In this chapter, several findings from various research studies on factors affecting unbound aggregate behavior, existing M_R predictive models, and successful applications of marginally low quality local aggregate sources were reviewed. Major factors influencing strength and resilient and permanent deformation responses were identified as the stress states and material properties. Corresponding resilient modulus predictive models/equations established from those major factors were reviewed as examples. In light of the shortage of high quality aggregates in many areas, the historical applications of local aggregate sources were documented. It is concluded that in spite of being classified as “out-of-specification,” certain local aggregate sources are still promising for use in road construction to achieve cost-effectiveness and promote sustainability, provided that proper guidelines are followed with care.

Chapter 3 Establishment of Aggregate Index Properties

3.1 Introduction

This chapter presents the establishment of general distribution and availability of local aggregate sources in Minnesota suitable for use in road construction, as well as aggregate index properties. Such information serves as the basis for the remaining sections of this report. The Aggregate Source Information System (ASIS) is a database developed by MnDOT's Office of Materials and Road Research to store and retrieve information on gravel pits, rock quarries and commercial aggregate sources. It is used primarily by MnDOT's Aggregate Unit at the Maplewood Lab and District Materials personnel as a data resource for recommending aggregate sources for construction projects. In addition, there is another aggregate index property database which presents individual aggregate test results in electronic data tables to be linked to quarry/pit locations. On the basis of such existing databases, the types, sources and properties of locally available aggregates in Minnesota were categorized with typical costs obtained accordingly. The aggregate index property database was obtained from MnDOT Office of Materials and Road Research with approximate aggregate pricing and estimated cost information.

3.2 Brief Description of ASIS Database

Since its development by the Office of Materials in Maplewood, Minnesota in 1985, ASIS database has been managed by the Grading, Base, & Aggregate Unit and used to store and retrieve information on gravel pits and rock quarries either owned or leased by MnDOT. Recently, an online web-based interactive map interface has been made available for a geographical representation of the gravel pit and rock quarry data stored in ASIS (<http://www.dot.state.mn.us/materials/asismap.html>). Included in this database is prospective sampling on aggregate used by engineers to recommend sources for future projects. One of the primary advantages of the ASIS database is that it, once integrated with Geographical Information System (GIS) techniques, allows the identification and further analyses of aggregate source quality (in terms of physical, chemical, and mechanical properties, etc.) based on geographical locations and then facilitate the establishment of linkages between aggregate source quality and pavement in-service performance.

In ASIS database, each aggregate source is assigned a unique source number with which other information including status classification, material class and quantity, aggregate source properties, and UTM coordinates, etc. is associated. Table 3.1 lists as examples part of the aggregate source properties stored in ASIS database; whereas a snapshot of the Excel spreadsheet retrieved from ASIS database is shown in Figure 3.1. From 2002 to 2007, series of laboratory tests were conducted on local aggregate sources to determine strength, modulus and deformation properties with all the test results included in the Laboratory Information Management System (LIMS) database as well as an additional strength and modulus database created to store all the testing undertaken by MnDOT. The ASIS, LIMS and the strength and modulus databases are the main digital databases collected for use in this research study.

The material properties in standard tests for selection purposes were recorded and archived in the ASIS database. Those tests performed on aggregate materials can be divided into engineering and mineralogical tests. The former includes particle size distribution, plasticity, particle hardness, shear strength (or structural capacity), compaction characteristics, whereas the latter includes mineralogical tests.

Table 3.1. Illustrative Examples of Aggregate Source Properties Stored in ASIS Database

Field Name	Description
PASS3QTR	Percent passing 3/4" sieve
PASSNUM4	Percent passing # 4 U.S. sieve
PASSNUM10	Percent passing # 10 U.S. sieve
PASSNUM40	Percent passing # 40 U.S. sieve
PASSNUM200	Percent passing # 200 U.S. sieve
SH4LO	Lowest value for % shale @ minus 4 mesh
SH4HI	Highest value for % shale @ minus 4 mesh
MINUS4AVG	Average value for % shale @ minus 4 mesh
MINUS4OF	Number of shale @ minus 4 mesh samples
MS3_2TO1	Magnesium Sulfate (Soundness), Size range 1-1/2" to 1"
LARLO	Lowest Los Angles Rattler value
LARHI	Highest Los Angles Rattler value
LARAVG	Average Los Angles Rattler value
LAROF	Number of Los Angles Rattler tests
PCTLIMESTO	Percent limestone
PCTSANDSTO	Percent sandstone
PCTSOFTROC	Percent soft rock
PCTHARDROC	Percent hard rock
TOTALSHALE	Percent total shale by mass
TOTALSPALL	Percent total spall by mass
UCHERT	Percentage of unsound chert
UCHERTOF	Number of unsound chert tests
IOXIDE	Percent iron oxide
IOXIDEOF	Number of iron oxide tests

	A	B	C	D	E	F	G	H	I
1	 All Aggregate Sources - Aggregate Source								
2	Source	SAM_ID	Status	Status2	County	Section	Township	Range	Rd
56	04054		O		Beltrami	32	156	38	W
57	04055		P		Beltrami	23	155	36	W
58	04056		P		Beltrami	23	155	36	W
59	04057		O		Beltrami	15	147	33	W
60	04058		O		Beltrami	24	151	30	W
61	04059		O		Beltrami	09	148	34	W

Figure 3.1. A Snapshot of the ASIS Excel Spreadsheet

3.3 Locations of Locally Available Aggregate Sources in Minnesota

As shown in Figure 3.2, 87 prospect pits with most reliable gradation data that are located across Minnesota were selected from those two databases to demonstrate the methodology to be presented in this report. An ArcGIS® based database management system (DBMS) was developed for storing, searching, retrieving, and displaying aggregate index properties. Figure 3.3 shows the interfaces for searching, retrieving and graphically displaying features of interest.

3.4 Compiled Aggregate Cost Information on Local Materials

Cost information items are included as fields in the ASIS database. Table 3.2 summarizes those aggregate material cost-related fields. For the selected 87 prospect pits, part of them has no cost information recorded. Under such circumstances, the missing cost information was estimated as the average of costs of closest aggregate pits by counties. Figure 3.4 illustrates those aggregate pits with aggregate classes and typical costs reported that were used for estimating unknown costs.

3.5 Summary

In this chapter, the general distribution and availability of local aggregate sources in Minnesota suitable for use in road construction was discussed and the associated aggregate index properties collected for this study were highlighted. The Aggregate Source Information System (ASIS) database, developed by MnDOT's Office of Materials and Road Research to store and retrieve information on gravel pits, rock quarries and commercial aggregate sources, and another aggregate index property database were utilized together to establish 87 prospect pits with aggregate properties collected to demonstrate the current research approach. On the basis of such existing databases, the types, sources and properties of locally available aggregates in Minnesota were categorized with typical costs obtained accordingly.

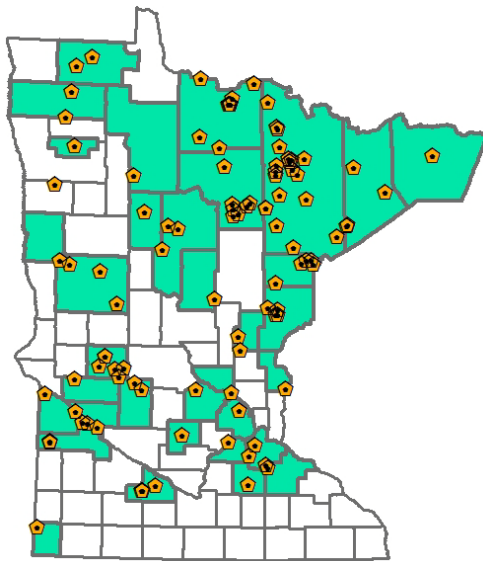
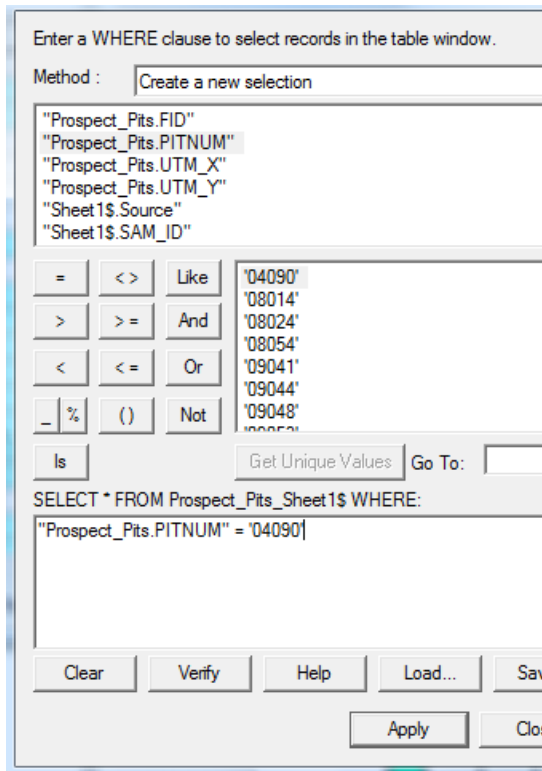
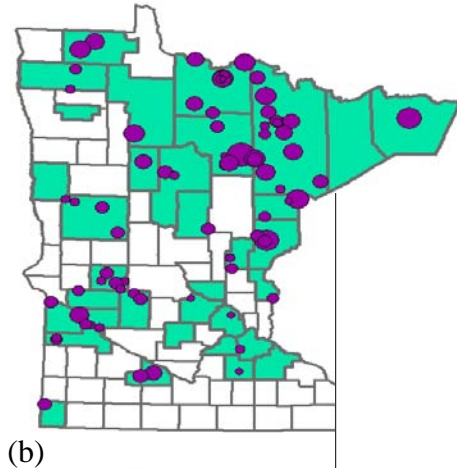


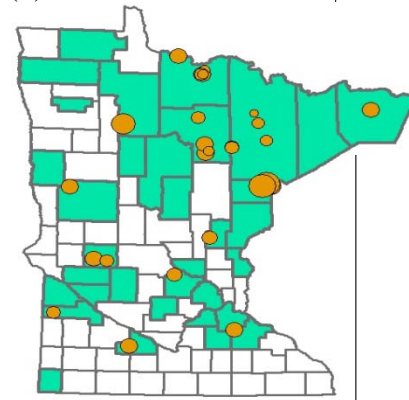
Figure 3.2. Geographical Locations of 87 Prospect Pits Selected for this Study



(a)



(b)



(c)

Figure 3.3. ArcGIS Based Database Management Interfaces for (a) Searching and Graphically Displaying (b) % Passing No.200 Sieve and (c) Material Cost Features

Table 3.2. Aggregate Cost Information Recorded in the ASIS Database

Field Name	Description
MCLASS1	Primary MnDOT material class
QUAN1	An estimate of quantity of primary material
COSTCYM1	Royalty rate (US dollars): cubic yards, loose volume (Vehicle Measure)
YRPRICECL1	Year cost for primary material updated
MCLASS2	Secondary MnDOT material class
QUAN2	An estimate of quantity of secondary material
COSTCYM2	Royalty rate (US dollars): cubic yards, loose volume (Vehicle Measure)
YRPRICECL2	Year cost for secondary material updated
MCLASS3	Third MnDOT material class
QUAN3	An estimate of quantity of third material
COSTCYM3	Royalty rate (US dollars): cubic yards, loose volume (Vehicle Measure)
YRPRICECL3	Year cost for third material updated

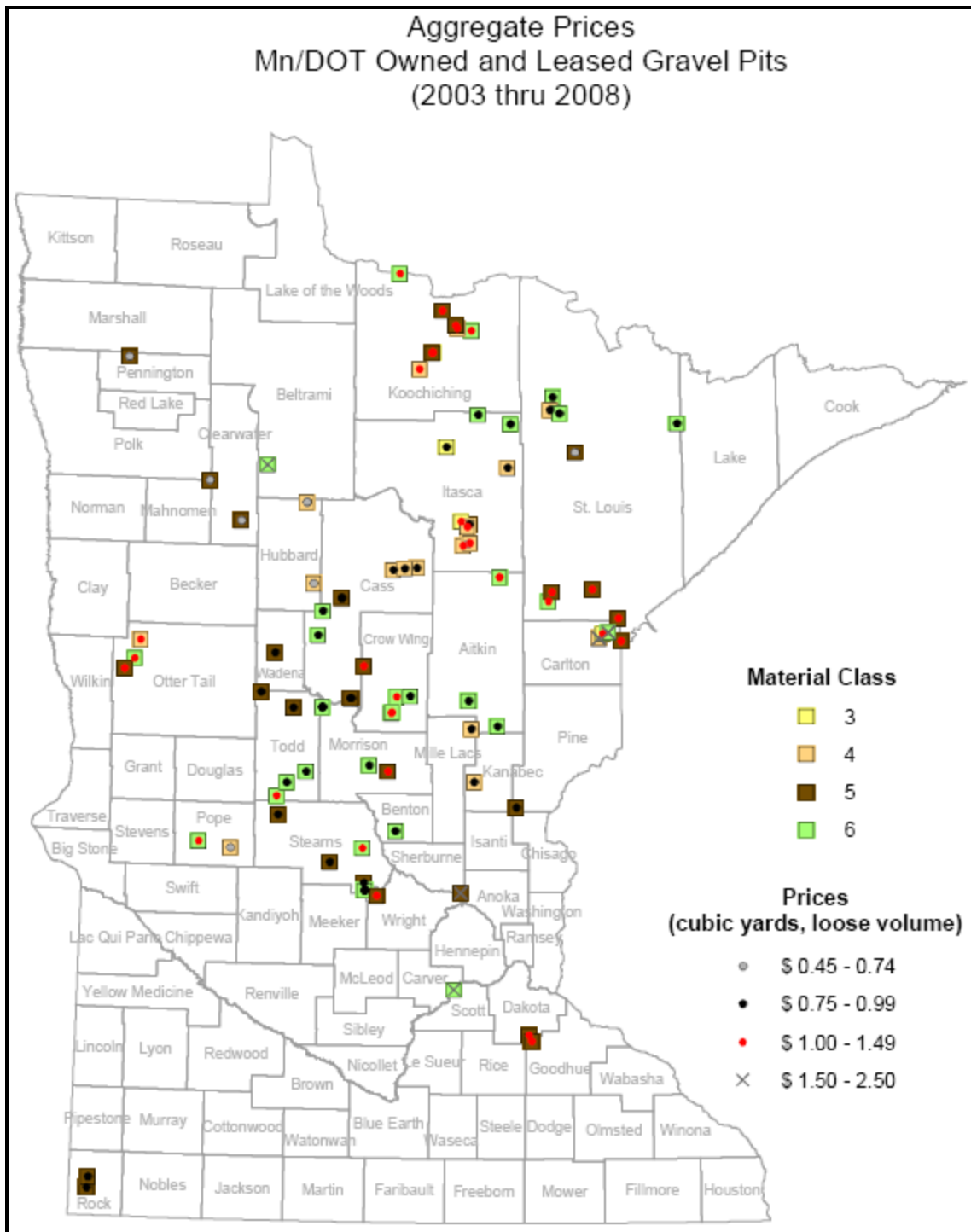


Figure 3.4. Typical Aggregate Costs Obtained from MnDOT

Chapter 4 Collection of Aggregate Strength and Modulus Data

4.1 Introduction

The Chapter presents all the databases from which mechanistic pavement analysis and design inputs as the strength and M_R data, along with corresponding aggregate index properties, were collected for unbound aggregate pavement base and subbase applications. The primary data source for this study is the existing laboratory and/or in situ test data for Minnesota's aggregates that were obtained from related research studies performed for/by MnDOT. Existing laboratory and in situ test data were also obtained for Minnesota aggregates from the LRBB Investigation 828 report, Davich et al. (2004) study, Kim and Labuz (2007) report and other related research studies performed for/by MnDOT. In addition, as part of a comprehensive literature search, strength and resilient modulus (M_R) data were also collected from other relevant research studies completed by the Principal Investigator (PI) for over a decade at the University of Illinois. The following sections of this Chapter are dedicated to the description and preliminary data analyses of the MnDOT aggregate databases; whereas the University of Illinois databases compiled are described in Appendix A for brevity purpose.

4.2 Description of MnDOT Aggregate Databases

4.2.1 Aggregate Resilient Modulus Database

4.2.1.1 Materials Tested

In the present study, the results of a variety of aggregate index property and resilient modulus tests conducted by the MnDOT Office of Materials and/or its contracting agencies on different Minnesota project materials were collected and evaluated. Two resultant databases, one for the MEPDG M_R constitutive model parameters k_1 , k_2 and k_3 and the other one for corresponding aggregate source properties, were created and used in the subsequent statistical correlation studies. Each of these two databases contains a total of 376 effective aggregate specimens after eliminating samples with incomplete information such as missing gradation or index properties. The majority of the tested materials are "standard" or traditional unbound aggregate base and subbase materials of Classes ranging from 3, 4, 5 to 6 according to the MnDOT classification, and no reclaimed/salvaged materials were included in the resilient modulus database provided by MnDOT due to the scope of this study.

4.2.1.2 Experimental Program

Resilient modulus test data includes the following load-time history information recorded for each load sequence: confining pressures, deviator stresses, and resilient strain and resilient deformation values. The laboratory M_R tests were conducted according to the NCHRP 1-28A protocol (Dai and Zollars, 2002). The load sequences start with 1,000 cycles of 207 kPa (30 psi) deviator stress at 103.5 kPa (15 psi) confining pressure for conditioning the specimen before M_R data collection and continue with cycles repeated 100 times for 30 loading sequences with different combinations of confining pressures and deviator stresses. The M_R is then calculated from recoverable axial strain and cyclic axial stress values from the last five cycles of each sequence. The moisture content of the specimens was within $\pm 0.5\%$ from the target moisture content. The vibratory hammer or gyratory compactor was used for compacting specimens to the

target dry densities. Not all the tests were carried out at the optimum moisture content. Detailed information about laboratory measured aggregate index properties includes AASHTO classification, MnDOT classification, material type, optimum moisture content, maximum dry density, actual sample moisture content, actual sample density, compaction method, gradation (i.e., percentages of materials passing specified sieves), silt content, clay content, liquid limit, plastic limit, and plasticity index.

Considering the well-recognized significant effects that coarse aggregate morphology, i.e., flat and elongation ratio, angularity, and surface texture, have on the strength and resilient and permanent strain behavior of unbound aggregate materials (Pan et al., 2005; Pan et al. 2006a-b; Tutumluer and Pan, 2008), twelve representative MnDOT aggregate resilient modulus (M_R) test samples were shipped to the University of Illinois Advanced Transportation Research and Engineering Laboratory (ATREL) for imaging based shape analysis using the University of Illinois Aggregate Image Analyzer (UIAIA). Identified and recommended by the NCHRP 4-30A project among the most promising aggregate imaging systems to provide an automated means to determine coarse aggregate size and shape properties, the UIAIA system can take images of an individual aggregate particle from three orthogonal views, which has been very effective in reconstructing three-dimensional (3-D) particle shape and computing accurately the volume and size and shape indices (Tutumluer et al., 2000; Rao, 2001).

Figure 4.1 shows all the twelve aggregate samples received, and Table 4.1 gives a listing and description of each. The summary of the image analysis results are given in Table 4.2. Note that the UIAIA could not scan and process the very fine-graded TH 47 SGB material and the dark colored TH 52 Taconite Tailings material, nor are very dark particles and particles smaller than #10 sieve size (2 mm). Some of these difficulties in imaging will be overcome in a new enhanced version of the UIAIA device that is currently being developed at the University of Illinois to feature an interchangeable background for correctly scanning both light and dark colored aggregates.

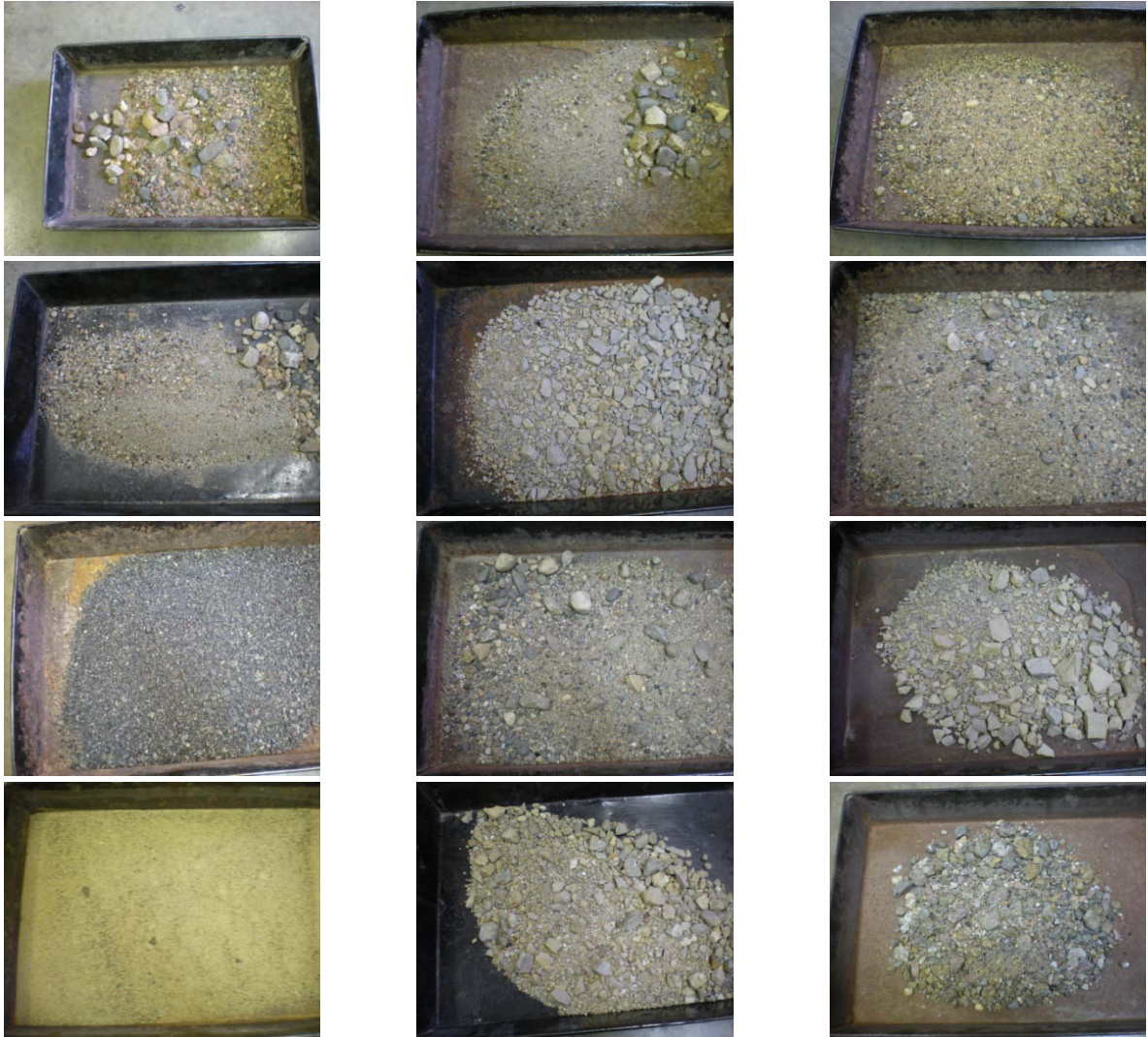


Figure 4.1. 12 MnDOT Aggregate Samples Received at the University of Illinois ATREL

Table 4.1. Description of M_R Samples Used for UIAIA Image Analyses

Label on Sample Bag	Soil Lab #	Number of data files from M _R Testing
TH 14/15 CL 5	CO-GS04-0034 CO-GS04-0035	17
CO RD 14 CL 5	CO-GS04-0130 CO-GS03-0142 CO-GS04-0131	9
TH 23 CL 6m	CO-GS05-0003	9
TH 371 CL 6	CO-GS04-0010 CO-GS03-0129 CO-GS03-0135	7
Olmsted CL 5	CO-GS02-0380 CO-GS02-0363 CO-GS02-0347 CO-GS020350	15
TH 16 CL 6	CO-GS03-0096 CO-GS03-0097 CO-GS04-0144	13
Olmsted CL 5 M	CO-GS04-0015 CO-GS02-0061 CO-GS02-0064	20
TH 52 SG	CO-GS04-0019 CO-GS04-0020 CO-GS03-0251	25
TH 23 CL 6 Granite waste	CO-GS05-0007	13

Table 4.2. Analysis Results of 9 MnDOT M_R Samples Processed Using UIAIA

Aggregate Sample	Average Values		
	F&E Ratio	Angularity Index (AI)	Surface Texture (ST)
TH14/15 CL5	2.7	307	0.9
CO RD14 CL5	2.0	344	1.0
TH23 CL6m	3.7	380	1.0
TH371 CL6	10.6	464	0.8
Olmsted CL5	2.1	414	1.6
TH16 CL6	1.8	453	1.5
Olmsted CL5M	2.0	431	1.6
TH23 CL6 Granite Waste	4.9	499	0.6
TH52 SG	7.4	400	0.8

4.2.2 Additional Aggregate Strength Database

4.2.2.1 Materials Tested

Additional aggregate strength spreadsheet files were received from MnDOT in January 2011 for conducting Task 4 analyses to validate the MnPAVE sensitivity analysis results. The first step of the analysis approach was to establish a database containing all the data elements to be analyzed. After examining both the previous and recently received aggregate strength data, a total of 266 datasets of peak deviator stress at failure (σ_{df}) were retrieved and matched with the corresponding resilient modulus data for base/subbase materials of different MnDOT Classes. The summary information of those aggregate samples is given in Table 4.3. It is worth mentioning that out of the 266 datasets only 35 did not have any gradation data while the rest had both M_R and gradation data. The shear strength test specimens were tested to failure at the last stage of M_R testing under constant confining pressures of 4 psi, 5 psi, 8 psi, or 10 psi.

Table 4.3. Details of the Aggregate Strength Data Compiled

Item	Description
Material type	Taconite Tailings, Gravel, Limestone, Granite, Reclaimed Concrete, RAP, and Soil
MnDOT Specification	Class 7 (B/C), Class 6 (special), Class 5 (special), Class 3, Class 4, FDR, Select Granular
Shear Strength Sample Type	Post M_R
Confining Pressure (psi)	4, 5, 8, or 10
Nominal Maximum Particle Size (NMPS) in mm	50, 37.5, 31.5, 25, 19, 16, 9.5, 4.75, 2.36, 2.0, 0.6, 0.425, and 0.3

Although the original resilient modulus (M_R) database provided by MnDOT did not include any reclaimed/salvaged materials, the additional shear strength database had the following materials included, i.e., “non-standard” taconite tailings (a waste mining material), reclaimed asphalt pavement (RAP) and reclaimed concrete aggregates (RCA) blended with virgin aggregates at different blending ratios, and materials recovered from full-depth reclamation (FDR) sites. All the materials were collected from road construction sites in Minnesota for testing at the MnDOT Office of Materials and Road Research laboratories and/or MnDOT’s contracting agencies/universities using consistent quality control procedures.

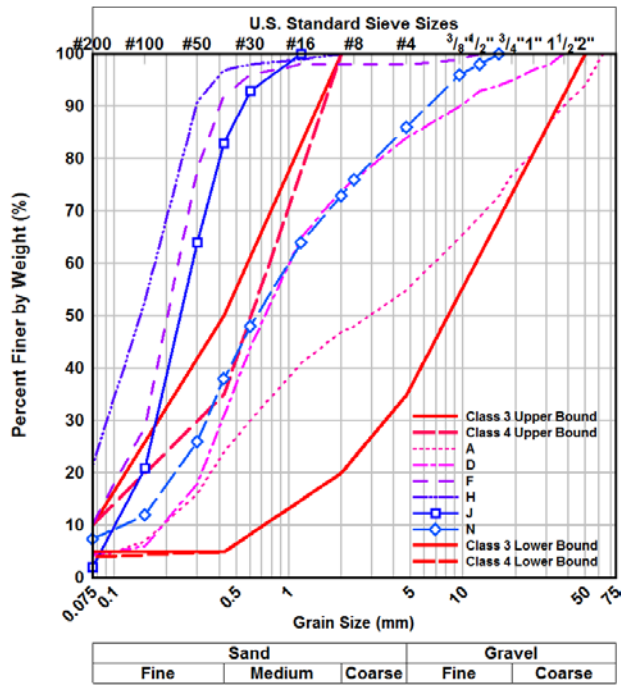
For those aggregate samples with modulus and strength data matched, Figures 4.2 and 4.3 present their grain size distributions in relation to current MnDOT specified gradation bands. Grouping them according to their rock type and mineralogy is to minimize the confounding effects that aggregate shape properties (form, texture and angularity), which have been demonstrated to be quite influential, have on analyses of gradation. It appears that quarried limestone and granite materials have much less variability in gradation than the others. Table 4.4 summarizes other sample details at optimum moisture conditions sorted from the database for subsequent correlation analyses, such as MnDOT specification designations and Nominal Maximum Particle Size (NMPS).

4.2.2.2 Experimental Program

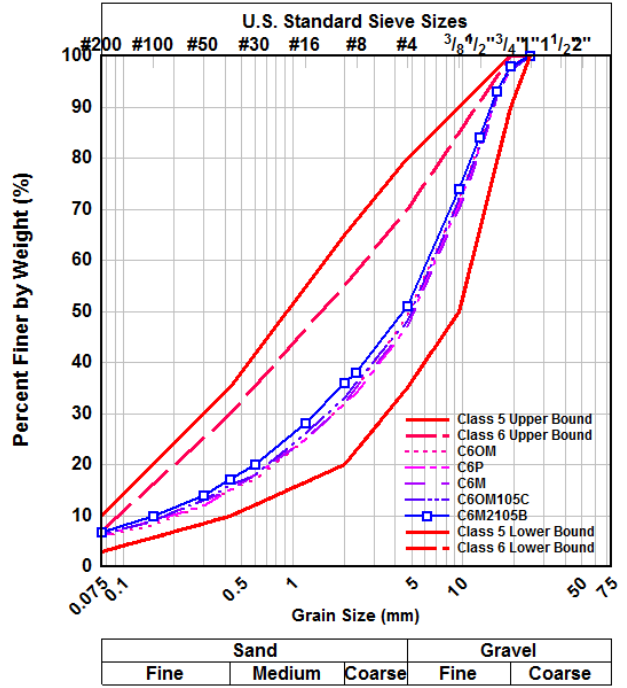
Proctor compaction tests were performed on the aggregate materials following the AASHTO T99 standard energy with index properties and optimum moisture contents and

maximum dry densities determined accordingly. Resilient modulus (M_R) tests were conducted on compacted specimens following the NCHRP 1-28A protocol. After completion of M_R tests, specimens were typically loaded to failure at constant confining pressures (σ_3) ranging from 4 to 10 psi (see Table 4.4) using a constant loading rate of 0.03 in./s (0.76 mm/s) to obtain the peak deviator stress (σ_{df}) values. Note that such shear strength tests performed after the completion of the repeated-load resilient modulus sequences were conditioned and thus included the effect of stress history as compared to unconditioned ones. The resilient modulus results of this database are analyzed in Chapter 5 to establish correlations between aggregate source properties and the MEPDG M_R constitutive model parameters for use in pavement design applications; whereas the shear strength results are analyzed in Chapter 7 to provide much more definite evaluation of base/subbase material quality and performance potential as compared to M_R .

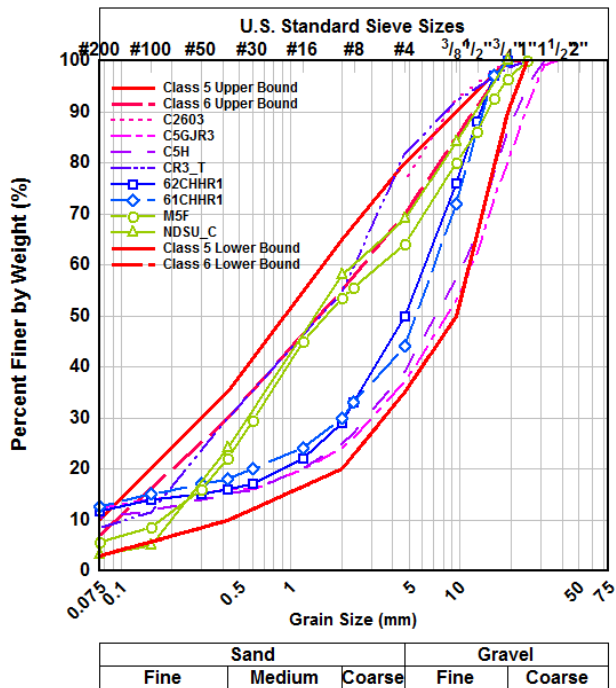
Considering the fact that permanent deformations were not recorded from the conditioning stages of M_R tests and saved in the database, the permanent deformation trends linked to field rutting performances were then indirectly evaluated for these aggregate materials from the peak deviator stresses at failure (σ_{df}) measured at a given confining pressure. The σ_{df} data described herein are therefore used subsequently as an indicator of the aggregate material's shear strength. Tutumluer and Pan (2008) observed good correlations between maximum σ_d at failure (at $\sigma_3=34.5$ kPa/5 psi) and permanent strains at the 10,000th load repetition for twenty-one unbound aggregate blends in a study of aggregate shape effects. Although the Mohr-Coulomb shear strength parameters, cohesion "c" and friction angle " ϕ ," could be determined for some of the samples, to be consistent, they are not explicitly used in the subsequent analyses.



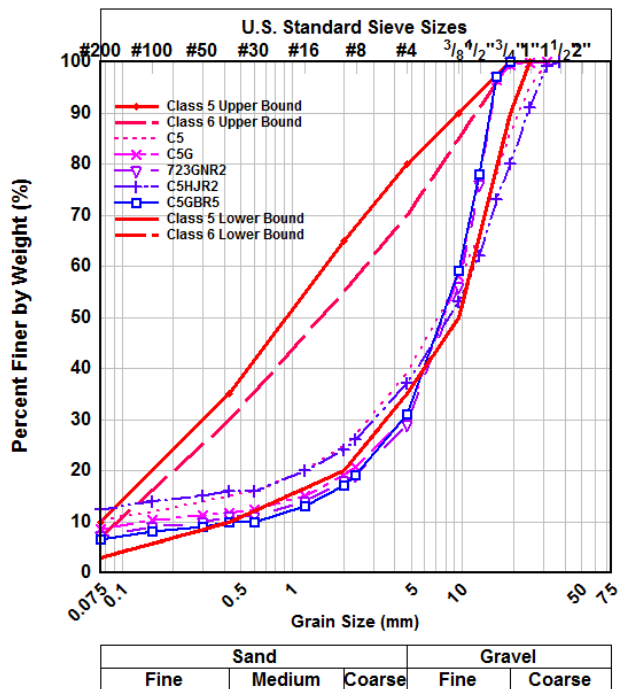
Select Granular



Granite

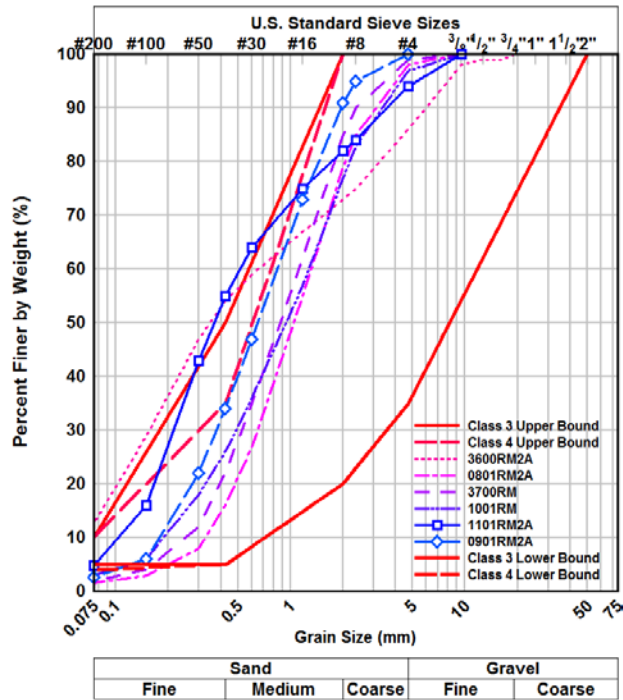


Gravel

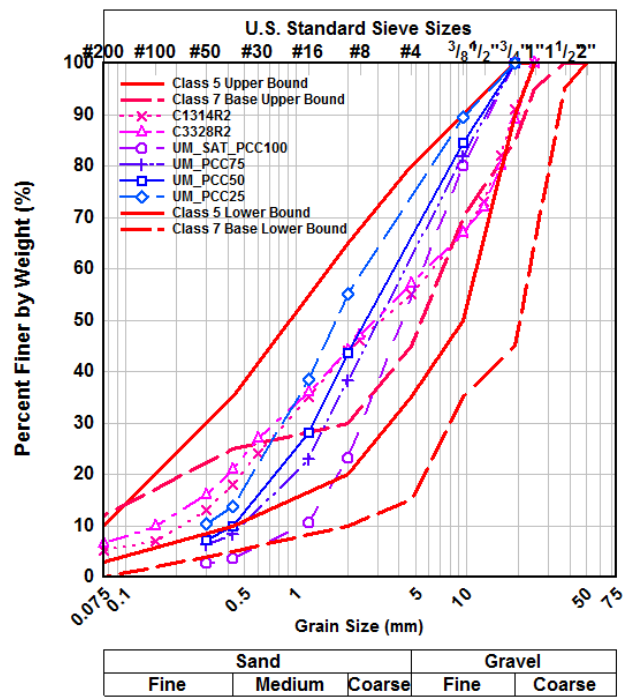


Limestone

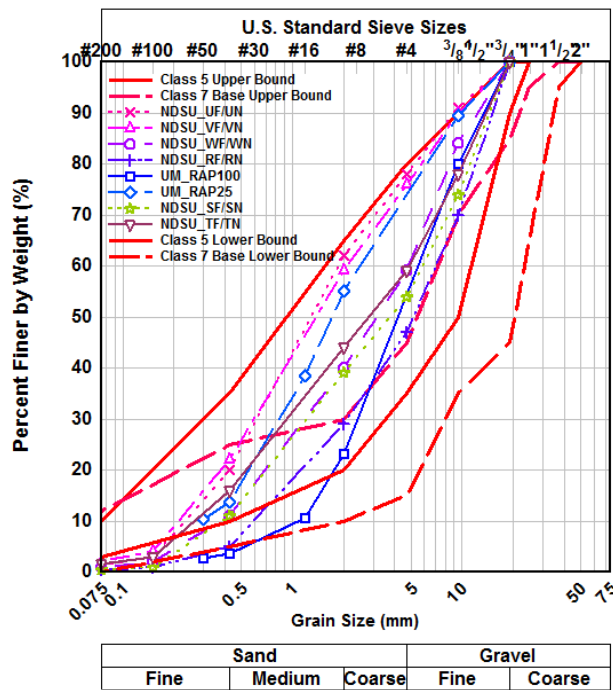
Figure 4.2. Gradations of Traditional Base/Subbase Materials in MnDOT Database: (a) Select Granular; (b) Granite; (c) Pit-run Gravel; and (d) Limestone



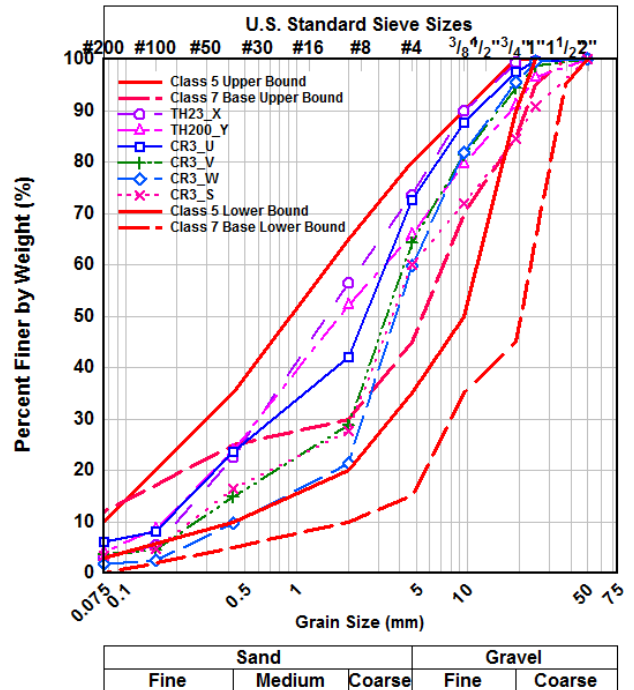
Taconite Tailings



Reclaimed Concrete (Class 7C)



Reclaimed Bituminous (Class 7B)



Full-depth Reclamation (FDR)

Figure 4.3. Gradations of Non-traditional Waste Base/Subbase Materials in MnDOT Database: (a) Taconite Tailings; (b) Reclaimed Concrete (Class 7C); (c) Reclaimed Bituminous (Class 7B); and (d) Full-depth Reclamation (FDR)

Table 4.4. Details of the Aggregate Materials Compiled in the MnDOT Strength Database

Material Type		MnDOT Specification	σ_3 for σ_{df} (psi)	NMPS (mm)	Major Gradation Type
“Standard”	Select Granular	Class 3/4	4, 8	0.425, 0.6, 9.5, 37.5	Fine-graded
	Granite	Class 6	4	16	Coarse-graded
	Gravel	Class 5	4, 5, 8, 10	9.5, 16, 19, 25, 31.5	Both
	Limestone	Class 5	4	16, 25, 31.5	Coarse-graded
“Non-standard”	Taconite Tailings	Class 3/4	4	2, 4.75, 9.5	Fine-graded
	Reclaimed Bituminous	Class 7B	4, 5, 8, 10	9.5, 19	Fine-graded
	Reclaimed Concrete	Class 7C	5, 10	19	Fine-graded
	FDR	Class 7	5, 10	19, 25	Fine-graded

Note: (1) No crushed/fractured particles are allowed for Class 3/4; (2) Class 5 requires at least 10% crushed particles; (3) Class 6 requires at least 15% crushed particles; (4) σ_3 and σ_{df} denote confining pressure and peak deviator stress at failure, respectively; and (5) 1 psi = 6.89 kPa, 1 in. = 25.4 mm.

4.3 Preliminary Analyses of Aggregate Source Properties Affecting Modulus and Strength Behavior

Resilient behavior and shear strength properties of aggregate base/granular subbase materials are affected by many factors, such as achieved density and moisture content. An attempt was made in this section to explain how M_R and shear resistance are distinctly affected by various aggregate source properties. To that end, parallel coordinate charts for the tested/analyzed aggregate materials of different MnDOT aggregate classes were prepared to simultaneously examine the effects of the various factors on both M_R and shear resistance.

To characterize the gradation, the primary control sieve (PCS), one of the core concepts in the Bailey asphalt mix design method, was used to define the separation between fine and coarse aggregate in the base/subbase materials. Then, the power law model proposed by Ruth et al. (2002) was followed to fit the gradation curves of both the coarse and fine aggregate portions. The power law equations used in this study are as follows:

$$\begin{aligned}
 P_{ca} &= a_{ca} (d)^{n_{ca}} \\
 P_{fa} &= a_{fa} (d)^{n_{fa}}
 \end{aligned}
 \tag{2.1}$$

where: P_{ca} or P_{fa} is the percent of material by weight passing a given sieve with opening size d ; a_{ca} and a_{fa} are the constants (intercepts) for the coarse and fine aggregate portions, respectively; n_{ca} and n_{fa} are the slopes (exponents) for the coarse and fine aggregate portions, respectively; d is the given sieve opening size in mm.

It was found that the intercept and the exponent (slope) in the power law model are correlated with each other for both fine and coarse aggregate portions. Hence, instead of using four parameters, only two independent parameters, n_{ca} and n_{fa} , are used to characterize the

gradation curves of the coarse and fine aggregate portions, respectively, which are separated by the primary control sieve (PCS) according to the Bailey method.

As shown in Figures 4.4 through 4.8, the achieved dry densities generally decrease for lower peak deviator stresses at failure indicating that shear resistance is more related to the achieved dry density of an aggregate sample when compared to other factors. As the peak deviator stress at failure keeps decreasing, the relative moisture content (achieved moisture content divided by optimum moisture content) also exhibits a somewhat increasing trend; however, resilient modulus fluctuates and shows no consistent trend. Small variations in relative moisture content seem to have more influence on M_R , albeit related to suction potential governed by aggregate matrix, as indicated by an inverse relationship.

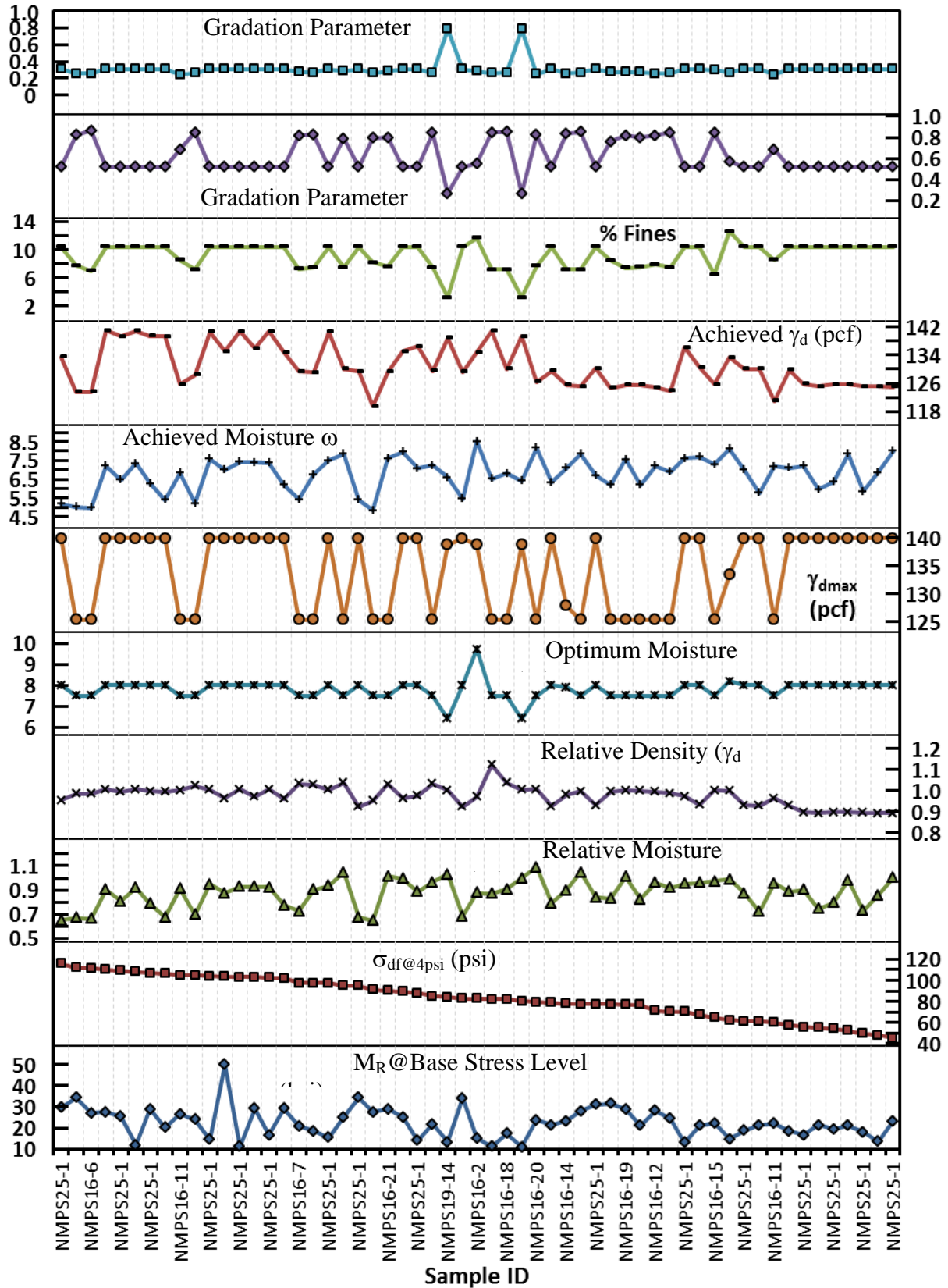


Figure 4.4. Factors Affecting Resilient Modulus and Peak Deviator Stress Results – Class 5

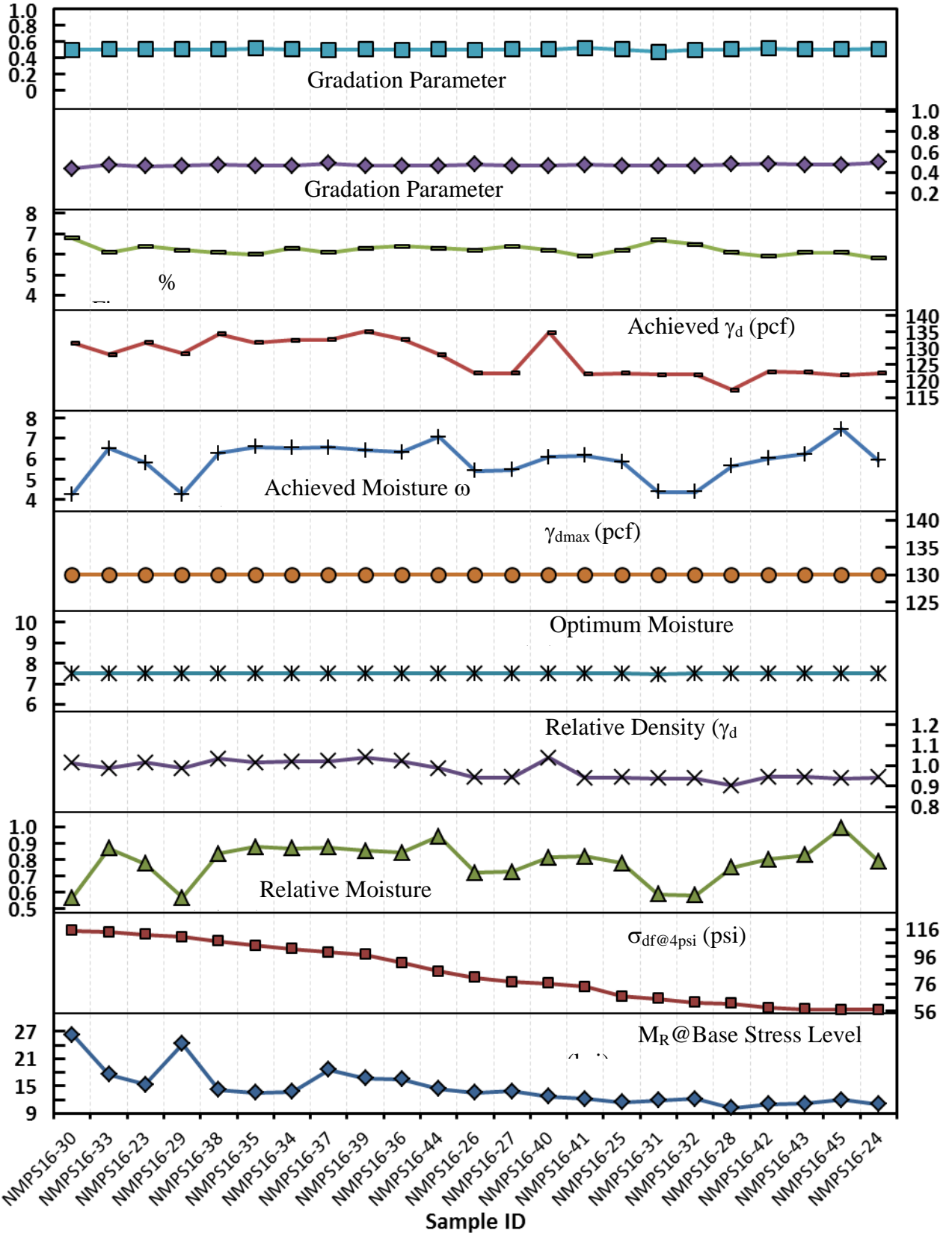


Figure 4.5. Factors Affecting Resilient Modulus and Peak Deviator Stress Results – Class 6

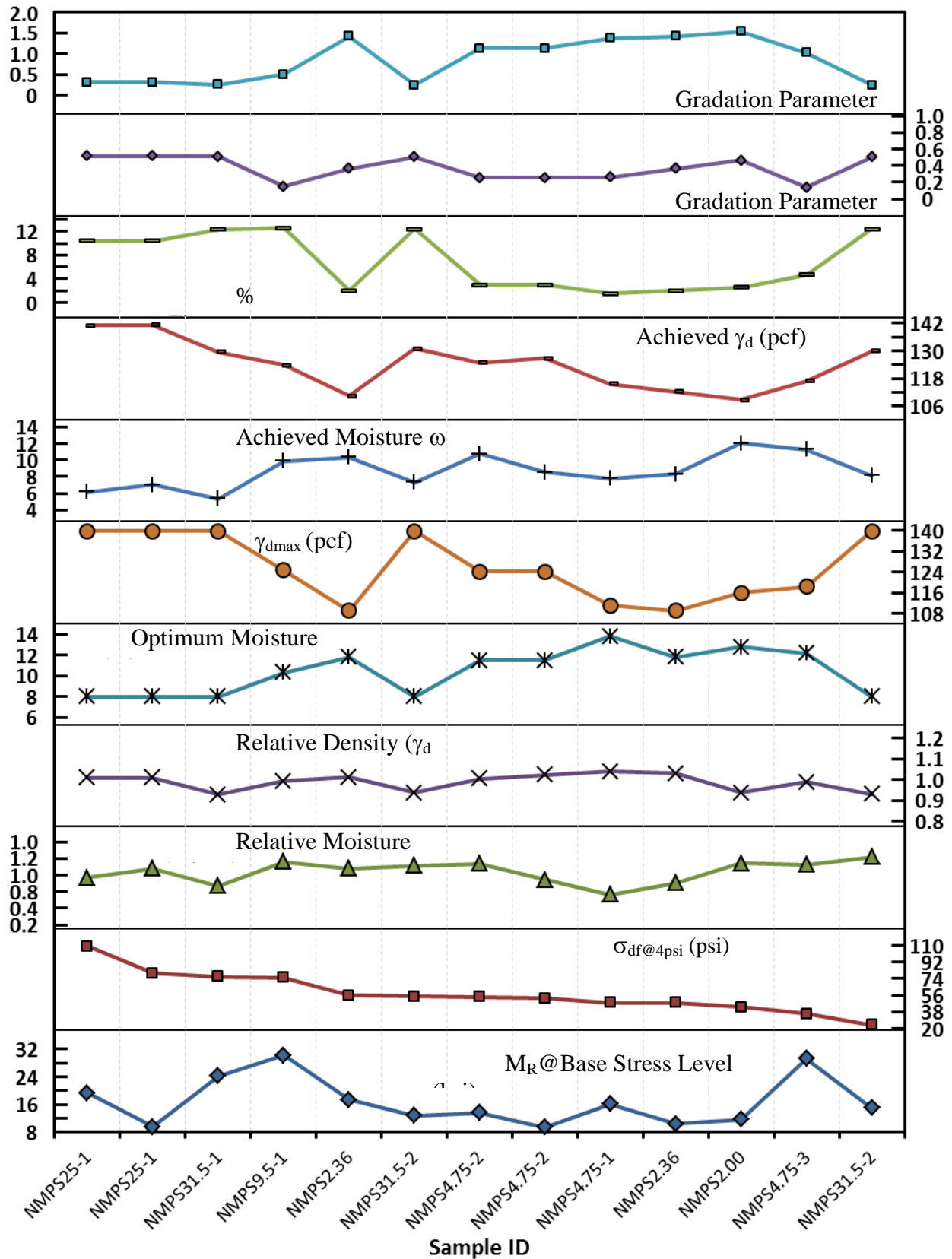


Figure 4.6. Factors Affecting Resilient Modulus and Peak Deviator Stress Results, Class 3/4

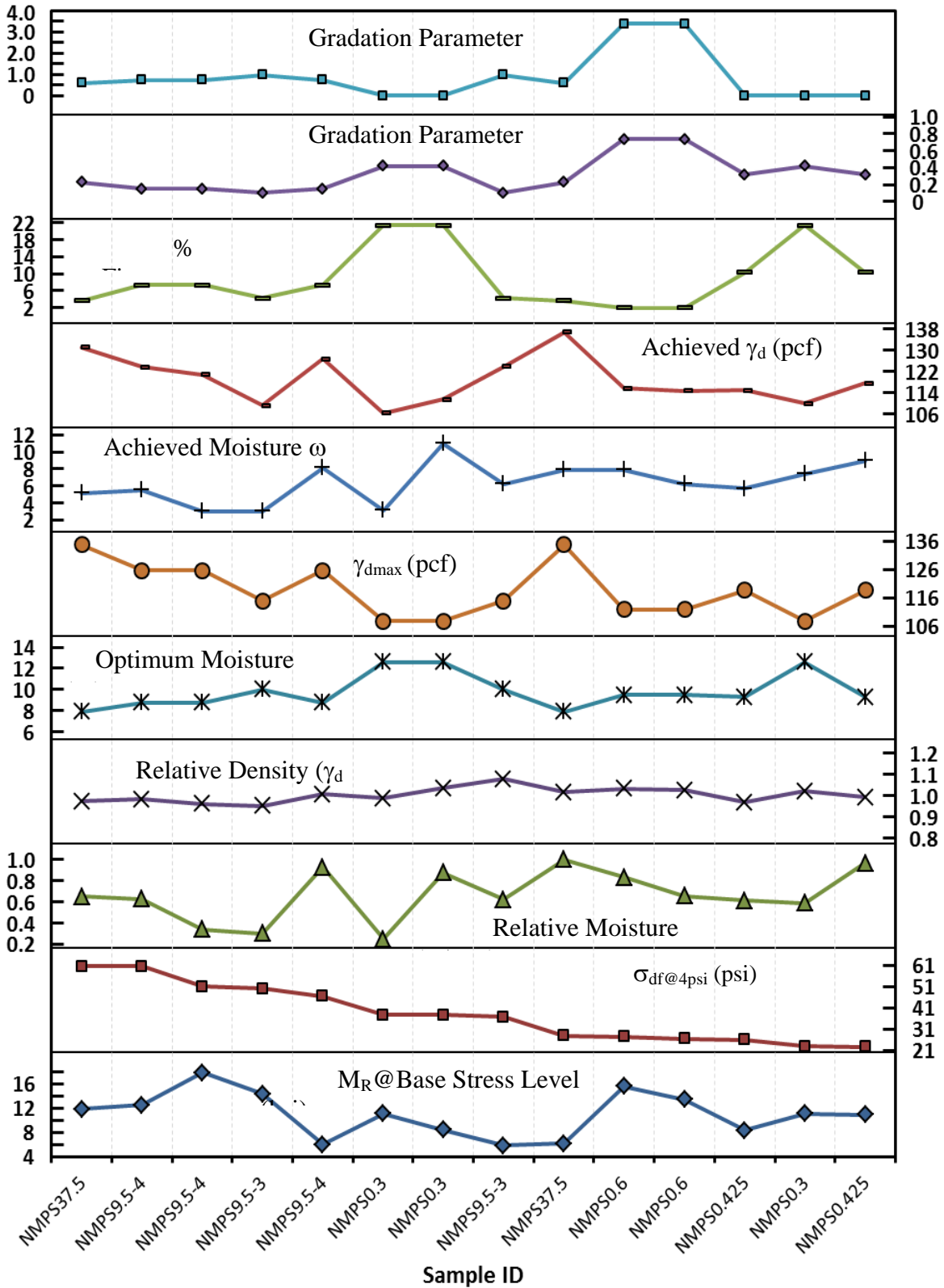


Figure 4.7. Factors Affecting Resilient Modulus and Peak Deviator Stress Results – Select Granular (4-psi Confining Pressure for σ_{df})

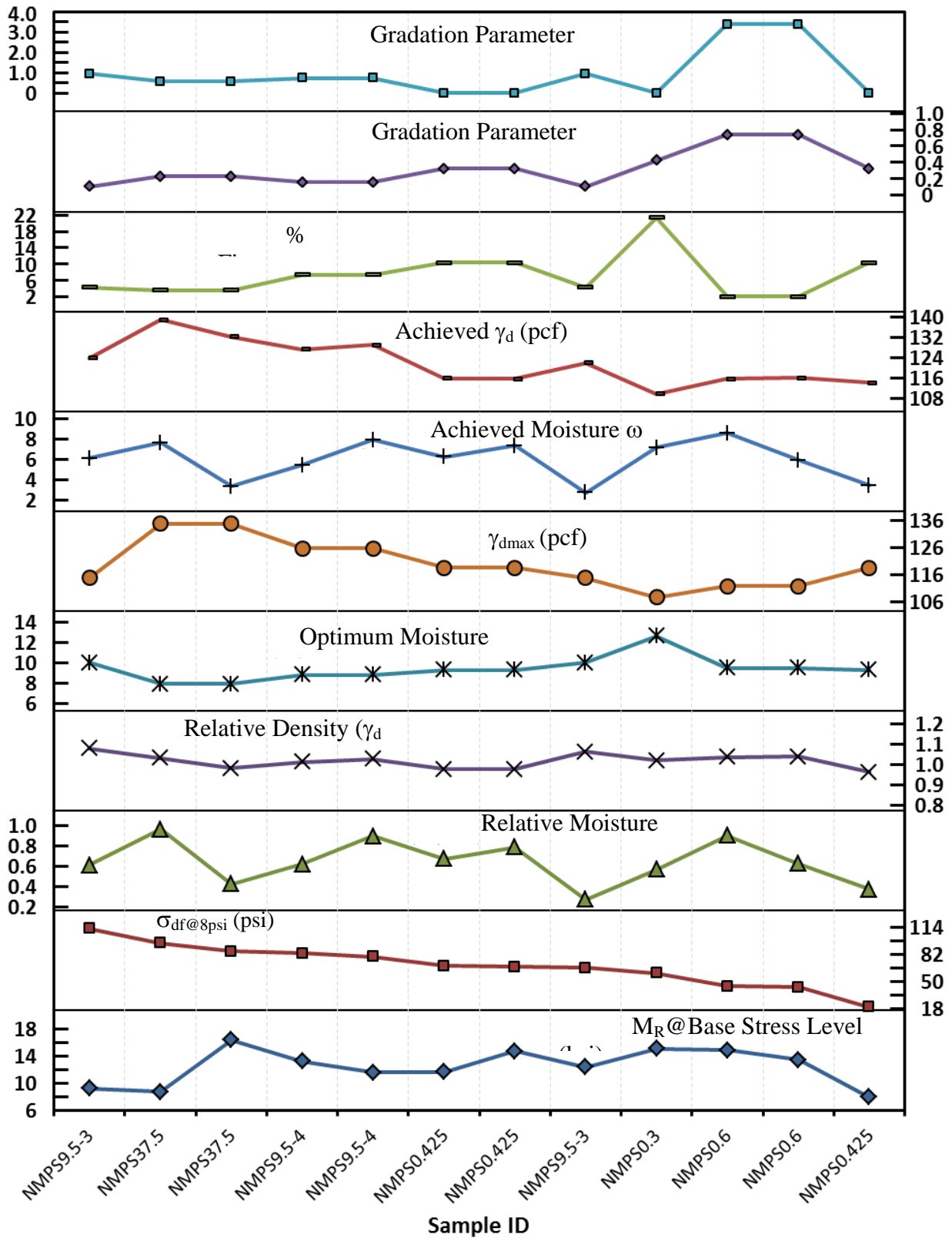


Figure 4.8. Factors Affecting Resilient Modulus and Peak Deviator Stress Results – Select Granular (8-psi Confining Pressure for σ_{df})

4.4 Summary

This chapter presented all the databases from which mechanistic pavement analysis and design inputs as the strength and M_R data were collected for unbound aggregate pavement base and subbase applications, as well as the corresponding aggregate index properties. Existing laboratory and in situ test data for Minnesota's aggregates were obtained from related research studies performed for/by MnDOT. In addition, as part of a comprehensive literature search, strength and resilient modulus (M_R) data were also collected from other relevant research efforts, such as a large database of laboratory M_R test results compiled by the Principal Investigator (PI) for over a decade at the University of Illinois. With any such strength and modulus data, corresponding aggregate index properties were collected and archived accordingly.

The preliminary data analysis reveals that the shear resistance of granular materials seems to be more affected by the achieved dry density than other influencing factors to stress the importance of adequate field compaction; whereas, the resilient modulus behavior is significantly influenced by small changes in the achieved moisture content in relation to the optimum moisture content, which may be linked to the moisture sensitivity of aggregate matrix suction potentials to emphasize the importance of taking into account environmental changes in the field.

All the resilient modulus load-time history data files, shear strength and aggregate index properties results were compiled as Excel spreadsheets submitted as task deliverables.

Chapter 5 Establishment of Linkages between Aggregate Properties and Design Inputs

5.1 Introduction

The evaluation of typical mechanistic design inputs is an important first step towards implementing new mechanistic-based pavement design procedures. Resilient modulus (M_R), a rational measure of the elastic response of unbound aggregate materials subjected to dynamic, repeated traffic loading, is a key mechanistic pavement analysis and design input. Laboratory testing for M_R requires expensive test equipment and time-consuming and detailed testing procedures. Therefore, using correlations to link M_R behavior with aggregate source properties would be more cost-effective in less advanced hierarchical level, Level 2 or 3, pavement design applications. Previous literature on resilient modulus prediction, based on either regression or Artificial Neural Network (ANN) techniques, was reviewed as examples in Chapter 2.

This chapter presents the establishment of regression based correlations between aggregate source properties and aggregate M_R data archived through modulus testing at the laboratories of MnDOT and University of Minnesota, for identifying mechanistic design moduli ranges of locally available materials in Level 2 pavement design applications. The effects of both stress sensitivity and seasonal variations are captured using the MEPDG M_R model with three model parameters, i.e., k_1 , k_2 , and k_3 . The commercial software, SAS[®], is used to develop the statistical correlations. Aggregate shape properties measured from the University of Illinois Aggregate Image Analyzer (UIAIA) and quantified through shape indices for 9 Minnesota aggregate samples are also included in the study to improve developed correlations. Finally, Monte Carlo type simulations using the software @Risk are presented to assess the sensitivities of M_R at given stress states to aggregate source properties.

5.2 Description of Study Data

Considering the fact that aggregate shape properties may not be tested and included in the MnDOT M_R database in the near future, the regression analysis was conducted separately for two different datasets: (1) the original 376 M_R observations without aggregate shape properties and (2) a subset of 135 M_R observations supplemented with aggregate shape properties measured from 9 MnDOT aggregate samples. Note that these 9 representative samples were provided by MnDOT and then tested for three shape indices, i.e., Flat and Elongation ratio (F&E ratio), Angularity Index (AI) and surface texture (ST) using the University of Illinois Aggregate Image Analyzer (UIAIA) (Tutumluer et al., 2000; Rao, 2001). An assumption was reasonably made that each sample tested for shape properties represented well the aggregate material source from which it was sampled.

Obviously, the major difference between these two regression data sets is that the first one does not include aggregate shape properties, whereas the second one considers three shape indices as predictor variables. Since recent research studies conducted at the University of Illinois have shown the importance of aggregate shape properties in accurate M_R prediction, the two separate regression analyses were conducted to further assess whether the inclusion of shape indices would significantly improve the accuracy of MnDOT modulus predictions.

Note that the laboratory prototype UIAIA was identified and recommended by the NCHRP 4-30A project among the most promising aggregate imaging systems to provide an

automated means to determine coarse aggregate size and shape properties (Tutumluer et al., 2000; Rao, 2001). The UIAIA system can take images of an individual aggregate particle from three orthogonal views, which has been very effective in reconstructing three-dimensional (3-D) particle shape and computing accurately the volume and size and shape indices. The UIAIA based image indicial data for coarse aggregate fall into the following two categories: (i) particle sizes, which include maximum, intermediate and minimum dimensions, and volume of the particle (Tutumluer et al., 2000; Rao, 2001); (ii) particle morphological or shape indices, which include the flat and elongated (F&E) ratio (Rao et al., 2001), angularity index AI (Rao et al., 2002), surface texture ST index (Rao et al., 2003). These two categories of imaging based coarse aggregate shape indices have been validated by successfully measuring aggregate properties and linking results to corresponding laboratory strength data and field rutting performances (Rao et al., 2002; Pan et al., 2004).

Eighty five percent of each of the two data sets was randomly selected for building the regression model, while the other 15 percent was used for model validation. Additionally, 6 extra M_R observations provided by MnDOT along with the shear strength data were also employed for model validation. The summary of data sets studied is as follows:

- (a) Model-building data set 1: 376 cases without aggregate shape properties extracted from MnDOT M_R database;
- (b) Model-building data set 2: 135 cases with aggregate shape properties (measured from 9 samples using UIAIA) extracted from those 376 cases;
- (c) Validation data set 1: 65 cases with shape properties extracted from Illinois DOT ICT R27-1 project M_R database;
- (d) Validation data set 2: Previously-compiled M_R database from Illinois DOT ICT R27-1 and other projects conducted at the University of Illinois; and
- (e) Validation data set 3: The 6 extra M_R cases provided by MnDOT along with the shear strength data.

Investigating effects of aggregate shape properties on the resilient modulus behavior has also been the subject of several recent research studies conducted at the University of Illinois with the most recent one being the ICT R27-1 project focusing on characterizing strength, stiffness and deformation behavior of three aggregate materials, i.e., limestone, dolomite and uncrushed gravel, commonly used in Illinois for subgrade replacement and subbase (item d above). The comprehensive laboratory test results of the ICT R27-1 study were also available to this project to compare and explore supporting trends from the developed modulus – aggregate property regression analyses.

5.3 Importance of Aggregate Shape Properties

Table 5.1 summarizes the variables used in the regression analysis. The final selected best models chosen from stepwise, forward selection and backward elimination regression methods are listed in Table 5.2. Several observations can be made related to these regression results:

Adding either predictor variable X25 (Angularity Index) or X26 (Surface Texture) into the regression equations for k_1 , k_2 and k_3 results in higher adjusted R^2 , indicating improved prediction accuracy. The last row of each response variable in Table 5.2 considers adding all

three shape indices (F&E ratio, AI and ST) into regression analysis to significantly improve the M_R predictions;

Among the three imaging shape indices examined (F&E ratio, AI and ST), based on the regression results herein, surface texture ST is statistically the most significant influencing k_1 predictions whereas AI is the most significant for k_2 and k_3 predictions, which should also be further validated with larger sample sizes;

The addition of aggregate shape properties into regression analysis can significantly improve the model prediction.

Table 5.1. Summary of the Variables Used in the Regression Analyses

Dependent Variable	Independent Variables	Note
K1	X1 - OMC	Optimum Moisture
K2	X2 - MDD	Maximum Density
K3	X3 - Cu	Coefficient of uniformity
	X4 - Cc	Coefficient of curvature
	X5 – PP_3"	Percent passing 75mm sieve
	X6 – PP_2-1/2"	Percent passing 63mm sieve
	X7 – PP_2"	Percent passing 50mm sieve
	X8 – PP_1-1/2"	Percent passing 37.5mm sieve
	X9 – PP_1-1/4"	Percent passing 31.5mm sieve
	X10 – PP_1"	Percent passing 25mm sieve
	X11 – PP_3/4"	Percent passing 19mm sieve
	X12 – PP_5/8"	Percent passing 16mm sieve
	X13 – PP_1/2"	Percent passing 12.5mm sieve
	X14 – PP_3/8"	Percent passing 9.5mm sieve
	X15 – PP_#4	Percent passing 4.75mm sieve
	X16 – PP_#8	Percent passing 2.36mm sieve
	X17 – PP_#10	Percent passing 2mm sieve
	X18 – PP_#16	Percent passing 1.18mm sieve
	X19 – PP_#30	Percent passing 600um sieve
	X20 – PP_#40	Percent passing 425um sieve
	X21 – PP_#50	Percent passing 300um sieve
	X22 – PP_#100	Percent passing 150um sieve
	X23 – PP_#200	Percent passing 75um sieve
	X24 – F&E Ratio	Flat & Elongation Ratio
	X25 – AI	Angularity Index
	X26 – ST	Surface Texture
	X27 – SA	Surface Area

Table 5.2. Summary of Regression Results for 9 MnDOT Aggregate Samples

Response Variables	Predictor Variables	Goodness of Regression
k ₁	X1, X2, X23	R ² = 0.898; Adj R ² = 0.837 (baseline*)
	X1, X2, X23, X24	R ² = 0.898; Adj R ² = 0.797 (↓)
	X1, X2, X23, X25	R ² = 0.935; Adj R ² = 0.871 (↑)
	X1, X2, X23, X26	R ² = 0.984; Adj R ² = 0.967 (↑)
	X1, X2, X23, X24, X25, X26	R ² = 0.989; Adj R ² = 0.957 (↑)
k ₂	X1, X2, X10, X23	R ² = 0.911; Adj R ² = 0.821 (baseline*)
	X1, X2, X10, X23, X24	R ² = 0.915; Adj R ² = 0.773 (↓)
	X1, X2, X10, X23, X25	R ² = 0.937; Adj R ² = 0.833 (↑)
	X1, X2, X10, X23, X26	R ² = 0.913; Adj R ² = 0.769 (↓)
	X1, X2, X10, X23, X24, X25, X26	R ² = 0.999; Adj R ² = 0.9995 (↑)
k ₃	X10, X13, X20	R ² = 0.746; Adj R ² = 0.593 (baseline*)
	X10, X13, X20, X24	R ² = 0.749; Adj R ² = 0.498 (↓)
	X10, X13, X20, X25	R ² = 0.889; Adj R ² = 0.778 (↑)
	X10, X13, X20, X26	R ² = 0.873; Adj R ² = 0.747 (↑)
	X10, X13, X20, X24, X25, X26	R ² = 0.933; Adj R ² = 0.730 (↑)

* Baseline predictions were reported earlier without shape properties included.

5.4 Regression Analysis Methodology

The flowchart description of the multiple linear regression analysis approach consists of the following consecutive steps: (i) determination of the pool of possible predictor variables to be regressed against response variables (i.e., k parameters): analysis of variance (ANOVA) method, to a certain extent, can be useful for assisting in selecting predictor variables that significantly influence the response variables; after identifying those predictor variables, some simple graphic diagnostics for each variable, such as Stem-and-Leaf plot and Box plot, are further considered to check if there are any outliers that could affect the appropriateness of the fitted regression function; (ii) identification of the functional forms in which the predictor variables should enter the regression model and important interactions that should be included in the model: scatter plots matrix and Pearson’s correlation coefficients matrix are powerful tools to visually examine if special nonlinear relationships exist between dependent and predictor variables and if strong linear associations exist between any two variables, respectively; (iii) reduction of predictor variables and identification of “good” subsets of potentially useful predictor variables to be included in the final regression model: effective automatic search procedures for model selection, including stepwise, forward selection and backward elimination regression methods are compared based on R₂, adjusted R₂, Mallows’ Cp, PRESS, VIF and other model selection criteria; (iv) selection of the ultimate regression models: formal tests for lack of fit, hypothesis tests for regression coefficients, and residual plots and analyses can be employed to identify any lack of fit, insignificant predictor variables, outliers, and influential observations; moreover, a rule-of-thumb here is that a model containing multiple types of physical properties would be better than that having only one type, given other conditions are similar; and (v) validation of the built regression models: the mean squared prediction error, denoted by MSPR in Eq. 5.1 below, is used as a means of measuring the actual prediction ability of the selected regression model;

hence, the calculated MSPR which is fairly close to MSE (mean squared error) is an indication of the appropriateness of the selected model.

$$MSPR = \frac{\sum_{i=1}^{n^*} (Y_i - \hat{Y}_i)^2}{n^*}$$

(5.1)

where Y_i = the value of the response variable in the i^{th} validation case;
 \hat{Y}_i = the predicted value for the i^{th} validation case based on the
 model-building data set;
 n^* = the number of cases in the validation data sets.

5.5 Regression Model Development

This section presents the establishment of the regression models for the three model parameters using the first model-building data set first without using shape properties and then with shape properties. The steps included in the regression analysis methodology are sequentially followed.

5.5.1 Selection and Diagnostics of Predictor Variables

To identify which aggregate index properties significantly affect the resilient modulus, ANOVA analysis via SAS[®] statistical software was conducted for both MnDOT and ICT R27-1 project databases. As introduced before, for the MnDOT database, the data set without shape properties has 376 observations, whereas the one with shape properties has 135 observations. In this application, each of those quantitative aggregate index properties to be studied is first grouped into different categories according to the magnitudes of their values. ANOVA then compares the means of the response variables, i.e., three k parameters here, for those newly-created categories. A predetermined level of significance, denoted as α , is compared against the resultant level of significance of the categories, namely the p value, through which a statistical difference between the mean values of those categories can be identified as significant or not. The null and alternative hypotheses used for ANOVA in this case are expressed as follows:

$$H_0: \mu_1 = \mu_2 = \dots = \mu_n;$$

H_a : At least one of the category means differs from the rest;

where μ_i is the mean value for the i^{th} category of each aggregate index property. If the resultant p value is less than the α value (usually 0.05), then conclude H_a , indicating the aggregate index property analyzed is important for the response variable; otherwise, this property is considered insignificant.

The significant aggregate index properties affecting resilient modulus are identified at $\alpha=0.05$ and summarized in Table 5.3. It should be noted that not all of these aggregate index properties identified as “significant” are necessarily to be included into the final regression models; instead, some of them might be substituted by others, because part of these aggregate index properties are highly correlated with each other in nature. The explanations of the notations given in Table 5.3 are presented in Table 5.4.

Table 5.3. Significant Aggregate Index Properties identified by ANOVA Analysis* ($\alpha=0.05$)

Database	Dependent Variables	Significant Aggregate Index Properties
MnDOT (w/o Shape Properties)	k ₁	$\omega_{opt}, \gamma_{max}, C_u, C_c, P_{\#4}, \& P_{200}$
	k ₂	$\omega_{opt}, \gamma_{max}, C_u, C_c, P_{\#4}, \& P_{200}$
	k ₃	$\omega_{opt}, \gamma_{max}, C_u, C_c, P_{\#4}, \& P_{200}$
MnDOT (with Shape Properties)	k ₁	$\omega_{opt}, \gamma_{max}, \omega_c, C_u, C_c, P_{\#4}, P_{200}, \mathbf{FE_Ratio, AI, ST}, (\gamma_{max})^2/P_{40}, \% \text{Gravel}, \% \text{Sand}, P_{40}, \& P_{3/8}$
	k ₂	$\omega_{opt}, \gamma_{max}, C_u, C_c, P_{\#4}, P_{200}, \mathbf{FE_Ratio, AI, and ST}, (\gamma_{max})^2/P_{40}, \% \text{Gravel}, \% \text{Sand}, P_{40}, P_{3/8}$, & $\omega_{achieved} / \omega_{opt}$
	k ₃	$\omega_{opt}, \gamma_{max}, \omega_{achieved}, C_u, C_c, P_{\#4}, P_{200}, \mathbf{FE_Ratio, AI, ST}, (\gamma_{max})^2/P_{40}, \% \text{Gravel}, \% \text{Sand}, P_{40}, \& P_{3/8}$
ICT R27-1	k ₁	$\omega_{opt}, \gamma_{max}, \omega_{achieved}, C_u, C_c, P_{200}, \mathbf{FE_Ratio, AI, \& ST}$
	k ₂	None
	k ₃	$\gamma_{max}, C_u, C_c, \mathbf{FE_Ratio, AI, and ST}$

* The explanations of the notations are presented in Table 5.4.

It is interesting to observe from Table 5.3 that none of the aggregate index properties are significant for the parameter k₂ of the ICT R27-1 database. One might suspect that the standard Proctor tests, but not the modified Proctor ones, employed in the ICT R27-1 project may have changed the strong trends in bulk stress dependency seen in higher density samples. Besides this interesting observation, the differences between these two databases need to be further investigated and compared.

In addition to the ANOVA analysis, scatter plots matrix and Pearson's correlation coefficients matrix are also powerful alternatives to identify important predictor variables for MR prediction models/equations. The principles of using scatter plots and Pearson's correlation coefficients for preliminary diagnostics for nonlinear relationships and strong interactions among those basic parameters are as follows: (1) predictor variables that are highly correlated, as indicated by the high R values (usually above 0.8) in Pearson's correlation matrix, are not combined due to strong multi-collinearity; (2) predictor variables that have the highest R values with dependent variables are selected first; and (3) it is desirable to select such predictor variables that are highly correlated with the dependent variable and, meanwhile, are less inter-correlated with other predictor variables. Due to space limitation, the scatter plots are not shown. The final selected pool of predictor variables is summarized in Table 5.4.

5.5.2 First-order Model

As no obvious nonlinear trends were observed in the scatter plots, a tentative first-order multiple linear regression model was examined first. All of the variables listed in Table 5.4 were included in the model development. Due to the large number of predictor variables and their inter-correlated nature, it was necessary to use different model selection criteria to select the most significant variables and thereby reduce the number of variables. In this process, a list of models was first obtained using RSQUARE selection criteria available in SAS. The RSQUARE criterion ranks the subsets of X variables according to the coefficient of multiple determination

R^2 , with a higher value of R^2 indicating a better model. Besides R^2 , other indicators, such as adjusted R^2 , Mallows' C_p , PRESS (Prediction sum of squares) and VIF (Variance Inflation Factor) were also examined while selecting a model. Since ordinary R^2 value always increases as more predictor variables are added to the regression model regardless of their relative significances to the response variable; the adjusted R^2 takes into account the number of parameters in the regression model through the degrees of freedom and thus can indeed decrease as the number of parameters increases. Therefore, a model which produces least predictor variables, highest adjusted R^2 , smallest C_p value near the total number of parameters, smallest PRESS value, and VIF value much less than 10, besides having highest R^2 value, was selected. The final selected models for three response variables were generated by the stepwise regression method shown in Table 5.5 to 5.7. Note that logarithmic transformation is demonstrated to be effective for k_1 .

Table 5.4. Significant Aggregate Index Properties Identified by ANOVA Analysis

Predictor Variable	Type	Description
ω_{opt}	Measured Property	Optimum Moisture Content
γ_{max}	Measured Property	Maximum Dry Density
\square	Measured Property	Achieved Moisture Content
γ_{dry}	Measured Property	Achieved Dry Density
C_u	Calculated Parameter	Coefficient of Uniformity
C_c	Calculated Parameter	Coefficient of Curvature
P_2	Measured Property	Percent Passing 2" sieve (50 mm)
$P_{1.5}$	Measured Property	Percent Passing 1-1/2" sieve (37.5 mm)
P_1	Measured Property	Percent Passing 1" sieve (25 mm)
$P_{3/4}$	Measured Property	Percent Passing 3/4" sieve (19 mm)
$P_{1/2}$	Measured Property	Percent Passing 1/2" sieve (12.5 mm)
$P_{3/8}$	Measured Property	Percent Passing 3/8" sieve (9.5 mm)
P_4	Measured Property	Percent Passing #4 sieve (4.75 mm)
P_{10}	Measured Property	Percent Passing #10 sieve (2 mm)
P_{40}	Measured Property	Percent Passing #40 sieve (0.425 mm)
P_{100}	Measured Property	Percent Passing #100 sieve (0.15 mm)
P_{200}	Measured Property	Percent Passing #200 sieve (0.075 mm)
GRAVEL	Calculated Parameter	Percent Gravel (75~2 mm)
CSAND	Calculated Parameter	Percent Coarse Sand (2~0.42 mm)
FSAND	Calculated Parameter	Percent Fine Sand (0.42~0.074 mm)
ω/ω_{opt}	Calculated Parameter	Moisture Ratio
$\gamma_{dry}/\gamma_{max}$	Calculated Parameter	Density Ratio
$\square_{max} P_{40}$	Calculated Parameter	/
$P_{200}/\log C_u$	Calculated Parameter	/

It can be seen from Tables 5.5 to 5.7 that the VIF values for all regression coefficients are much less than 10, indicating that each predictor variable is approximately uncorrelated with others; and that the p values of all regression coefficients are much less than the significance level of 0.05 (reject null hypothesis), indicating all predictor variables included are statistically significant, though the adjusted R^2 values for three models are very low. The reason may be that

all the aggregate samples studied came from different sources and locations and were tested for MR in different laboratories by different personnel, which may amplify the measurement variance and obscure the real statistical regression correlations.

To better test the significance of one regression model and/or the significance of some specific regression coefficients, the corresponding hypothesis tests are conducted for the general multiple linear regression model as follows:

$$Y = \beta_0 + \sum_{i=1}^{p-1} \beta_i X_i + \varepsilon_i$$

The overall F test of whether or not there is a regression relation between the response variable Y and the set of X variables:

$$H_0: \beta_1 = \beta_2 = \dots = \beta_{p-1} = 0$$

$$H_a: \text{not all } k \in \{1, \dots, p-1\} \text{ equal zero}$$

The partial F test of whether a particular regression coefficient β_k equals zero:

$$H_0: \beta_k = 0$$

$$H_a: \beta_k \neq 0$$

If the p-value of the corresponding hypothesis test is greater than the predetermined α value (e.g., 0.05), then the null hypothesis H_0 is concluded; otherwise, the alternative hypothesis H_a is concluded. It is clearly listed in Tables 5.5 to 5.7 that, not only all the three multiple linear regression models are significant because of the small p values (<0.0001), but all the individual predictor variables are also significant in the corresponding models as indicated by the individual p values, which are much less than the predetermined level of significance (i.e., $\alpha=0.05$).

Another noteworthy characteristic of the developed three regression models is that the variance inflation factor (VIF) value for each individual predictor variable is less than the critical value of 10. As a rule of thumb, a maximum VIF value in excess of 10 is frequently indicative of serious multi-collinearity problems, whereas a VIF value close to 1 is taken as an indication that the predictor variable of interest is not linearly related to others. Therefore, it appears that multi-collinearity is not a serious issue in this case. The magnitudes of standard errors of estimated regression coefficients are also reasonably low.

Table 5.5. Summary of Multiple Linear Regression (MLR) Analysis Results for Identifying Properties Used to Predict $\log k_1$ of M_R Constitutive Equation

Model Parameters	Case 1 (376 observations)			Case 2 (115 observations)		
	Parameter Estimate	Pr> t	Variance Inflation	Parameter Estimate	Pr> t	Variance Inflation
Intercept	1.379	<.0001	0	4.323	<.0001	0
ω_{opt}	-0.041	<.0001	1.51	-0.026	0.0031	1.74
γ_d	-0.005	0.0044	1.86			
ω/ω_{opt}	-0.294	<.0001	1.12	-0.555	<.0001	1.63
FSAND	0.001	0.0441	1.85			
FE_Ratio				-0.052	<.0001	2.49
ST				-0.060	<.0001	1.68
P _{1"}				-0.025	0.0001	1.33
P _{#100}				-0.064	<.0001	3.71
R ²	0.14			0.58		
Adj. R ²	0.13			0.56		
Root MSE	0.16			0.12		
Pr>F	<.0001 (F=15.09)			<.0001 (F=25.36)		

Table 5.6. Summary of MLR Analysis Results for Identifying Properties Used to Predict k_2 Parameter of M_R Constitutive Equation

Model Parameters	Case 1 (376 observations)			Case 2 (115 observations)		
	Parameter Estimate	Pr> t	Variance Inflation	Parameter Estimate	Pr> t	Variance Inflation
Intercept	1.606	<.0001	0	1.785	<.0001	0
ω	-0.012	0.0311	1.25			
γ_d	0.006	0.0021	2.27			
$(\gamma_{dmax})^2/P_{\#40}$	-0.0002	<.0001	1.86	-0.001	<.0001	6.09
C _u	-0.004	<.0001	3.97			
C _c	-0.427	0.0102	5.71			
P _{3/4"}	-0.011	<.0001	2.39			
AI				-0.001	0.0297	4.35
P _{#200} /logC _u				-0.073	<.0001	4.40
GRAVEL				0.008	<.0001	5.42
R ²	0.32			0.50		
Adj. R ²	0.31			0.48		
Root MSE	0.16			0.12		
Pr>F	<.0001 (F=28.64)			<.0001 (F=27.29)		

Table 5.7. Summary of MLR Analysis Results for Identifying Properties Used to Predict k_3 Parameter of M_R Constitutive Equation

Model Parameters	Case 1 (376 observations)			Case 2 (115 observations)		
	Parameter Estimate	Pr> t	Variance Inflation	Parameter Estimate	Pr> t	Variance Inflation
Intercept	-9.867	<.0001	0	-8.602	0.0002	0
ω/ω_{opt}				0.528	0.0314	1.45
$(\gamma_{dmax})^2/P_{\#40}$	0.001	<.0001	4.46	0.001	<.0001	1.63
C_u	0.007	<.0001	3.25			
$P_{2''}$	0.067	0.0023	1.52			
$P_{1.5''}$				0.131	<.0001	2.20
$P_{1''}$				-0.062	0.0015	1.71
$P_{3/4''}$	0.015	0.0604	3.33			
$P_{\#40}$	0.009	0.0001	4.59			
R^2	0.394			0.53		
Adj. R^2	0.386			0.52		
Root MSE	0.42			0.32		
Pr>F	<.0001 (F=48.12)			<.0001 (F=31.34)		

5.5.3 Examine and Test for Normality and Constant Variance

Several graphic diagnostics executed are presented in Appendix E for examining whether the model assumptions have been violated: 1) linearity of regression functions, 2) constant error variance; and 3) normality of error terms.

From a residual plot against the predicted values, whether a linear regression function is appropriate for the data being analyzed can be studied. Both the Residual and Studentized Residual (RStudent) plots against predicted values for k_1 show that the residuals approximately fall within a horizontal band centered around 0 with some outlying observations; therefore, no systematic tendencies towards positive and negative are displayed indicating a linear regression model is somewhat appropriate. The plots of Residual by Regressors also reveal that no clear increasing or decreasing tendencies between residual and regressors exist, thus the non-constancy of error variance is not an issue in this case. The normality of error terms can be roughly studied from the histogram of residuals, namely Percent against Residual and the plot of Residual against Quantile. The facts that the histogram is more or less close to the normal distribution, and that the plot of Residual against Quantile almost falls on a straight line support the assumption of normality of error terms. The diagnostics analysis for model parameters k_2 and k_3 are similar to that for k_1 . It is concluded that all the inherent statistical assumptions embedded in the multiple linear regression analyses are satisfied here.

5.5.4 Model Validation Using 15% Data

To validate regression models developed with shape properties, the following data sets were used: 1) 20 randomly-selected cases (around 15%) out of the 135 model-building cases; 2) 65 cases from ICT R27-1 project; 3) 6 extra M_R cases received from MnDOT. However, due to the missing Proctor data for achieved moisture content and dry density, the 6 extra M_R cases could not be used effectively. Further, the developed regression models with shape properties,

based on validation results, cannot predict M_R with satisfactory accuracy for the 65 cases from the IDOT ICT R27-1 project, which indirectly demonstrates that M_R is sensitive to aggregate sources, types and physical properties. Hence, one M_R predictive model suitable for one state or region (Minnesota in this case) may not necessarily be suitable for other states/regions, e.g., Illinois.

The validation results in terms of MSPR values for the remaining 20 cases are presented in Table 5.8 below. As listed, the MSE and MSPR values are very close for these three regression models, which is indicative of the satisfactory model prediction ability. Furthermore, the measured values versus the predicted values for three k parameters are plotted in Figures 5.1 to 5.3. Accordingly, the developed models would have fairly good prediction abilities when used in the MEPDG level 2 or level 3 design analyses as long as no extrapolations were made during the use of these regression models.

Table 5.8. Comparisons between MSPR and MSE Values for the Three k Parameters

Validation Dataset	Dependent Variables	MSE	MSPR
20 cases from MnDOT (with Shape Properties)	k_1	0.01479	0.013205
	k_2	0.01530	0.017817
	k_3	0.10537	0.10791

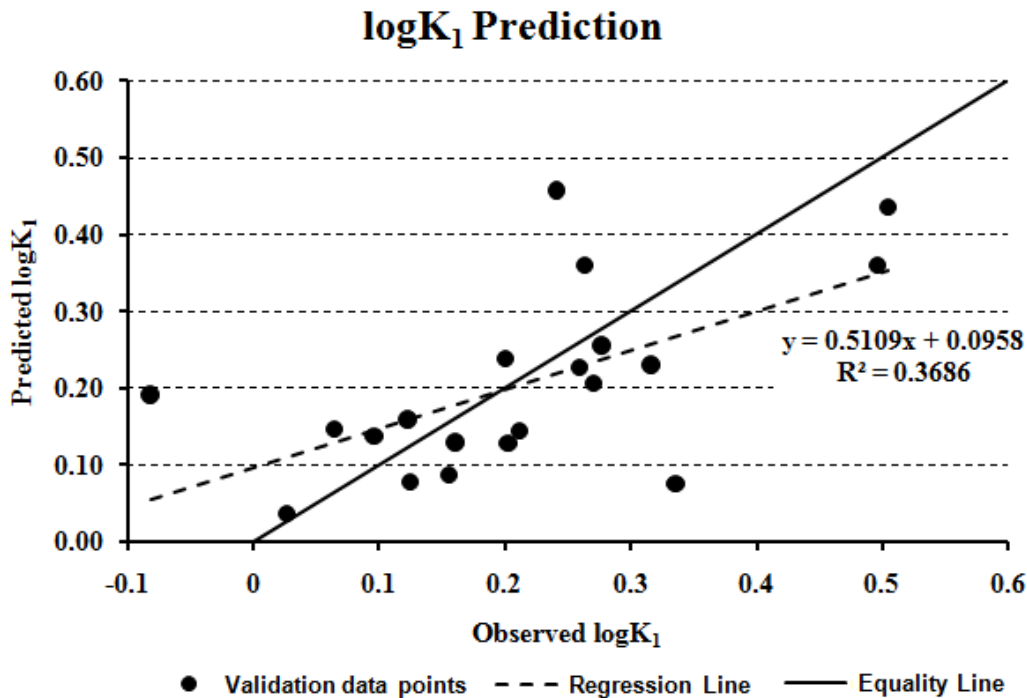


Figure 5.1. Measured vs. Predicted Values for $\log k_1$

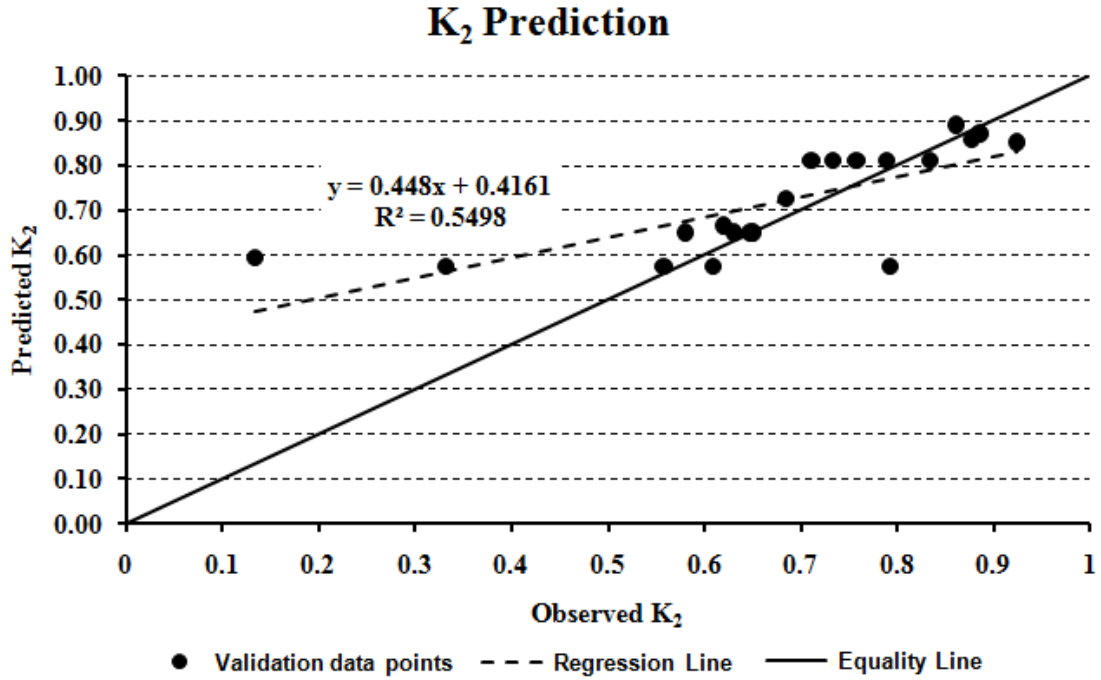


Figure 5.2. Measured vs. Predicted Values for k₂

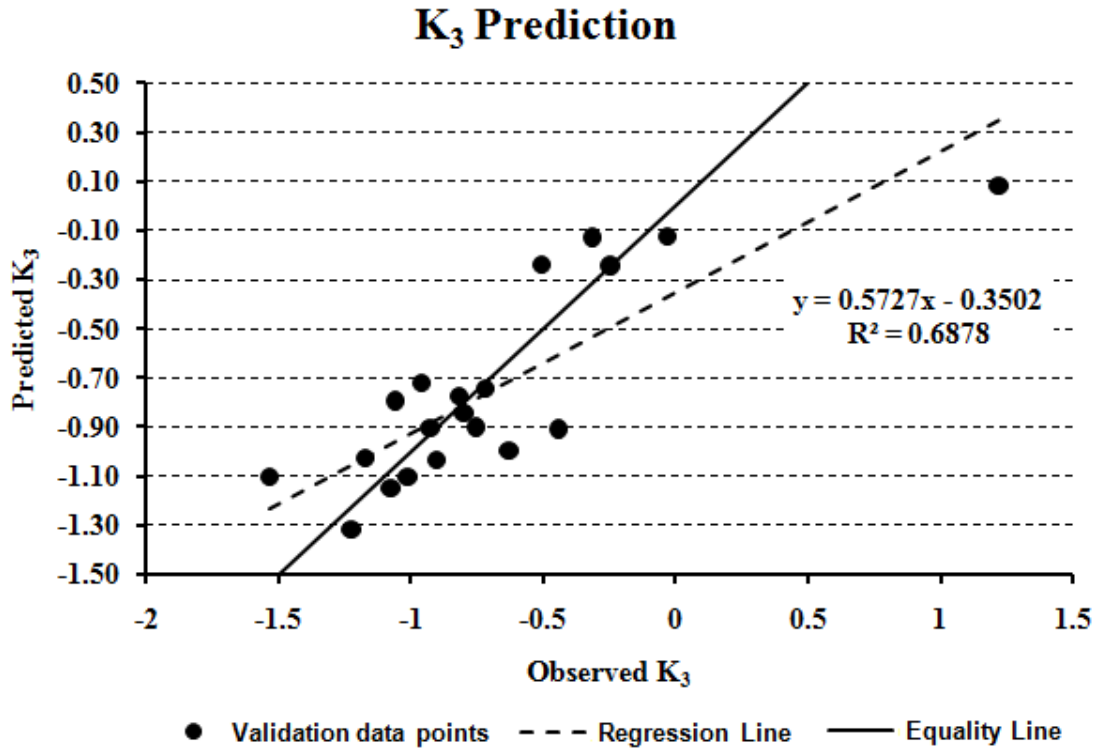


Figure 5.3. Measured vs. Predicted Values for k₃

5.5.5 Model Development with Combined Data Sets

As the regression models developed using the model-building data set have been validated using the cross validation data set, it is then customary practice to re-develop the models by combining both the model-building and validation data sets as one single data set. The rebuilt regression models using the combined data set are presented in Equation 5.2. The residuals of model k_1 pass all the tests for normality; however, the residuals of model k_2 and k_3 both fail to pass some of the tests for normality. The histograms of all the residuals are approximately close to normal distribution. Failing some of the tests for normality would not seriously violate the normality assumption of error terms; indeed, it still indicates that the residuals still approximate normal distribution to a reasonable extent.

It is noteworthy that the regression models rebuilt from the combined data set should be used for M_R prediction in the future. The following sensitivity analysis is also based on the rebuilt regression models. The developed regression models with shape indices for k parameters are given by Equation 5.2 as follows:

$$\left\{ \begin{array}{l}
 M_R = k_1 P_a \left(\frac{\theta}{P_a} \right)^{k_2} \left(\frac{\tau_{oct}}{P_a} + 1 \right)^{k_3} \\
 k_1 = 10^{(0.132 - 0.016 FE_Ratio - 0.05 ST - 0.026 \omega_{opt} - 0.628 \frac{\omega}{\omega_{opt}} + 0.0004 \frac{\gamma_{max}^2}{P_{40}} + 1.197 C_c)} \\
 (R^2 = 0.5523; \text{Adj. } R^2 = 0.5313; p < 0.0001; \text{MSE} = 0.01478) \\
 k_2 = 1.573 + 0.007 \gamma_d - 0.0009 \frac{\gamma_{max}^2}{P_{40}} - 0.013 P_{10} - 0.046 P_{200} \\
 (R^2 = 0.5062; \text{Adj. } R^2 = 0.4910; p < 0.0001; \text{MSE} = 0.01543) \\
 k_3 = -15.914 + 0.041 FE_Ratio + 0.004 AI + 0.015 \gamma_d + 0.488 \frac{\omega}{\omega_{opt}} - 0.0008 \frac{\gamma_{max}^2}{P_{40}} \\
 + 0.246 \frac{P_{200}}{\log C_u} + 0.145 P_{2^n} - 0.057 P_{1^n} \\
 (R^2 = 0.6633; \text{Adj. } R^2 = 0.6419; p < 0.0001; \text{MSE} = 0.08328)
 \end{array} \right. \quad (5.2)$$

The validation results in terms of MSPR values for the remaining 15% data indicated that the MSE and MSPR values are very close for these three regression models, which is indicative of the satisfactory predictive capability of these models. Therefore, the developed models are believed to have fairly good predictive capabilities to be used in MEPDG level 2 or level 3 design analysis, as long as no extrapolations are made during the use of those regression models. Not only are all the three multiple linear regression models significant because of the small p values (< 0.0001), but all the individual predictor variables are also significant in the corresponding models, as indicated by the individual p values which are much less than the predetermined level of significance (i.e., $\alpha = 0.05$). The variance inflation factor (VIF) value for each individual predictor variable is less than the critical value of 10. According to the rule of thumb, it appears that multicollinearity is not a serious issue in this case. The magnitudes of standard errors of estimated regression coefficients are also reasonably low. No serious

violations of the linearity, constancy and normality assumptions have been found in these three regression models developed with shape properties.

5.6 Monte Carlo Simulation of Resilient Modulus

To investigate sensitivities of resilient moduli of aggregate base/granular subbase materials to various input parameters (i.e., aggregate source properties) and their inherent variability, advanced risk modeling by Monte Carlo type simulation was performed via @RISK. The Monte Carlo type simulation models each input parameter as a stochastic variable with a distribution function assigned such that the distribution of the output values can be predicted.

5.6.1 Development of M_R Predictive Model

After the developed regression models for Case 2 (with aggregate shape indices) were validated using the cross-validation dataset, basic procedures of a customary practice were followed to re-develop the models by combining both the model-building and validation datasets as one single model development dataset. The resultant regression models for the k parameters were then entered into the MEPDG M_R constitutive model, leading to the following analytical model that expresses M_R as a function of the applied stress states and aggregate source properties. To calculate M_R values, the stress terms included in the model given below, i.e., bulk stress θ and octahedral shear stress τ_{oct} , must be specified. Based on the MnPAVE program default layer modulus inputs and the 18-kip dual-tire axle loads (ESALs) applied, Table 5.9 lists the representative stress levels calculated in MnDOT aggregate base, granular subbase, and subgrade layers, respectively.

$$M_R = 10^{\left(0.132 - 0.016 FE_Ratio - 0.05 ST - 0.026 \omega_{opt} - 0.628 \frac{\omega}{\omega_{opt}} + 0.0004 \frac{\gamma_{max}^2}{P_{40}} + 1.197 C_c\right)} P_a \times \left(\frac{\theta}{P_a}\right)^{\left(1.573 + 0.007 \gamma_d - 0.0009 \frac{\gamma_{max}^2}{P_{40}} - 0.013 P_{10} - 0.046 P_{200}\right)} \times \left(\frac{\tau_{oct}}{P_a} + 1\right)^{\left(-15.914 + 0.041 FE_Ratio + 0.004 AI + 0.015 \gamma_d + 0.488 \frac{\omega}{\omega_{opt}} - 0.0008 \frac{\gamma_{max}^2}{P_{40}} + 0.246 \frac{P_{200}}{\log C_u} + 0.145 P_2 - 0.057 P_1\right)} \quad (5.3)$$

where: $\theta = \sigma_1 + 2\sigma_3$; $\sigma_d = \sigma_1 - \sigma_3$; $\tau_{oct} = \frac{1}{3} \sqrt{(\sigma_1 - \sigma_2)^2 + (\sigma_1 - \sigma_3)^2 + (\sigma_2 - \sigma_3)^2}$

Atmospheric (normalizing) pressure $p_a = 101.35$ -kPa (14.7-psi)

log k_1 model: $R^2 = 0.55$, Adj. $R^2 = 0.53$, $P < .0001$, SSE=1.89

k_2 model: $R^2 = 0.51$, Adj. $R^2 = 0.49$, $P < .0001$, SSE=2.01

k_3 model: $R^2 = 0.66$, Adj. $R^2 = 0.64$, $P < .0001$, SSE=10.49

Table 5.9. Representative Stress Levels in Typical MnDOT Pavement Layers*

MnDOT Layer Material	Layer Thickness		Representative Stress Levels		MnPAVE <i>Fall</i> Design Moduli	
	in.	cm	psi	kPa	ksi	MPa
HMA: PG 58-34	6	15.2	-	-	-	-
Aggregate Base: Class 6	6	15.2	$\sigma_1=9.0$ $\sigma_3=1.0$	$\sigma_1=62.1$ $\sigma_3=6.9$	24	164
Granular Subbase: Select Granular	18	45.7	$\sigma_1=5.0$ $\sigma_3=1.0$	$\sigma_1=34.5$ $\sigma_3=6.9$	11.7	81
Subgrade: Engineered Soil	12	30.5	$\sigma_1=4.5$ $\sigma_3=1.0$	$\sigma_1=31.0$ $\sigma_3=6.9$	-	-

* Data source from MnDOT.

5.6.2 Simulation Results

The Monte Carlo simulation was performed using the software @RISK which allows for the analysis to be performed in Excel spreadsheets. The Latin Hypercube sampling and 100,000 iterations were adopted. The Monte Carlo simulation properly captured the distribution function for each input parameter. The initial distributions assigned to each of the input parameters, as detailed in Table 5.10, were fitted from the databases collected. Summary statistics for the resulting distribution of calculated M_R are presented in Table 5.11. As shown in Table 5.11, the MnPAVE fall-season design moduli listed in Table 5.9 for aggregate base and granular subbase have the reliability of at least 95% and 85% in the specified pavement structure, respectively. The mean M_R values under both typical base and subbase stress levels are above the minimum MnPAVE requirement of 5 ksi, and the listed statistics are also within reasonable limits.

Table 5.10. Input Parameters and Distributions

Input Parameters	Mean	Std. Dev.	Min.	Max.	Distribution
ω_{opt} (%)	8.7	1.8	6.2	12.2	Log-logistic
ω/ω_{opt}	0.83	0.16	0.33	1.21	Weibull
γ_d (pcf)	128	5	119	141	Beta general
γ_{dmax} (pcf)	128	6	122	140	Log-logistic
$(\gamma_{dmax})^2/P_{\#40}$	897	311	404	1573	Log-logistic
$P_{2''}$ (%)	99.4	1.6	95	100	Weibull
$P_{1''}$ (%)	98.7	2.2	91	100	Weibull
$P_{\#10}$ (%)	48.6	20.0	17	71	Beta general
$P_{\#200}$ (%)	6.3	2.4	2.9	12.4	Johnson SB
C_c	0.56	0.11	0.36	0.70	Johnson SB
$P_{\#200}/\log C_u$	4.97	1.51	3.48	8.35	Beta general
FE_Ratio	4.1	2.4	1.8	10.6	Johnson SB
AI	425	61	307	499	Inverse Gauss
ST	2.5	2.3	0.6	1.6	Pareto

Table 5.11. Monte Carlo Simulation Results for M_R (Unit: ksi; 1 ksi=6.9 MPa)

Statistics	M_R at Base Stress Level	M_R at Subbase Stress Level
Minimum	0	0
Maximum	898.8*	4225.3*
Mean	7.8	8.1
Std Dev	6.0	19.2
Median	6.9	6.1
95% Percentile	15.6	18.5
75% Percentile	9.4	9.3
25% Percentile	5.0	4.0
MnPAVE M_R reliability	>95%	85%

* Unreliable extreme outliers

Figure 5.4 shows the sensitivity charts for aggregate base and granular subbase M_R from which the relative influences of aggregate source properties on M_R can be compared. At the representative aggregate base stress levels, the term $(\gamma_{dmax})^2/P_{\#40}$ positively affects M_R the most, while the moisture content ratio and the optimum moisture content are the primary negative factors. The same trends are also observed at granular subbase stress levels. As one would expect, larger F&E ratio and less angularity result in lower M_R levels. However, the M_R is found to increase with increased percent passing No.200 sieve (fines). The reason for that is probably the maximum percent fines found around 12% in the database; i.e., the coarse aggregate particle contact is not seriously severed by excessive fines. In general, the sensitivities of M_R to aggregate source properties are in accordance with expectations, indicating that the developed correlations are reasonable.

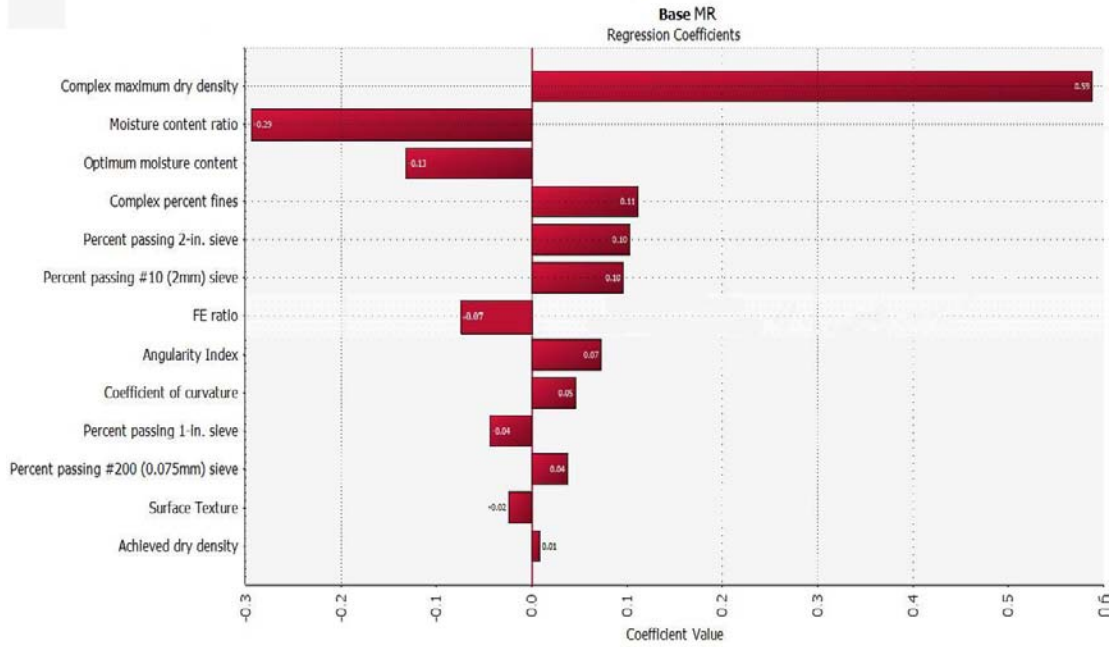
5.7 Reliability-Based Evaluation of Aggregate Source Properties Affecting Resilient Modulus Behavior

5.7.1 Limit State Function Used

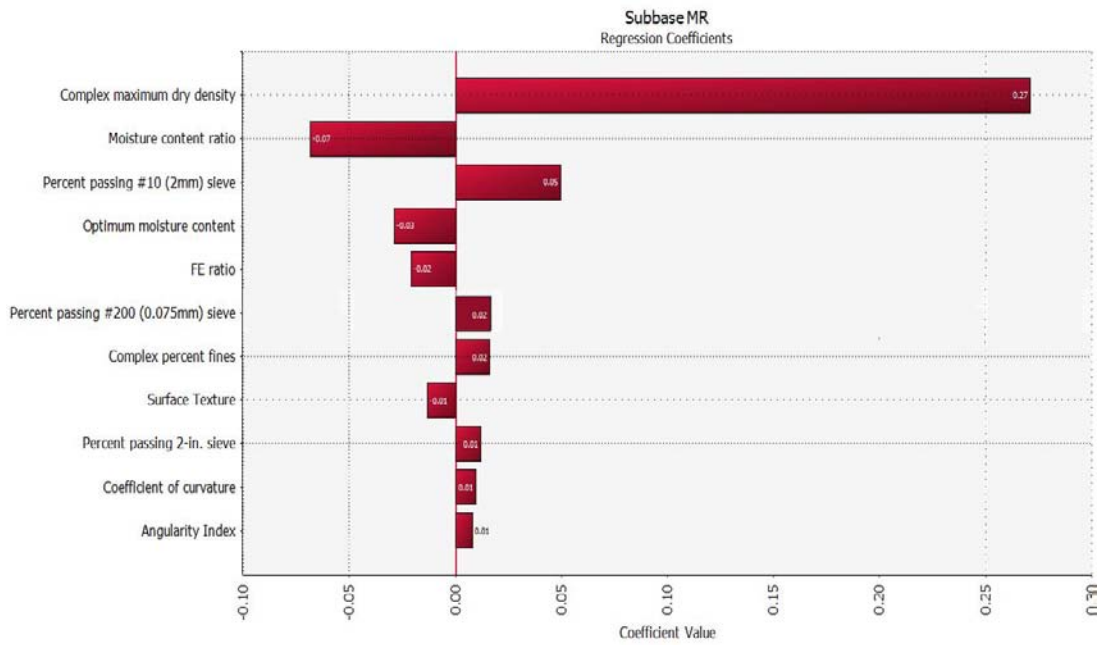
The failure mode of this problem is defined as when the measured resilient modulus is below the designed value of resilient modulus. Therefore, the limit state function is expressed as follows:

$$g(\mathbf{X}) = M_R - M_{R_design} \quad (5.4)$$

A typical conventional pavement structure used in Minnesota was selected to calculate the representative stress levels in aggregate base layer. The stress results were tabulated in Table 5.12, as well the standard design modulus specified by Minnesota Department of Transportation for Class 6 aggregate base materials.



(a) M_R at Stress Levels in Aggregate Base



(b) M_R at Stress Levels in Granular Subbase

Figure 5.4. Sensitivity Charts for M_R

Table 5.12. Representative Stress Level and Design Modulus for Aggregate Base Layer in a Typical Conventional Pavement Structure

Layer Material	Layer Thickness	Representative Stress Levels	Design Modulus
Units	(in.)	(psi)	(ksi)
Aggregate Base: Class 6	6	$\sigma_1=9.0$ $\sigma_3=1.0$	24

The resilient modulus constitutive equation used in this study is the model just developed and presented previously. The reason to use this model is that the database for this model was generated from real laboratory tests done on aggregate materials collected from different construction projects through Minnesota. This model also included all significant variables affecting resilient modulus behavior. Table 5.13 gives the abbreviations of variables used in this study.

Table 5.13. Abbreviations and Brief Descriptions of Significant Variables Influencing Resilient Modulus Behavior

Abbreviation	Brief description
<i>FE ratio</i>	Flat and Elongated ratio
<i>ST</i>	Surface Texture index
ω_{opt}	Optimum Moisture Content
ω / ω_{opt}	Moisture content ratio
γ_{max}^2 / P_{40}	Complex maximum dry density
C_c	Coefficient of Curvature
γ_d	Achieved dry density
P_{10}	Percent passing #10 (2mm) size sieve
P_{200}	Percent passing #200 (0.075mm) size sieve
<i>AI</i>	Angularity Index
$P_{200} / \log C_u$	Complex percent fines

It is worth mentioning that the effects of variables $P_{1''}$ and $P_{2''}$ (percent passing 1'' and 2'' sieves, respectively) were not included because most of the samples do not have sizes larger than 1'' in diameter and the values of these two variables in most of the observed datasets thus remained constant (100 percent passing). Gradation was quantified by parameters $P_{\#10}$, $P_{\#200}$, C_c , and $P_{\#200}/\log C_u$. Moisture and density were quantified by parameters γ_{max}^2 / P_{40} , γ_d , ω_{opt} , and ω / ω_{opt} . Aggregate particle shape or morphology was quantified as Flat and Elongated (F&E) ratio, Angularity Index (AI), and Surface Texture (ST) index measured by the University of Illinois Aggregate Image Analyzer (UIAIA).

5.7.2 Variables and Distributions

Totally 135 M_R observations from MnDOT database supplemented with aggregate shape properties measured from 9 MnDOT samples via University of Illinois Aggregate Image Analyzer (UIAIA) were employed in this study. The initial distribution assigned to each of the random variables, as detailed in Table 5.14, were obtained by distribution fitting tool in MATLAB[®] from the databases collected. Corresponding distribution parameters were also calculated and presented in Table 5.14.

The correlation matrix, as shown in Table 5.15, was established from the 135 datasets and adjusted according to definitions and characteristics of variables wherever necessary. Reasonable Assumptions were reasonably made for shape properties (FE ratio, ST and AI) that they are not correlated to other variables except density (γ_{\max}^2 / P_{40} and γ_d), and that FE ratio is not correlated to AI or ST.

Table 5.14. Basic Statistics of Aggregate Source Properties Used

Property	Variable	Distribution	Mean	Standard Deviation
<i>FE ratio</i>	X1	Lognormal	4.110	2.446
<i>ST</i>	X2	Exponential	2.504	2.300
ω_{opt}	X3	Gumbel	8.653	1.761
ω / ω_{opt}	X4	Weibull	0.828	0.156
γ_{\max}^2 / P_{40}	X5	Weibull	898.897	309.842
C_c	X6	Uniform	0.529	0.097
γ_d	X7	Lognormal	128.390	4.880
P_{10}	X8	Uniform	44.000	15.820
P_{200}	X9	Lognormal	6.351	2.689
<i>AI</i>	X10	Normal	424.809	60.895
$P_{200} / \log C_u$	X11	Lognormal	4.958	1.386

5.7.3 Form Analysis

Statistical analysis was performed using a First Order Reliability Method (FORM). The FORM algorithm approximates the integral of the joint probability distribution function of the basic variables X over the portion of the sample space that corresponds to failure of a component (Madsen et al., 1986). The function which defines this region is the limit-state function, ($g(X) = 0$). FORM uses an one-to-one transformation of the random variables into a standardized normal space as shown below:

$$X = (X_1, X_2, \dots, X_n) \rightarrow U = (U_1, U_2, \dots, U_n) \quad (5.5)$$

where U_1, U_2, \dots, U_n are uncorrelated random variables with standard normal distributions. Next, the limit-state surface in the X-space is mapped on the corresponding limit-state surface in the U-space. The probability content of the failure set in the U-space is obtained by a search for the minimum distance β (also called the reliability index) from the origin to a point u^* on the failure space (see Figure 5.5). The point u^* is also known as the design point, or the most likely failure point. While various software/programs are available to perform these calculations, the FERUM program developed by Haukaas and Kiureghian (1999) at the University of California, Berkeley is used in this study.

Table 5.15. Correlation Coefficients of Variables

	<i>FE ratio</i>	<i>ST</i>	ω_{opt}	ω / ω_{opt}	γ_{max}^2 / P_{40}	C_c	γ_d	P_{10}	P_{200}	<i>AI</i>	$P_{200} / \log C_u$
<i>FE ratio</i>	1	0	0	0	-0.3	0	-0.1	0	0	0	0
<i>ST</i>		1	0	0	0.1	0	0.2	0	0	0.5	0
ω_{opt}			1	-0.3	-0.3	0.5	-0.4	0.5	0	0	0.3
ω / ω_{opt}				1	0	0	0	0	0	0	-0.1
γ_{max}^2 / P_{40}					1	-0.5	0.5	-0.5	0	0.4	-0.4
C_c						1	-0.5	0.5	-0.2	0	0.4
γ_d			Symmetric				1	-0.4	0	0.4	-0.4
P_{10}								1	0	0	0.4
P_{200}									1	0	0.5
<i>AI</i>										1	0
$P_{200} / \log C_u$											1

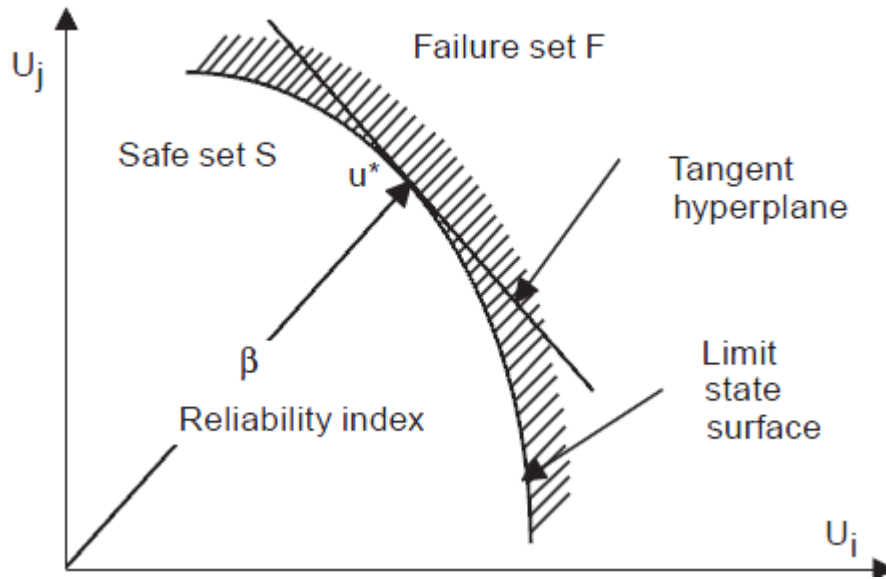


Figure 5.5. FORM Approximations (Haukaas and Kiureghian, 1999)

Table 5.16 and Figure 5.6 show the calculated importance vector from FERUM. Negative sign of Importance Vector γ means that the variable in the original space is capacity type and as the increase of the value of this variable, resilient modulus will increase. Positive sign of Importance Vector γ means that the variable in the original space is demand type and as the increase of the value of this variable, resilient modulus will decrease. $P_{200} / \log C_u$, AI , P_{200} , P_{10} , γ_d , c_c , and γ_{\max}^2 / P_{40} were found to be capacity type and ω / ω_{opt} , ω_{opt} , ST , and $FE Ratio$ were found to be demand type.

5.7.4 Sensitivity of Variables to the Reliability Index

The relative contribution of each variable can be examined by comparing the magnitude of γ^2 . Figure 5.7 shows that γ_{\max}^2 / P_{40} has the most important contribution to resilient modulus behavior, followed by c_c , ω / ω_{opt} , ST , ω_{opt} , $P_{200} / \log C_u$, and P_{10} . The contributions of $FE Ratio$, γ_d , P_{200} , and AI were found to be insignificant as compared to others.

A sensitivity analysis was used to quantify the effect of the variability of the parameters of those different random variables included in the analysis. This was done by taking the partial derivative of the reliability index β , with respect to the parameters considered. The results as summarized in Table 5.17 showed that the resilient modulus behavior is most sensitive to the variability in c_c and ω / ω_{opt} .

Table 5.16. Importance Vector of Variables Obtained from FERUM Program

Source Properties	Importance Vector γ
$FE\ ratio$	0.0689
ST	0.292
ω_{opt}	0.1954
ω / ω_{opt}	0.4277
γ_{max}^2 / P_{40}	-0.5771
C_c	-0.5463
γ_d	-0.0122
P_{10}	-0.145
P_{200}	-0.058
AI	-0.0999
$P_{200} / \log C_u$	-0.1514

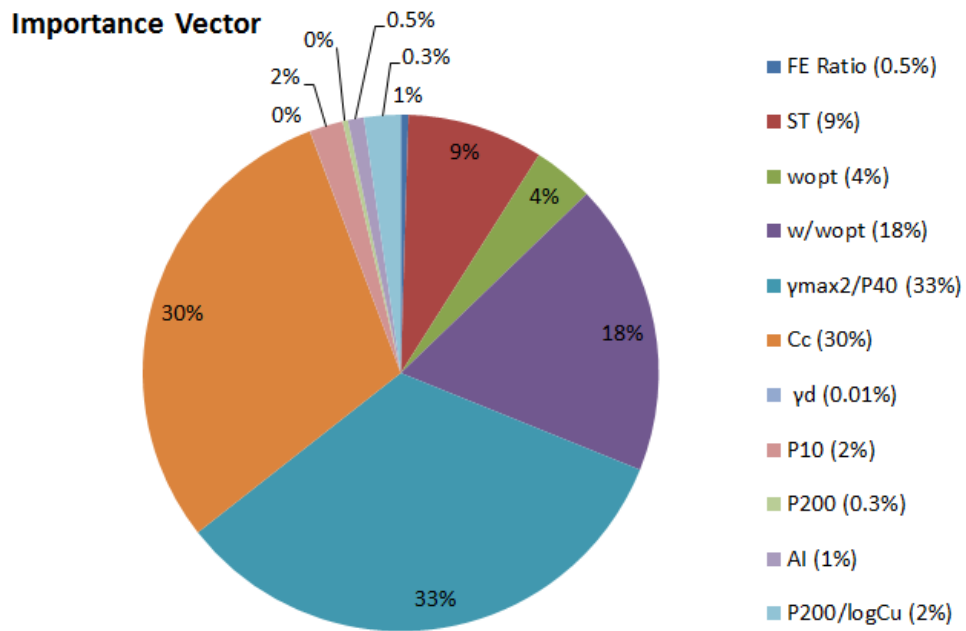


Figure 5.6. Relative Contributions of Various Variables to Resilient Modulus (M_R)

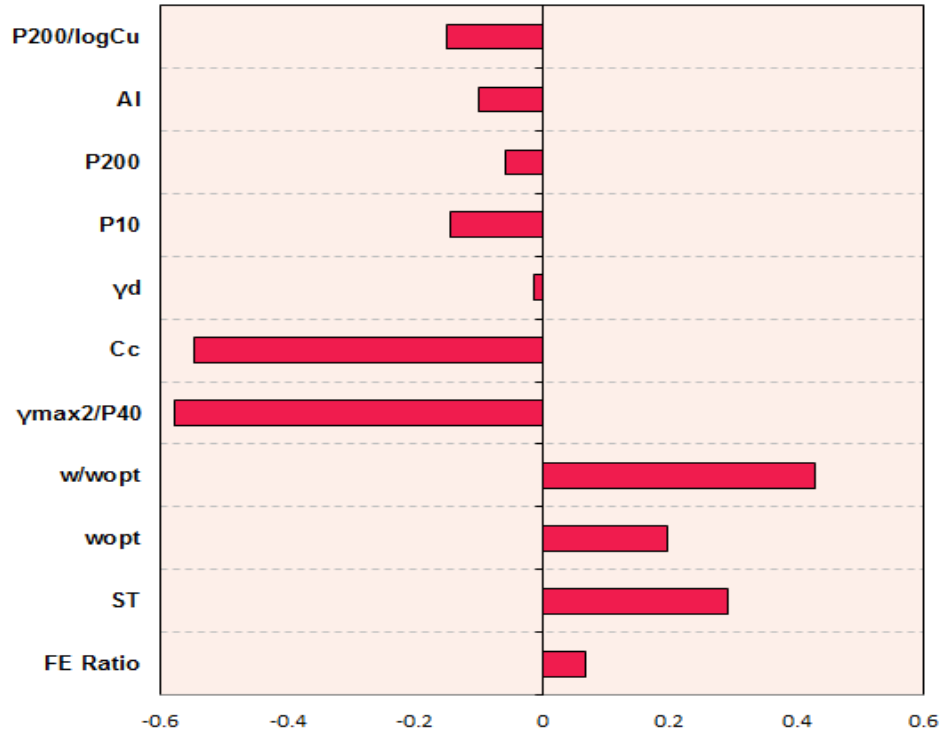


Figure 5.7. The Relative Contribution of Each Variable to Resilient Modulus (M_R)

Table 5.17. Sensitivity of Variables Studied with the Reliability Index

	Sensitivity with respect to Mean	Sensitivity with respect to Standard Deviation
<i>FE ratio</i>	-0.063	0.038
<i>ST</i>	-0.277	0.160
ω_{opt}	-0.144	-0.030
ω / ω_{opt}	-3.261	3.095
γ_{max}^2 / P_{40}	0.002	0.001
C_c	6.636	5.376
γ_d	0.003	0
P_{10}	0.009	0.003
P_{200}	0.034	-0.010
<i>AI</i>	0.002	0.001
$P_{200} / \log C_u$	0.141	0.031

5.8 Summary

This chapter presented the establishment of regression based correlations between aggregate source properties and aggregate M_R data archived through modulus testing at the laboratories of MnDOT and University of Minnesota, for identifying mechanistic design moduli ranges of locally available materials in Level 2 pavement design applications. The effects of both stress sensitivity and seasonal variations are captured using the MEPDG M_R model with three model parameters, i.e., k_1 , k_2 , and k_3 . The commercial software, SAS[®], is used to develop the statistical correlations. Aggregate shape properties measured from the University of Illinois Aggregate Image Analyzer (UIAIA) and quantified through shape indices for 9 Minnesota aggregate samples are also included in the study to improve developed correlations.

Monte Carlo type simulations using the software @Risk and the FORM analysis are presented to assess the sensitivities of M_R at given stress states to aggregate source properties. The detrimental effect of excessive moisture within pavement layers was also confirmed from the Monte Carlo simulation. The currently used aggregate base/granular subbase design moduli in MnPAVE Minnesota DOT mechanistic analysis and design program for the standard fall season were compared with the simulated M_R distributions, and the design reliability of at least 85% was achieved for the selected conventional flexible pavement structure with aggregate base and granular subbase.

FORM analysis was performed using FERUM program based on the developed model for estimating M_R . The importance vector and the sensitivity of reliability index with respect to distribution parameters of different variables were investigated. It was concluded that the complex maximum dry density (γ_{\max}^2 / P_{40}), coefficient of curvature (C_c), and relative moisture content ratio (ω / ω_{opt}) have the most important contributions to the resilient modulus behavior, and that the resilient modulus behavior is most sensitive to the variability in the distribution of coefficient of curvature (C_c) and relative moisture content ratio (ω / ω_{opt}). Future work is needed to refine the distributions of those aggregate source property variables provided that more data are available; moreover, the significant negative correlations existing between several variables caused problems when running FERUM program, leading to the slight modification of those correlation coefficients. This issue will also need to be looked into in more detail.

Chapter 6 MnPAVE Sensitivity Analyses of Design Inputs to Pavement Life Expectancies

6.1 Introduction

The main objective of this chapter is to investigate effects of unbound aggregate layer characteristics (i.e., material quality affecting modulus input and layer thickness) on conventional flexible pavement performances predicted from MnPAVE program. It is expected that the findings will help verify the current understanding of pavement performance and assist design engineers in selecting better and more appropriate strategies including the optimized use of locally available aggregate materials in pavements in order to achieve cost-effective and satisfactory pavement performance.

A comprehensive mechanistic analysis matrix was carefully designed with various scenarios considering pavement structure and climatic effects. Two mechanistic aggregate inputs, i.e., resilient modulus and peak deviator stress at failure, were used to uniquely characterize the approximately 376 different Minnesota aggregates considered for quality ranges in the sensitivity analyses. The MEPDG stress-dependent M_R models were used to identify k_1 - k_2 - k_3 model parameters associated with high, medium and low M_R levels of representative aggregate materials, i.e., MnDOT Class 5 and 6 materials for aggregate base and Class 3 and 4 materials for granular subbase from MnDOT laboratory-tested M_R database. Using the MEPDG stress dependent models, the GT-PAVE nonlinear finite element (FE) program predicted modulus distributions in the base and subbase layers. Averaging the moduli along the load axis throughout each layer depth established equivalent single M_R values in base and subbase for subsequent input into MnPAVE program so that fatigue and rutting life expectancies could be studied.

6.2 Representative Aggregate Quality Levels

According to the literature review, classifying unbound aggregates into different quality levels by mechanistic means requires the simultaneous examination of resilient modulus and permanent deformation behavior; the second linked to shear strength properties. Provided that the MEPDG M_R model is selected to characterize the nonlinear stress-dependent behavior of unbound aggregate materials, the corresponding M_R model parameters k_1 - k_2 - k_3 then can be assigned based on material quality. If one combination of parameters k_1 - k_2 - k_3 results in the greatest calculated M_R value for any predetermined stress level, then the aggregate material from which this combination was determined would most probably have the highest quality level in terms of resilient behavior; however, in order to avoid potential exceptions, permanent deformation behavior and shear strength properties should also be checked to confirm these levels identified according to M_R values. To accomplish this, regression-based predictive models for strength and resilient modulus characteristics were developed for up to 376 Minnesota aggregate materials according to their source properties in Chapter 5. In addition to gradation, fines content (or percent passing No. 200 sieve), moisture content and dry density, aggregate particle shape properties, such as texture and angularity quantified by imaging based indices, were also included as predictor variables in those correlations. The main goal was to estimate mechanistic design inputs from aggregate properties without the need for conducting time-consuming and costly laboratory performance tests.

The MnDOT M_R database used in this study includes the results of M_R tests conducted by the MnDOT Office of Materials and Road Research and/or its contracting agencies on different Minnesota project base and subbase materials of different MnDOT classes. After completion of M_R tests, specimens were typically loaded to failure at 4-psi (27.5-kPa) confining pressure and a constant rate of 0.03-in./s (0.76-mm/s) to obtain the peak deviator stress values. As compared to the cohesion “c” and friction angle “ ϕ ” which may not be consistent when individually compared, such peak deviator stresses at failure can be used to consistently compare shear strength characteristics of different aggregate samples. Note that the three representative aggregate materials with high, medium, and low modulus results were selected from a pool of 124 Class 5 and 6 aggregate base materials and 64 Class 3 and 4 granular subbase materials. As illustrated in Figure 6.1(a) and (b), two typical stress levels were chosen associated with field unbound aggregate base and granular subbase conditions, respectively, and the averaged M_R values are also shown for each stress level.

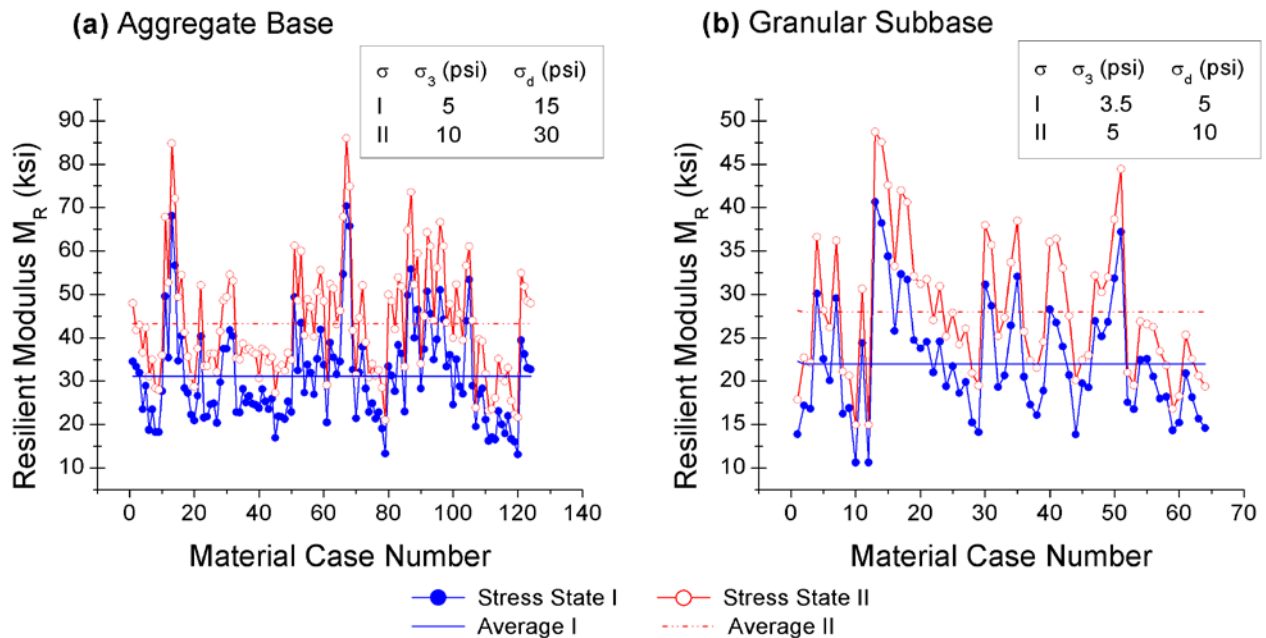


Figure 6.1. Computed Resilient Moduli for Different Unbound (a) Aggregate Base and (b) Granular Subbase Materials (1 psi = 6.89 kPa)

The selected M_R model parameters k_1 - k_2 - k_3 for the three modulus/quality levels are listed in Table 6.1 for the MEPDG and Uzan (1987) characterization models. The particle size distributions of those selected aggregate materials and the MnDOT gradation specifications for different material classes are shown in Figure 6.2. Note that similar aggregate gradations shown in Figure 6.2 may have in fact significant differences in mechanical properties as depicted from Table 6.1. Further, the peak deviator stresses at failure for those selected unbound base and subbase materials, also listed in Table 6.1, confirm the representative quality levels assigned from resilient moduli. In other words, higher peak deviator stresses at failure are postulated to be associated with higher calculated M_R values to adequately represent high, medium, and low quality levels.

6.3 Sensitivity Analysis Matrix

To better evaluate the effects of various design features and site factors on predicted pavement performance, a full factorial sensitivity matrix was designed for MnPAVE analysis and design. The variables considered in the full factorial are listed in Table 6.2. Since the environmental conditions may have a significant effect on the performance of conventional flexible pavements, two representative climate zones in Minnesota, i.e., Beltrami County in north and Olmsted County in south, were selected. With regard to the two climate zones studied, a move to Beltrami County in the north from Olmsted County in south Minnesota brings the following seasonal considerations into pavement analysis and design: (i) lower winter temperatures, (ii) lower summer temperatures, (iii) longer winter and shorter summer durations; and (iv) no seasonal factor differences to base, subbase, or soil. Different pavement sections were also analyzed to represent a wide spectrum of structural designs. Since the main goal was to investigate effects of unbound aggregate quality and layer thicknesses on pavement performance, the unrealistic pavement design alternatives, which might be found in the developed sensitivity analysis matrix, were not specifically excluded from the mechanistic analyses. Both aggregate base and granular subbase layers were modeled as nonlinear isotropic materials using the MEPDG resilient modulus models. The asphalt concrete surface layer using PG58-34 binder and the subgrade, however, were simplified as linear elastic materials. It is worth noting that the elastic modulus of asphalt concrete layer was taken from the default value in MnPAVE program; and that the elastic modulus of natural subgrade was taken as 50 percent of that of engineered subgrade. A total number of 2,592 pavement section combinations were analyzed.

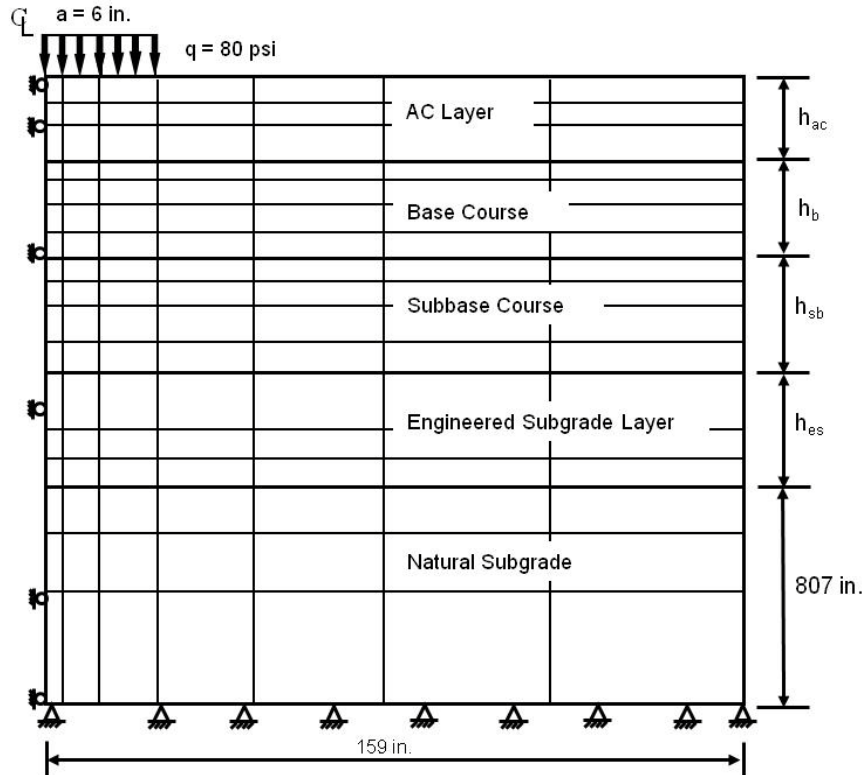
Table 6.2. Input Values for All the Variables Used in the Sensitivity Analysis

Input Category	Input Variables		Number of Variables
Climate Zones	Beltrami and Olmsted		2
Design Traffic Volume (20-year ESALs in Millions)	0.2, 0.6, 1.5, 3, and 6		5
Asphalt Concrete (AC) Layer	Type of Asphalt Binder	PG58-34	1
	Layer Thickness (in.)	4, 6, and 8	3
Aggregate Base Layer	Quality Levels	Low, Medium, and High quality Class 5/6	3
	Layer Thickness (in.)	3, 6, 9, and 12	4
Granular Subbase Layer	Quality Levels	Low, Medium, and High quality Class 3/4	3
	Layer Thickness (in.)	6, 12, and 18	3
Engineered Subgrade Layer	Elastic Modulus (ksi)	2, 4, 7, and 10	4
	Layer Thickness (in.)	12, and 36	2

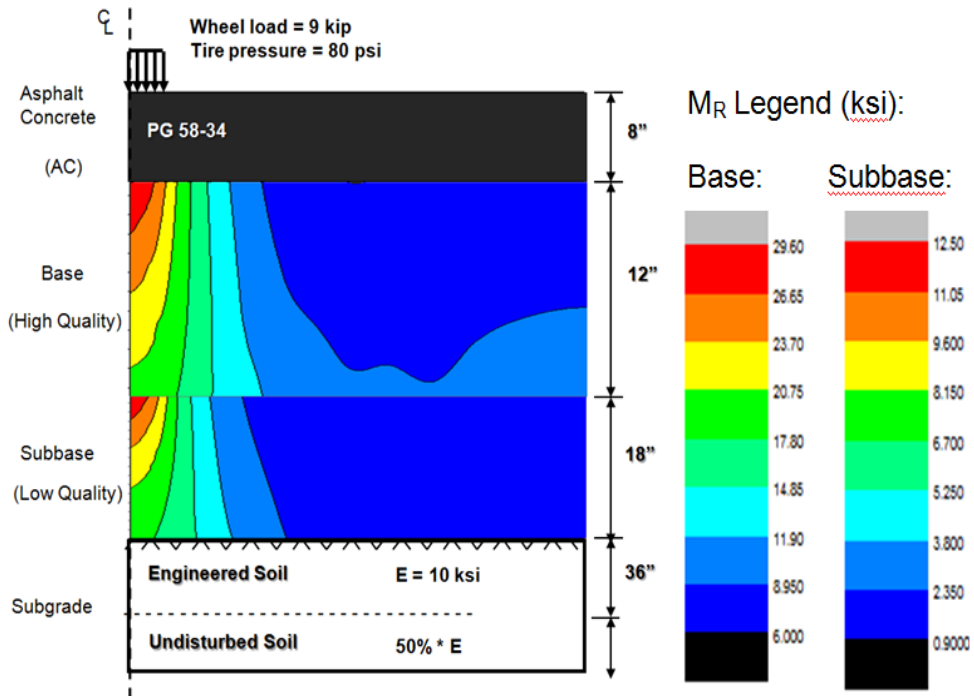
Note: 1 ksi = 6.89 MPa; 1 in. = 25.4 mm.

6.4 GT-PAVE Structural FE Modeling

Developed at Georgia Institute of Technology in 1996, the nonlinear finite element program GT-PAVE uses isoparametric eight-node quadrilateral elements to analyze a flexible pavement as an axisymmetric solid consisting of either linear or nonlinear elastic layers with an optional cross-anisotropic characterization of the granular layers (Tutumluer, 1995). For the analyses of conventional flexible pavements, predicted responses by the axisymmetric GT-PAVE finite element (FE) program have been validated in several instances in the past with measured data from instrumented full-scale pavement sections as well as verified with similar computed responses by the commercial ABAQUSTM FE program (Tutumluer, 1995; Kim, 2007). In this study, the Uzan base/subbase models were employed in GT-PAVE for the characterization of the unbound aggregate base and granular subbase layers. The GT-PAVE FE mesh designed consisted of 780 isoparametric eight-node quadrilateral elements used to analyze each pavement section consistently with the same mesh in the sensitivity matrix. The FE mesh used and the typical distributions of predicted stress dependent moduli in both aggregate base and granular subbase layers are illustrated in Figure 6.3 for one pavement section studied out of 2,592 analyses.



(a) Finite Element Mesh of Pavement Structure (Not to Scale)



(Not to Scale)

(b) Predicted Modulus Distributions in the Base and Subbase (1 ksi=6.89 MPa; 1 in.=25.4 mm)

Figure 6.3. Illustrations of GT-PAVE (a) Finite Element Mesh and (b) Modeling Results

The single wheel load of 9 kip (40 kN) was applied as a uniform pressure of 80 psi (552 kPa) over a circular area of radius 6 in. (152 mm). The Poisson's ratios for asphalt concrete, unbound aggregate base/granular subbase, and engineered/natural subgrade were taken as 0.3, 0.4, and 0.45, respectively. The MnPAVE default elastic modulus of 490 ksi (3,380 MPa) in the Fall season was used for the PG58-34 asphalt concrete. The equivalent single M_R values for the aggregate base/granular subbase to be used in subsequent linear elastic MnPAVE analyses were obtained by averaging moduli throughout each layer depth from the elements located at the load axis. The results of such equivalent M_R values linked to high, medium and low aggregate quality levels are presented in Figure 6.4. Note that the equivalent M_R value associated with each quality level was averaged from all the pavement sections studied in the sensitivity matrix. It is worth noting that in some cases the granular subbase material had much larger moduli than the aggregate base (see Figure 6.4).

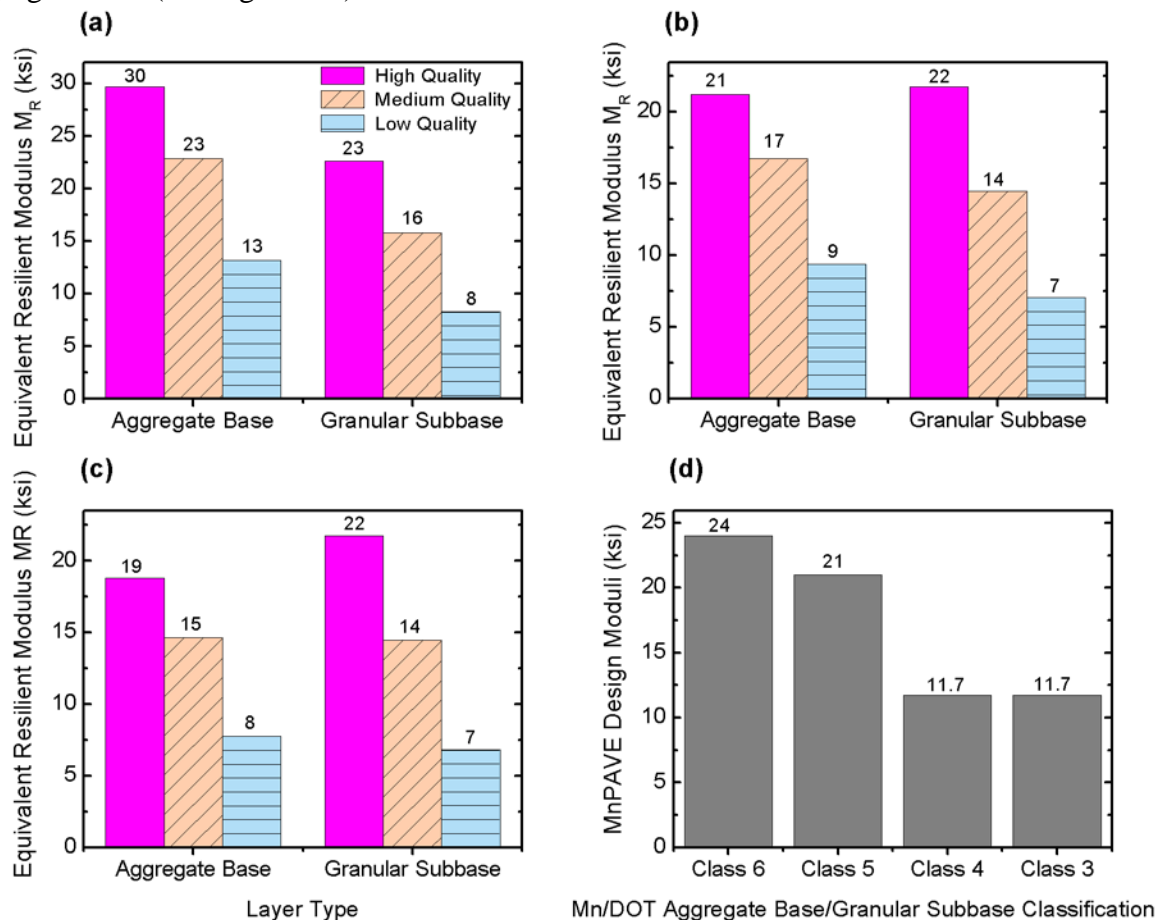


Figure 6.4. Equivalent M_R Values Linked to Aggregate Quality for (a) 4-in., (b) 6-in., (c) 8-in. Asphalt Surface Thicknesses and (d) Current Default MnPAVE Fall Design Moduli (1 in. = 25.4 mm; 1 ksi = 6.89 MPa)

6.5 Sensitivity Analysis Results and Discussion

The nonlinear FE program GT-PAVE predictions were a key step for establishing the single equivalent M_R values for the high (H), Medium (M) and low (L) modulus levels of aggregate base and granular subbase as shown in Figure 6.4. Those equivalent M_R values,

assumed to closely represent the related H, M, and L material quality standards, were subsequently input during MnPAVE analyses to calculate fatigue and rutting life expectancies. The MnPAVE program was run for all 51,840 combinations with each run generating an Excel spreadsheet file including the damage details. The major damage indicators are fatigue life, rutting life, fatigue damage ratio, and rutting damage ratio, though other distress indicators including International Roughness Index (IRI), alligator cracks (% of length), and rutting ≥ 0.5 in. (% of length) can also be predicted using empirical regression equations. In this section, pavement performance is mainly referred to rutting life and fatigue life, and the effects of various variables on rutting life and fatigue life were identified using the results from the cases studied.

6.5.1 Effect of Aggregate Quality on Fatigue Life Performance

Figure 6.5 shows pavement fatigue lives predicted according to the five design traffic levels studied for each base/subbase quality combinations in Beltrami and Olmsted Counties. The standard pavement structure consisted of 4-in. (102-mm) asphalt concrete surfacing over 12-in. (305-mm) of base and 12-in. (305-mm) of subbase over a 12-in. (305-mm) engineered subgrade ($E = 2$ ksi or 14 MPa) considered in Beltrami and Olmsted Counties. For low traffic designs, less than 0.6 million equivalent single axle loads (ESALs), base and subbase quality is less important for achieving 20-year fatigue and rutting performance lives, even in the case of 4-in. (102-mm) thick asphalt concrete surfacing (see Figure 6.5). For low-volume roads, using locally available and somewhat marginal materials may therefore be quite cost-effective. However, for traffic designs greater than 1.5 million ESALs, aggregate material quality becomes quite critical for the fatigue performance.

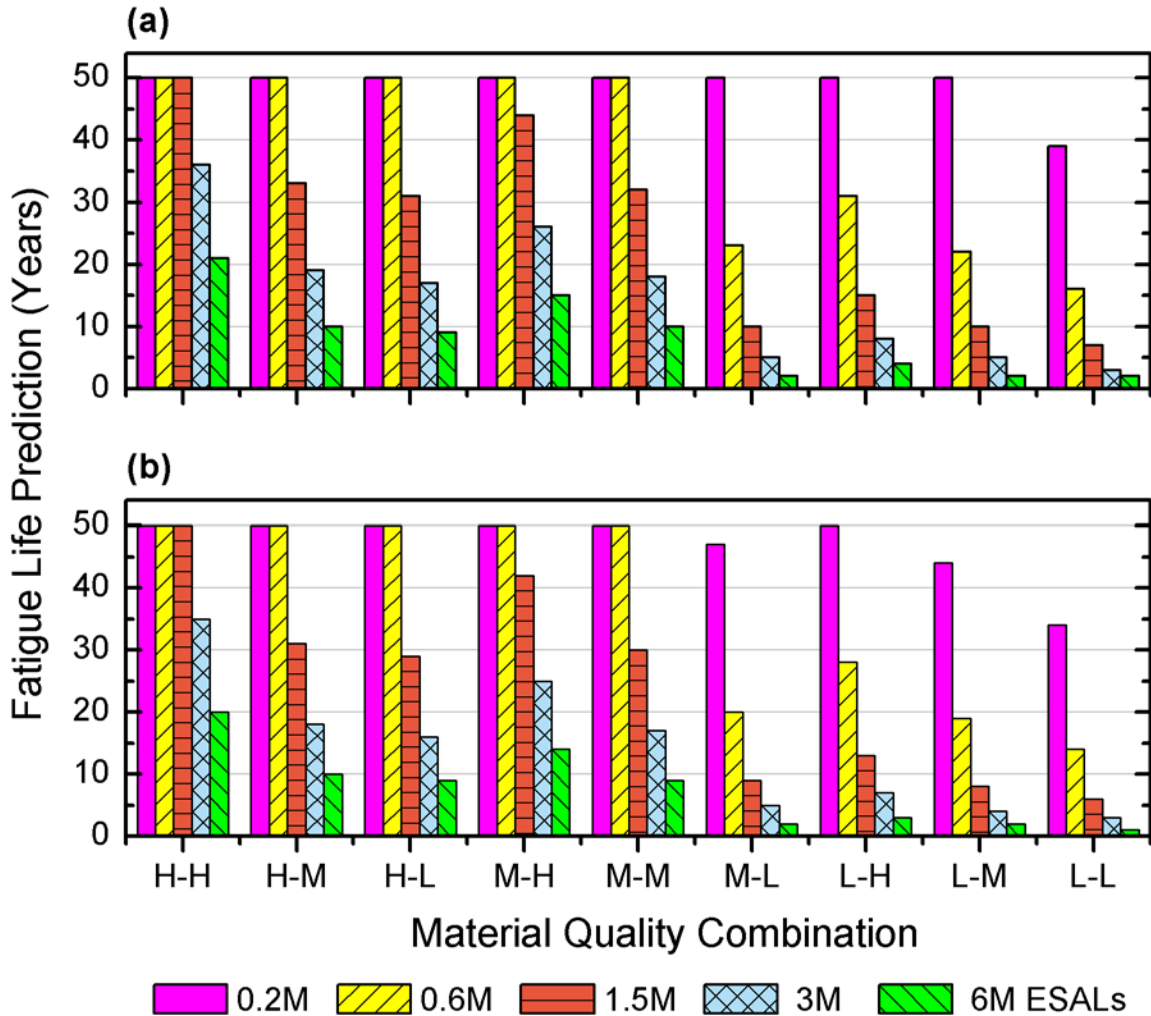


Figure 6.5. Fatigue Life Predictions for Different Base-Subbase Qualities in (a) Beltrami and (b) Olmsted Counties (M-L Stands for Medium Quality Base and Low Quality Subbase)

The main effect of this change is expected to be on asphalt pavement surface temperatures and accordingly on fatigue performances, which was also supported by the similar results for the case of Olmsted County (see Figure 6.5b).

The effect of unbound aggregate quality on pavement fatigue life prediction is further illustrated in Figure 6.6 for the case of Beltrami County. Figure 6.6 shows the percentages of pavement sections (y-axis) having service lives greater than a certain target performance life (x-axis). Important conclusions can be drawn from Figure 6.6 in terms of overall fatigue life, using high (H) quality base and low (L) quality subbase material combinations does not make any significant difference from the use of low quality (L) base and high (H) quality subbase material combinations; however, a large decrease in fatigue life can be seen when the qualities of base and subbase materials both are changed from high (H) to low (L). Further, the quality of base layer has been found to directly impact fatigue life expectancy. With low quality materials used in the base, increasing base layer thickness does not seem to improve fatigue life as there is not enough support under the asphalt concrete surfacing to minimize bending under wheel loading.

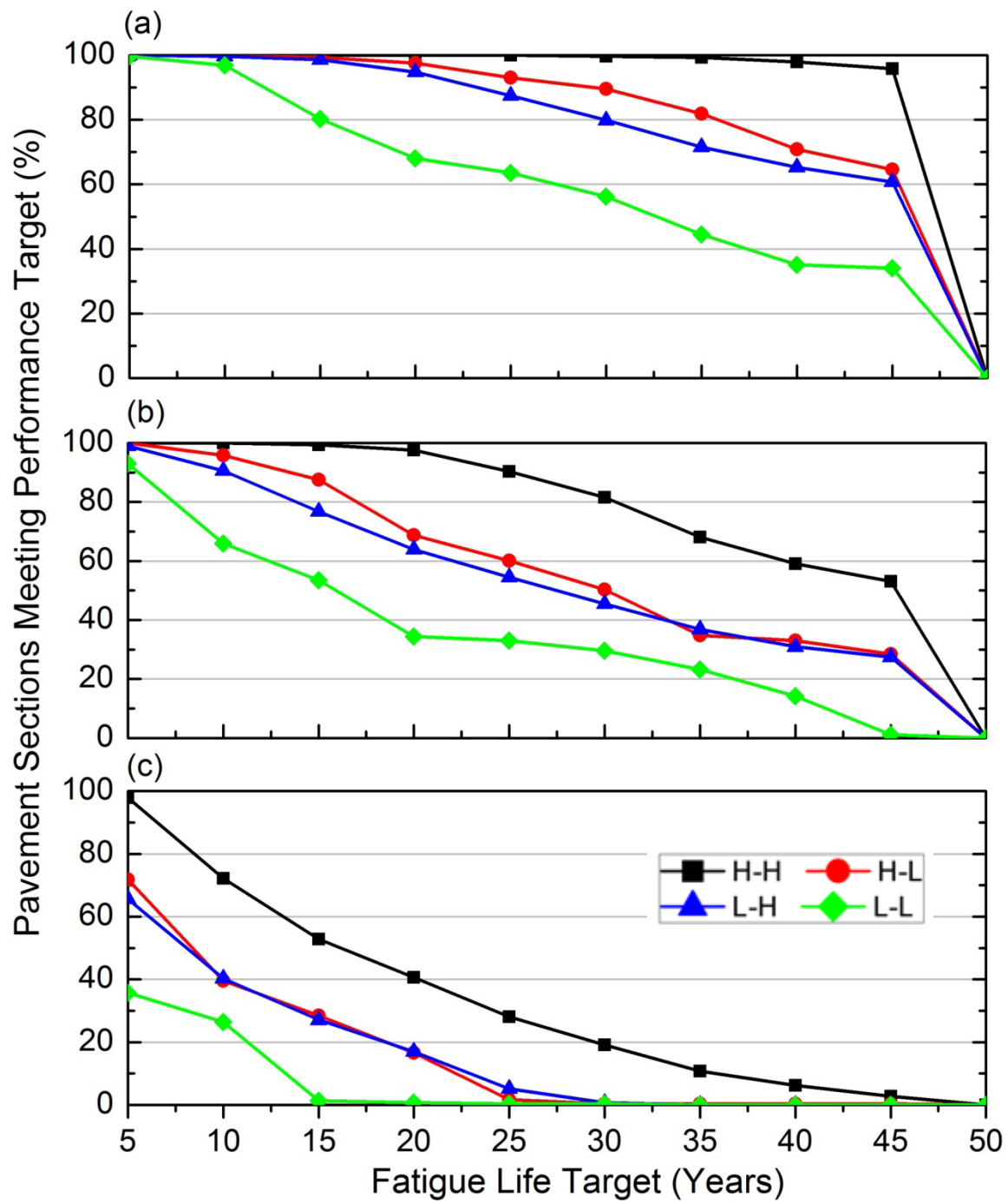


Figure 6.6. Effects of Unbound Granular Material Quality on Fatigue Life for Beltrami County: (a) 0.6 Million ESALs; (b) 1.5 Million ESALs; and (c) 6 Million ESALs (H-L Stands for High Quality Base and Low Quality Subbase)

6.5.2 Effect of Aggregate Quality on Rutting Life Performance

The effect of unbound aggregate quality on pavement rutting life prediction is illustrated in Figure 6.7 for both Beltrami and Olmsted Counties. The standard pavement structure again consisted of 4-in. (102-mm) asphalt concrete surfacing over 12-in. (305-mm) of base and 12-in. (305-mm) of subbase over a 12-in. (305-mm) engineered subgrade ($E = 2$ ksi or 14 MPa) considered in Beltrami and Olmsted Counties. For this pavement structure with the thinnest asphalt concrete thickness (4 in. or 102 mm), pavement rutting life decreases as the quality standards of base and subbase layers decrease from the high (H) to low (L), indicating stiff granular layers are required to maintain structural integrity and protect subgrade.

It can be seen from Figure 6.8 that, if the aggregate base quality decreases from high (H) to low (L), its effect on rutting performance is almost negligible for any traffic designs from 0.6 million to 6.0 million ESALs. Whereas, if a similar high (H) to low (L) quality drop is observed in the subbase, the rutting life is shortened more rapidly. Such a difference in the subbase behavior has been proven to be statistically significant when all the sensitivity results were analyzed. Accordingly, a high quality, stiff subbase exhibits a bridging effect to better protect the subgrade and offset some of the detrimental effects of low base stiffness, and as a result, the quality of base materials becomes less important. Note that this is the same concept as utilized in the South-African “Inverted Pavement” designs, which often use a cement-stabilized subbase over soft soils to effectively protect the subgrade while providing a very stiff underlying layer for the base course above, which enables compaction of aggregate base materials in excess of 100% Proctor densities.

The comparison between Beltrami and Olmsted County results revealed a less significant effect of climate on rutting performance, which might be attributed to a constant seasonal pore suction resistance factor of 1.0 used in these MnPAVE analyses.

The effects of different base and subbase material quality combinations on fatigue and rutting life predictions were statistically confirmed in the form of the notched box plots which compare two median values differing at the 95% confidence level and also from one-way Analysis of Variance (ANOVA) (McGill et al., 1978). According to the statistical analysis results, the granular subbase material quality makes a significant difference/impact on both predicted fatigue and rutting lives even for low quality aggregate base; however, aggregate base quality is primarily related to pavement fatigue performance.

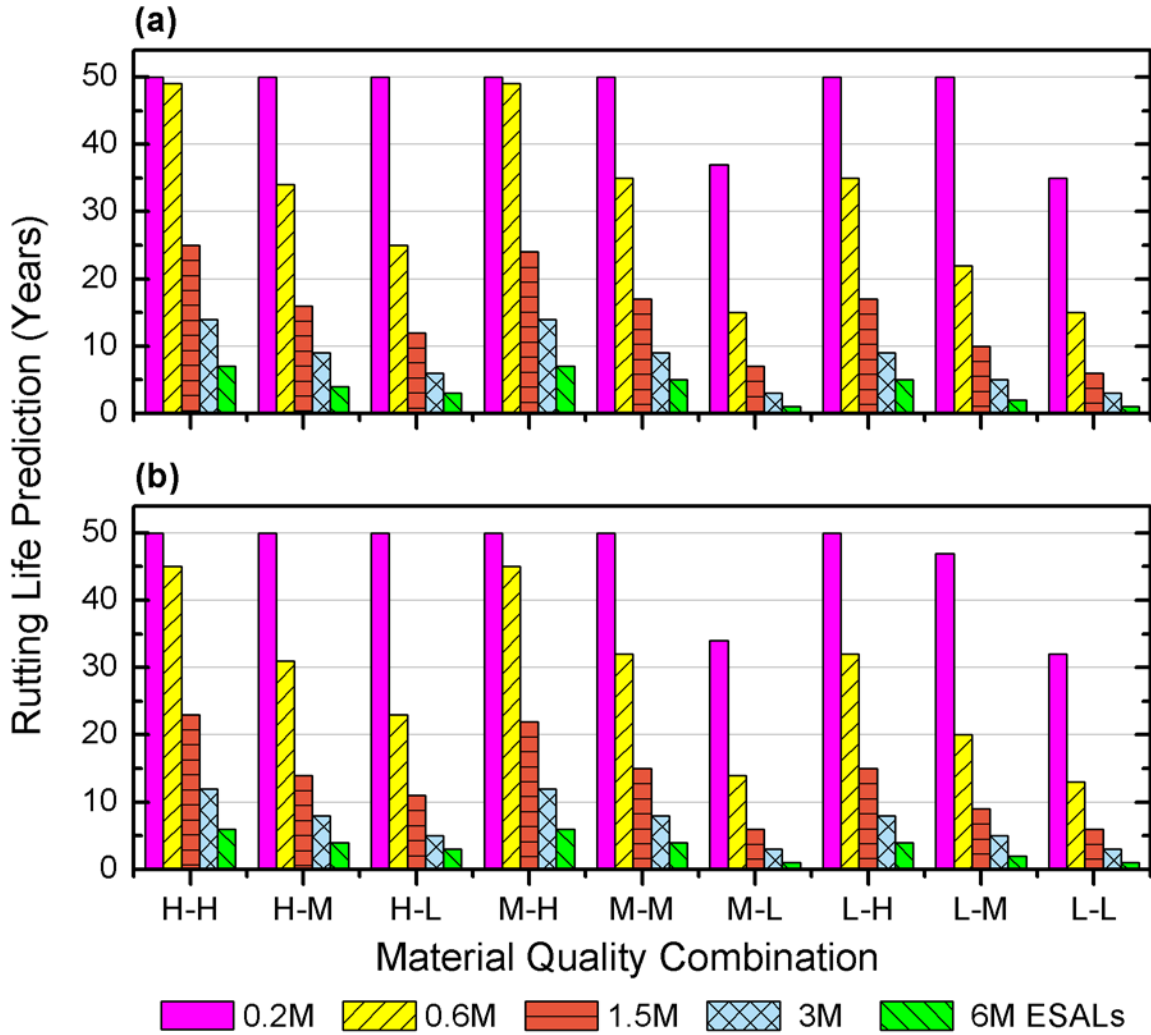


Figure 6.7. Rutting Life Predictions for Different Base-Subbase Qualities in (a) Beltrami and (b) Olmsted Counties (M-L Stands for Medium Quality Base and Low Quality Subbase)

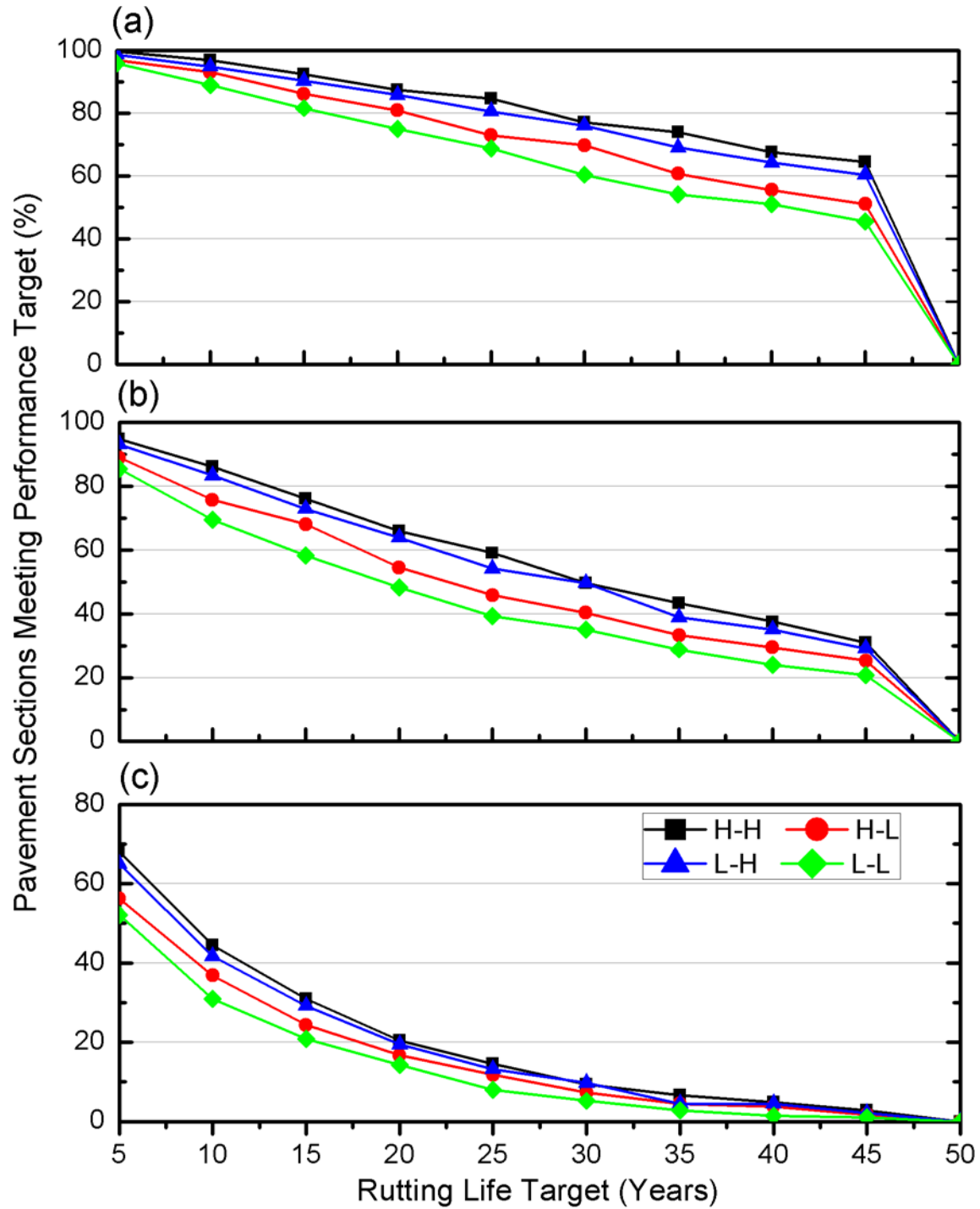


Figure 6.8. Effects of Unbound Granular Material Quality on Rutting Life for Beltrami County: (a) 0.6 Million ESALs; (b) 1.5 Million ESALs; and (c) 6 Million ESALs (H-L Stands for High Quality Base and Low Quality Subbase)

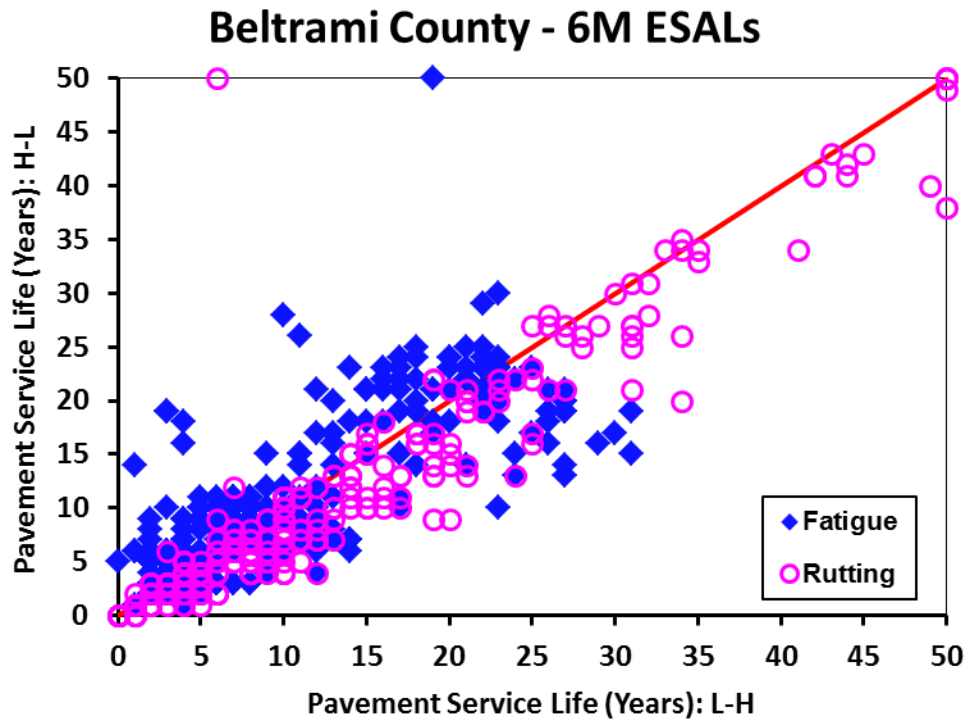


Figure 6.9. Pavement Service Life Comparison for Different Base and Subbase Quality Combinations (H-L Stands for High Quality Base and Low Quality Subbase)

Figure 6.9 shows the base and subbase quality combination effects in a different way for pavement structures in the Beltrami County with 6-million ESALs. Note that each data point in Figure 6.9 represents one pavement structure and pavement service lives greater than 50 years are treated as 50 years. It is clearly shown that all the data points corresponding to rutting lives are below the equality line, indicating low quality base and high quality subbase combinations result in rutting lives greater than high quality base and low quality subbase combinations. This demonstrates the importance of subbase quality on pavement rutting life expectancies.

From the sensitivity analyses the following general observations can also be made. Both fatigue and rutting life performances improve as asphalt concrete (AC) thickness increases, with higher fatigue performance and less rutting performance improvements expected for AC thickness increasing from 6 in. to 8 in. (152 mm to 203 mm) than from 4 in. to 6 in. (102 mm to 152 mm). Increasing aggregate base thickness may also result in longer fatigue life and significantly improved subgrade rutting life performance. For the same AC thickness, the rutting life performance increases considerably with increasing aggregate base thickness; and for the same AC and aggregate base thicknesses, the rutting life performance increases with increasing subgrade stiffness. Interestingly, increasing granular subbase thickness seems to significantly improve both rutting and fatigue performances. As compared to fatigue performance, rutting performance can benefit much more from an increase in granular subbase thickness. As expected, a stronger engineered subgrade contributes significantly to improved rutting performance.

6.6 Summary

A comprehensive matrix of conventional flexible pavement layer thicknesses and mechanistic design moduli was carefully designed to conduct MnPAVE sensitivity analyses to account for structural adequacy and performance requirements of different pavement sections in two climatic regions in north and south Minnesota. The type and quality of unbound aggregate materials were represented by one of the key mechanistic analysis inputs, the resilient modulus (M_R). Three representative sets of the MEPDG stress-dependent M_R model parameters, k_1 , k_2 , and k_3 , were selected for the aggregate base and subbase layers from the MnDOT laboratory-tested MR database studied under Task 3. The materials considered for base were MnDOT classes 5 and 6; and for subbase, material classes 3 and 4 were used. Typical representative stress states considered within aggregate base and subbase layers were identified to establish the M_R model parameters associated with high (H), medium (M), and low (L) MR levels. The nonlinear finite element (FE) program GT-PAVE was then used to determine the single equivalent M_R values for the granular base and subbase by averaging layer moduli distributions computed from the nonlinear GT-PAVE FE analyses. Those equivalent M_R values, assumed to closely represent the related H, M, and L material quality standards, were subsequently inputted into MnPAVE analyses to calculate fatigue and rutting life expectancies for the comprehensive matrix of pavement structures considered.

The findings from the MnPAVE analyses indicate that for low traffic designs, less than 0.6 million equivalent single axle loads (ESALs), base and subbase quality is not so significant for achieving 20-year fatigue and rutting performance lives, even in the case of 4-in. thick asphalt concrete surfacing. For low-volume roads, using locally available and somewhat marginal materials may therefore be quite cost-effective. However, for traffic designs greater than 1.5 million ESALs, aggregate material quality becomes critical for the fatigue and rutting performances. The quality of base layer has been found to directly impact fatigue life expectancy. With low quality materials used in the base, increasing base layer thickness does not seem to improve fatigue life as there is not enough support under the asphalt concrete surfacing to minimize bending under wheel loading. Whereas, increasing base thickness significantly improves subgrade rutting performance. As expected, a stronger Engineered Subgrade contributes significantly to improved rutting performance. Increasing engineered subgrade thickness from 12 in. to 36 in. has negligible effects on both rutting and fatigue performances when the underlying soil is stable which assures compaction of the engineered subgrade and overlying subbase and base courses. Interestingly, increasing subbase thickness seems to significantly improve both rutting and fatigue performances. As compared to fatigue performance, rutting performance can benefit much more from an increase in subbase thickness.

A move to Beltrami County in the north from Olmsted County in southern Minnesota also brings the following seasonal changes into pavement analysis and design: (i) lower winter temperatures, (ii) lower summer temperatures, and (iii) longer winter and shorter summer durations. The main effect of this change is on asphalt pavement surface temperatures and accordingly on fatigue performances. A less significant effect of climate on rutting performance may be attributed to a constant seasonal pore suction resistance factor of 1.0 used in all the MnPAVE analyses at this stage.

Instead of using both high (H) quality base and subbase materials, if either one of the base or subbase quality decreases from the high (H) to low (L), a similar percent reduction in fatigue life has been determined for any traffic designs in the range of 0.6 million to 6.0 million ESALs.

The most interesting of all, subbase material quality seems to much more significantly impact rutting performance than the quality standards of base materials. If the base quality decreases from high (H) to low (L), its effect on rutting performance is almost negligible for any traffic designs from 0.6 million to 6.0 million ESALs. Whereas, if a similar high (H) to low (L) quality drop, e.g. material degradation of an existing subbase by subgrade intrusion, etc., is observed in the subbase, the rutting life is shortened more rapidly. According to the analysis results, a high quality, stiff subbase exhibits a bridging effect to better protect the subgrade and offset any detrimental effects of low base stiffness and as a result, the quality of base materials is less important. Note that this is the same concept as utilized in the South-African “Inverted Pavement” designs, which often use a stabilized subbase over soft soils to effectively protect the subgrade while providing a very stiff layer to enable compaction of the overlying granular base materials often in excess of 100% of achieved Proctor densities.

Chapter 7 Validation of Sensitivity Analysis Results Using Additional Aggregate Strength Data

7.1 Introduction

Resilient modulus (M_R) is an important mechanistic-empirical design input for computing pavement structural responses and linking them to performance through transfer functions. When two aggregate materials used in a pavement layer happen to exhibit similar modulus characteristics, the resilient load responses (stresses, strains, deflections) of the pavement system are similar regardless of the differences in the granular material types and properties. However, those two pavements that display similar load responses can perform quite differently thus addressing the need to distinguish between the structural response and the pavement performance. Unbound aggregate base/subbase layer performance is measured by rutting resistance primarily influenced by aggregate shear strength rather than “resilient modulus.” Shear strength property has been shown to be linked to granular material permanent deformation behavior, which corresponds to field rutting performance (Thompson, 1998). Low shear strength granular materials are more susceptible to permanent deformation. Past Mn/ROAD experience has shown that aggregate base/granular base permanent deformation may contribute significantly to the overall flexible pavement surface ruts (Dai et al., 2007). Therefore, careful attention must be directed to having not only high modulus but also sufficient shear strength in unbound aggregate layers so that contribution of these granular materials to pavement rutting can be minimized.

The relationship between modulus and strength was investigated for different MnDOT aggregate classes using additional aggregate strength data (peak deviator stresses at failure) from available MnDOT laboratory studies, as described in Chapter 4. Due to the limited number of datasets collected, the primary objective, however, was to verify if any consistent trends existed between modulus and strength (e.g., high shear strength for high modulus, etc.) for each MnDOT aggregate class. For MnPAVE sensitivity analyses presented in Chapter 6, it was postulated from limited M_R datasets that different M_R levels could be linked to high (H), medium (M), and low (L) material quality standards, in relation to strength properties. In other words, higher modulus was assumed in the sensitivity analysis to be indicative of better quality and lower pavement responses leading to higher pavement performance, i.e., shear strength/rutting resistance. Findings regarding modulus-strength relationships for Minnesota aggregate materials are of utmost importance to accurately interpret sensitivity analysis results in relation to ensuring relevant strength properties of the established material quality standards.

7.2 Modulus-Strength Relationships Observed for Different MnDOT Aggregate Classes

The resilient modulus values were calculated at the two representative stress levels (low and high) using the MEPDG M_R model with its model parameters k_1 , k_2 , and k_3 retrieved from the M_R database. As tabulated in Table 7.1, these representative stress levels were adopted as typical stress states within aggregate base and granular subbase from MnPAVE analysis by using default pavement-load combination in Minnesota (i.e., 18-kip single wheel load).

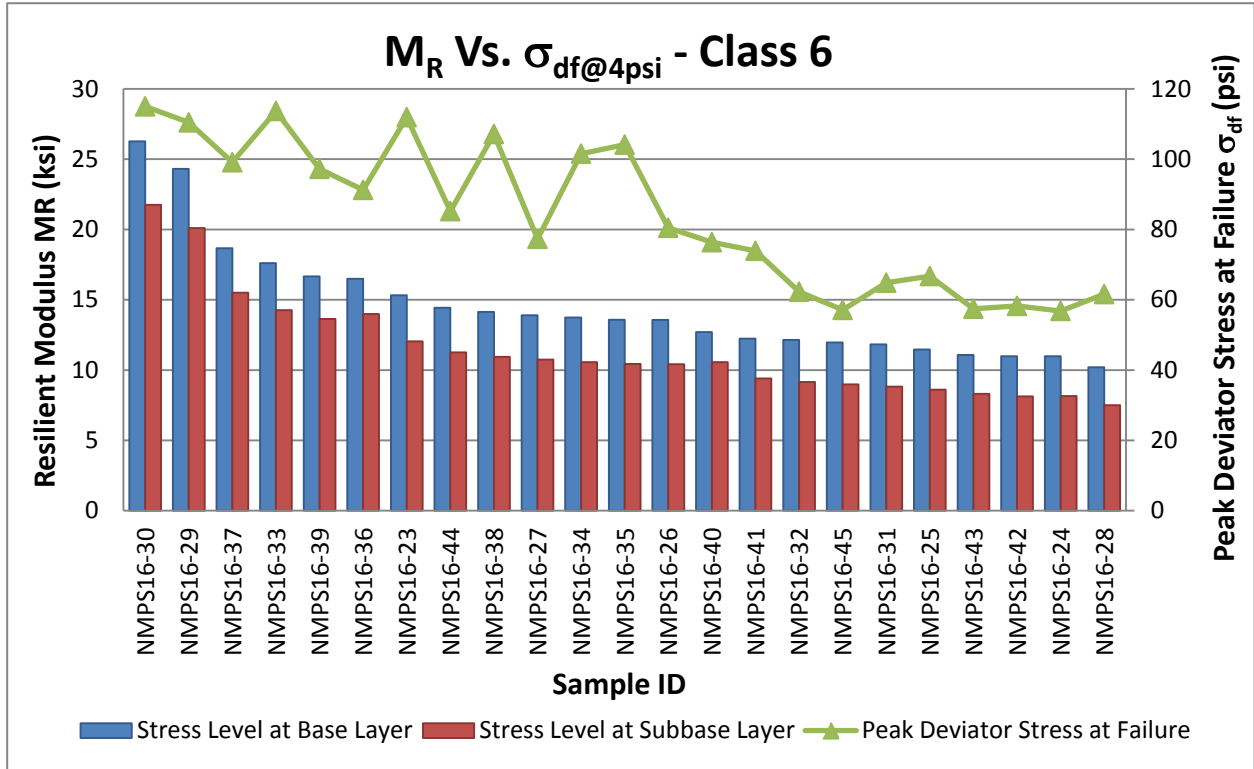
Table 7.1. Representative Stress Levels in Typical MnDOT Pavement Layers

MnDOT Pavement Layer	Layer Thickness		Representative Stress Levels		MnPAVE Fall Design Moduli	
	in.	cm	psi	kPa	ksi	MPa
HMA: PG 58-34	6	15.2	-	-	-	-
Aggregate Base: Class 6	6	15.2	$\sigma_1=9.0$ $\sigma_3=1.0$	$\sigma_1=62.1$ $\sigma_3=6.9$	24	164
Granular Subbase: Select Granular	18	45.7	$\sigma_1=5.0$ $\sigma_3=1.0$	$\sigma_1=34.5$ $\sigma_3=6.9$	11.7	81
Subgrade: Engineered Soil	12	30.5	$\sigma_1=4.5$ $\sigma_3=1.0$	$\sigma_1=31.0$ $\sigma_3=6.9$	-	-

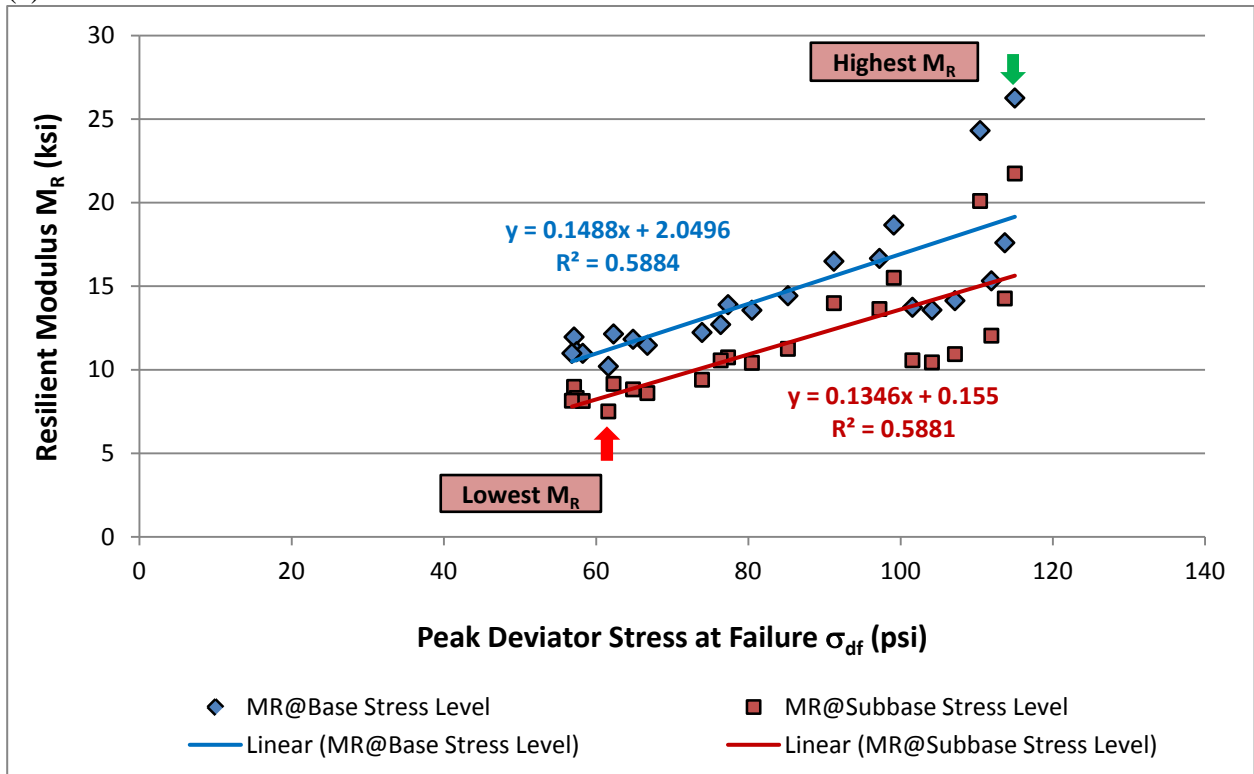
7.2.1 Aggregate Base Materials (Class 5/6)

Modulus-strength trends for Class 5/6 aggregate base materials are illustrated in Figure 7.1 and Figure 7.2. As the shear resistance of Class 6 aggregate materials, measured by the peak deviator stress at failure, decreases, M_R generally decreases except for a few cases where increased shear strength is observed (see Figure 7.1a). Overall, there exists a positive correlation between resilient modulus and the peak deviator stress at failure as highlighted in Figure 7.1b, and this correlation is reasonably significant with an R^2 value of 0.59.

For Class 5 aggregates, Figure 7.2a shows the peak deviator stress at failure (σ_{df}) to fluctuate as M_R decreases indicating somewhat inconsistent trends between modulus and shear strength. A positive correlation seems to exist between the modulus and shear strength as illustrated in Figure 7.2b. The sample IDs were renamed according to the Nominal Maximum Particle Size (NMPS), which was taken as one sieve size larger than the first sieve with more than 10% materials retained. The sample having the highest M_R (ID: NMPS25-1 denoting the 1st sample with NMPS of 25 mm or 1 in.) still has high enough shear resistance whereas the one with the lowest M_R value (ID: NMPS16-46) ends up having the lowest shear resistance. That is, the assumption made in MnPAVE sensitivity analysis, i.e., different M_R levels could be linked to high (H), medium (M), and low (L) material quality standards in relation to strength properties, is reasonably supported to a certain extent. In general, gravel materials exhibit lower M_R and shear strength than limestone samples.

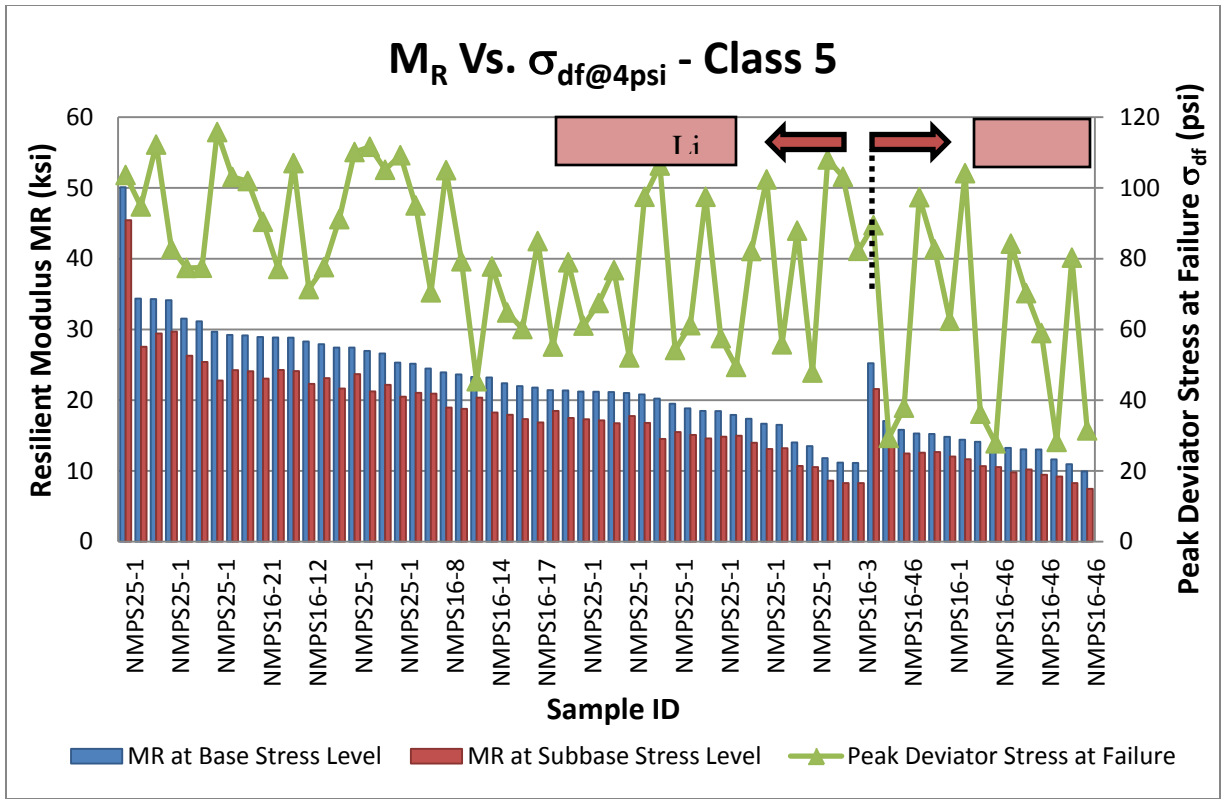


(a)

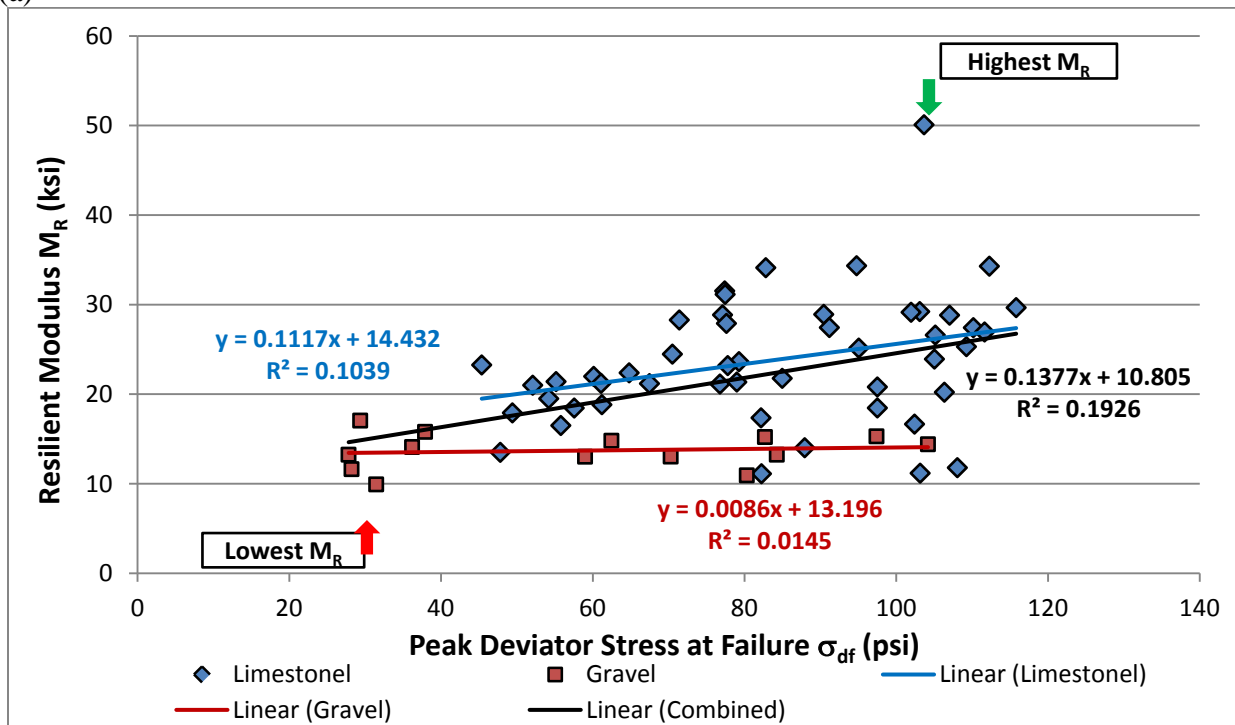


(b)

Figure 7.1. Resilient Modulus and Peak Deviator Stress (σ_{df@4psi}) Results – Class 6 Aggregates (NMPS16-30, for Example, Denotes the 30th Sample with NMPS of 16 in.)



(a)



(b)

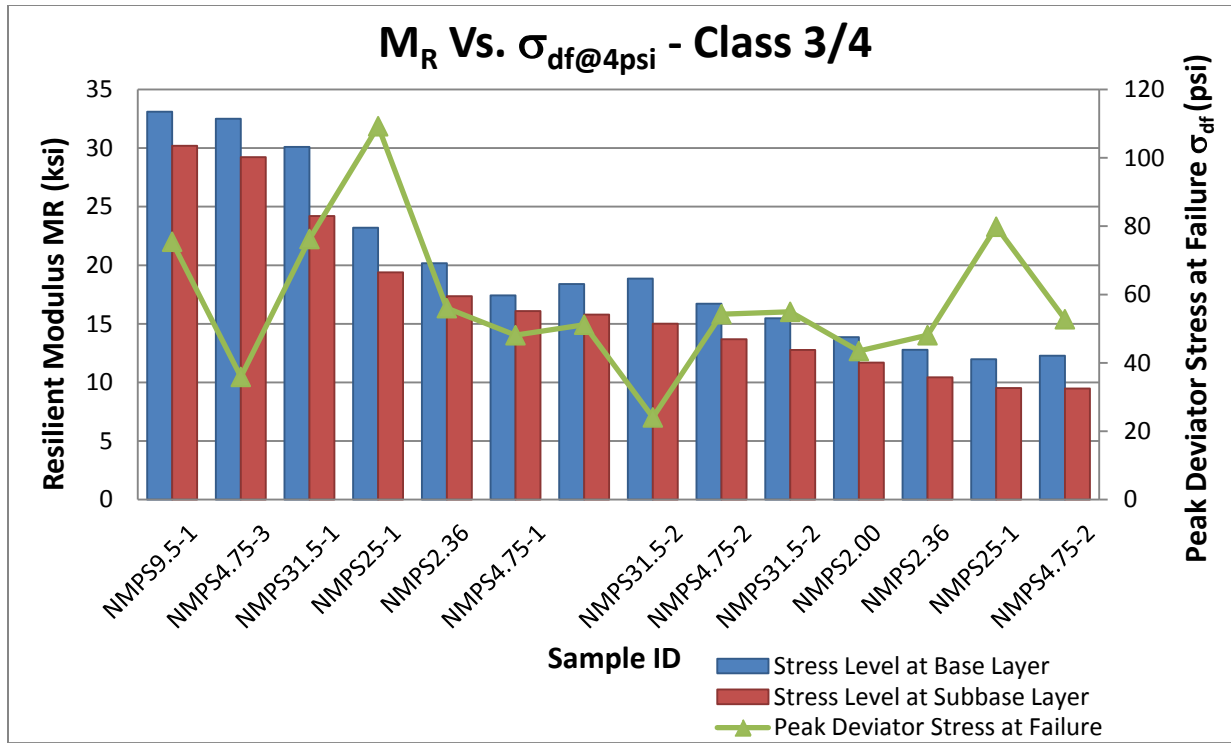
Figure 7.2. Resilient Modulus and Peak Deviator Stress (σ_{df@4psi}) Results – Class 5 Aggregates

Therefore, the three aggregate quality levels postulated in MnPAVE sensitivity analysis for Class 5 and 6 materials are somewhat in line with the strength data analyzed, i.e., high quality with high M_R gives somewhat high shear resistance, and low quality material with low M_R has reduced shear resistance. This observation, however, becomes much weaker for Class 5 materials to make them more susceptible to accumulate permanent deformation or potential rutting damage when constructed in pavements even though they are assigned a high layer modulus.

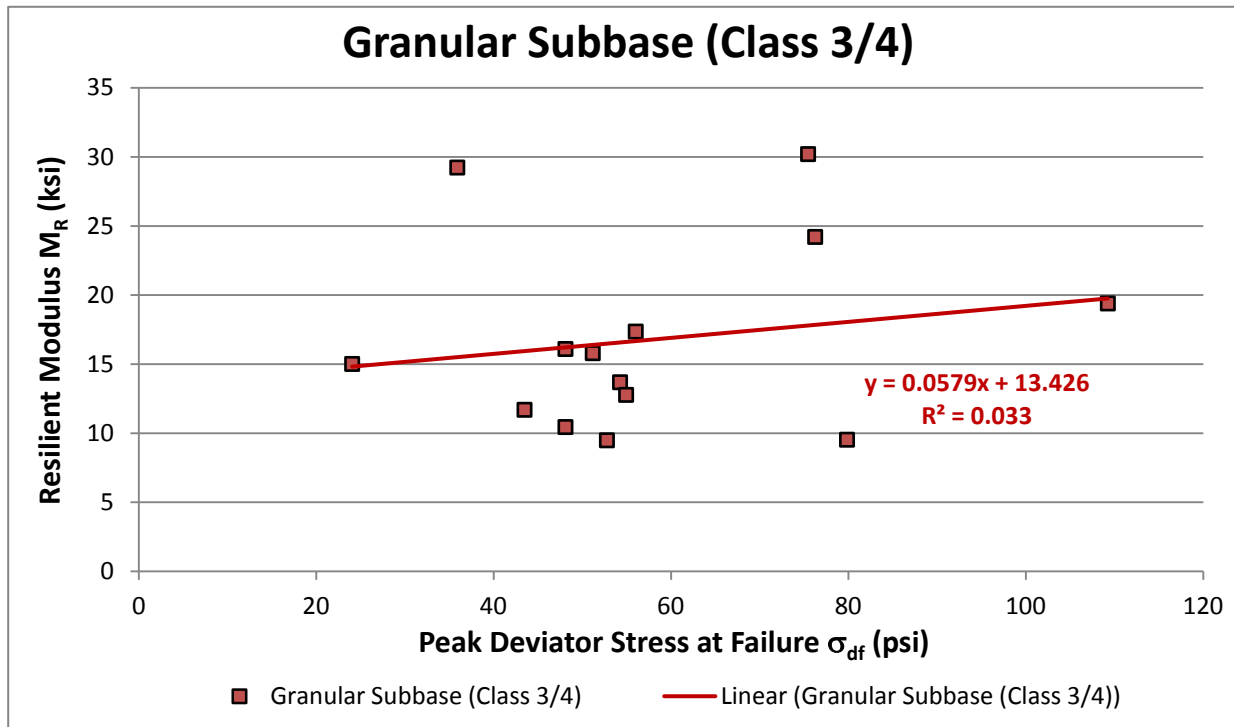
7.2.2 Granular Subbase Materials (Class 3/4)

Figure 7.3 explores the modulus-shear strength trends for Class 3/4 granular subbase materials combined. Note that the samples could not be further categorized into individual Class 3 or Class 4 due to the lack of such information in the database. In general, when M_R values steadily decrease, shear resistance stays more or less the same for these granular subbase materials except for one sample which exhibits low modulus but relatively high shear resistance and two samples that exhibit high to medium modulus but low shear resistance. A somewhat positive but statistically insignificant correlation exists between the modulus and shear resistance for Class 3/4 materials. The fact that some granular subbase materials exhibit high M_R but low shear strength may disqualify them from being considered as “high quality” for use in subbase layers as recommended in MnPAVE sensitivity analysis results. Note that the potential of a shear/rutting type failure associated with Class 3/4 granular subbase materials requires particular caution and further detailed investigation for proper pavement performance.

Another type of common subbase material, i.e., select granular, was also studied for modulus-shear strength trends, with results illustrated in Figure 7.4. The samples were separated into two groups according to the applied confining pressure at which the peak deviator stress at failure was obtained (either 4 psi or 8 psi).

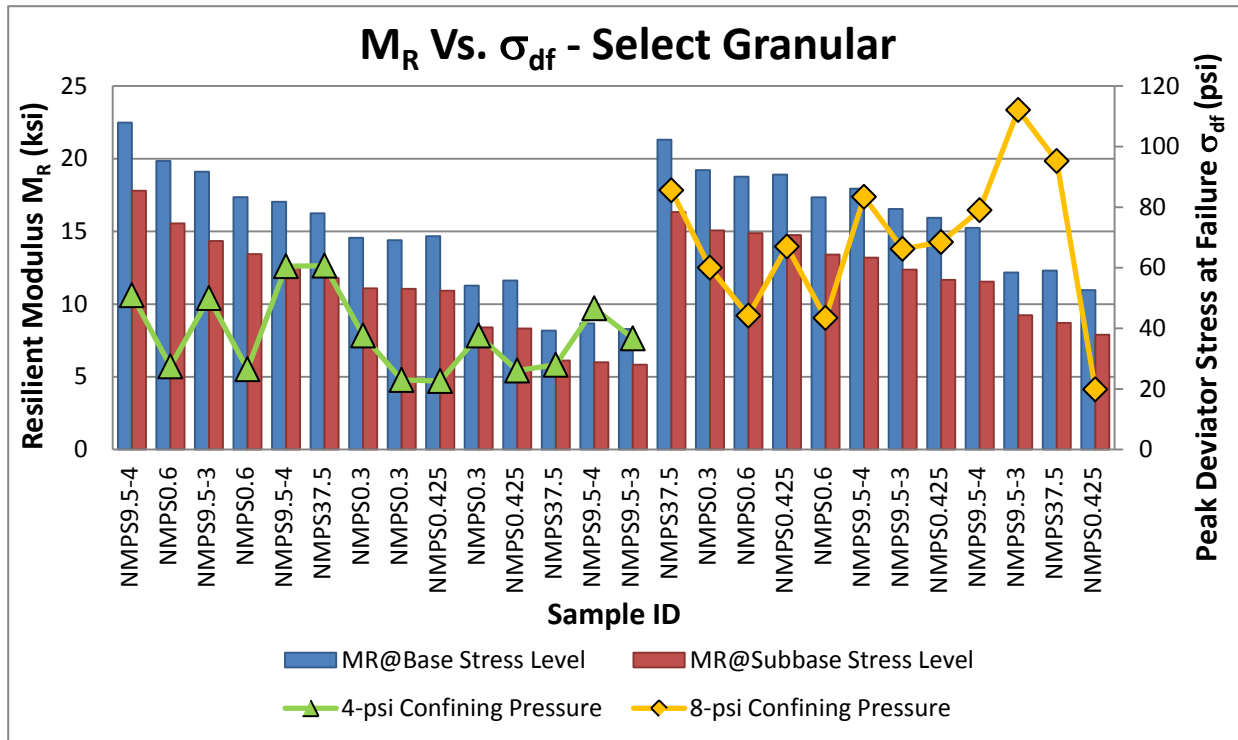


(a)

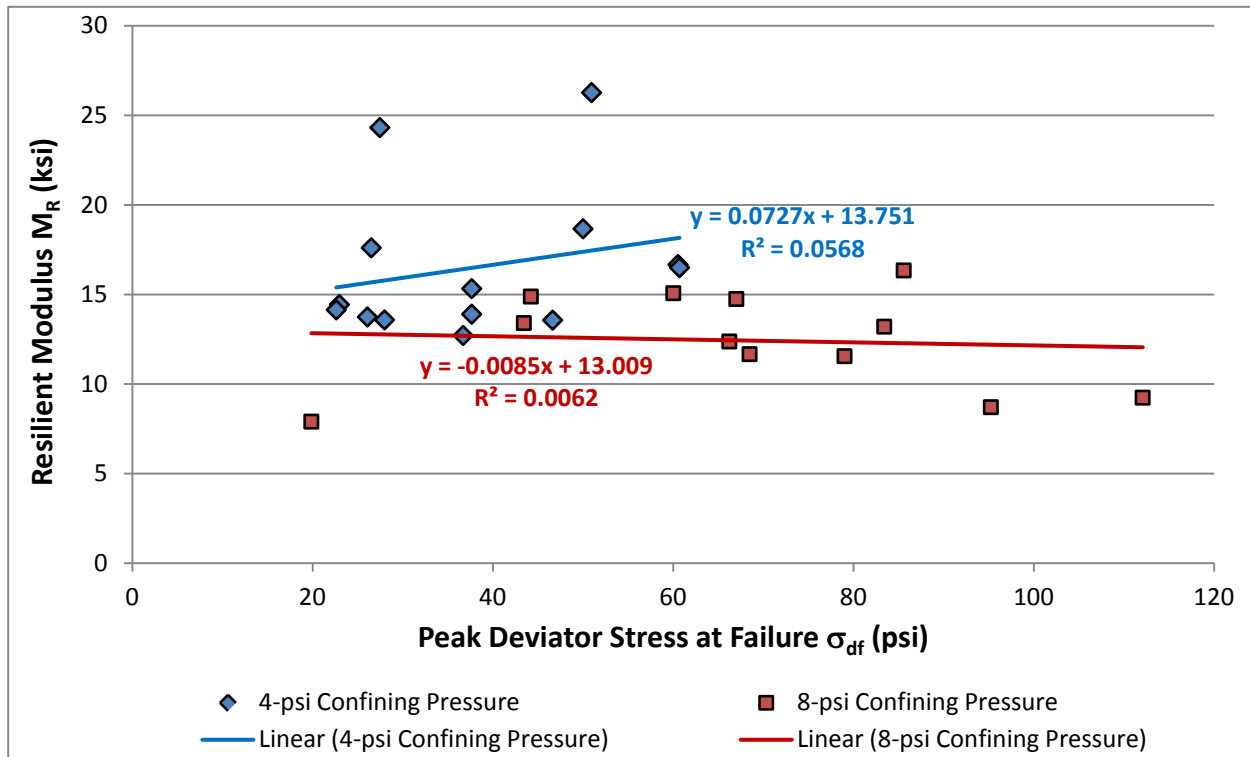


(b)

Figure 7.3. Resilient Modulus and Peak Deviator Stress ($\sigma_{df@4psi}$) Results for Combined Class 3 and 4 Granular Subbase Materials



(a)



(b)

Figure 7.4. Resilient Modulus and Peak Deviator Stress (σ_{df}) Results for Select Granular (Granular Subbase) Materials

As shown in Figure 7.4, no consistent trends could be observed for the two groups. In fact, surprisingly, samples with low to medium moduli exhibited the highest shear resistance; while some high M_R samples yielded low shear strengths, as mentioned previously. Figure 7.4b indicates that there is no statistically significant correlation between modulus and shear strength for the select granular samples studied.

In summary, strength and modulus properties of granular subbase materials may be governed by different factors as they do not follow consistent trends. Special caution should be used when applying MnPAVE sensitivity analysis results to pavement design practices. That is, the high modulus associated with high quality subbase materials as assumed in MnPAVE sensitivity analyses will be necessary for achieving high layer stiffness but it may not be sufficient for certain field applications and designs where subbase shear failure might be of a concern. A proper selection of aggregate materials to be used in aggregate base/granular subbase layers should provide both (1) high enough layer stiffness to minimize critical pavement responses, e.g., vertical strain/stress on top of subgrade, and (2) adequate shear strength to prevent rutting in the granular layer for a satisfactory pavement performance.

7.2.3 Salvaged Materials (Class 7)

Although beyond the original scope of this study, all the salvaged materials included in the additional strength data, such as Full Depth Reclamation (FDR), Recycled Asphalt Pavement (RAP), and Recycled Concrete Aggregate (RCA) were categorized as Class 7 and studied accordingly. Figure 7.5 shows four groups of materials formed according to the confining pressure (4, 5, 8, or 10 psi) at which the peak deviator stress at failure was recorded. Observed once again is that there are samples having medium to high modulus properties but low shear resistance. It is worth emphasizing that the mechanical behaviors of salvaged materials are quite complicated and still not well understood yet. Hence, the findings made here regarding salvaged materials are phenomenological only and not intended to be conclusive.

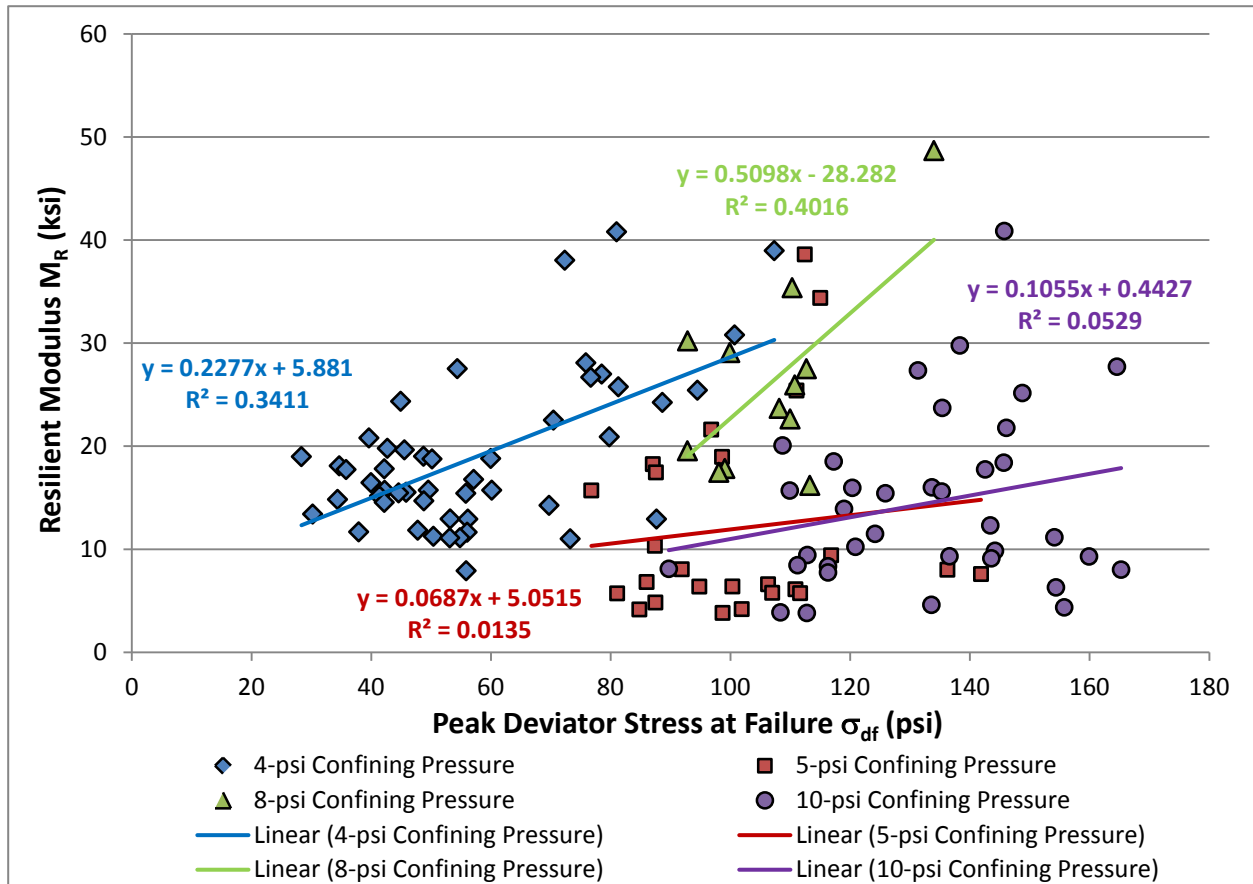


Figure 7.5. Resilient Modulus and Peak Deviator Stress (σ_{df}) Results for Class 7 Salvaged Materials

7.2.4 Important Implications

Note that all the previous observations were made from aggregate samples at varying moisture and density conditions in relation to optimum ones. It is revealed from literature reviewed in Chapter 2 that both resilient modulus and shear strength are affected significantly by the moisture and density deviations from optimum ones; therefore, it may be desired to minimize such deviations so that more confirmative observations can be made. To serve this purpose, “standard” aggregate samples with molded moisture contents within $\pm 0.5\%$ of the targeted optimum, as per the NCHRP 1-28A protocol, were chosen for further modulus-strength relationship investigation. This way, samples compared were closely kept at near optimum conditions with only gradations varying. Unlike the moisture contents, the achieved dry densities were not found to influence results significantly in this study, as the average relative compaction level (achieved dry density over the maximum dry density) was 98.9% with a standard deviation of 3.5% for all the samples tested.

The refined modulus-strength relationships are shown in Figure 7.6a for aggregate base materials and Figure 7.6b for granular subbase ones. It is obvious that for standard high quality crushed stones, such as granite, high resilient moduli generally correspond to high shear strength properties; while this trend is surprisingly reversed for weaker subbase materials such as select granular. Overall, there seems to be no clear and significant modulus-strength relationship for all

aggregate materials studied, which is probably due to the fact that the shear strength test is destructive in nature; whereas the M_R test, by contrast, is nondestructive in nature. By testing materials close to maximum dry density and optimum moisture conditions, Thompson and Smith (1990) pointed out that permanent deformation under repeated loading, instead of resilient modulus, was a better and more definite property for ranking granular base performance potential. Bilodeau et al. (2009) tested materials at three water contents (+2% higher than the absorption, near saturation, and drained water contents) and also found that the permanent strain behavior of all source aggregates were related to grain-size properties of the smaller fractions; while the resilient behavior (at saturated water content) depended highly on the grain-size distribution of the gravel (or coarse) fraction for crushed rocks or on the gradation uniformity for partially crushed gneiss. These findings may partly explain the results shown in Figure 7.1 through 7.6, although further in-depth analysis is needed on suction stress which reportedly has different relative effects on resilience and strength.

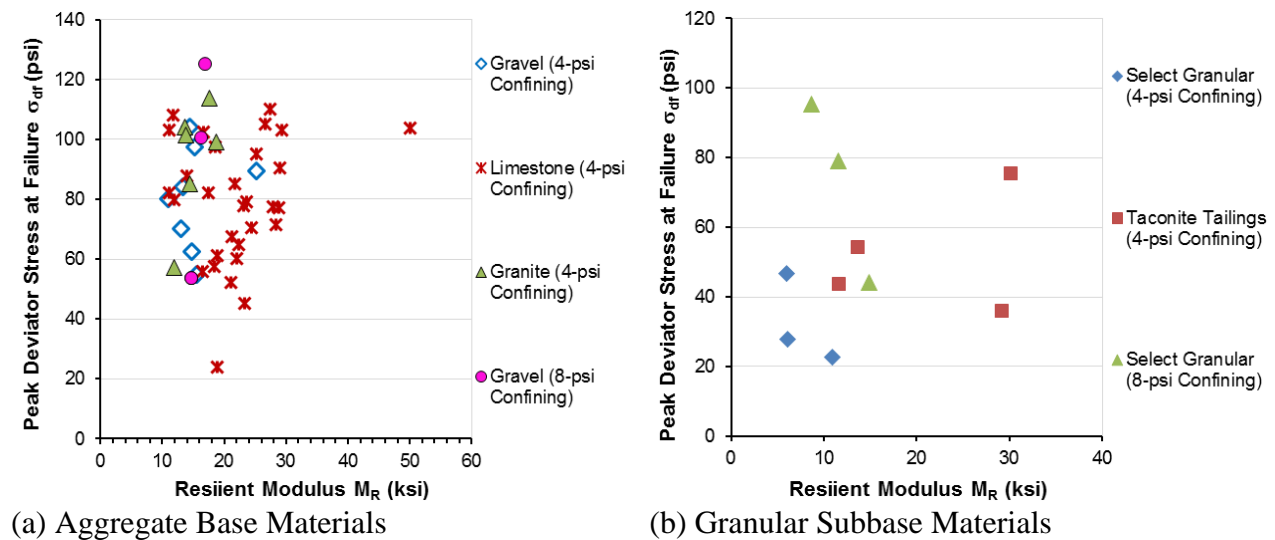


Figure 7.6. Resilient Modulus-Shear Strength Relationships for “Standard” (a) Aggregate Base and (b) Granular Subbase Materials at Near Optimum Moisture Conditions [1 psi = 6.89 kPa]

Contrary to the conventional wisdom that the load-carrying capacity of base/subbase materials increases with larger aggregate top sizes, it was observed for the data graphed in Figure 7.6 (although not explicitly shown) that gradations with larger top sizes did not necessarily perform better than those with smaller top sizes in terms of both resilient modulus and shear strength characteristics, i.e., the top size appears to have no definite effect on resilient modulus and shear strength, which was also reported by Lindly et al. (1995).

Based on similar findings, a limiting shear stress ratio (applied shear stress over shear strength) is recommended for implementation in the MnPAVE flexible pavement analysis and design program so that potential rutting performances of aggregate base and especially granular subbase courses in Minnesota could be taken into account. Such an approach would avoid any catastrophic shear failure in base/subbase layer, such as the one reported by Mulvaney and Worel (2002) in Mn/ROAD forensic case studies. In additions, gradation seems to govern the resilient modulus and shear strength behavior of unbound aggregate base/granular subbase materials, as

samples at optimum compaction conditions but with varying gradations exhibit distinct shear resistance. This could justify the development of performance-based gradation selection guidelines so that shear strength and permanent deformation characteristics can be maximized, especially for local aggregate sources which often have lesser quality.

7.3 Preliminary Gradation Refinement Guidelines for Optimized Strength Behavior

7.3.1 Motivation

Particle size distribution or gradation is a key factor influencing the mechanical response behavior of unbound aggregates characterized by resilient modulus (M_R), shear strength and permanent deformation. To ensure adequate pavement performance, MnDOT, among many other state highway agencies, currently employs “recipe-based” specifications for unbound aggregates used in road base/subbase construction (see Figure 2.5). These empirical gradation bands used in pavement applications specify different aggregate classes from 1 to 7 and source rock quality, etc., which reportedly have no robust linkage with actual performance in the field (Mulvaney and Worel, 2002). Such requirements based on various grading envelopes (e.g., well-graded, uniformly-graded, etc.) and limits of maximum particle size may not only be conflicting in regards to pavement layer stability and drainability but may also fail to distinguish different gradations within the specified bands, especially when aggregates from different sources are used (Tian et al., 1998; Tao et al., 2008). With “standard” materials becoming increasingly scarce and expensive, such traditional gradation specifications may potentially result in less than optimal placement of locally available lower cost materials. Recent research demonstrated that marginal materials could become quite economical for use in low-volume roads and serve properly the design traffic levels and the operating environment (Bullen, 2003). Therefore, development of performance based gradation specifications can help maximize beneficial use of the locally available materials that is potentially a green and sustainable transportation infrastructure alternative.

Establishing robust linkages between gradation and satisfactory unbound aggregate mechanical behavior is essential for the development of performance based gradation specifications. The qualitative gradation descriptions (e.g., upper, median, and lower limits), as documented in previous laboratory experiments investigating gradation influences, are certainly not applicable for this purpose (Thompson and Smith, 1990; Tian et al., 1997; Molenaar and Van Niekerk, 2002; Cunningham, 2009). With the advent of analytical gradation models and aggregate packing theories, recent research efforts have focused on quantifying gradation curves as numbers on a continuous scale to better relate them to mechanistic behavior trends (Kim et al., 2007; Bilodeau et al., 2009). These analytical gradation measures can quantify the change in performance of a given aggregate material within specified gradation bands leading to optimized gradation zones for desirable mechanical and hydraulic performance based on site-specific traffic and environmental conditions, respectively.

The primary objective of this section is to explore from MnDOT aggregate database analysis robust linkages between quantitative gradation parameters and critical mechanical behavior of aggregate base/granular subbase materials. More broadly, when such linkages were established and validated, improved performance based specifications would provide sustainable outcomes for utilizing limited aggregate sources with optimal properties by matching site-specific design traffic levels and operating environmental conditions. The comprehensive MnDOT aggregate database includes experimental results of the resilient modulus and peak

deviator stress at failure for standard material aggregate classes as well as waste/reclaimed base/subbase course materials. There is no unique relationship between modulus and shear strength properties. Statistical correlations established between critical gradation parameters, quantified using aforementioned characterization methods, and the strength, modulus, and moisture properties indicate Gravel-to-Sand ratio as an important gradation parameter.

7.3.2 Critical Gradation Parameter(s) Governing Shear Strength Behavior

To develop correlations between gradation parameters and the resilient modulus and peak deviator stress responses of base/subbase materials, the first step was to establish datasets containing all the independent and dependent variables. It was necessary to eliminate any differences among samples related to compaction moisture and density conditions. This was accomplished by choosing samples with only molded moisture contents within $\pm 0.5\%$ of the targeted optimum, as per the NCHRP 1-28A protocol, for subsequent investigation. It is worth mentioning that all the results presented here were in fact based on the $\pm 1\%$ moisture content criterion, such a trial relaxation of $\pm 0.5\%$ criterion to $\pm 1\%$ increased the sample population but did not change the results and the trends observed in statistical analyses, and, the data included in the analyses were referred to as “near optimum conditions.” As mentioned previously, the achieved dry densities were not found to influence results significantly in this study.

The current gradation quantification methods reviewed in Appendix B were employed one by one to calculate gradation parameters for all the samples selected; thus, the independent variables considered were: 1) maximum particle size D_{\max} and shape factor n from the Talbot equation; 2) mean aggregate size D_m and spread factor n from the Rosin-Rammler distribution function; 3) uniformity coefficient C_u , curvature coefficient C_c , the fines percentage $\%F$, and the diameter values corresponding to 60, 50, 30, and 10% passing in weights d_{60} , d_{50} , d_{30} , and d_{10} from the USCS, respectively; 4) the Gravel-to-Sand (G/S) ratio; and 5) three aggregate ratios of the Bailey method aggregate (CA , FA_c , and FA_f). It is worth emphasizing here that the G/S ratios for MnDOT database gradations studied were calculated using Equation (7.1) that was derived from the two parameters of the Talbot equation (D_{\max} and n) fitted from the percent passing data, according to the “Gravel” and “Sand” definitions of the USCS. This way, percentages passing all sieve sizes, but not just No. 4 (4.75-mm) and No. 200 (75- μm), were used.

$$\frac{G}{S} = \frac{P_{75\text{mm}} - P_{4.75\text{mm}}}{P_{4.75\text{mm}} - P_{0.075\text{mm}}} = \frac{1 - \left(\frac{4.75}{D_{\max}}\right)^n}{\left(\frac{4.75}{D_{\max}}\right)^n - \left(\frac{0.075}{D_{\max}}\right)^n} = \frac{(D_{\max})^n - 4.75^n}{4.75^n - 0.075^n} \quad (7.1)$$

To identify the most important gradation parameter(s) governing the shear strength behavior of base/subbase materials, a bivariate analysis, useful for identifying bivariate unusual points and bivariate collinearities, was employed to investigate relationships between the dependent variable (σ_{df} at given confining pressure) and explanatory variables (gradation parameters). The coefficients of determination (R^2 and adjusted R^2) were the criteria for evaluating the strength of association between each pair of these parameters. The statistical normality of each parameter was also verified with the Shapiro-Wilk test.

Among those calculated gradation parameters, the Gravel-to-Sand (G/S) ratio, in spite of its relative simplicity, was found to exhibit the best correlation with σ_{df} for all the materials

studied at various confining pressures, as shown in Figure 7.7. For instance, aggregate ratios of the Bailey method, which were thought to be very promising for governing influential factors, were found to be statistically insignificant except for the fine aggregate coarse ratio (FA_c). For brevity, weaker correlations found are not described here.

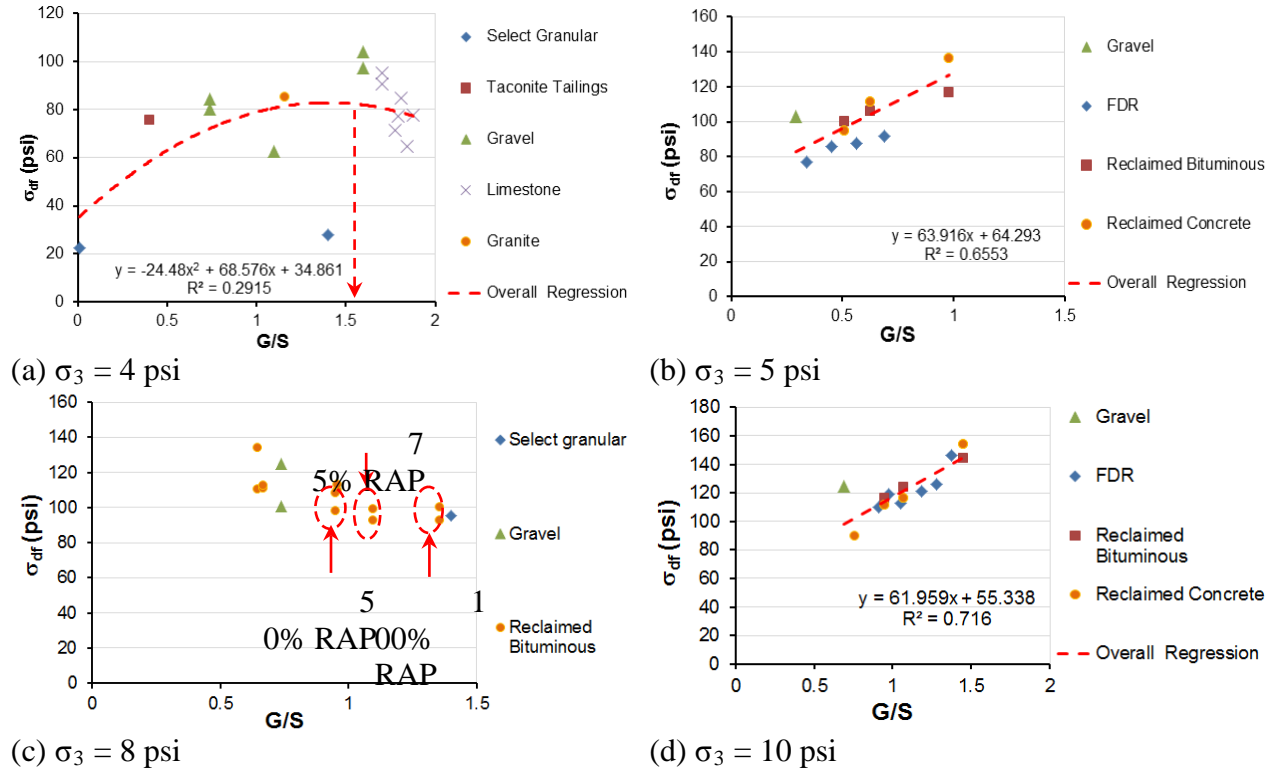


Figure 7.7. Peak Deviator Stress at Failure (σ_{df}) vs Gravel-to-Sand (G/S) Ratio for Various Aggregates: (a) 4-psi, (b) 5-psi, (c) 8-psi, and (d) 10-psi Confining Pressure [1 psi = 6.89kPa; 1 pcf = 16.02 kg/m³]

As shown in Figure 7.7a, the Gravel-to-Sand (G/S) ratio appears to have an optimal value somewhere between 1.5 and 2 at which maximum σ_{df} was computed for different gradations. Limestone samples exhibited decreased peak deviator stress at failure with increased G/S ratio (larger than a possible optimal G/S ratio). The examination of Figure 7.7b and 7.7d tends to confirm the inference made from Figure 7.7a, as σ_{df} values increase with larger G/S ratios regardless of aggregate types and gradations when G/S ratio is less than 1.5. The trend in Figure 7.7c however is less obvious. As reported by Kim and Labuz (2007), specimens with increased RAP percentages exhibited higher permanent deformation. Almost the same σ_{df} level for those three different RAP percentages in Figure 7.7c may be attributed to the increasing G/S ratios (less than 1.5 still), which could to a certain extent offset the detrimental effect of increasing RAP percentages (further study is needed to make this inference conclusive). In other words, it appears that when G/S ratios gradually approach about 1.5, shear strength behavior is improved.

7.3.3 Interpretation of the Gravel-to-Sand Ratio

The profound effect of the Gravel-to-Sand (G/S) ratio on the peak deviator stress at failure (or shear strength behavior) can also be interpreted from the particle packing and porosity

characteristics acquired by different relative concentrations of gravel and sand size particles (as per ASTM D2487-11). Aggregate base/granular subbase materials, in essence, are mixtures of the gravel fractions, sand fractions and fines. Coarse aggregate grains can be deemed to enclose a void space in which finer sand particles fill; whereas the fines (passing No. 200 sieve or smaller than 0.075 mm) basically fill the void space created by the sand particles (see Figure 7.8).

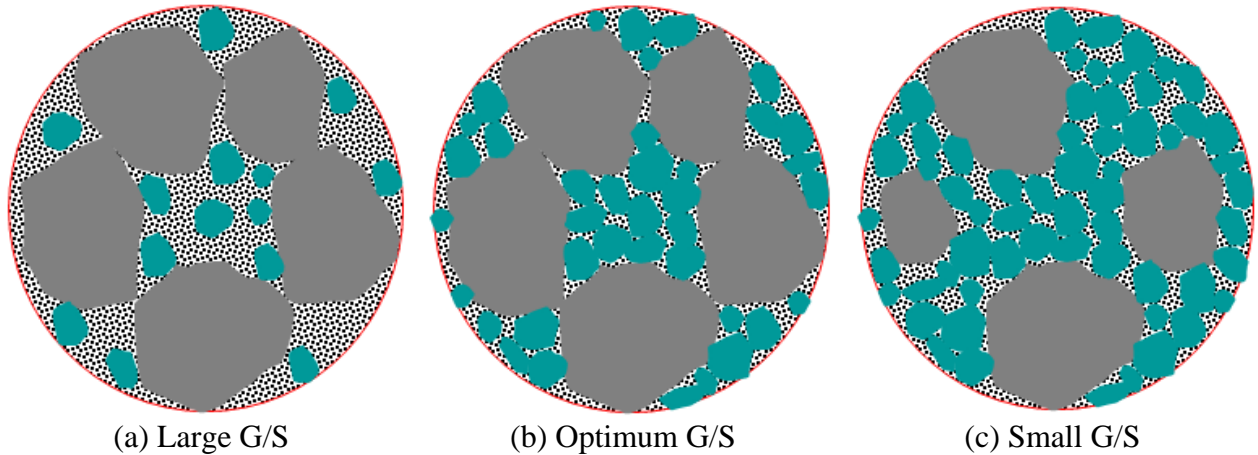
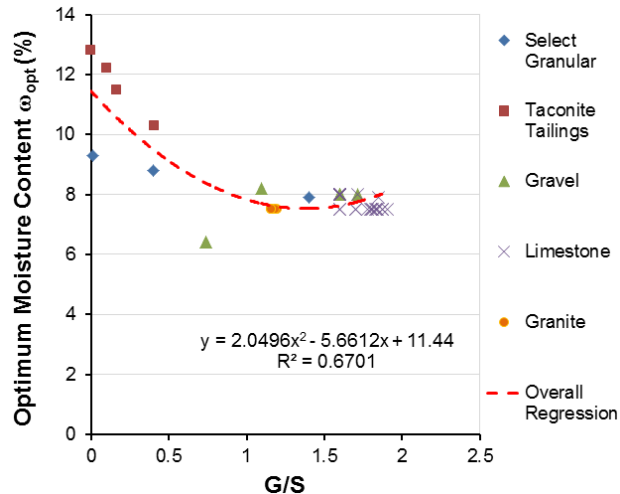
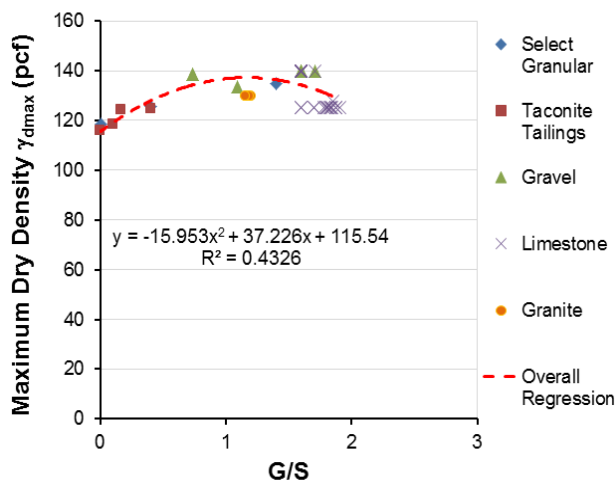


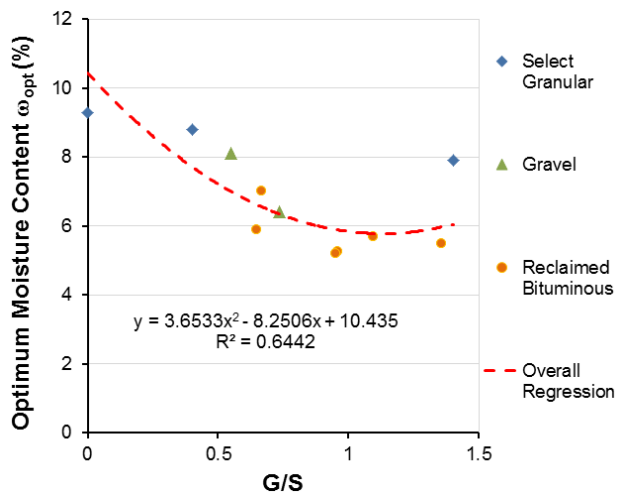
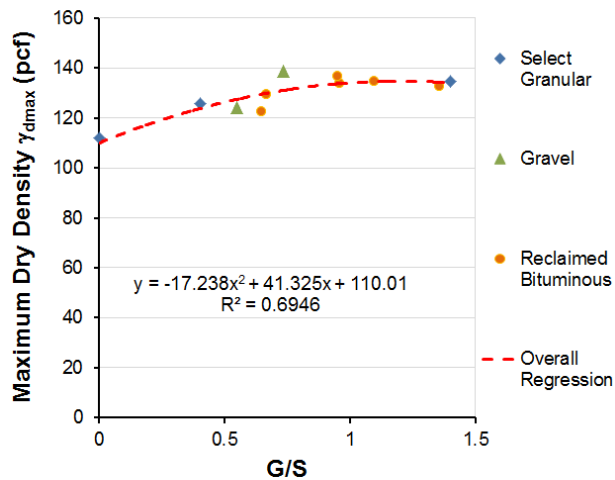
Figure 7.8. Different Packing States of Gravel-Sand-Fines Mixture with Different Gravel/Sand Ratios (Small Black Dots Represent Fines Fraction)

Figure 7.8a indicates the packing state resulting in the largest G/S ratio as almost no sand grains to occupy a portion of the voids between the coarse aggregate particles. Mixtures at this state develop shear or permanent deformation resistance primarily by friction resistance between gravel size particles and may not be very stable depending on the grading of the gravel-size particle distribution. G/S ratio decreases when more sand fractions exist until an optimal packing configuration is reached at the ideal state shown in Figure 7.8b. This ideal state means the voids between the gravel size particles are completely occupied by the bulk volume of the sand grains, developing the condition of minimum porosity. The minimum porosity of the mixture can be theoretically interpreted as the boundary between a gravel-controlled and a sand-controlled mixture. The phase diagram analysis of Figure 7.8b can also derive that the minimum porosity of the mixture is the product of the porosity of each individual fraction (i.e., $n_{\min} = n_G * n_S * n_f$) with the same specific gravity assumed for all fractions. After that, if sand fractions keep increasing (or G/S ratio decreases), then packing conditions will dictate gravel (or coarse) particles to “float” in the sand-fine matrix and have trivial control over shear strength behavior of the mixture (see Figure 7.8c).

To validate such inferences made above, the trends between the maximum dry density (γ_{dmax}) and optimum moisture content (ω_{opt}) and the Gravel-to-Sand (G/S) ratio are plotted in Figure 7.9 for those materials studied. Intuitively, the maximum dry density and optimum moisture content obtained under a given compactive effort can serve as indicators of the porosity of the mixture, with lower maximum dry density and higher optimum moisture content representing greater porosity. The porosity is then related to the shear strength developed, and the maximum shear strength of the mixture tends to occur at an optimum range of low porosity values.



(a) $\sigma_3 = 4$ psi



(b) $\sigma_3 = 8$ psi

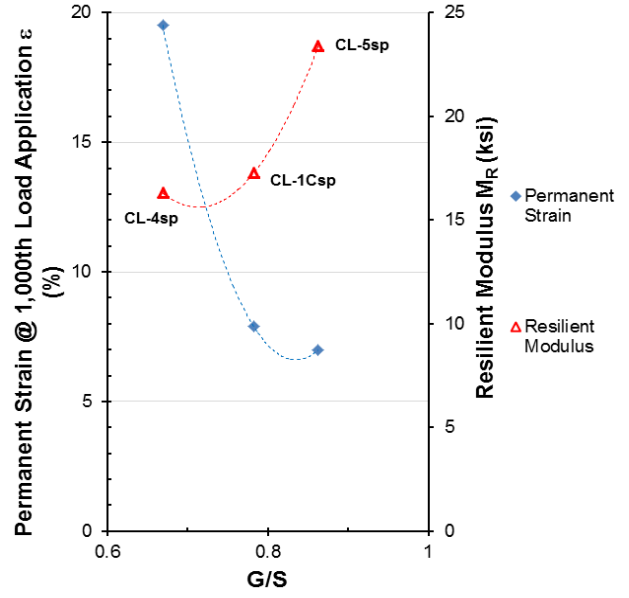
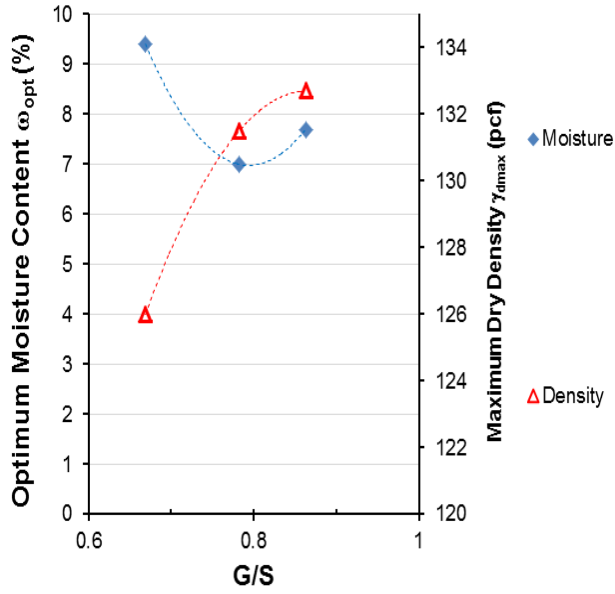
Figure 7.9. Maximum Dry Density (γ_{dmax}) and Optimum Moisture Content (ω_{opt}) vs Gravel-to-Sand Ratio (G/S) at (a) 4-psi and (b) 8-psi Confining Pressure [1 psi = 6.89kPa; 1 pcf = 16.02 kg/m³]

As shown in Figure 7.9, maximum dry density approaches a maxima and optimum moisture content reaches a minima when the G/S ratio is around 1.5, indicating the minimum possible porosity achieved by mixtures with G/S of around 1.5. The relative importance of the suction stress is also reduced as the G/S ratio increases and the optimum moisture content decreases. Since mixtures with G/S ratios of around 1.5 at the moment is at the possibly densest packing state, it explains well why peak deviator stress at failure has a maxima at this point, as presented previously. Note that the minimum porosity of a mixture is a function of porosities of both coarse aggregate particles and fine aggregate particles. Therefore, the approximate value of 1.5 found here may change when different material sources (e.g., with different bulk specific gravity) with different gradations are used. Nevertheless, such optimal proportions of gravel and sand fractions (as per ASTM D2487-11) may exist when the mixture reaches its minimum porosity, gets packed to the densest state, and thus yields the highest shear strength.

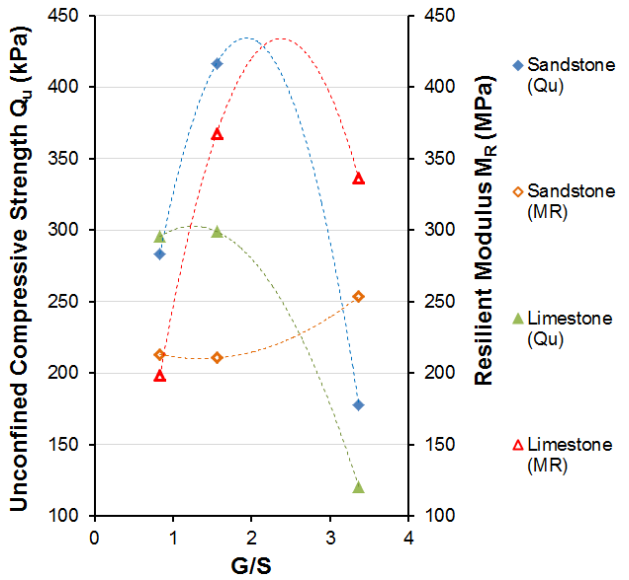
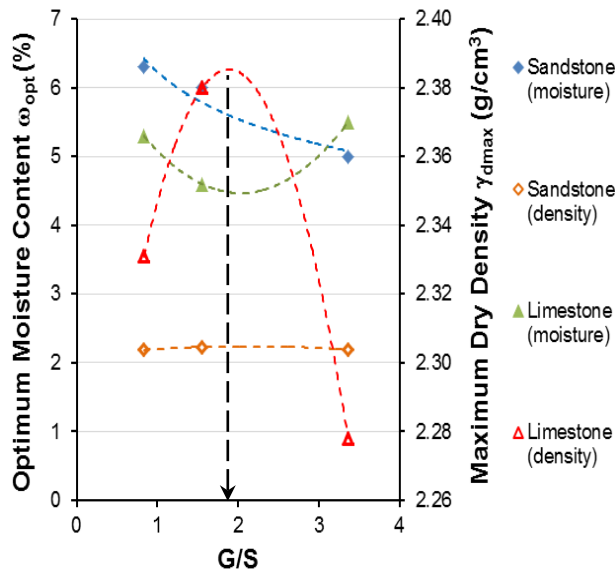
The G/S ratio may also help better understand effects of unsaturated hydraulic conductivity on the suction behavior of base/subbase materials, especially those with broad particle size distributions. The G/S ratio reflects the relative concentrations of larger gravel (or coarse aggregate) and smaller sand particles which according to Gupta et al. (2005) control the saturated hydraulic conductivity and the water retention characteristics, respectively. Future research in this area could potentially explain how moisture suction may become more controlling with smaller G/S ratios.

7.3.4 Analyses of Other Aggregate Databases Collected

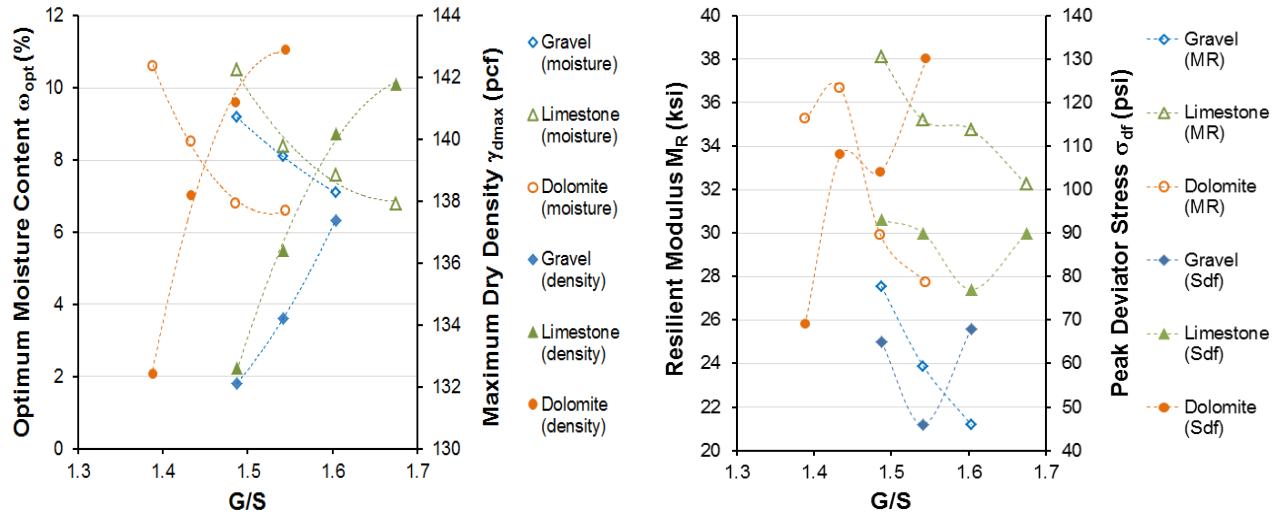
To support the observed gradation effects and G/S ratio trends summarized so far, similar analysis results from other aggregate databases collected from the literature are also presented in this section. The first data source was collected from the comprehensive laboratory testing program performed by Garg and Thompson (1997) in which six base and subbase materials (CL-1Fsp, CL-1Csp, CL-3sp, CL-4sp, CL-5sp, and CL-6sp) collected from the Mn/ROAD flexible pavement test sections were characterized for shear strength, resilient modulus, and rutting potential from rapid shear and repeated load triaxial tests. Since samples were tested in that study at varying moisture and density levels, to be consistent, only results of three samples (CL-1Csp, CL-4sp, and CL-5sp) tested at reported maximum dry density and optimum moisture content values (AASHTO T99) are presented here. In Figure 7.10a, the calculated G/S ratios are plotted against the maximum dry density, optimum moisture content, resilient modulus calculated at 100-psi bulk stress, and permanent strain calculated at the 1,000th load application from the reported values of “A” and “b” ($\epsilon_p \% = AN^b$), respectively. It clearly shows that as the G/S ratio increases, the optimum moisture content decreases and maximum dry density increases, indicating the densification trend towards the minimum porosity. Note that higher permanent strain (at the 1,000th load application) represents increased rutting potential and lower shear strength. The decreased permanent strain or increased shear strength is also observed for increasing G/S ratio, which agrees with the previous findings. Although aggregate class CL-5sp required 10-15% crushed/fractured particles and no crushed/fractured particles were allowed in CL-1Csp or CL-4sp, a permanent strain decrease of up to 64% from CL-5sp to CL-4sp demonstrates the significant role of G/S ratio for improving shear strength. Interestingly, resilient modulus increases with decreased permanent strain or increased shear strength.



from Garg and Thompson (1997)



(b) from Tian et al. (1998)



(c) from Tutumluer et al. (2009)

Figure 7.10. The Gravel-to-Sand Ratio Effects Observed in Other Databases Collected from: (a) Garg and Thompson (1997); (b) Tian et al. (1998); and (c) Tutumluer et al. (2009) [1 psi = 6.89kPa; 1 pcf = 16.02 kg/m³]

The second data source collected was from the study of Tian et al. (1998) aimed at investigating resilient modulus and shear strength characteristics of two good quality aggregates commonly used in Oklahoma as base/subbase materials at three different gradations (finer, median, and coarser limits). As shown in Figure 7.10(b), the calculated G/S ratios (from actual gradation curves) are plotted against the unconfined compressive strength (Q_u), maximum dry density (AASHTO T180), and optimum moisture content, respectively. The resilient modulus values were obtained at 689-kPa (100-psi) bulk stress. As indicated in Figure 7.10(b), both aggregates have an optimal G/S ratio of around 2 where mixture porosity reaches its minimum and the shear strength reaches its maximum values. The greater optimal G/S ratio found here may be possibly attributed to higher compaction energy used (AASHTO T180 rather than T99). In addition, the modulus-strength relationship does not show any consistent or unique trends similar to the previous MnDOT aggregate database findings.

Tutumluer et al. (2009) recently characterized strength, stiffness, and deformation behavior of three aggregate materials (limestone, dolomite, and uncrushed pit-run gravel) with controlled gradations for subgrade replacement and subbase applications through a comprehensive laboratory test matrix. This comprehensive database was also analyzed for verification purpose. To be consistent, only samples that had nonplastic fines at optimum moisture conditions were studied here for the G/S ratio effects. The results are shown in Figure 7.10(c). Note that the peak deviator stress values were recorded at 15-psi confining pressure, and MR values were calculated at 345-kPa (50-psi) bulk stress. The increasing maximum dry density (AASHTO T99) and decreasing optimum moisture content trends are consistent and indicate that the minimum porosity levels for the uncrushed gravel, crushed limestone, and crushed dolomite materials approximately take place at the G/S ratios of 1.6, 1.68, and 1.56, respectively. Considering the specific gravity variations of those three materials, the three very close G/S ratios can actually be regarded as the same. Note that investigation of the gradation effect was in fact not the primary objective of this research study, so the gradations were well controlled and engineered by only varying percent fines. Although the peak deviator stress values do not

consistently increase with increasing G/S ratios (or decreasing porosity), overall, the peak deviator stress values at the maximum G/S ratios for all three different aggregate materials are still approximately the maximum ones. Once again, no definite relationship exists between modulus and shear strength trends, which may require further investigation into effects of moisture-related suction stress for various fines percentages.

7.3.5 Preliminary Performance-based Gradation Guidelines

Commonly used gradation quantification methods, including the Talbot equation, the Rosin-Rammler distribution function, the Unified Classification System parameters, the conventional Gravel-to-Sand ratio, as well as the Bailey method, were employed to identify key gradation parameters governing the shear strength behavior of the studied aggregate materials. While other gradation parameters seemed to be less significant, the Gravel-to-Sand (G/S) ratio was found to control the shear strength behavior of both “standard” and reclaimed materials. For the MnDOT database samples studied, the highest shear strength was reached around an optimal G/S ratio of 1.5 where void spaces enclosed by the coarse aggregate fraction were probably filled completely by the sand size particles and fines. Further, there was inconclusive evidence of an apparent modulus-strength relationship which suggested incorporating a limiting working shear stress to strength ratio to avoid catastrophic shear failure in base and especially subbase courses.

Previous studies on soil/sand-gravel mixtures indicated that for large gravel (or coarse aggregate) concentrations, the friction resistance between gravel particles controls the shear strength behavior of mixtures; while at low gravel concentrations, the friction resistance of sand/soil grains controls the shear strength behavior (Vallejo, 2001). By applying this observation to this study, interpretation regarding the role of G/S was made, which well explained the validity of the optimal G/S ratio of 1.5 in this case. Additional aggregate databases collected from literature also confirmed the existence of such an optimal G/S ratio and the significant influence of the G/S ratio gradation parameter.

In light of these findings, current gradation specification bands, which may reject non-standard base/subbase materials for use in cost-effective road constructions, can be further revised and transferred into performance-based specifications in which the G/S ratio, together with other important factors, can be used to utilize available aggregate sources to match the site-specific design traffic levels and operating environmental conditions, for the sake of promoting sustainability. It is postulated here that within the current MnDOT specified gradation bands, those with the same G/S value of around 1.5 may exhibit similar shear strength behavior regardless of their maximum particle size, provided that other properties such as fines content, moisture and density conditions (AASHTO T99), and aggregate shape are not considerably different from each other. Note that in the context of this report, the gradations of locally available aggregate materials were not intended to go beyond the current MnDOT specified gradation bands.

7.4 Recommendations for Aggregate Strength Input in MnPAVE Analysis

According to the findings made so far, aggregate shear strength properties would be helpful to establish a valid measure of evaluating rutting potentials of aggregate base and granular subbase layers. Certain limiting criteria are recommended in this section for inclusion in the MnPAVE flexible pavement analysis and design program. Similar in concept to the subgrade stress ratio proposed by Thompson (NCHRP 1-26, 1990) for controlling rutting behavior of

subgrade soils, a shear stress ratio can be adopted to evaluate aggregate permanent deformation tendencies under various confining stress conditions (Kim and Tutumluer, 2005). Accordingly, one can determine a maximum allowable working stress for a constant, limiting shear stress ratio and the permanent deformation or rut accumulation potential of an unbound aggregate layer can then be evaluated by comparing the stress states predicted from MnPAVE analysis to the maximum allowable working stress.

To protect aggregate base from shear failure, MnPAVE program currently implements a maximum allowable stress criterion which is also based on the traditional Mohr-Coulomb criteria. The ratio of the maximum applied shear stress σ_1 to the critical value $\sigma_{1_critical}$, $SR = \frac{\sigma_1}{\sigma_{1_critical}}$, is regarded as an indicator of how close the base is to shear failure under the application of axle loading. The critical major principal stress $\sigma_{1_critical}$ is calculated as follows:

$$\sigma_1 < \sigma_{1_critical} = \sigma_3 \tan^2 \left(45 + \frac{\phi}{2} \right) + 2c \tan \left(45 + \frac{\phi}{2} \right) \quad (7.2)$$

Considering the significant variability of shear strength properties observed for aggregate base/granular subbase materials of different MnDOT Classes, proper procedures based on either laboratory testing or predictive methods should be adopted to establish the Mohr-Coulomb criterion parameters, c and ϕ . Checking the applicability of both the shear stress ratio and major principal stress ratio concepts for preventing aggregate base/subbase shear failure would also be desirable through field validation.

7.5 Summary

The relationship between modulus and strength was investigated for different MnDOT aggregate classes using additional aggregate strength data (peak deviator stresses at failure) from available MnDOT laboratory studies. The primary objective, however, is to verify if any consistent trends existed between modulus and strength (e.g., high shear strength for high modulus, etc.) for each MnDOT aggregate class. For comparison purposes, the peak deviator stress recorded at specimen failure was used as an indicator to evaluate the shear strength behavior of an aggregate sample. The resilient modulus (M_R) values were calculated from the MEPDG M_R constitutive model using typical stress levels within aggregate base/granular subbase courses. Major research findings are summarized below.

7.5.1 Observed Modulus-Strength Relationships

Some kind of a correlation between aggregate modulus and strength properties is commonly expected; however, as revealed from the laboratory data analysis in this Chapter, it appears that there are no strong correlations and sometimes even possible trends to rely on. The fact that modulus behavior and shear resistance are not directly related can be explained with the destructive nature of the shear failure test, which is a measure of the shear strength of the aggregate material; while the M_R test and the subsequently calculated resilient moduli as a function of applied stress states, by contrast, are nondestructive in nature. Although both resilient modulus and shear strength are likely to be affected by the same aggregate source properties and specimen compaction conditions, such as achieved density and moisture content, it is questionable to assume that a strong correlation may exist between the two very important

mechanical properties. This was also indicated by the findings from the Minnesota Road Research Project field study conducted by Newcomb et al. back in 1996.

Based on the findings in this task, it would not be sufficient to establish the quality of aggregate base/granular subbase materials based solely on resilient modulus. This is because certain aggregate materials exhibiting similar high or low resilient moduli were observed to show considerable differences in shear resistance, i.e. shear strength, which primarily dictates pavement performance through rutting resistance. Therefore, a proper selection of aggregate materials to be used in aggregate base/granular subbase layers should provide both (1) high enough layer stiffness to minimize critical pavement responses, e.g., vertical strain/stress on top of subgrade, and (2) adequate shear strength to prevent rutting in the granular layer for a satisfactory pavement performance.

7.5.2 Validation of MnPAVE Sensitivity Analysis Results

As presented in Chapter 6, MnPAVE sensitivity analysis results concerning base/subbase stiffness requirements to minimize subgrade vertical strain and hot mix asphalt tensile bending strain are still applicable as long as special care is taken for protecting base/subbase against potential shear failure. This is especially important for granular subbase materials evaluated in this study since they tend to provide high modulus/stiffness properties, yet, they may exhibit low shear resistance and prone to permanent deformation accumulation or shear failure under detrimental stress states induced by wheel and/or environmental loadings.

7.5.3 Preliminary Performance-based Gradation Selection Guidelines

While other quantitative gradation parameters seemed to be less significant, the Gravel-to-Sand (G/S) ratio was found to control the shear strength behavior of both “standard” and reclaimed materials. For the MnDOT database samples studied, the highest shear strength was reached around an optimal G/S ratio of 1.5 where void spaces enclosed by the coarse aggregate fraction were probably filled completely by the sand size particles and fines. It is postulated here that within the current MnDOT specified gradation bands, those with the same G/S value of around 1.5 may exhibit similar shear strength behavior regardless of their maximum particle size, provided that other properties such as fines content, moisture and density conditions, and aggregate shape are not dramatically different from each other. In light of these findings, current gradation specification bands can be further revised and transferred into performance-based specifications in which the G/S ratio, together with other important factors, can be used to utilize available aggregate sources to match the site-specific design traffic levels and operating environmental conditions, for the sake of promoting sustainability.

To better understand the underlying mechanism of the G/S ratio from a microscopic level, further efforts aided by, for example, the Discrete Element Modeling (DEM) approach will be definitely needed and helpful, as well-validated by several recent research studies (Tutumluer et al., 2009; Yohannes et al., 2009). The goal will be to simulate aggregate shear strength tests so that optimum contact and packing arrangements from various gradations can be identified for improved aggregate interlock. More aggregate material types and gradations will definitely be helpful in terms of better understanding the modulus-strength relationships and further validating/quantifying effects of the G/S ratio on mechanical behavior of aggregate base/granular subbase materials.

Chapter 8 Development of Best Value Granular Material Selection Tool Components

8.1 Introduction

This chapter essentially involves the implementation challenge of the research study findings as MnPAVE Best Value Granular Material components. As shown in Figure 8.1, the following three components have been envisioned for incorporation into the MnPAVE program to implement mechanistic-based pavement design concepts in aggregate selection/utilization: (1) GIS-based Aggregate Source Management Component, (2) Aggregate Property Selection Component for Design, and (3) Aggregate Source Selection/Utilization Component. With implementation of these three modules envisioned in current and future studies, the immediate attention has been focused to the second component for implementation priority. To successfully accomplish this task, the final coding and development of MnPAVE software with the proposed/envisioned components/modules has been coordinated with MnDOT personnel for implementation.

8.1.1 GIS Based Aggregate Source Management Component

This component is proposed/envisioned for incorporation into MnPAVE “Climate” module as a new “selection button”, **Aggregate Source**, which is similar as other options including “Counties”, “Coordinates”, and “Soil Class”.

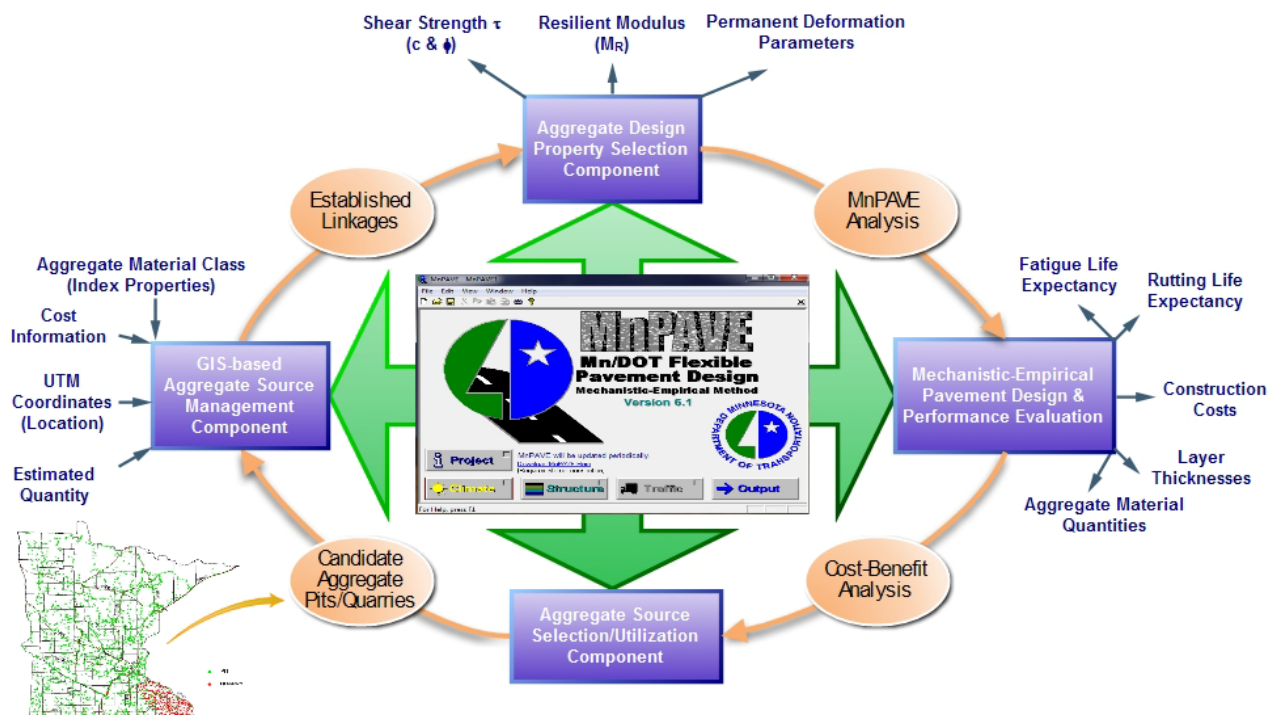
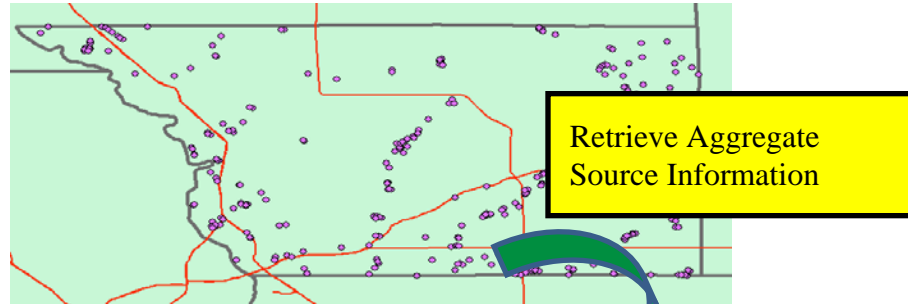


Figure 8.1. Overview of the Proposed/Envisioned MnPAVE Best Value Granular Material Components

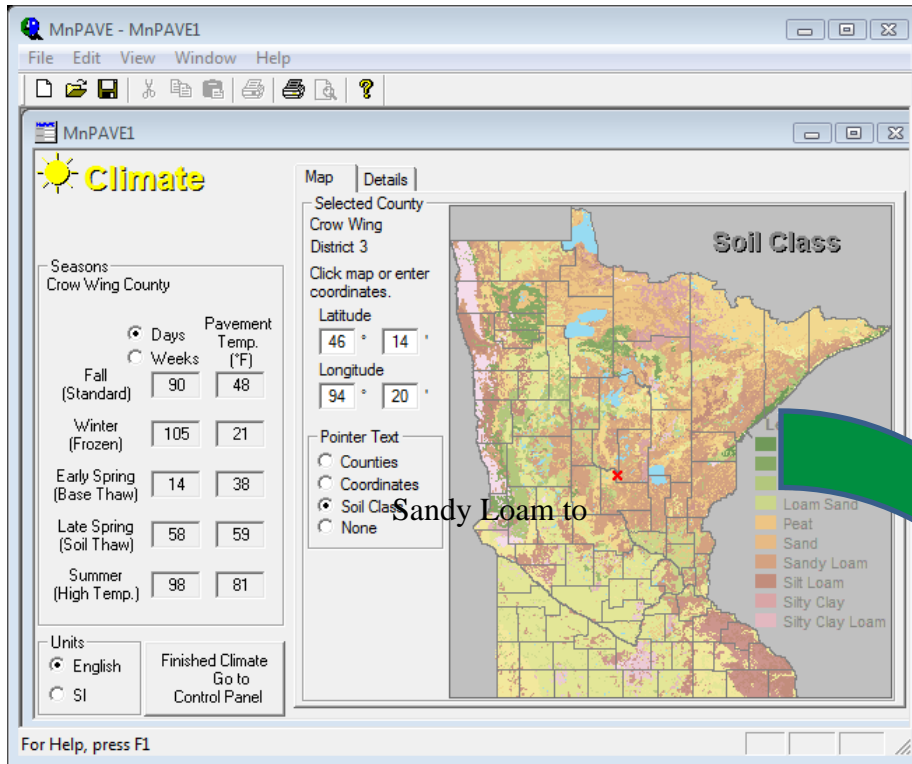
The currently-used MnDOT online “Interactive Aggregate Source Information System Map” (<http://www.mnrapps.dot.state.mn.us/gisweb/viewer.htm?activelayer=8>) can be used as a protocol for this component. Specifically, the corresponding inputs and outputs of this component are listed as follows: (1) the “Aggregate Source” button enables the user to visually identify the potential aggregate sources close to the specific project site, which is similar as the following “Soil Class” function; and (2) by clicking on the map of Aggregate Sources, the aggregate source properties (i.e., quality characteristics) and other information including quantity and costs associated with each aggregate source can be retrieved for both visual examination and internal program calculation.



An Illustrative Map Showing the State Trunk Highway Network & the Active Gravel Pits (for example Benton County, MN)

Source	Status	Status2	County	Section	Township	Range	Role	Pri	Legal Description	Nearest City	Owner	Source Name	District	Mclass1	Quan1	Costcym1	Ypric
3	05001	C	Benton	26	036	30	W	4		St Cloud	laurely Bro	Blank Pit	3				
4	05002	C	Benton	32	036	29	W	4		St Cloud	Hardives	Juelm Pit (Hanson)	3				
5	05003	O	Benton	26	036	30	W	4	S1/2 SW1/4	St Cloud	Becker G		3				
6	05004	O	Benton	02	038	32	W	4	SE1/4 NE1/4	Royalton	Isen, Bird	Elgelow	3				
7	05005	O	Benton	11	036	30	W	4	W1/2 SE1/4	Sauk Rapids	soetteman P		3				
8	05006	O	Benton	12	037	31	W	4	SW1/4	Oak Park	McCook J		3				
9	05007	O	Benton	25	036	31	W	4	SW1/4 NW1/4	Sartell	Blattner D		3				
10	05008	O	Benton	14	036	31	W	4	S1/2 SW1/4	Sartell	Larson J		3				
11	05009	O	Benton	19	037	28	W	4	NW1/4 SE1/4	Oak Park	Andersdahl R		3				
12	05010	O	Benton	12	036	28	W	4	NE1/4 SE1/4	Glendorado	Ford J		3				
13	05011	I	Benton	20	036	29	W	4	SW1/4 SE1/4	Duelm	Mfalter, Leo		3	6			
14	05012	C	Benton	12	037	28	W	4	NW1/4	Oak Park	auery Bro	Murray	3	6			
15	05013	P	Benton	36	036	28	W	4	NE1/4 SW1/4	Glendorado	Larson N		3	6	10000		
16	05014	O	Benton	21	036	28	W	4	NE1/4 NE1/4	Glendorado	Gleson O		3				
17	05015	I	Benton	30	036	29	W	4	SE1/4	Duelm	Rau P		3				
18	05015	M	Benton	21	036	28	W	4	1/4 NE1/4 & E1/2 SW1/4 NE	Glendorado	DOT	Mn/DOT Pit	3				
19	05017	M	Benton	11	036	30	W	4	E1/2 SW1/4	Sauk Rapids	DOT	Mn/DOT Pit	3	6	18000	0.83000	200
20	05018	I	Benton	04	036	31	W	4	Lot 4	Sartell	Benton Co		3				
21	05019	O	Benton	26	036	31	W	4	Lot 9, Block 14	Sauk Rapids	nan W, Olson C		3				
22	05020	I	Benton	13	037	30	W	4	E1/2 SW1/4	Bushville	Sendy E		3				
23	05021	P	Benton	17	038	29	W	4	NW1/4 SW1/4	North Benton	reck A & Son		3	6	74000		
24	05022	P	Benton	17	038	29	W	4	SW1/4 NW1/4	North Benton	reck A & Son		3	6			
25	05023	I	Benton	09	036	29	W	4	NE1/4 SE1/4	Parent	Kapboth J		3				
26	05024	I	Benton	09	036	29	W	4	SE1/4 SE1/4	Parent	Rau A		3				
27	05025	I	Benton	10	036	29	W	4	NW1/4 SW1/4	Parent	Rau A		3				
28	05026	P	Benton	24	036	31	W	4	Part SW1/4 NW1/4	Sauk Rapids	Daniel J		3	5	23000		
29	05027	P	Benton	27	036	29	W	4	N1/2 NE1/4 & W1/2 NE1/4	Duelm	omigan, Don		3	6	100000		
30	05028	O	Benton	02	036	29	W	4	NE1/4 SW1/4	Duelm	Kaprich C		3				
31	05029	P	Benton	10	037	28	W	4	SW1/4 SW1/4	Oak Park	enton County		3	6	10000		
32	05030	P	Benton	15	037	28	W	4	NW1/4 NW1/4	Oak Park	ssiewski C&F		3	5	15000		
33	05031	I	Benton	20	037	28	W	4	SW1/4 NE1/4	Ronneby	orgenson G		3				
34	05032	I	Benton	20	037	28	W	4	NW1/4 NE1/4	Ronneby	imonskoski L		3				
35	05033	O	Benton	20	037	28	W	4	NW1/4 NE1/4	Ronneby	Brady J		3				
36	05034	I	Benton	25	037	29	W	4	SE1/4 NE1/4	Foley	Towne C		3				
37	05035	P	Benton	17	038	29	W	4	SW1/4 SW1/4	North Benton	Shiba A		3	4			
38	05036	P	Benton	29	036	28	W	4	S1/2 NE1/4	Glendorado	Kosloski J		3	6	142000	0.25000	
39	05037	P	Benton	11	038	32	W	4	NW1/4 NE1/4	Royalton	Beam J		3	5	8000		
40	05038	P	Benton	11	038	32	W	4	NE1/4 NE1/4	Royalton	Pasch L		3				
41	05039	I	Benton	15	036	31	W	4	NW1/4 NE1/4	Sartell	Schoun L		3	6			
42	05040	P	Benton	11	038	32	W	4	NW1/4 SE1/4	Royalton	Pasch L		3	5	40000		
43	05041	D	Benton	16	037	31	W	4	SE1/4 SE1/4	Wasson	Mueschler		3	4			

Figure 8.2. Design Concepts for the Aggregate Source Management Component



The “Soil Class” button enables the user to visually determine for any specified project site the soil class by simply clicking the map.

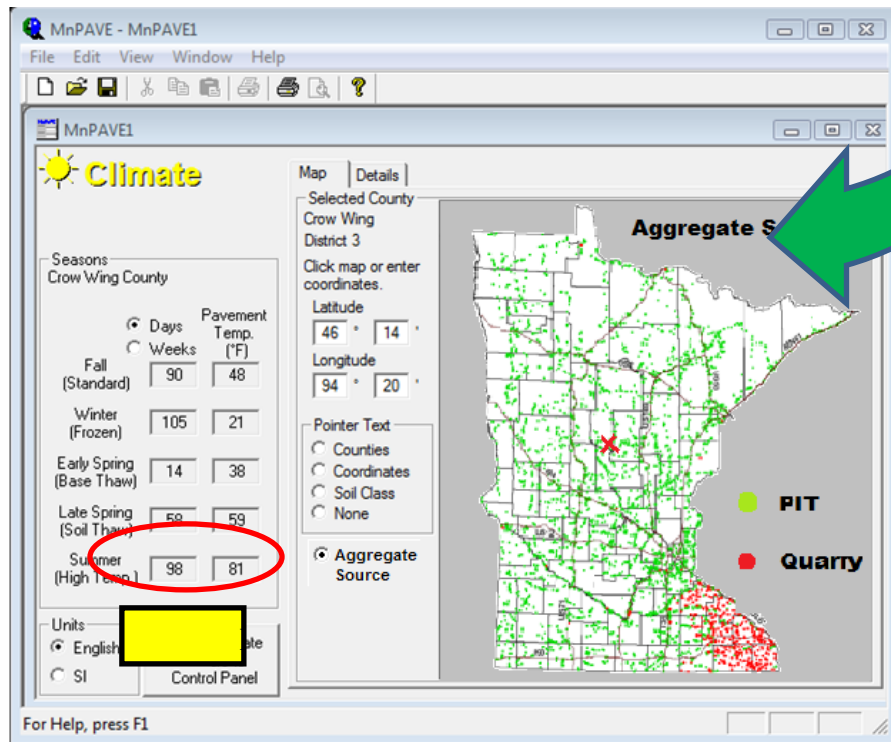
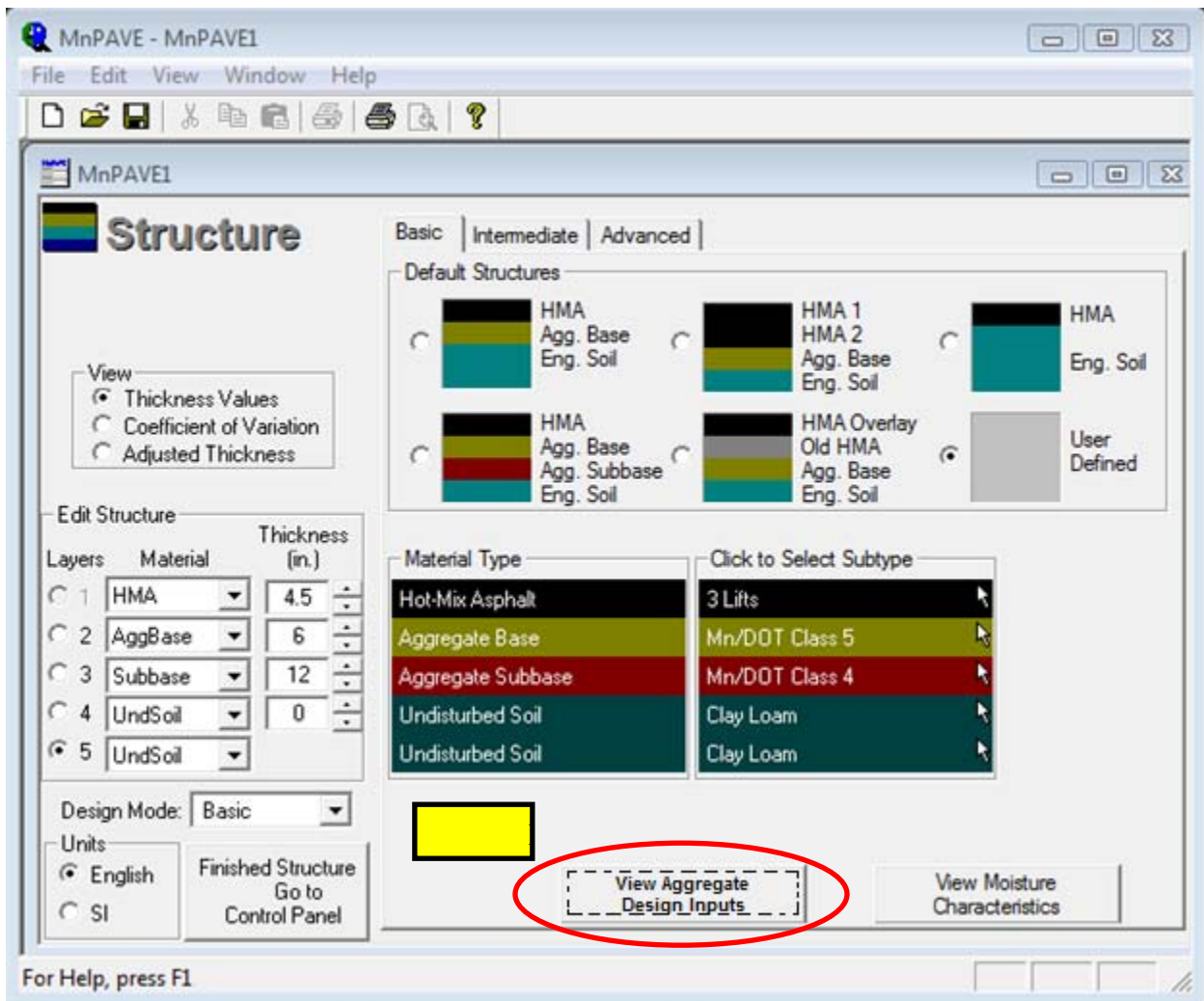


Figure 8.3. Conceptual Windows Proposed for the Aggregate Source Management Component

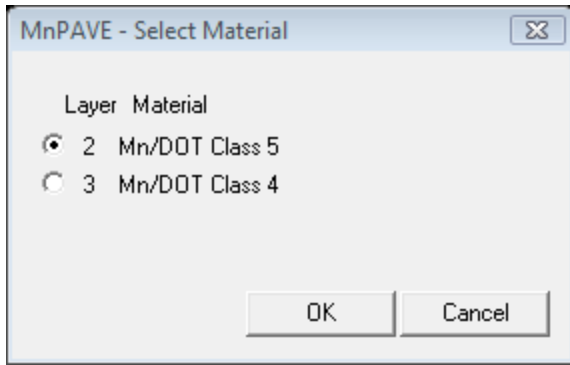
8.1.2 Aggregate Property Selection Component for Pavement Design

This component is proposed for incorporation into MnPAVE “Structure” module. MnPAVE consists of three design levels: Basic, Intermediate, and Advanced. Note that the advanced level requires the determination of modulus values of aggregate materials over the expected operating range of moisture and temperature. The regression-based correlations were developed in the previous tasks for relating resilient modulus model parameters and peak deviator stress at failure with aggregate source properties. In the absence of laboratory test data, those correlations, however, could be employed to predict mechanistic pavement design inputs of aggregate base/granular subbase materials for use in Basic and Intermediate levels. Serving the purpose of selecting proper basic default values for mechanistic design inputs, the design concept of this component is illustrated below. Note that the default parameter values shown in Figure 8.4(c) are the mean values from MnDOT aggregate database statistical analyses, and only the first thirteen regression model parameters are shown (from a_1 to a_{13}) for illustration purpose.



(Conceptual Window)





(a)

MnPAVE - Aggregate Properties

Material: Mn/DOT Class 5

Bulk Spec. Grav. (Gsb) 2.7

Dry Bulk Density 120 pcf

Units: English SI

Least haul distance 15.5 mile

Least haul time (h) 0.5

View Transportation

Sieve Size	Passing
1"	100
3/4"	95
3/8"	70
#4	58
#10	43
#40	23
#200	7
Not Used	
Not Used	
Not Used	

Gradation graph showing Percent Passing vs Sieve Size, mm. Legend: Gradation (black line), Mn/DOT Specification (red line).

Select other aggregate sources

Aggregate Source Number:

Or

District: County:

Section: Township: Range:

Buttons: Submit, Reset

(Conceptual Window)

(b)

MnPAVE - Aggregate Resilient Modulus Parameter Equation

Print Window Help

An empirical equation derived from Mn/DOT test database

$$M_R = 10^{\left(0.132 - 0.016FE_Ratio - 0.053ST - 0.026AI - 0.028\omega_{opt} - 0.0004\gamma_{max} - 1.197C_u\right)} \times P_2 \times \left(\frac{\theta}{P_2}\right)^{\left(1.573 - 0.007\gamma_{max} - 0.0009\frac{\gamma_{max}}{P_2} - 0.013P_2 - 0.046P_{200}\right)}$$

$$\left(\frac{\tau_{oct}}{P_2} + 1\right)^{\left(-15.914 - 0.041FE_Ratio - 0.004AI - 0.015\gamma_{max} - 0.488\frac{\omega}{\omega_{opt}} - 0.0008\frac{\gamma_{max}}{P_2} - 0.246\frac{P_{200}}{\log C_u} - 0.145P_2 - 0.057P_2\right)}$$

From regression

Aggregate Source Properties		Modulus Coefficients	
FE_Ratio	4.1	Flat & Elongation ratio	
ST	2.5	Surface Texture	
AI	425	Angularity Index	
ω_{opt}	8.7	Optimum Moisture Content	
γ_{max}	128.3	Maximum Dry Density	
ω	7.0	Achieved Moisture Content	
γ_{dry}	128.4	Achieved Dry Density	
C_u	36.2	Coefficient of Uniformity	
C_c	0.6	Coefficient of Curvature	
P_{20}	99.4	Percent Passing 2" sieve (50 mm)	a_0 0.132
P_{10}	98.7	Percent Passing 1" sieve (25 mm)	a_1 -0.016
$P_{4.75}$	48.6	Percent Passing #10 sieve (2 mm)	a_2 -0.05
P_{200}	6.3	Percent Passing #200 sieve (0.075 mm)	a_3 -0.026
ω/ω_{opt}	0.83	Moisture Ratio	a_4 -0.628
			a_5 0.0004
			a_6 1.197
			a_7 1.573
			a_8 0.007
			a_9 -0.0009
			a_{10} -0.013
			a_{11} -0.046
			a_{12} -15.914
			a_{13} 0.041

Stress Level
 $\theta = \sigma_1 + \sigma_2 + \sigma_3$
 $\tau_{oct} = \sqrt{(\sigma_1 - \sigma_2)^2 + (\sigma_1 - \sigma_3)^2 + (\sigma_2 - \sigma_3)^2}$
 θ τ_{oct}

OK

(Conceptual Window)

MnPAVE - MnPAVE1

File Edit View Window Help

MnPAVE1

Structure Basic Intermediate Advanced

View
 Thickness Values
 Coefficient of Variation
 Adjusted Thickness

Edit Structure

Layers	Material	Thickness (in.)
1	HMA	4.5
2	AggBase	6
3	Subbase	12
4	UndrSoil	0
5	UndrSoil	0

Design Mode: Basic

Units
 English
 SI

Finished Structure
 Go to Control Panel

View
 Test Results
 Poisson's Ratio
 Resistance Factors
 Coefficient of Variation (COV)

Uncheck to use Basic defaults.

HMA Modulus

Agg. Test Type
 Lab Mr, ksi
 R-Value
 DCP, mm/blow

Soil Test Type
 Lab Mr, ksi
 R-Value
 DCP, mm/blow
 Silt % Clay %

Other Design Modulus, ksi

Moisture Data
 Mohr-Coulomb

For Help, press F1

(c)

Figure 8.4. Conceptual Windows Proposed for the Aggregate Property Selection Component

8.1.3 Aggregate Source Selection/Utilization Component

This component is essentially proposed for identifying, within a panel of potential gravel pits/rock quarries, those of best location for the supply of aggregate materials with respect to their transport costs to a specific highway construction project, yet still satisfying pavement design performance requirements (i.e., structural adequacy). This proposed component, entitled “Aggregate Selection/Utilization Optimization”, is envisioned to be embedded into MnPAVE’s “Output” module since both pavement performance and construction cost (A.K.A Life-cycle Cost Analysis) need to be considered.

8.2 Aggregate Property Selection Component for Pavement Design

8.2.1 Implementation Plan

MnPAVE is a multi-layer elastic theory program currently used by Minnesota Department of Transportation (MnDOT) for mechanistic-based flexible pavement design. To calculate critical pavement responses including stresses, strains, and deflections in flexible pavements, MnPAVE requires as input a single value of the modulus of elasticity for each pavement layer material. Depending on the specific design level selected, i.e., Basic, Intermediate, or Advanced, the modulus input can be default/empirical values from experiences and/or similar projects, estimated values from correlations or in-situ tests, or even realistic values determined from laboratory testing, respectively. To provide reasonable modulus inputs without the need to conduct laboratory repeated load triaxial testing, multiple linear regression based correlations have been developed from MnDOT aggregate resilient modulus (M_R) databases to estimate the MEPDG M_R model parameters k_1 - k_2 - k_3 from aggregate source properties including shape properties.

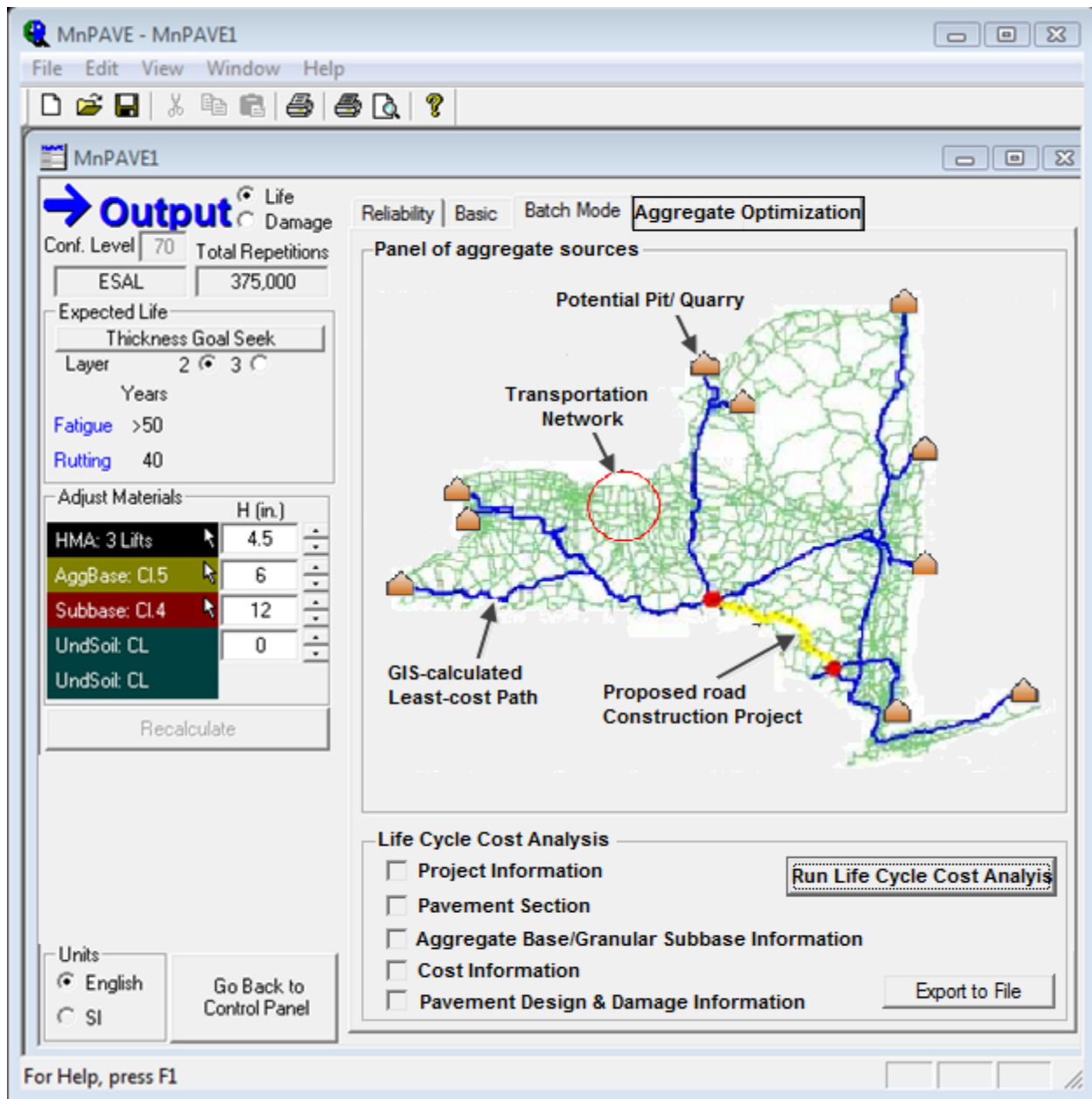


Figure 8.5. Conceptual Windows Proposed for the Aggregate Source Selection/Utilization Component

The stress dependent M_R model parameters k_1 - k_2 - k_3 can be directly used as inputs for finite element based pavement analysis programs such as ILLI-PAVE, GT-PAVE, etc.; however, for the use in the multi-layer elastic theory analysis, those parameters need to be converted into a single representative value of the modulus of elasticity using an iterative procedure which takes into account the stress states/distribution in individual nonlinear pavement granular layers. Although the finite element approach is the most accurate one for incorporating nonlinear granular modulus behavior, the use of multi-layered elastic theory and corresponding programs in flexible pavement analysis and design still receives widespread acceptance because of simple requirements. Thus, the primary objective of this component, as illustrated in Figure 8.4, is to

determine the equivalent one layer base/subbase modulus from an iterative elastic layered approach that directly accounts for the nonlinear base/subbase behavior.

Overall, this component is to be implemented into MnPAVE “Structure” module for use in either Basic or Intermediate design level, in the absence of lab test data. Conceptually, this component will be built in as a button to function as follows: once the user inputs all the necessary aggregate source properties included in the M_R predictive equation and then clicks the “OK” button, as shown in the first window of Figure 8.4, the iterative elastic layered analysis, which will be discussed in detail subsequently, will be initiated in the background of MnPAVE program to generate the equivalent one layer modulus. All the iteration steps will run in the background and the convergence will output the equivalent one layer modulus to be displayed on the screen and automatically used by the program in any subsequent analyses. In the following subsections, literature on this iterative elastic layered analysis framework is briefly reviewed, followed by the presentation of detailed implementation work.

8.2.2 Literature Review

The use of an iterative stress-modulus approach allows incorporating nonlinear or stress dependent properties of unbound materials into layered linear elastic models. Since the stress states are used in the M_R characterization model, the stresses computed in the previous iteration at a certain location in the granular layer are used to compute the modulus. Basically, there are several different ways to determine this conceptual stress point: 1) subdividing each nonlinear granular layer into a number of sub-layers, and then using the stresses at the mid-depth of each layer to determine the modulus; 2) considering the granular layer as a single layer, and then selecting an appropriate stress point, usually between the upper quarter and upper third of the layer, to compute the modulus; and 3) defining the stress point at a certain point on the pavement surface, by a slope of load distribution, SLD, and by a z coordinate, ZCNOL, as adopted in the KENLAYER program (Huang, 1993). Note that stresses actually vary with both in the horizontal and vertical distances from the load and the modulus should also change both vertically and horizontally and is not uniform throughout the layer.

Another important aspect of nonlinear analysis is the stress adjustment/modification for computing equivalent single modulus values for nonlinear granular layers. It is a well-known fact that most unbound granular materials cannot take any tension, unless the horizontal stresses in tension due to applied loads are smaller than the pre-compression caused by compaction-related residual stresses, geostatic stresses, and/or other in-situ stresses. Therefore, it is not possible that the computed total horizontal stress due to initial compaction (residual stress) and loading will become negative. It is thus imperative to adjust the total stress that the actual stress cannot exceed the strength of the granular material. This adjustment/modification, however, applies only to the determination of the equivalent single modulus of granular materials and does not change computed stress state due to loading. Among several methods commonly used for stress adjustment/modification in nonlinear analysis is the one based on Mohr-Coulomb theory, as incorporated into ILLI-PAVE and MICH-PAVE. It assumes that when a granular material with an angle of internal friction ϕ , and a hypothesized zero cohesion fails, the Mohr's circle based on the major and minor principal stresses must be tangent to the failure envelope, and no circle should cut and lie outside the envelope, so no minor and major principal stresses σ_3 and σ_1 should be smaller than the $(\sigma_3)_{\min}$ and greater than the $(\sigma_1)_{\max}$ as computed by the following equations, respectively:

$$\begin{aligned}
(\sigma_3)_{\min} &= \sigma_V \tan^2 \left(45^\circ - \frac{\phi}{2} \right) \\
(\sigma_1)_{\max} &= \sigma_V \tan^2 \left(45^\circ + \frac{\phi}{2} \right)
\end{aligned}
\tag{8.1}$$

If the computed minor principal stress σ_3 , including the horizontal geostatic stress, is smaller than the computed $(\sigma_3)_{\min}$, it must be increased to $(\sigma_3)_{\min}$ to satisfy the Mohr-Coulomb failure envelope requirement. Similarly, the computed major principal stress σ_3 should be reduced accordingly if it is greater than $(\sigma_1)_{\max}$ (Huang, 1993).

In summary, after reviewing relevant approaches in nonlinear analysis, two main methods are found to be promising for implementation. The first approach is to subdivide the granular layer into a number of sublayers and take the stress point for determining the modulus located at the mid-depth of each sublayer. In regard to the stress adjustment/modification, the horizontal stress (including the geostatic stress) that is negative or in tension can be set to zero to avoid negative bulk stress θ . With horizontal stresses being equal to 0, the modulus is then dependent on the vertical stress only. The second method considers the granular layer as a single layer, and thus its accuracy primarily depends on the proper selection of the single stress point. The weakness of the second method lies in its failure to represent the actual case of decreasing modulus with depth. With this method, it is very difficult, if not impossible; to reproduce the same critical pavement responses as those obtained by multiple layers or finite element based programs.

MEPDG adopted, with minor modification, the procedure proposed by Witczak and Smith (1981). The recommended procedure is in essence similar to the second method in the previous paragraph. Khazanovich et al. (2006) proposed several refinements of the MEPDG procedure after their consultations with the NCHRP Project 1-40B team. Those refinements further specified the critical points within unbound pavement layers where the stress state should be calculated, as well as the wheel load used for computation of the traffic stresses. As shown in Figure 8.6, the critical point for each unbound layer except the last one is located at the one-fourth of the layer depth; whereas the critical point for the last layer, i.e., subgrade soils, is 18 in. from the top surface. A Falling Weight Deflectometer (FWD) type single wheel load of 9,000 lbs. is assumed for computing the traffic induced stresses. The iterative framework shown in Figure 8.7 is relatively intuitive and simple; however, the implementation is quite time-consuming due to the fact that each iteration requires performing one multi-layer elastic theory analysis run. Note that the maximum relative error of 1% between the predicted modulus and modulus from last iteration was proposed as the convergence criteria.

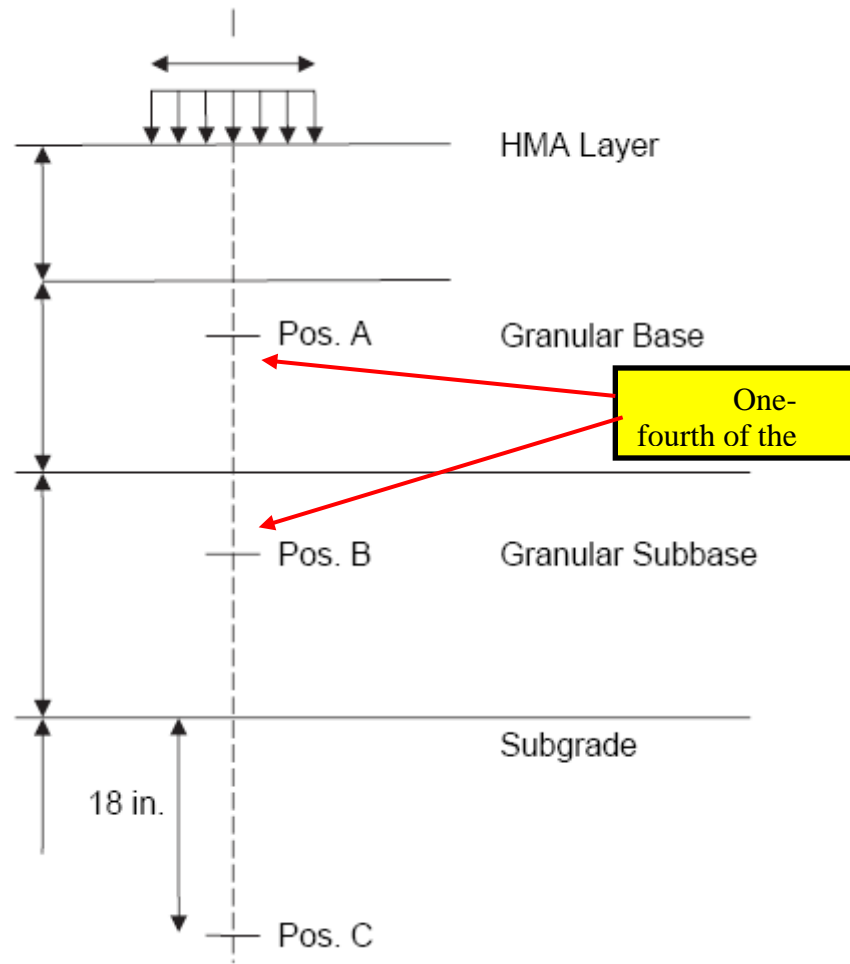


Figure 8.6. Pavement System and Evaluation Points Used for Stress State Analysis (Khazanovich et al., 2006)

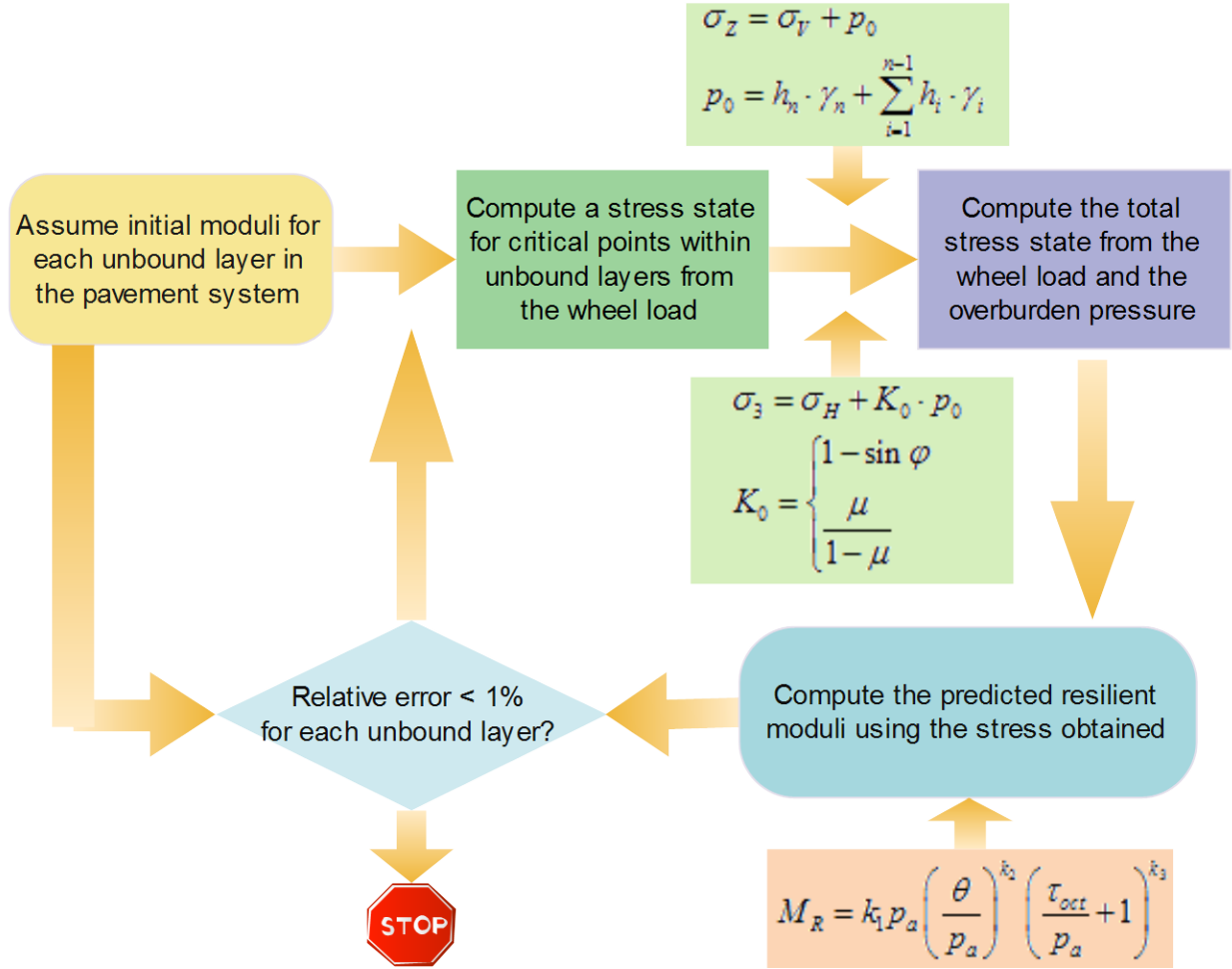


Figure 8.7. The Iterative Procedure Adopted by MEPDG for Obtaining One Single Modulus (Khazanovich et al., 2006)

8.2.3 Constitutive Relationship

This section uses the MEPDG resilient modulus (M_R) model as the constitutive relationship for both aggregate base and granular subbase materials. The constitutive relationship between resilient modulus and the stress state can be expressed as:

$$M_R = K_1 \cdot P_a \cdot \left(\frac{\theta}{P_a} \right)^{K_2} \cdot \left(\frac{\tau_{oct}}{P_a} + 1 \right)^{K_3} \quad (8.2)$$

where,

M_R = Resilient modulus;

θ = Bulk stress = $\sigma_1 + \sigma_2 + \sigma_3$;

σ_1 = Major principal stress;

σ_2 = Intermediate principal stress = σ_3 for M_R test on cylindrical specimen;

σ_3 = Minor principal stress or confining pressure in the triaxial tests;

σ_d = Deviator stress = $\sigma_1 - \sigma_2 = \sigma_1 - \sigma_3$;

τ_{oct} = Octahedral shear stress,

$$\begin{aligned} & \frac{1}{3} \sqrt{(\sigma_1 - \sigma_2)^2 + (\sigma_1 - \sigma_3)^2 + (\sigma_2 - \sigma_3)^2} \\ &= \frac{\sqrt{2}}{3} (\sigma_1 - \sigma_3) \end{aligned}$$

for cylindrical specimen in triaxial tests;

Pa = Normalizing stress (atmospheric pressure = 100 kPa = 14.7 psi);

K₁, K₂, K₃ = Model parameters obtained from regression analysis.

By replacing the M_R model parameters K₁-K₂-K₃ with the previously developed regression based correlations, Eq. (8.3) can be rewritten as:

$$\begin{aligned} M_R = 10 & \left(0.132 - 0.016 FE_Ratio - 0.05 ST - 0.026 \omega_{opt} - 0.628 \frac{\omega}{\omega_{opt}} + 0.0004 \frac{\gamma_{max}^2}{P_{40}} + 1.197 C_c \right) P_a \times \\ & \left(\frac{\theta}{P_a} \right) \left(1.573 + 0.007 \gamma_d - 0.0009 \frac{\gamma_{max}^2}{P_{40}} - 0.013 P_{10} - 0.046 P_{200} \right) \times \\ & \left(\frac{\tau_{oct}}{P_a} + 1 \right) \left(-15.914 + 0.041 FE_Ratio + 0.004 AI + 0.015 \gamma_d + 0.488 \frac{\omega}{\omega_{opt}} - 0.0008 \frac{\gamma_{max}^2}{P_{40}} + 0.246 \frac{P_{200}}{\log C_u} + 0.145 P_2 - 0.057 P_1 \right) \end{aligned} \quad (8.3)$$

where: logk₁ model: R²=0.55, Adj.R² = 0.53, P<.0001, SSE=1.89

k₂ model: R²=0.51, Adj.R² = 0.49, P<.0001, SSE=2.01

k₃ model: R²=0.66, Adj.R² = 0.64, P<.0001, SSE=10.49

Note that θ is the stress invariant, which can be either the sum of three normal stresses, σ_x, σ_y, and σ_z, or the sum of three principal stresses, σ₁, σ₂, and σ₃:

$$\theta = \sigma_1 + \sigma_2 + \sigma_3 = \sigma_x + \sigma_y + \sigma_z \quad (8.4)$$

If the density of a layered system is given and the body weight is considered, then θ is given as:

$$\theta = \sigma_x + \sigma_y + \sigma_z + \gamma z (1 + 2K_0) \quad (8.5)$$

where γ is the average unit weight, z is the distance below pavement surface at which the modulus is to be determined, and K₀ is the coefficient of earth pressure at rest.

8.2.4 Iterative Framework

The iterative framework to be used will need to be decided upon first. The sublayering method is preferred due to its higher accuracy, as compared to the method with one single stress point in the entire layer. If the single layer method with one single stress point is eventually selected for use, the locations used by Khazanovich et al. (2006) can be tentatively implemented to check if the procedure for selecting the optimum stress point location works adequately. To do this, critical pavement responses from the two aforementioned methods are compared with those computed by validated finite element programs such as GT-PAVE and ILLI-PAVE and the best approach is determined for accuracy.

The sublayering procedure is illustrated in Figure 8.8. The base or subbase is divided into a pre-determined number of “imaginary” sublayers with the stress computation point for each sublayer taken at the mid-depth of that sublayer. Each sublayer is somewhat analogous to the elements used in the finite element method, except that each sub-layer is infinite in the horizontal direction and thus cannot capture the horizontal modulus variation. Note that those “imaginary” sublayers are not physically analyzed in MnPAVE layer elastic analysis.

It should be noted that the solution engine utilized in MnPAVE for computing stresses, strains, and displacements is the “WESLEA” program from the U.S. Army Corps of Engineers Waterways Experiment Station Layered Elastic Analysis method (Van Cauwelaert et al., 1989). The “WESLEA” only allows up to 5 layers in the pavement system. Accordingly, we cannot physically divide the actual base or subbase layer into sublayers for pavement analysis using MnPAVE; instead, we can use the “imaginary” sublayering approach for calculating stresses in those “imaginary” sublayer mid-layer points for computing modulus values in each iteration, and at the end of each iteration, those imaginary sublayers are then transformed into one single layer with one modulus but equivalent thickness using the Odemark method. How to achieve convergence in such a scheme needs to be studied thoroughly.

The following steps detail the iterative elastic layered analysis framework for the revised sublayering method based on the Odemark method proposed.

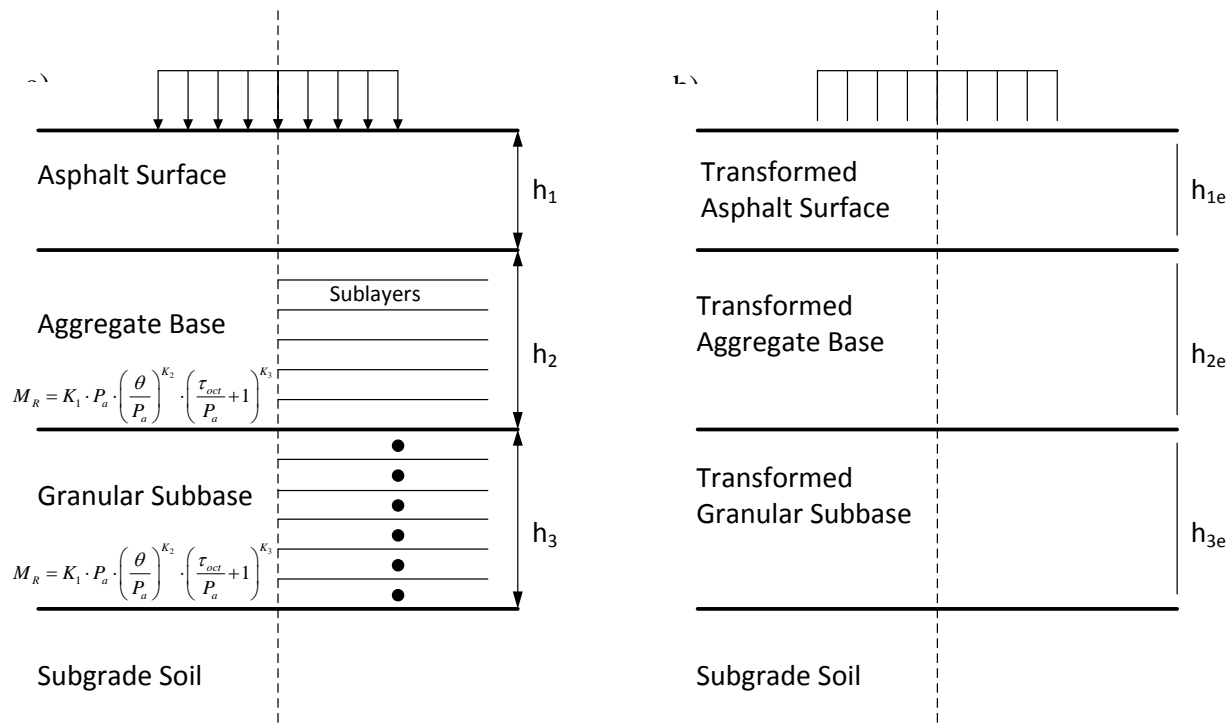


Figure 8.8. The Iterative Procedure of (a) Subdividing Each Nonlinear Granular Layer into a Number of “Imaginary” Sublayers and (b) Transforming “Imaginary” Sublayers into Single Equivalent (subscript “e”) Layers Using the Odemark Method

8.2.4.1 Assume Initial Modulus for Aggregate Base and/or for Granular Subbase

An optional “Nonlinear” mode, as highlighted in Figure 8.9, is envisioned for operating this iterative framework in MnPAVE program, taking advantage of the Climate Module in

MnPAVE for seasonal and geographical effects on modulus. The initial moduli can be either reasonable guesses or empirical values. MnPAVE default design values can also be used. Note that the closer to the actual value the initial modulus is, the faster the iteration process converges. Here, another modular ratio based approach currently used in Austroads (mechanistic-empirical flexible pavement design program used in Australia and New Zealand) is cited as an example for assigning initial moduli to those imaginary sublayers (Saleh et al., 2009).

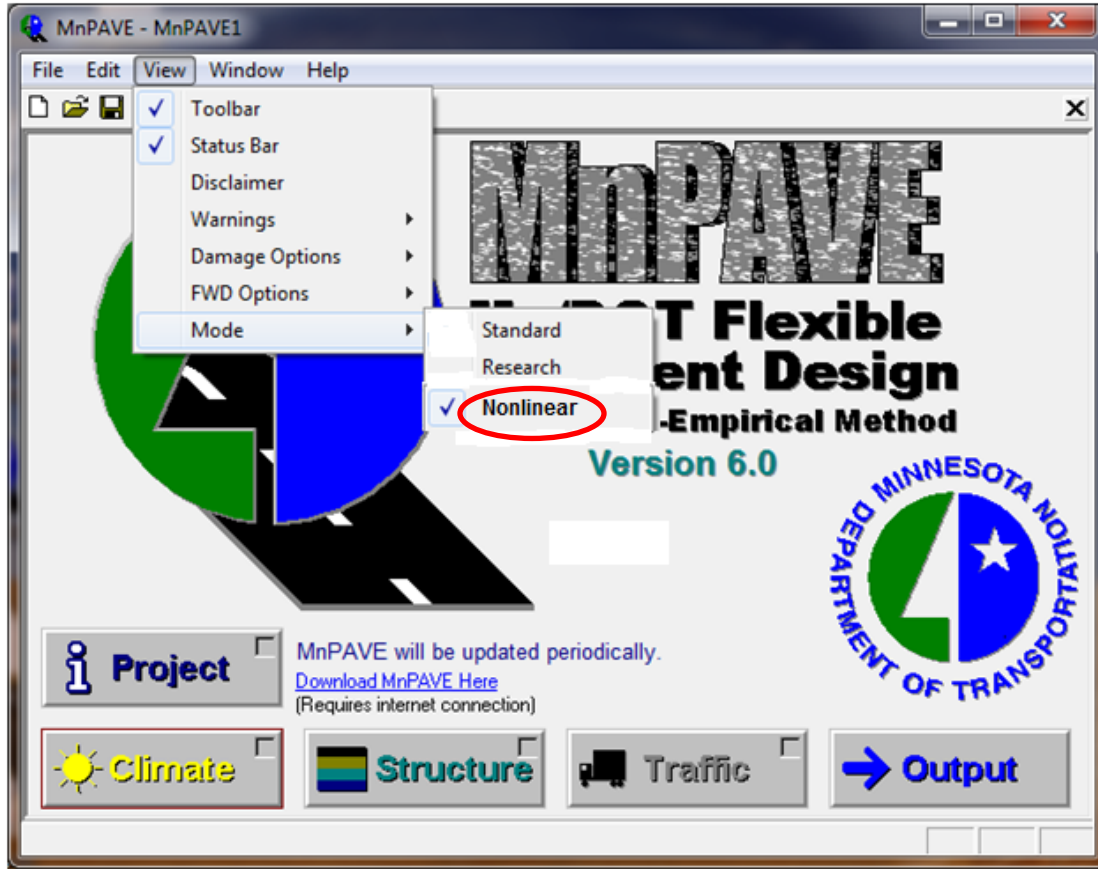


Figure 8.9. The Conceptual Window Showing the Proposed Nonlinear Mode in MnPAVE

$$E_{base,i} = E_{base,1} / \left(\frac{E_{base,1}}{E_{subbase,1}} \right)^{1/n_{base}}$$

$$E_{subbase,i} = E_{subbase,1} / \left(\frac{E_{subbase,1}}{E_{subgrade}} \right)^{1/n_{subbase}} \quad (8.6)$$

where: $E_{base,1}$, $E_{base,i}$ are elastic moduli of the 1st and i-th sub-layers of base course, respectively; $E_{subbase,1}$, $E_{subbase,i}$ are elastic moduli of the 1st and i-th sublayers of subbase course, respectively; $E_{subgrade}$ is elastic modulus of the top subgrade; and n_{base} , $n_{subbase}$ are the number of sublayers for base and subbase courses, respectively.

As given in Equation 8.6, once the initial moduli for top base, subbase and subgrade courses are assumed, the initial moduli for those remaining base/subbase sublayers can then be determined from Equation 8.6 using the corresponding number of sublayers. This way, the decreasing trend of the moduli in the vertical direction can somewhat be represented.

8.2.4.2 Compute Wheel Load Stresses at Critical Points within Each Nonlinear Unbound Aggregate Layer

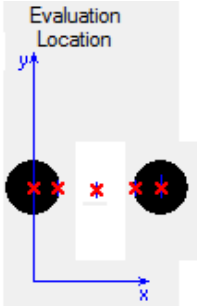
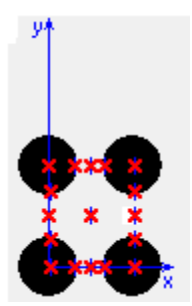
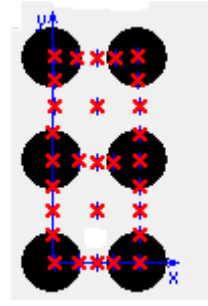
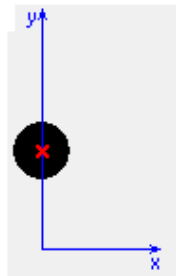
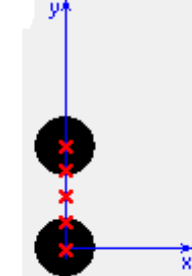
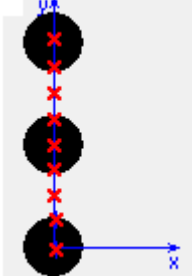
As mentioned previously, MnPAVE is developed based on WESLEA which can solve for a maximum of 5 layers; therefore, instead of increasing the number of layers in the layer elastic analysis, the sublayers locations are used only to compute stresses and capture the decreasing trend of resilient modulus with depth. The number of sublayers (stress computation points) to be used can be determined according to the thickness of base/subbase. Table 8.1 lists the recommended number of sublayers to use for base/subbase layer thickness less than 24 in.

Table 8.1. Recommendations for Determining the Number of Sublayers

Granular Layer Thickness h (in.) for Nonlinear Analysis	Number of Sublayers (Equal thickness)
$0 < h \leq 8$	8
$8 < h \leq 16$	16
$16 < h \leq 24$	24

After selecting the number of sublayers, a Falling Weight Deflectometer (FWD) type single wheel load of 9,000 lbs. can be used for computing traffic induced stresses. Currently, MnPAVE analyzes 7 different axle types, i.e., 18-kip ESAL, Dual Tire, Dual Tandem, Dual Tridem, Single Tire, Single Tandem, and Single Tridem (MnDOT, 2010). Table 8.2 lists the proposed locations of stress points within each sub-layer for each axle type included in MnPAVE program. The reason for the stress point locations is to search for maximum or critical pavement responses. The pavement responses that MnPAVE calculates include normal stresses (σ_x , σ_y , and σ_z), shear stresses (τ_{xy} , τ_{xz} , and τ_{yz}), principal stresses (σ_1 , σ_2 , and σ_3), strains (ϵ_x , ϵ_y , and ϵ_z), and displacements (δ_x , δ_y , and δ_z).

Table 8.2. Proposed Stress Points Locations within Each Sublayer

Axle Type			
Locations of Stress Points			
Axle Type			
Locations of Stress Points			

8.2.4.3 Compute Total Stresses (Wheel Load Stresses + Overburden Pressures)

The vertical and horizontal overburden pressures can be computed using the following equations, respectively.

$$\sigma_z = \sigma_v + p_0$$

$$p_0 = h_n \cdot \gamma_n + \sum_{i=1}^{n-1} h_i \cdot \gamma_i \quad (8.7)$$

where: p_0 is the at-rest vertical pressure from the overburden of other layers; ϕ is the angle of shearing resistance for non-cohesive soils such as gravel and sand (as per ASTM D2487-11), respectively; σ_v is the vertical normal stress applied by the wheel load; and σ_z is the total vertical stress for determining the resilient modulus of nonlinear granular layer.

$$\sigma_{X/Y} = \sigma_H + K_0 \cdot p_0$$

$$K_0 = \begin{cases} 1 - \sin \varphi & \text{for noncohesive soils} \\ \frac{\mu}{1 - \mu} & \text{for cohesive soils} \end{cases} \quad (8.8)$$

where: K_0 is the at-rest pressure coefficient; h_i and γ_i are the thickness and unit weight of the i -th layer; μ is the Poisson's ratio for cohesive soils such as clays; σ_H is the horizontal normal stress applied by the wheel load; and $\sigma_{X/Y}$ is the total lateral stress for determining the resilient modulus of nonlinear granular layer.

The corresponding principal stresses can be calculated at each stress point from vertical and lateral stress components, as the resilient modulus constitutive model requires the use of principal stresses.

8.2.4.4 Compute Predicted Resilient Modulus Using Adjusted/Modified Total Principal Stresses

After adjusting/modifying total principal stresses to satisfy the Mohr-Coulomb theory requirement, those stresses can then be plugged into the M_R model (Equation 8.3) to predict the resilient modulus and start the iterative process. To initiate next iteration, a single modulus is averaged from those sublayer moduli and used for the layered elastic analysis. The convergence check is then applied to determine whether or not the iterative process should be terminated.

8.2.4.5 Convergence Criteria: Check if Relative Error between Predicted New Modulus and Old Modulus from Previous Iteration is less than a Certain Value

The convergence criteria used in GT-PAVE and ILLI-PAVE can be employed here with minor modifications (Tutumluer, 1995). To facilitate converge during each iteration, a damping factor λ (which has value between 0 and 1) can be used to obtain an improved estimate of the resilient modulus for the next iteration in the form below:

$$M_R^j = (1 - \lambda) M_R^{j-1} + \lambda M_{R_{Model}}^j \quad (8.9)$$

where: M_R^j is the actual M_R to be used at the end of iteration number j ; M_R^{j-1} is the M_R used at the end of iteration number $(j-1)$; and $M_{R_{Model}}^j$ is the M_R averaged from corresponding sublayer moduli computed from the M_R constitutive model at the end of iteration number j .

Typical values of λ needed for adequate convergence will be determined after the iterative procedure is implemented into MnPAVE. The convergence criteria proposed for use in this study consist of (i) a maximum of 1% difference between the old and new values of averaged resilient modulus (from sublayer moduli) at each iteration for each nonlinear granular layer and (ii) a temporary 0.2% maximum cumulative error (E_c) criterion which is similar to the one used in the GT-PAVE program (Tutumluer, 1995).

$$E_c = \frac{\sum_{i=1}^n (M_R^j - M_R^{j-1})^2}{\sum_{i=1}^n (M_R^j)^2} \quad (8.10)$$

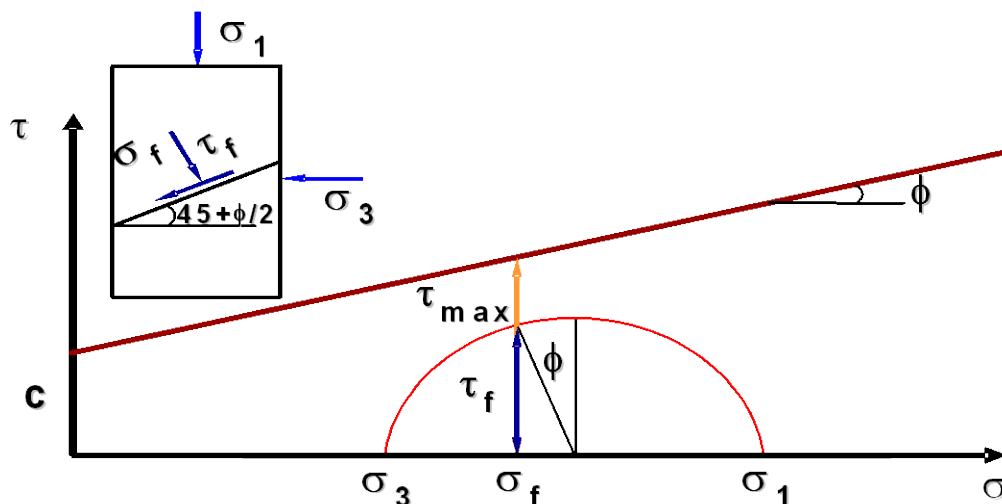
where: n is the total number of stress points in the pavement system; j is the iteration number; and M_R^j is the M_R computed at each stress point from the M_R constitutive equation at the end of iteration number j .

It should be emphasized that the 1% individual and 0.2% cumulative error criteria are proposed here based on previous experience with the GT-PAVE and ILLI-PAVE finite element solutions. The final criteria, i.e. actual error percentages that would work the best for providing convergent MnPAVE solutions will have to be studied after the iterative procedure is fully implemented into MnPAVE.

If convergence is observed, then the iteration process terminates and the converged modulus is displayed to the user and automatically saved by MnPAVE program for use in any subsequent analyses; otherwise, the iterations go back to step 1 and re-start the iteration loop until final convergence is achieved.

8.2.4.6 Evaluation of Granular Material Shear Failure

As mentioned previously, unbound granular materials cannot take tensile stresses. In this study, the Mohr-Coulomb theory is recommended for implementing the shear stress ratio concept presented previously provided that the shear properties of granular materials are available, i.e., the angle of internal friction, ϕ , and the cohesion, c . Figure 8.10 illustrates the shear strength and corresponding failure envelope. This process applies to the final stress point used to compute pavement critical responses.



$$\text{Shear Stress Ratio: } \frac{\text{Applied Shear Stress } (\tau_f)}{\text{Shear Strength } (\tau_{\max})}$$

Figure 8.10. Mohr-Coulomb Representation of Shear Strength and the Failure Envelope

8.3 Summary

This chapter focused on the implementation challenge of the research study findings as MnPAVE Best Value Granular Material components. The following three components were proposed for incorporation into the MnPAVE program to implement mechanistic-based pavement design concepts: (1) GIS-based Aggregate Source Management Component, (2) Aggregate Property Selection Component for Design, and (3) Aggregate Source

Selection/Utilization Component. Immediate attention has been given to the second component for the highest priority in implementation. Accordingly, a methodology has been outlined to determine an equivalent one layer base/subbase modulus from an iterative elastic layered approach that directly accounts for the nonlinear base/subbase behavior in MnPAVE pavement analysis and design software.

Chapter 9 Conclusions and Recommendations

The main objective of this research is to demonstrate that locally available materials can be economically efficient in the implementation of the available mechanistic-based design procedures in Minnesota through the MnPAVE mechanistic-empirical flexible pavement design method. The goal is to develop the components of a new granular material best value software module to be added to the MnPAVE program.

The Minnesota Office of Materials Aggregate Source Information System (ASIS) is a database used to store and retrieve information on gravel pits, rock quarries and commercial aggregate sources. The ASIS database and other aggregate index property databases have been utilized to obtain aggregate properties to categorize locally available aggregate base and granular subbase materials from quarries and borrow pits around the State. Existing laboratory and in situ strength and resilient modulus test data have also been collected from MnDOT sponsored research studies with the intention to define reasonable mechanistic target value design inputs for aggregate base and subbase layers from the established database aggregate index properties. By assigning resilient modulus values to different MnDOT aggregate classes and to aggregate materials having different properties, sensitivity analyses were conducted using the MnPAVE program for generated pavement life expectancies. As a result, certain important performance trends and guidelines have been established to choose a range of design moduli for different MnDOT aggregate classes and modulus-strength correlations and recommendations have been established for pavement design applications. These recommendations involving target values for strength, modulus, and thickness for different design scenarios involving various types and qualities of locally available aggregate materials will need to be incorporated into MnPAVE best value granular materials components also envisioned in this study for future implementation.

9.1 Major Research Findings

9.1.1 *Linkages Established between Aggregate Source Properties and Mechanistic Design Inputs*

Importance of aggregate shape properties was identified through statistical analyses for establishing resilient modulus correlations with aggregate properties. The addition of aggregate shape properties into regression analysis significantly improved the resilient modulus model parameter correlations. The significant aggregate index properties affecting resilient modulus were identified accordingly using Analysis of Variance (ANOVA) at the confidence level of $\alpha=0.05$. Adding as quantifiable predictor variables the imaging based Angularity Index (AI) or Surface Texture (ST) index into the regression equations for the stress-dependent resilient modulus model parameters k_1 , k_2 , and k_3 resulted in higher adjusted R^2 , thus indicating improved prediction accuracy.

Among the three imaging shape indices examined (F&E Ratio, AI and ST), based on the regression results obtained, surface texture (ST) is statistically the most significant influencing k_1 predictions; whereas AI is the most significant for k_2 and k_3 predictions, which should also be further validated with larger aggregate databases.

9.1.2 *Sensitivity Analyses of Mechanistic Design Inputs on Pavement Life Expectancy*

The findings from the MnPAVE sensitivity analyses indicate that for low traffic designs, less than 0.6 million equivalent single axle loads (ESALs), base and subbase quality is somewhat

less significant for achieving 20-year fatigue and rutting performance lives, even in the case of 4-in. thick asphalt concrete surfacing. For low-volume roads, using locally available and somewhat marginal materials may therefore be quite cost-effective. However, for traffic designs greater than 1.5 million ESALs, aggregate material quality becomes quite critical for the fatigue and rutting performances.

The quality of base layer has been found to directly impact fatigue life expectancy. With low quality materials used in the base, increasing base layer thickness does not seem to improve fatigue life as there is not enough support under the asphalt concrete surfacing to minimize bending under wheel loading. Whereas, increasing base thickness significantly improves subgrade rutting performance.

As expected, a stronger engineered subgrade contributes significantly to improved rutting performance. However, increasing engineered subgrade thickness from 12 in. to 36 in. appears to have negligible effects on both rutting and fatigue performances if the underlying subgrade soil provides adequate support.

Interestingly, increasing subbase thickness seems to significantly improve both rutting and fatigue performances. As compared to fatigue performance, rutting performance can benefit much more from an increase in subbase thickness.

A move to Beltrami County in the north from Olmsted County in the south also brings the following seasonal changes into pavement analysis and design: (i) lower winter temperatures, (ii) lower summer temperatures, and (iii) longer winter and shorter summer durations. The main effect of this change is on asphalt pavement surface temperatures and accordingly on fatigue performances. A less significant effect of climate on rutting performance may be attributed to a constant seasonal pore suction resistance factor of 1.0 used during these analyses.

Instead of using both high (H) quality base and subbase materials, if either one of the base or subbase quality decreases from the high (H) to low (L), a similar percent reduction in fatigue life has been determined for any traffic designs in the range of 0.6 million to 6.0 million ESALs. Of course, such a pavement structure still performs better in fatigue than the worst case scenario when both the base and subbase materials are of low (L) quality standards.

Subbase material quality, again linked to modulus characteristics only here, seems to much more significantly impact rutting performance than the quality standards of base materials. According to the results, a high quality, stiff subbase exhibits a bridging effect to better protect the subgrade and offset detrimental effects of low base stiffness.

For low to medium volume roads in Minnesota, locally available and somewhat marginal materials may be used in base layer while higher quality materials can be used in subbase for a greater resistance to subgrade rutting and hence improved long-term pavement performance, provide that shear failure potential in both base and subbase layers can be properly addressed.

9.1.3 Validation of Sensitivity Analyses Using MnDOT Aggregate Strength Data

As revealed from data analyses on the laboratory resilient modulus (M_R) and peak deviator stress to failure at given confining pressure (σ_{df}), it appears that although both resilient modulus and shear strength are likely to be affected by the same set of aggregate source properties and specimen compaction conditions, the modulus behavior and shear resistance are not directly related. Therefore, it may be inappropriate to expect a strong correlation between those two very important mechanistic properties.

It may be insufficient to establish the quality of aggregate base/granular subbase materials based solely on resilient modulus, as certain aggregate materials exhibiting similarly

high or low resilient moduli were observed to show considerable differences in shear resistance, i.e. shear strength. Therefore, a proper selection of aggregate materials to be used in aggregate base/granular subbase layers should provide both (1) high enough layer stiffness to minimize critical pavement responses, e.g., vertical strain/stress on top of subgrade, and (2) adequate shear strength to prevent rutting in the granular layer for a satisfactory pavement performance.

Sensitivity analysis results concerning base/subbase stiffness requirements to minimize subgrade vertical strain and hot mix asphalt tensile bending strain are still applicable as long as special care is taken for protecting base/subbase against potential shear failure. This is especially important for granular subbase materials evaluated in this study since they tend to provide high modulus/stiffness properties, yet, they may exhibit low shear resistance.

The shear resistance of granular materials seems to be more affected by the achieved dry density than other influencing factors, thus indicating the importance of adequate field compaction; whereas the resilient modulus behavior is significantly influenced by even small changes in the achieved moisture content in relation to the optimum moisture content, which may be linked to the moisture sensitivity of aggregate matrix suction potentials to emphasize the importance of properly considering environmental changes in the field.

9.2 Recommendations for Future Research

When developing regression models with the inclusion of shape properties, an assumption was reasonably made that each sample tested for shape properties represented well the aggregate material source from which it was sampled. More aggregate materials from other aggregate sources would definitely improve the developed correlations. Despite the demonstrated significant contribution of aggregate shape (especially surface texture ST), such properties may not be readily measured in MnDOT's material laboratories in the near future. To reasonably overcome this limitation, some guidelines can be prepared for entering visual characterization categories (such as rounded, subrounded, subangular, angular, etc.) and linking those categories to the actual quantifiable shape index variables (FE_Ratio, AI and ST) needed in the equations in accordance with the ranges established for the MnDOT database. In addition, rapid field imaging technologies deserve further exploration for this purpose.

Permanent strain (or deformation) data from preconditioning cycles of laboratory repeated load triaxial tests, if available in the future, should also be analyzed to confirm the observed aggregate quality aspects.

The three components were proposed and outlined for incorporation into the MnPAVE program (1) GIS-based Aggregate Source Management Component, (2) Aggregate Property Selection Component for Design, and (3) Aggregate Source Selection/Utilization Component. These MnPAVE components/modules will bring a major improvement for aggregate design property selection while utilizing best value granular materials for mechanistic pavement design and improved performance. Immediate attention has been given to the second component for the highest priority in implementation. The final coding and development of MnPAVE software with the developed components will be further pursued through follow up MnDOT projects.

References

- Allen, J. (1973). *The Effect of Non-constant Lateral Pressures of the Resilient Response of Granular Materials*. Ph.D. Thesis, University of Illinois at Urbana-Champaign, Urbana, IL.
- Allen, J.J. and Thompson, M.R. (1974). "Resilient Response of Granular Materials Subjected to Time Dependent Lateral Stresses," *Transportation Research Record*, 510, pp. 1-13.
- ASTM Standard D2487-11 (2011). *Standard Practice for Classification of Soils for Engineering Purpose (Unified Soil Classification System)*. ASTM International, West Conshohocken, PA, DOI: 10.1520/D2487-11, www.astm.org.
- AUSTROADS (2003a). "Development of Performance-based Specifications for Unbound Granular Materials." *Part A: Issues and Recommendations*. AP-T29/03, Sydney, Australia.
- Barksdale, R.D. (1972). "Laboratory evaluation of rutting in basecourse materials." *Proceedings of the 3rd International Conference on Structural Design of Asphalt Pavements*, pp. 161-174.
- Barksdale, R.D. and Itani, S.Y. (1989). "Influence of Aggregate Shape on Base Behavior." *Transportation Research Record*, 1227, pp. 173-182.
- Bilodeau, J.-P., Dore, G., and Pierre, P. (2007). "Erosion Susceptibility of Granular Pavement Materials." *International Journal of Pavement Engineering*, 8(1), pp. 55-66.
- Bilodeau, J.-P., Dore, G., and Pierre, P. (2008). "Gradation Influence on Frost Susceptibility of Base Granular Materials." *International Journal of Pavement Engineering*, 9(6), pp. 397-411.
- Bilodeau, J.-P., Dore, G., and Pierre, P. (2009). "Pavement Base Unbound Granular Materials Gradation Optimization." *Proceedings of the 8th International Conference on the Bearing Capacity of Roads, Railways and Airfields*, 1, pp. 145-154.
- Bullen, F. (2003). *Design and Construction of Low-Cost, Low-Volume Roads in Australia*. Paper No. LVR8-1116, TRR 1819, School of Engineering, University of Tasmania, Hobart, Australia.
- Carmichael, R. and Stuart, E. (1978). "Predicting Resilient Modulus: A Study to Determine the Mechanical Properties of Subgrade Soils." *Transportation Research Record*, 1043, pp. 20-28.
- Clyne, T.R., Johnson, E.N., and Worel, B.J. (2010). *Use of Taconite Aggregates in Pavement Applications*. Final Report MN/RC-2010-24, Minnesota Department of Transportation, St. Paul, MN.
- Cook, J.R. and Gourley, C.S. (2003). *A Framework for the Appropriate Use of Marginal Materials*. World Road Association-(PIARC), Technical Committee C12 Seminar, Mongolia.

- Cunningham, C.N. (2009). *Mechanical Response of Crushed Stone Mixtures*. M.S. Thesis, Department of Civil Engineering, North Carolina State University, Raleigh, NC.
- Dai, S. and Zollars, J. (2002). “Resilient Modulus of Minnesota Road Research Project Subgrade Soil.” *Transportation Research Record*, 1786, pp. 20-28.
- Dai, S., Boerner, D. and Isackson, C. (2007). “Failure Analysis of Flexible Pavement Section on MnROAD.” *Transportation Research Board 86th Annual Meeting Compendium of Papers CD-ROM*, Transportation Research Board, Washington D.C.
- Davich, P., Labuz, J.F., Guzina, B., and Drescher, A. (2004). *Small Strain and Resilient Modulus Testing of Granular Soils*. Final Report 2004-39, Minnesota Department of Transportation, St. Paul, MN.
- Dawson, A.R., Thom, N.H., and Paute, J.L. (1996). “Mechanical characteristics of unbound granular materials as a function of condition.” *Flexible Pavements, Proceedings of European Symposium of Euroflex 1993*, A. G. Correia, ed., Balkema, Rotterdam, The Netherlands, pp. 35–44.
- Dempsey, B.J. (1982). “Laboratory and Field Studies of Channeling and Pumping.” *Transportation Research Record*, 849.
- Drumm, E., Boateng-Poku, Y. and Johnson Pierce, T. (1900). “Estimation of Subgrade Resilient Modulus from Standard Tests.” *Journal of Geotechnical Engineering*, 116(5), pp. 774-789.
- Elliot, R.P. and Thornton, S.I. (1988). “Resilient Modulus and AASHTO Pavement Design.” *Transportation Research Record*, 1196, pp. 116-124.
- Garg, N., and Thompson, M.R. (1997). “Triaxial Characterization of Minnesota Road Research Project Granular Materials.” *Transportation Research Record*, 1577.
- George, K.P. (2004). *Resilient Modulus Prediction Employing Soil Index Properties*. Final Report FHWA/MS-DOT-RD-04-172, Mississippi Department of Transportation, Jackson, MS.
- Gray, J.E. (1962). “Characteristics of Graded Base Course Aggregates Determined by Triaxial Tests.” *Engineering Research Bulletin*, 12.
- Gupta, S., Singh, A., and Ranaivoson, A. (2005). *Moisture Retention Characteristics of Base and Sub-base Materials*. Technical Report MN/RC-2005-06, Minnesota Department of Transportation, St. Paul, MN.
- Gupta, S., Ranaivoson, A., Edil, T., Benson, C., and Sawangsuriya, A. (2007). *Use of Taconite Aggregates in Pavement Applications*. Final Report MN/RC-2007-11, Minnesota Department of Transportation, St. Paul, MN.

- Haukaas, T. and Kiureghian, A.D. (1999). "Parameter sensitivity and importance measures in nonlinear finite element reliability analysis." *Journal of Engineering Mechanics*, 131(10), pp. 1013-1026.
- Hicks, R.G. and Monismith, C.L. (1971). "Factors Influencing the Resilient Properties of Granular Materials." *Transportation Research Record*, 345, pp. 15-31.
- Holubec, I. (1969). *Cyclic Creep of Granular Materials*. Report No. RR147, Department of Highways, Ontario, Canada.
- Huang, Y.H. (1993). *Pavement Analysis and Design*. Prentice Hall, Englewood Cliffs, N.J., pp. 103-141.
- Khazanovich, L., Celauro, C., Chadbourn, B., Zollars, J., and Dai, S. (2006). "Evaluation of Subgrade Resilient Modulus Predictive Model for Use in Mechanistic-Empirical Pavement Design Guide." *Transportation Research Record*, 1947, pp. 155-166.
- Khogali, W.E.I. and Mohamed, E.H.H. (2007). "Mechanistic Classification of Unbound Materials." *Transportation Research Record*, 2016.
- Kim, M. (2007). *Three-dimensional Finite Element Analysis of Flexible Pavements Considering Nonlinear Pavement Foundation Behavior*. Ph.D. Dissertation, Department of Civil and Environmental Engineering, University of Illinois at Urbana-Champaign, Urbana, IL.
- Kim, S.-H., Tutumluer, E., Little, N.L., and Kim, N. (2007). "Effect of Gradation on Nonlinear Stress-Dependent Behavior of a Sandy Flexible Pavement Subgrade." *Journal of Transportation Engineering*, 133(10), pp. 582-589.
- Kim, W. and Labuz, J.F. (2007). *Resilient Modulus and Strength of Base Course with Recycled Bituminous Material*. Technical Report MN/RC-2007-05, Minnesota Department of Transportation, St. Paul, MN.
- Knutson, R.M. and Thompson, M.R. (1977). "Resilient Response of Railway Ballast." *Transportation Research Record*, 651, pp. 31-39.
- Lekarp, F., Isacsson, U., and Dawson, A. (2000). "State of the art I: Resilient Response of Unbound Aggregates." *Journal of Transportation Engineering*, 126(1), pp. 66-75.
- Lindly, J., Townsend, J.T., and Elsayed, A. (1995). "How Top-Size Affects the Resilient Modulus of Roadway Base Materials." *Engineering Journal of University of Qatar*, 8, pp. 127-138.
- Madsen, H.O., Krenk, S., and Lind, N.C. (1986). *Methods of structural safety*. Prentice-Hall, Inc., Englewood Cliffs, N.J.

- Mohammad, L., Huang, B., Puppala, A. and Allen, A. (1999). "Regression Model for Resilient Modulus of Subgrade Soils." *Transportation Research Record*, 1442, pp. 47-54.
- Morgan, J.R. (1966). "The Response of Granular Materials to Repeated Loading." *Proceedings of the 3rd Conference, Australian Road Research Board*, Sydney, Australia, pp. 1178-1192.
- Mulvaney, R. and Worel, B. (2002). *MnROAD Cell 26 Forensic Investigation*. Technical Report No. 2002-06, Minnesota Department of Transportation, St. Paul, MN.
- Pan, T., Tutumluer, E., and Carpenter, S.H. (2005). "Effect of Coarse Aggregate Morphology on Resilient Modulus of Hot-Mix Asphalt." *Transportation Research Record*, 1929, pp. 1-9.
- Pan, T. and Tutumluer, E. (2005). "Imaging Based Evaluation of Coarse Aggregate Size and Shape Properties Affecting Pavement Performance." *Advances In Pavement Engineering*, ASCE Geotechnical Special Publication No. 130, C.W. Schwartz, E. Tutumluer, and L. Tashman, eds.
- Paute, J.L., Hornych, P., and Benaben, J.P. (1994). "Comportement mécanique des graves non traitées." *Bulletin de Liaison des Laboratoires des Ponts et Chaussées*, 190, pp. 27-38.
- Pumphrey, Jr., N.D., and Lentz, R.W. (1986). "A Deformation Analysis of Florida Highway Subgrade Sand Subjected to Repeated Load Triaxial Tests." *Transportation Research Record*, 1089, pp. 49-56.
- Puppala, A.J. (2008). *Estimating Stiffness of Subgrade and Unbound Materials for Pavement Design*. NCHRP Synthesis 382, TRB, National Research Council, Washington, D.C.
- Rahim, A. and George, K. (2004). "Subgrade Soil Index Properties to Estimate Resilient Modulus." *Proceedings of the 83rd Annual Meeting of Transportation Research Board*, Washington, D.C.
- Rao, C., Tutumluer, E., and Stefanski, J.A. (2001). "Flat and Elongated Ratios and Gradation of Coarse Aggregates Using a New Image Analyzer." *ASTM Journal of Testing and Standard*, 29(5), pp. 79-89.
- Rao, C., Tutumluer, E., and Kim, I.T. (2002). "Quantification of Coarse Aggregate Angularity based on Image Analysis." *Transportation Research Record*, 1787, pp. 17-124.
- Rowshanzamir, M.A. (1995). *Resilient Cross-Anisotropic Behavior of Granular Base Materials Under Repetitive Loading*. Ph.D. Thesis, University of New South Wales, School of Civil Engineering, Australia.
- Ruth, B.E., Roque, R., and Nukunya, B. (2002). "Aggregate Gradation Characterization Factors and Their Relationships to Fracture Energy and Failure Strain of Asphalt Mixtures." *Journal of Association of Asphalt Paving Technologists*, 71, pp. 310-344.

- Saeed, A., Hall, J., and Barker, W. (2001). *Performance-related Tests of Aggregates for Use in Unbound Pavement Layers*. NCHRP Report No.453, National Academy Press, Washington, D.C.
- Saleh, M., Dixit, V., and Radwan, E. (2009). "Validation of the Austroads Quasi Nonlinear Sublayering Approach for the Design of Flexible Pavements." *Road & Transport Research*, 8(2), pp. 27-38.
- Sandefur, K. (2003). *Correlation of Resilient Modulus of Fine-grained Soils with Common Soil Parameters for Use in Design of Flexible Pavements*. M.Sc. Thesis, University of Hawaii, Manoa, HI.
- Santha, B.L. (2009). "Resilient Modulus of Subgrade Soil: Comparison of Two Constitutive Equations." *Transportation Research Record*, 1462, pp. 79-90.
- Seyhan, U., and Tutumluer, E. (2002). "Anisotropic Modular Ratios as Unbound Aggregate Performance Indicators." *Journal of Materials in Civil Engineering*, 14(5), pp. 409-416.
- Smith, B.E. and Witczak, M.W. (1981). "Prediction of Equivalent Granular Base Moduli Incorporating Stress Dependent Behavior in Flexible Pavement." *Journal of Transportation Engineering*, 107(6), pp. 635-652.
- Tao, M., Abu-Farsakh, M., and Zhang, Z. (2008). "Optimize Drainable Unbound Aggregate Through Laboratory Tests." *Proceedings of GeoCongress 2008: Characterization, Monitoring, and Modeling of Geosystems*, GSP 179, pp. 28-35.
- Tao, M., Louay, M.N., Munir, N.D., Zhang, Z., and Wu, Z. (2010). "Application of Shakedown Theory in Characterizing Traditional and Recycled Pavement Base Materials." *Journal of Transportation Engineering*, 136(3), pp. 214-222.
- Tian, P., Zaman, M.M., and Laguros, J.G. (1998). "Gradation and Moisture Effects on Resilient Moduli of Aggregate Bases." *Transportation Research Record*, 1619, pp. 7-17.
- Titi, H., Elias, M. and Helwany, S. (2006). *Determination of Typical Resilient Modulus Values for Selected Soils in Wisconsin*. Final Technical Report, Wisconsin Highway Research Program Project ID 0092-03-11, Department of Civil Engineering and Mechanics, University of Wisconsin-Milwaukee, Milwaukee, WI.
- Thom, N.H. and Brown, S.F. (1987). "Effect of moisture on the structural performance of a crushed-limestone road base." *Transportation Research Record*, 1121, pp. 50-56.
- Thom, N.H. and Brown, S.F. (1988). "The Effect of Grading and Density on the Mechanical Properties of a Crushed Dolomitic Limestone." *Proceedings of the 14th ARRB Conference*, Part 7, pp. 94-100.

- Thompson, M.R. and Robnett, Q.L. (1979). "Resilient Properties of Subgrade Soils." *Transportation Engineering Journal*, 105(1), pp. 71-89.
- Thompson, M.R. and Smith, K.L. (1990). "Repeated Triaxial Characterization of Granular Bases." *Transportation Research Record*, 1278, pp. 7-17.
- Thompson, M.R. (1998). "State-Of-The-Art: Unbound Base Performance." *Proceedings of the 6th Annual Symposium of International Center for Aggregate Research (ICAR)*, Austin, TX.
- Tutumluer, E. (1995). *Predicting Behavior of Flexible Pavements with Granular Bases*. Ph.D. Dissertation, School of Civil and Environmental Engineering, Georgia Institute of Technology, Atlanta, GA.
- Tutumluer, E. and Seyhan, U. (1998). "Neural Network Modeling of Anisotropic Aggregate Behavior from Repeated Load Triaxial Tests." *Transportation Research Record*, 1615, pp. 86-93.
- Tutumluer, E., Rao, C., and Stefanski, J.A. (2000). *Video Image Analysis of Aggregates*. Final Project Report, FHWA-IL-UI-278, Civil Engineering Studies UILU-ENG-2000-2015, University of Illinois Urbana-Champaign, Urbana, IL.
- Tutumluer, E. and Seyhan, U. (2000). "Effects of Fines Content on the Anisotropic Response and Characterization of Unbound Aggregate Bases." *Proceedings of the 5th International Symposium on Unbound Aggregates in Roads (UNBAR5), Unbound Aggregates in Road Construction*, A.R. Dawson and A.A. Balkema, eds., University of Nottingham, UK, pp. 153-161.
- Tutumluer, E. and Pan, T. (2008). "Aggregate Morphology Affecting Strength and Permanent Deformation Behavior of Unbound Aggregate Materials." *Journal of Materials in Civil Engineering*, 20(9), pp. 617-627.
- Tutumluer, E., Mishra, D., and Butt, A.A. (2009). *Characterization of Illinois Aggregate for Subgrade Replacement and Subbase*. Technical Report FHWA-ICT-09-060, Illinois Center for Transportation (www.ict.illinois.edu), pp. 1-179.
- Tutumluer, E., Huang, H., Hashash, Y.M.A., and Ghaboussi, J. (2009). "AREMA Gradations Affecting Ballast Performance Using Discrete Element Modeling (DEM) Approach." *Proceedings of the AREMA 2009 Annual Conference*, Chicago, IL, September 20-23.
- Uzan, J. (1985). "Characterization of Granular Materials." *Transportation Research Record*, 1022, pp. 52-59.
- Vallejo, L.E. (2001). "Interpretation of the Limits in Shear Strength in Binary Granular Mixtures." *Canadian Geotechnical Journal*, 38, pp. 1097-1104.

- Van Cauwelaert, F.J., Alexander, D.R., White, T.D., and Barker, W.R. (1989). "Multilayer Elastic Program for Backcalculating Layer Moduli in Pavement Evaluation." *Nondestructive Testing of Pavements and Backcalculation of Moduli*, ASTM STP 1026, A.J. Bush II and G.Y. Baladi, eds., American Society for Testing and Materials, Philadelphia, PA, pp. 171-188.
- Van Niekerk, A.A. (2002). *Mechanical Behavior and Performance of Granular Bases and Sub-Bases in Pavements*. Ph. D. Thesis, Technische Universiteit Delft, Delft, The Netherlands.
- Witczak, M.W., and Uzan, J. (1988). *The Universal Airport Pavement Design System Report I of V: Granular Materials Characterization*. University of Maryland, College Park, MD, pp. 79.
- Wood, D.M. (1982). "Laboratory Investigations of the Behavior of Soils under Cyclic Loading: A Review." *Soil Mechanics-Transient and Cycle Loads*. G.N. Pance and O.C. Zienkiewicz, eds. John Wiley and Sons Inc., New York, NY, pp. 513-582.
- Woodbridge, M.E. (1999). "Use of Soft Limestone for Road-Base Construction in Belize." *Proceedings of the 7th International Conference on Low-Volume Roads*, Baton Rouge, LA.
- Yau, A. and Von Quintus, H. (2004). "Predicting Elastic Response Characteristics of Unbound Materials and Soils." *Transportation Research Record*, 1874, pp. 47-56.
- Yohannes, B., Hill, K., and Khazanovich, L. (2009). *Mechanistic Modeling of Unbound Granular Materials*. Technical Report MN/RC-2009-21, Minnesota Department of Transportation, St. Paul, MN.

**Appendix A: University of Illinois Laboratory Databases of
Aggregate Modulus and Strength Test Results**

A.1 NCHRP 4-23 Research Project Database

A.1.1 Types and Properties of Aggregate Materials Tested

As part of the NCHRP 4-23 Phase II laboratory testing program, UI-FastCell testing was undertaken to determine directional dependency (anisotropy) of M_R at various stress states and then to correlate anisotropic modular ratios to the quality and strength properties of the aggregate. Twelve aggregates with varying material types and properties were selected for M_R testing using the UI-FastCell. In the selection process, consideration was given to both good and poor performing granular base/subbase materials obtained from seven different states. A realistic range of aggregate qualities and properties, such as average and top sizes, gradations (both uniform and well-graded samples), particle shapes (rounded gravel to angular crushed stone), and fines contents, i.e., materials less than 0.075 mm (No. 200 sieve) size, were represented. The variations among the aggregate types and properties were considered essential for studying the effects of material properties on the anisotropic resilient behavior under the application of vertical and radial pulse loadings. To establish a consistent test procedure to successfully discern anisotropy in aggregate specimen responses, a synthetic calibration specimen with known isotropic material properties was also tested.

Gradation curves for the twelve aggregates are given in Figures A.1 and A.2. Except for the two uniformly graded aggregates, PA Good Quality and the IN Section #2421, the materials studied can generally be considered as well-graded. The top sizes vary from 25-mm (1-in.) to 51-mm (2-in.). Both crushed aggregates composed of angular particles having rough surfaces such as the MN Fountain Quarry, and rounded gravels such as the MN Shiely Elk River material can be found in the material mix. There is a considerable variation in the fines content values ranging from less than 1% in the case of PA Good Quality to 17.9% for the TX Subgrade 1426 material.

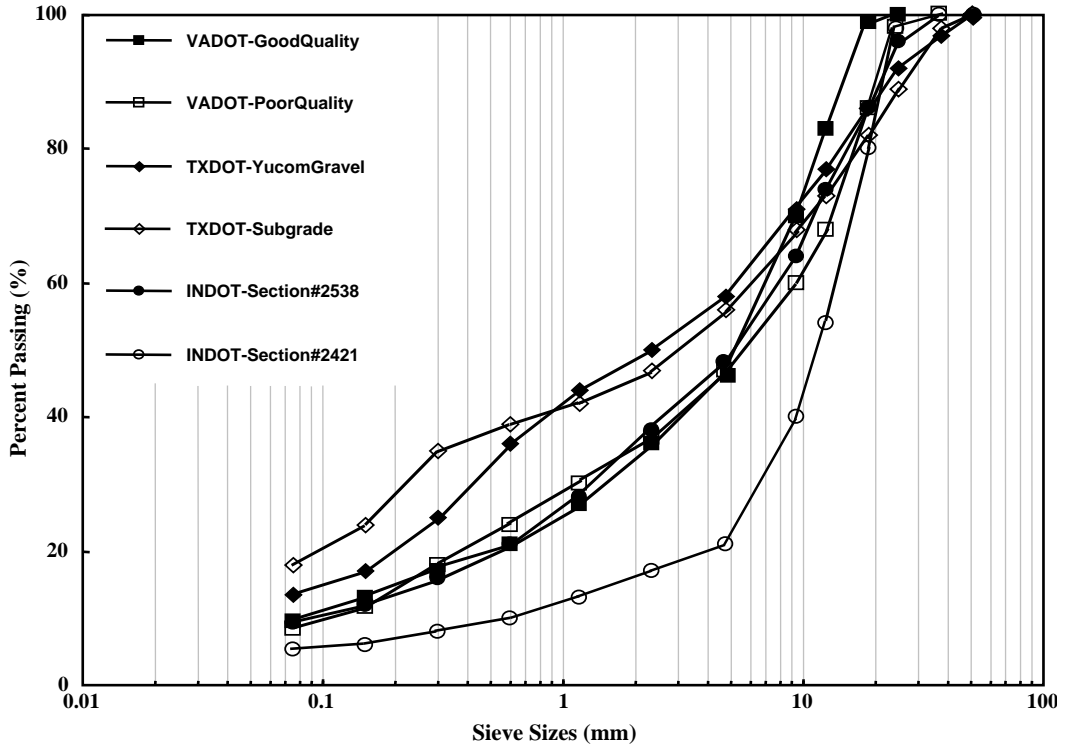


Figure A.1. Gradation Curves for Virginia, Texas, and Indiana Aggregates (Seyhan and Tutumluer, 2000)

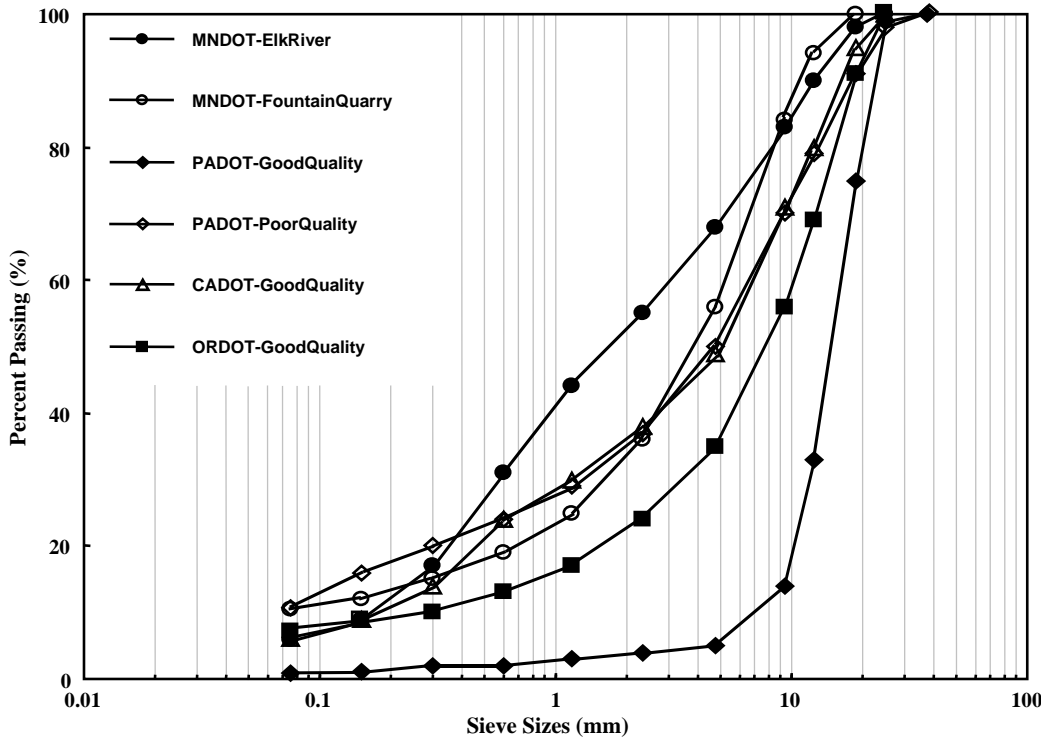


Figure A.2. Gradation Curves for Minnesota, Pennsylvania, California, and Oregon Aggregates (Seyhan and Tutumluer, 2000)

Table A.1 reports the strength and compaction properties of the twelve aggregates as obtained from tests performed by Braun Intertec, Inc. of Minneapolis, MN. The static strength properties were obtained from standard triaxial tests (ASTM D 2850) conducted at confining pressures of 35, 69, and 104 kPa (5, 10, 15 psi) on samples compacted at optimum moisture states. The maximum dry densities and the optimum moisture contents are for modified Proctor tests (AASHTO T-180). In addition, Table A.1 also gives for each aggregate the fines content and specific gravity (G_s) and the theoretical moisture contents computed at both 90% and 100% saturation using the maximum dry density and the G_s information.

Table A.1 Strength, Compaction, and Material Properties for 12 Aggregates Tested (Seyhan and Tutumluer, 2000)

State	Material	c (opt) kpa (psi)	ϕ (opt) (degree)	Fines Content (%)	Specific Gravity G _s	Max	Opt	100%	90%
						Dry Density γ_{max} g/cm ³ (pcf)	Moist. Content W _{opt} (%)	Sat. Moist. Content W (%)	Sat. Moist. Content W (%)
MN	Class 5 Fountain Quarry	0.0 (0.0)	58.0	10.40	2.71	2.28 (142.3)	6.1	6.9	6.3
MN	Class 5 Shiely Elk River	0.0 (0.0)	55.1	6.00	2.72	2.20 (137.3)	6.5	8.7	7.8
TX	#17 Yucom County Gravel	26.9 (3.9)	48.3	13.5	2.64	2.16 (135.0)	6.2	8.3	7.5
TX	#13 Subgrade 1426	9.6 (1.4)	45.9	17.90	2.62	2.03 (126.6)	8.5	11.2	10.0
IN	Section #2538	57.2 (8.3)	56.4	9.3	2.73	2.07 (129.5)	11.0	11.8	10.4
IN	Section #2421	44.1 (6.4)	52.0	5.2	2.82	2.20 (137.0)	9.5	10.2	9.1
VA	Good Quality w/o Mica	77.2 (11.2)	48.9	9.6	2.76	2.29 (143.0)	5.5	7.3	6.7
VA	Poor Quality with Mica	84.1 (12.2)	40.9	8.5	2.66	2.20 (137.0)	5.5	8.0	7.2
CA	Good Quality Aggregate	69.0 (10.0)	53.7	6.2	2.78	2.28 (142.0)	7.5	8.0	7.2
OR	Good Quality Aggregate	87.6 (12.7)	50.2	7.2	2.89	2.25 (140.5)	7.6	10.0	8.8
PA	Good Quality Aggregate	46.9 (6.8)	48.8	0.9	2.71	2.12 (132.0)	8.6	10.3	9.4
PA	Poor Quality Aggregate	9.7 (1.4)	49.8	10.7	2.71	2.21 (138.0)	6.8	8.4	7.5

A.1.2 Sample Preparation Procedure

Cylindrical specimens, 150 mm in diameter by 150 mm high (approximately 6-in. in diameter by 6-in. high), were prepared to fit in the confinement chamber of the UI-FastCell for the repeated load triaxial testing. A total of 46 specimens, four samples for each aggregate except for only two samples tested for the PA Good Quality material, were prepared using a pneumatic vibratory compactor. The dry densities and moisture contents recorded for a total of 46 samples of the twelve aggregates are listed in Table A.2. For each material, samples were prepared at two moisture contents: (i) optimum moisture content corresponding to maximum dry density and (ii) wet of optimum moisture content near saturation. The achieved dry densities at optimum moisture contents match closely with the maximum Proctor densities. For the PA Good Quality material that had only 5% minus 4.75 mm (No. 4 sieve) size and 0.9% minus 0.075 mm (No. 200 sieve) size, only one moisture content could be consistently achieved. The achieved water contents are in general very close to the optimum values for the rest of the samples tested at optimum moisture contents. For the wet of optimum tests, minimum moisture contents that provided at least 90% saturation were typically achieved.

Table A.2 Achieved Dry Densities and Water Contents for All Samples Tested (Seyhan and Tutumluer, 2000)

State	Material	Optimum Moisture Content				Wet of Optimum Moisture Content			
		Sample #1 Achieved		Sample #2 Achieved		Sample #3 Achieved		Sample #4 Achieved	
		w (%)	γ (pcf)	w (%)	γ (pcf)	w (%)	γ (pcf)	w (%)	γ (pcf)
MN	Class 5 Fountain Quarry	5.00	2.30 (143.79)	5.60	2.29 (142.97)	6.27	2.29 (143.14)	6.80	2.28 (142.43)
MN	Class 5 Shiely Elk River	6.46	2.20 (137.35)	6.49	2.20 (137.31)	8.40	2.21 (137.68)	8.70	2.20 (137.30)
TX	#17 Yucom County Gravel	6.35	2.16 (134.81)	6.75	2.15 (134.30)	8.30	2.16 (135.00)	8.30	2.16 (135.00)
TX	#13 Subgrade 1426	8.45	2.03 (126.66)	8.35	2.03 (126.78)	12.00	2.01 (125.70)	11.20	2.03 (126.60)
IN	Section #2538	10.30	2.09 (130.32)	10.60	2.08 (129.97)	11.60	2.08 (129.73)	13.00	2.05 (128.12)
IN	Section #2421	8.50	2.22 (138.26)	9.60	2.19 (136.88)	10.00	2.20 (137.25)	10.40	2.19 (136.75)
VA	Good Quality w/o Mica	5.20	2.30 (143.41)	5.50	2.29 (143.00)	6.90	2.30 (143.54)	8.10	2.27 (141.94)
VA	Poor Quality with Mica	5.30	2.20 (137.26)	5.70	2.19 (136.74)	8.40	2.19 (136.49)	8.10	2.19 (136.87)
CA	Good Quality Aggregate	7.10	2.28 (142.53)	7.40	2.28 (142.13)	8.10	2.27 (141.87)	7.70	2.28 (142.40)
OR	Good Quality Aggregate	7.30	2.26 (140.89)	6.90	2.27 (141.42)	10.30	2.25 (140.12)	10.20	2.25 (140.25)
PA	Good Quality Aggregate	4.35	1.82 (113.56)	4.74	1.81 (113.14)	---	---	---	---
PA	Poor Quality Aggregate	7.30	2.20 (137.36)	7.10	2.20 (137.61)	9.20	2.19 (136.99)	8.10	2.22 (138.38)

A.1.3 Resilient Modulus Test Procedure

The UI-FastCell cyclic loading system used is a Universal Testing Machine (UTM), a Closed-Loop Servo Control material testing machine. The main part of the system consists of loading frame, triaxial cell, air power supply, Control and Data Acquisition System (CDAS), and personal computer with an integrated software package. The specimens were not conditioned before the actual testing sequence. Following the standard AASHTO T294-94 procedure, the specimens were subjected to 15 triaxial stress states that are typically less than the failure stress states. A haversine load waveform was applied with a load pulse duration of 0.1-seconds (10-Hz), and a rest period of 0.9-seconds. After the 2-kPa (0.3-psi) hydrostatic seating stress was applied on the specimen, resilient modulus testing was conducted in both the vertical (direction 1) and radial (direction 3) pulsing directions with the applied (pulsed) deviator stresses σ_{nd} ($n = 1$ or 3). Two replicate specimens for each moisture state were tested following the test procedures A and B at a total of 30 stress states each to study the effects of stress history built in the samples (Seyhan and Tutumluer, 2000).

The pulsed deviator stresses, σ_{nd} , ranged from 21 to 276 kPa (3 to 40 psi) in both axial and radial directions whereas the hydrostatic pressures ranged from 21 to 138 kPa (3 to 20 psi). The applied stress ratios, defined as the total stress in any direction divided by the hydrostatic stress $[(\sigma_{nd} + \sigma_{hydrostatic}) / \sigma_{hydrostatic}]$, ranged from 1.66 to 4. One hundred load repetitions were applied at each stress state. Typically, the same vertical and radial recoverable deformations were measured between the 50th and 100th load repetitions.

A.2 Federal Aviation Administration (FAA) Granular Base/Subbase Material Study Database

A.2.1 Types and Properties of Aggregate Materials Tested

The FAA specified granular base and subbase materials, NAPTF P209 and P154, both crushed aggregate were selected for permanent deformation testing in the laboratory and for studying the effects of moving wheel loads and the degree of compaction (Kim and Tutumluer,

2007). The NAPTF P209 and P154 are one of FAA material items specified in terms of usage of materials. They are usually used for airport pavement constructions. In particular, the NAPTF P209 is referred to a crushed aggregate base course (crushed limestone) and the NAPTF P154 is referred to a subbase course (manufactured screenings) according to FAA Advisory Circular 150/5370-10B. Therefore, it is necessary to review the material properties of NAPTF P209, classified as A-1-a according to AASHTO procedure and as GP-GM (poorly graded gravel with silt) according to ASTM procedure, and P154, classified as A-1-b according to AASHTO procedure and as SW-SM (well graded sand with silt) according to ASTM procedure, as FAA base/subbase granular materials.

Figure A.3 shows the gradation curves for the NAPTF P209 and P154 materials used in the FAA's NAPTF granular base and subbase courses. The NAPTF P209 had a maximum size of 50-mm (2-in) and 6.7 % fines content, whereas the NAPTF P154 had a maximum size of 12.5-mm (0.5-in) and 10% fines content. The mean particle sizes for the NAPTF P209 and P154 were 8-mm and 1.7-mm, respectively. The dry densities and moisture contents for the NAPTF P209 and P154 aggregates were determined following the procedure of the modified Proctor (AASHTO T180) test. Results of the modified Proctor tests are given in Table A.3.

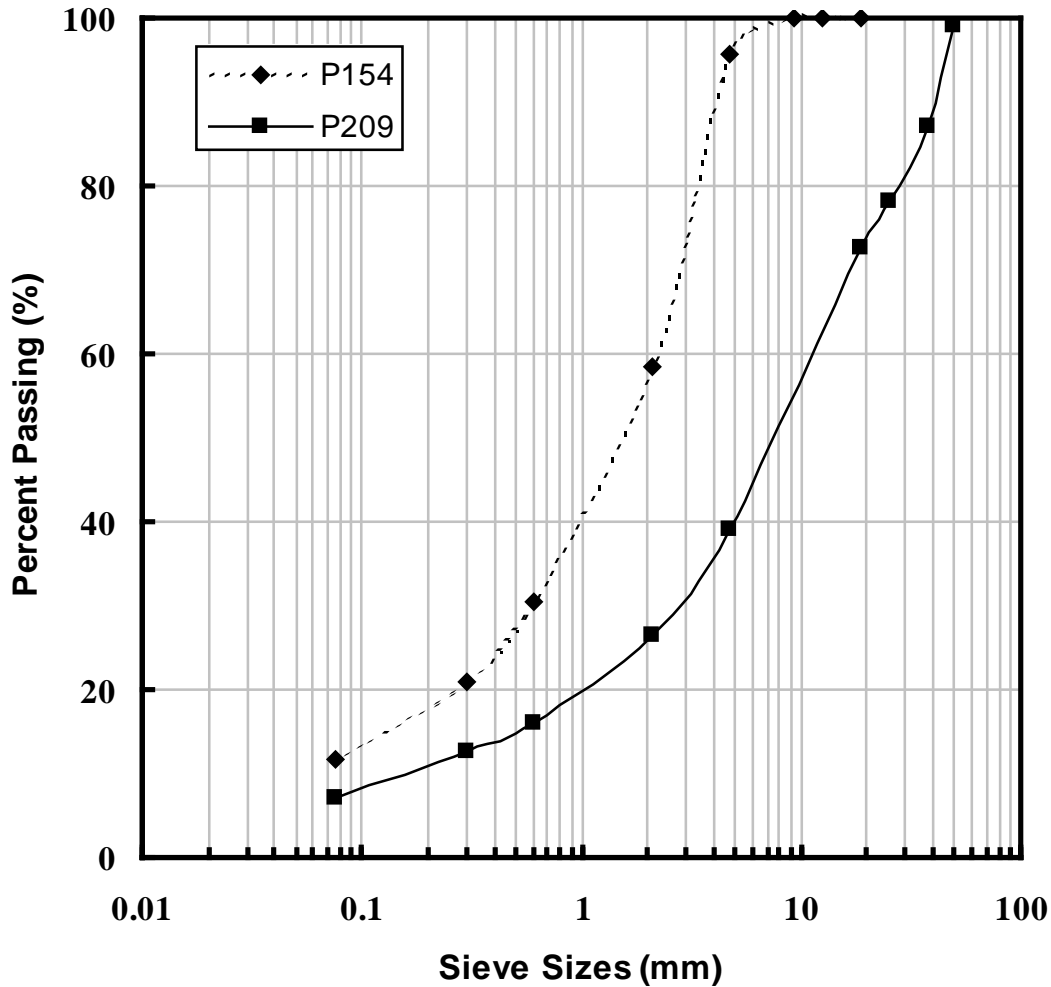


Figure A.3 Gradation Curves for the NAPTF P209 and P154 Materials (Kim, 2007)

Table A.3 Modified Proctor Test Results for NAPTF P209 and P154 (Kim, 2007)

Material	Maximum Dry Density, kN/m ³	Optimum Moisture Content, %
NAPTF P209	24.19	4.7
NAPTF P154	20.04	6.5

A.2.2 Resilient Modulus Test Procedure

The standard AASHTO T307-99 modulus test procedures were followed for NAPTF P209 and P154, respectively. The moduli obtained at the 15 AASHTO stress states were also plotted with bulk stress, $\Theta = \sigma_d + 3\sigma_3$, where σ_d is the deviator stress and σ_3 is the confining pressure. For the stronger NAPTF P209 granular base material, resilient moduli obtained vary between 200 MPa (30 ksi) and 430 MPa (62 ksi) while the P154 subbase material has resilient moduli ranging from 120 MPa (17 ksi) to 285 MPa (41 ksi) for the same stress states.

A.2.3 Shear Strength Test Procedure

Compared to the conventional triaxial shear tests, a very high loading rate of 3.8cm/second (1.5 in./second) is typically applied in rapid shear tests, causing 12.5% deformation in a 305mm (12-in) high specimen, to better simulate the conditions of the actual pavement layer under the dynamic application of a moving wheel load. Rapid shear tests were conducted at 35, 69, and 104 kPa (5, 10, and 15 psi) confining pressures. Typically, higher peak stresses were obtained in the samples when compared to the results of conventional tests. The NAPTF P209 aggregate had a friction angle of 61.7° with a cohesion intercept of 132 kPa and the NAPTF P154 material had a friction angle of 44° with a cohesion intercept of 182 kPa.

A.3 Fines Content Study

A.3.1 Types and Properties of Aggregate Materials Tested

A crushed dolomite classified as A-1-a according to AASHTO procedure was selected for modulus testing using the UI-FC and for studying the effects of stress path loading on resilient moduli (Seyhan and Tutumluer, 1999). This is a well-graded angular aggregate that is commonly used in pavement construction by the Illinois Department of Transportation and designated for its standard gradation as the CA-6 material. Using only one aggregate type to prepare replicate samples was considered essential for studying the effects of loading on the anisotropic resilient behavior under the application of vertical and radial pulse loadings. The use of a synthetic calibration specimen with known isotropic material properties was also considered for verifying the accuracy of UI-FC test results and interpretation of test data.

Table A.4 reports the modified Proctor dry density (AASHTO T-180) and the corresponding optimum moisture content for the CA-6 aggregate. The material was composed of angular particles having rough surfaces, a fines content of 7.7%, and a top size of 25-mm.

Table A.4 Properties of the CA-6 Crushed Aggregate (Seyhan and Tutumluer, 1999)

Gradation		Material Properties		
Sieve Size (mm)	% Passing	c (kPa)	ϕ (degrees)	
		166	48	
25	100.0	Opt. Water Content, w_{opt} (%)	Max. Dry Density γ_{dry} (kN/m ³)	
18.75	97.1	5.4	22.81	
12.5	80.1	Stress Path m	Achieved w (%)	Achieved γ_{dry} (kN/m ³)
9.375	71.0		5.0	23.15
4.75	47.8	3.0, -1.5	4.6	22.92
2.36	31.9	0.75	4.4	22.96
1.18	21.9	1.5	4.9	22.85
0.3	11.8	-0.6	4.5	22.94
0.075	7.7	-1.5		

A.3.2 Testing Program

The cylindrical specimens were compacted by the pneumatic vibratory compactor during the sample preparation stage at or near the optimum moisture content according to the AASHTO T-180 procedure (see Table A.4). This compaction effort on the specimens was assumed to represent the initial conditions of the granular layers in the field just after pavement construction. Therefore, the specimens were not conditioned before the actual testing sequence.

A total of six tests were conducted on the CA-6 samples for the selected constant stress path slopes. Figure A.4 and Table A.5 present together the summary of the stress path testing program and the 15 combined, static (subscript s) and dynamic (subscript d), triaxial stress states that the specimens were subjected to following closely the standard AASHTO (T294-94) test procedure. A haversine load waveform was applied during testing with a load pulse duration of 0.1-seconds (10-Hz), and a rest period of 0.9-seconds. After the 2-kPa hydrostatic seating stress was applied on the specimen, resilient modulus testing was conducted by loading first hydrostatically and then by: (1) pulsing only in the vertical (σ_{1d}) or radial (σ_{3d}) direction for CCP1 compression or CCP2 extension tests, respectively, or (2) pulsing both in the vertical (σ_{1d}) and radial (σ_{3d}) directions for VCP tests. For the compression VCP1 and VCP2 tests with positive stress path slopes ($m = q/p$), full values of σ_{1d} shown in Table 4.5 were always pulsed. Similarly, for the extension VCP3 and VCP4 tests with negative slopes, the values shown in Table A.5 were always pulsed for σ_{3d} at each hydrostatic pressure p_0 . One hundred load repetitions were applied at each stress state. Typically, the same vertical and radial recoverable deformations were measured between the 50th and 100th load repetitions.

Table A.5 Properties of the CA-6 Crushed Aggregate (Seyhan and Tutumluer, 1999)

	$p_0 = \sigma_{\text{hydrostatic}} = \sigma_{1s} = \sigma_{3s}$ (kPa)				
	21	34	69	103	138
σ_{1d}	21^1	34^4	69^7	69^{10}	103^{13}
or	41^2	69^5	138^8	103^{11}	138^{14}
σ_{3d} (kPa)	62^3	103^6	207^9	207^{12}	276^{15}

1 : testing sequence number,
 σ_{1d} : compression, σ_{3d} : extension.

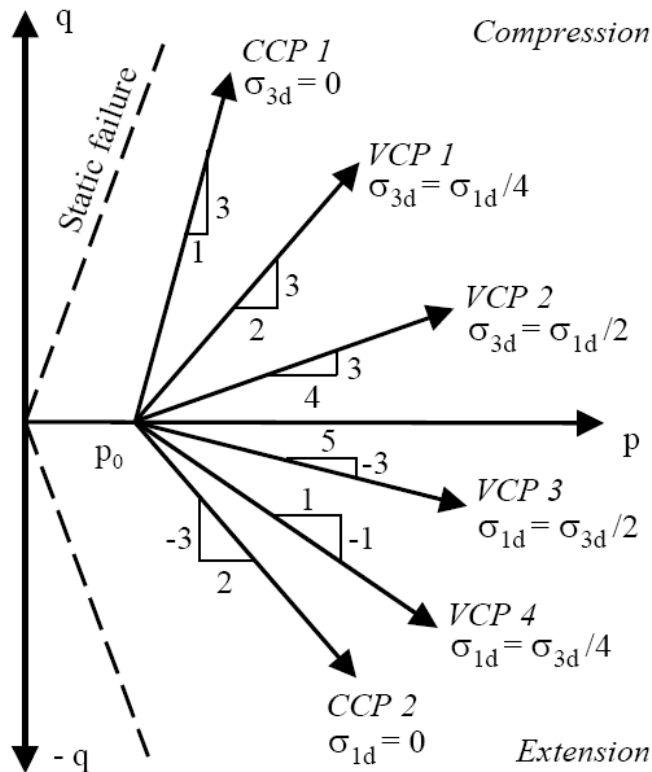


Figure A.4. Summary of UI-FastCell Testing Program for Fines Content Study (Seyhan and Tutumluer, 1999)

A.4 Illinois Center for Transportation R27-1 Research Project Database

A.4.1 Types and Properties of Aggregate Materials Tested

The laboratory testing effort for this research project was designed so as to enable the researchers to assess the relative importance of different parameters affecting aggregate behavior. The focus was on the characteristics and performances of dense graded structural layers for developing various aggregate property correction factors to determine aggregate working platform thickness. Based on IDOT Standard Specifications, CA-6 gradations which are often required for constructing aggregate layers as subgrade replacement and subbase were selected for use. A comprehensive experimental test matrix was developed for the three most commonly used aggregate types in Illinois: uncrushed gravel, limestone, and dolomite. The primary objective was to establish ranges for major aggregate properties that primarily influence strength, modulus, and deformation behavior of aggregates thus governing the behavior of aggregate layers (both unbound and bound) in any pavement system. These major properties include: [1] fines content (defined in this research study as the amount of material passing sieve # 200 or 0.075 mm), [2] Plasticity Index (PI) of fines, [3] particle shape (flatness and elongation), angularity and surface texture, and [4] moisture content and dry density (compaction) properties.

For studying the effect of fines on aggregate behavior, laboratory specimens with four different target fines contents, i.e., 4%, 8%, 12% and 16% material passing sieve size # 200, were fabricated and tested. To study the effect of type of fines on aggregate behavior, two different types of fines were used: one was non-plastic in nature such as mineral filler type (PI = 0), and the other was plastic such as cohesive fin-grained soil type (PI in the range of 10-12). The plasticity of fines was determined by testing the material passing sieve size # 40, as required by IDOT specifications. The effect of moisture content on aggregate performance was studied by testing the blended aggregate specimens at three different moisture contents: (1) optimum moisture content (OMC or wopt), (2) 90% of wopt, and (3) 110% of wopt, where the wopt was established through the standard Proctor (AASHTO T-99) test for each aggregate gradation. Therefore, in the end, the laboratory test matrix ended up being a 4x2x3 factorial (4 different fines contents, 2 different types of fines, 3 different moisture contents) for each aggregate type.

Unsoaked CBR or IBV penetration test was performed on each standard Proctor (AASHTO T-99) test specimen. The moisture-density tests were performed using a 6-in. mold. Each Rapid Shear Strength test comprised of 3 different samples tested at 3 different confining pressures (5, 10 and 15 psi, respectively). The total number of samples tested was 72 for each aggregate type.

A.4.2 Resilient Modulus and Permanent Deformation Tests

Resilient modulus and permanent deformation tests were performed on specimens with applied confining pressures and deviator stresses according to AASHTO T307-99. The specimens were first conditioned for 1,000 load cycles to characterize their permanent deformation behavior at an applied stress state of 15 psi deviator stress and 15 psi confining pressure. Then, resilient modulus tests were conducted at the 15 AASHTO T307 stress states.

Once again, the University of Illinois-FastCell (UI-FastCell), an innovative testing device having provisions for switching and pulsing of the major principal stresses both in the vertical and radial directions by the use of the two independently controlled stress channels, was used to

perform directional modulus tests. Table A.6 presents the cyclic stress sequences for the constant confining pressure (CCP) condition.

Table A.6 Laboratory Test Program for the CCP condition

Sequence No.	Confining Pressure (σ_{nc}) (psi)/(kPa)	Max Axial Stress (σ_{nd}) (psi)/(kPa)	No. of Load Applications
1	3 / 20.7	3 / 20.7	100
2	3 / 20.7	6 / 41.4	100
3	3 / 20.7	9 / 62.1	100
4	5 / 34.5	5 / 34.5	100
5	5 / 34.5	10 / 68.9	100
6	5 / 34.5	15 / 137.9	100
7	10 / 68.9	10 / 68.9	100
8	10 / 68.9	20 / 137.9	100
9	10 / 68.9	30 / 206.8	100
10	15 / 103.4	10 / 68.9	100
11	15 / 103.4	15 / 103.4	100
12	15 / 103.4	30 / 206.8	100
13	20 / 137.9	15 / 103.4	100
14	20 / 137.9	20 / 137.9	100
15	20 / 137.9	40 / 275.8	100

A.4.3 Rapid Shear Strength Testing of Aggregates

To study the effect of different aggregate properties on the shear strength behavior, triaxial shear strength tests were run on the aggregate samples. The test procedure followed was that of “Rapid Shear Strength Test,” commonly performed at the University of Illinois ATREL on highway geomaterials. Compared to the conventional triaxial shear tests, a very high loading rate of 1.5 in./second is applied in rapid shear tests, causing 12.5% deformation in a 12-in. high specimen instantly. Due to the high loading rate, this test gives slightly higher peak stresses as compared to results from conventional shear strength tests. However, rapid shear tests are believed to better simulate the conditions of the actual pavement layer under the dynamic application of a moving wheel load.

Three different samples were tested at confining pressures of 5, 10, and 15 psi to determine the shear strength properties, friction angle and cohesion, of the aggregate materials. Each shear strength test actually involved testing of three different samples, resulting in a total of 216 samples tested for rapid shear strength determination. Instead of friction angle and cohesion, the maximum deviator stress at failure or the peak deviator stress values can also be compared to evaluate strength properties of different aggregate samples.

Appendix B: Determination of MnPAVE Equivalent Single Modulus Input from GT-PAVE Finite Element (FE) Modeling

MnPAVE is a multi-layer elastic theory (MLET) program that requires as input a single value of the modulus of elasticity, i.e., resilient modulus, for each pavement layer material to calculate critical pavement responses including stresses, strains, and deflections in flexible pavements. Several methods currently exist that determine equivalent single resilient modulus input for use with MLET analysis, among which is the iterative approach as recommended by the MEPDG and used later by Khazanovich et al. (2006). This iterative procedure, despite its simplicity, is actually time-consuming to implement due to the large number of MLET iterations involved; therefore, a validated finite element (FE) based pavement analysis program, GT-PAVE, was used instead to calculate the equivalent single resilient modulus input for MnPAVE from the stress-dependent M_R model parameters K1-K2-K3. The detailed steps of this procedure are presented as follows.

Step 1. Select basic parameters for finite element analyses

The single wheel load of 9 kips (40 kN) is applied as a uniform pressure of 80 psi (552 kPa) over a circular area of radius 6 in. (152 mm). The Poisson's ratios for asphalt concrete, unbound aggregate base/granular subbase, and engineered/natural subgrade are taken as 0.3, 0.4, and 0.45, respectively. The MnPAVE default modulus of 490 ksi (3,380 MPa) in the Fall season is used for the PG58-34 asphalt concrete. The example pavement structure considered here consists of 4-in. (102-mm) asphalt concrete surfacing (PG58-34) over 12-in. (305-mm) of high quality (H) aggregate base and 12-in. (305-mm) of low quality (L) granular subbase over a 12-in. (305-mm) engineered subgrade ($E=M_R=2$ ksi or 14 MPa). The stress-dependent M_R model parameters K1-K2-K3 for high quality (H) aggregate base and low quality (L) granular subbase materials are selected from Table 6.1.

Step 2. Conduct GT-PAVE nonlinear finite element analyses to compute modulus distributions in base and subbase layers

The Uzan base/subbase models are employed in GT-PAVE for the characterization of the unbound aggregate base and granular subbase layers. The GT-PAVE FE mesh designed consists of 780 isoparametric eight-node quadrilateral elements used to analyze this example pavement section in the sensitivity matrix. For illustration purposes, Table B.1 lists part of the modulus results of subbase layer elements calculated from GT-PAVE. The unit of modulus is in pound per square inches (psi). Note that nonlinear isotropic analyses were performed here, although GT-PAVE has the capability of cross-anisotropic modulus characterization.

Table B.1 GT-PAVE Calculated Element Moduli (in psi) for the Example Pavement Structure

ELEMENT	MODULUS IN Z-DIR	MODULUS IN R-DIR	SIGMA 1	SIGMA 2	SIGMA 3
495	.6737776E+04	.6737776E+04	.9979698E+00	-.2826605E+01	-.2827656E+01
496	.6748167E+04	.6748167E+04	.9943458E+00	-.2812132E+01	-.2821007E+01
497	.6789700E+04	.6789700E+04	.9856187E+00	-.2784446E+01	-.2810438E+01
498	.6851783E+04	.6851783E+04	.9681523E+00	-.2718243E+01	-.2781644E+01
499	.6981500E+04	.6981500E+04	.9260089E+00	-.2540729E+01	-.2690234E+01
500	.7358511E+04	.7358511E+04	.8233388E+00	-.2182291E+01	-.2511259E+01
501	.7951920E+04	.7951920E+04	.6586626E+00	-.1590787E+01	-.2172746E+01
502	.8681137E+04	.8681137E+04	.5156291E+00	-.9262601E+00	-.1698025E+01
503	.9707963E+04	.9707963E+04	.3889450E+00	-.3330090E+00	-.1185225E+01
504	.1070454E+05	.1070454E+05	.3607660E+00	.2281817E-01	-.6819882E+00
505	.1153608E+05	.1153608E+05	.4628634E+00	.9191473E-01	-.3013931E+00
506	.1067285E+05	.1067285E+05	.5564645E+00	.6206706E-01	.1203982E-01
507	.9773005E+04	.9773005E+04	.5560549E+00	.1823411E+00	.4065511E-01
508	.6835322E+04	.6835322E+04	.1085325E+01	-.2673203E+01	-.2674254E+01
509	.6845917E+04	.6845917E+04	.1083560E+01	-.2662401E+01	-.2668593E+01
510	.6876608E+04	.6876608E+04	.1073169E+01	-.2630973E+01	-.2655052E+01
511	.6951101E+04	.6951101E+04	.1057983E+01	-.2574271E+01	-.2630459E+01
512	.7076860E+04	.7076860E+04	.1010766E+01	-.2413905E+01	-.2545864E+01
513	.7405583E+04	.7405583E+04	.9028457E+00	-.2083296E+01	-.2367020E+01
514	.7957233E+04	.7957233E+04	.7257899E+00	-.1537016E+01	-.2045265E+01
515	.8623030E+04	.8623030E+04	.5742900E+00	-.9189295E+00	-.1592503E+01
516	.9575387E+04	.9575387E+04	.4399406E+00	-.3678079E+00	-.1108688E+01
517	.1056213E+05	.1056213E+05	.3844698E+00	-.7925239E-02	-.6378473E+00

Step 3. Calculate the equivalent single M_R inputs of aggregate base and granular subbase layers for subsequent MnPAVE analyses, respectively

Once the element modulus values are calculated from the GT-PAVE runs, the equivalent single M_R values for the aggregate base/granular subbase to be used in subsequent linear elastic MnPAVE analyses are obtained by averaging moduli throughout the depth from the elements located at the load axis of symmetry. Specifically, this requires (i) identifying those elements located at the load axis for both base and subbase layers, respectively; (ii) obtaining from GT-PAVE outputs the corresponding modulus values for those elements identified; and then, (iii) averaging those values to determine an equivalent single M_R input to be used in subsequent MnPAVE analysis.

The results of such equivalent M_R values linked to high, medium and low aggregate quality levels for both base and subbase are summarized in Table B.2. Note that for each base/subbase material quality level (H, M, or L), all the pavement sections in the sensitivity matrix corresponding to such a specific quality level are included to calculate the mean values and the ranges of equivalent M_R value.

Table B.2 Base and Subbase Equivalent Single Resilient Moduli (M_R) from GT-PAVE Analyses

Material Quality	Base M_R , ksi		Subbase M_R , ksi	
	Mean Value	Ranges	Mean Value	Ranges
High (H)	23.23	12.43 – 62.07	22.03	15.87- 38.85
Medium (M)	18.54	8.59 – 44.77	14.92	10.13 – 25.82
Low (L)	10.12	3.38 – 25.98	7.39	3.86 – 15.97

Appendix C: Review of Gradation Quantification Methods

Among the various mathematical functions proposed to describe aggregate particle size distribution, the Talbot equation was quite possibly one of the earliest to describe a maximum density curve for a given maximum aggregate size (Talbot, 1923). By regressing percent passing data (p_i) against sieve sizes (D_i) as per Equation C.1, a given gradation curve can be represented as a “point” with coordinates (n, D_{\max}) in a similar Cartesian plane where shape factor n is on x-axis and D_{\max} is on y-axis. Using this representation, Sánchez-Leal (2007) proposed a gradation-chart approach to promote “free design” in which a calculated Gravel-to-Sand ratio was used in lieu of the traditional gradation bands to ensure that required Hot Mix Asphalt (HMA) performance was met by available aggregate sources. According to Sánchez-Leal (2007), an increasing Gravel-to-Sand ratio markedly resulted in diminished workability, greater rutting resistance, and increased permeability.

$$p_i = \left(\frac{D_i}{D_{\max}} \right)^n \quad (C.1)$$

where p_i is the percentage of material by weight passing the i^{th} sieve size; D_i is the opening size of this particular i^{th} sieve; D_{\max} is the maximum size of aggregate; and n is called the shape factor of the gradation curve.

It is worth mentioning that the above gradation-chart approach was developed from gradation curves explained by the Talbot equation with R^2 values greater than 0.97, and that extending such an approach to gradation curves with R^2 values less than 0.97 still remains unexplored. For gradations other than well-graded ones (e.g., open-graded) that may not be well explained by the Talbot equation, the Rosin-Rammler distribution function described by Djamarani and Clark (Djamarani and Clark, 1997) can outperform others, as it is reported to be particularly suitable for describing the particle size distribution of powders of various nature and sizes as generated by grinding, milling, and crushing operations. As given in Equation C.2, two parameters, the mean particle size D_m and the measure of the spread of particle size distribution n , are used to represent the Rosin-Rammler function.

$$p_i = 1 - \exp \left[- \left(\frac{D_i}{D_m} \right)^n \right] \quad (C.2)$$

where p_i is the percentage of material by weight passing the i^{th} sieve size; D_i is the i^{th} sieve opening size; D_m is the mean size of aggregate; and n is called the spread factor.

The Unified Soil Classification System (USCS), as per ASTM D 2487-11 (2011), quantifies the gradation of a soil with less than 12% of fines using two parameters, i.e., coefficient of uniformity, C_u (D_{60}/D_{10}), and coefficient of curvature, C_c ($D_{30}^2/D_{60}D_{10}$). Soils are considered very poorly graded when $C_u < 3$; whereas gravels and sands are deemed well-graded when C_u is larger than 4 and 6, respectively. Note that C_c for well-graded soils or aggregates often ranges between 1 and 3. The definitions for “gravel” and “sand” are not unique, with USCS defining “gravel” as particles passing 75-mm (3-in.) sieve and retained on 4.75-mm (No. 4) sieve and “sand” as particles passing 4.75-mm (No. 4) sieve and retained on 75- μm (No. 200) sieve. Thus, an aggregate would be classified as gravel or sand (coarse aggregate or fine aggregate) depending on whichever proportion present is larger.

The influence of gravel (or coarse aggregate) content on the shear strength of cohesionless soil-gravel/sand-gravel mixtures has been the topic of investigation by many

geotechnical researchers. According to Vallejo (2001), the frictional resistance between the gravel particles controlled the shear strength of the soil/sand-gravel mixtures when the percentage by weight of gravel was on average greater than 70%; whereas the gravel particles with a concentration by weight less than average 49% basically had no control over the shear strength of the mixtures. This scientific observation could imply that the relative contents of gravel and sand particles (as per ASTM D2487-11) in aggregate base/granular subbase materials may possibly be an inherent factor controlling mixture performance mechanically and/or hydraulically, as supported by findings of Sánchez-Leal (2007) from HMA studies.

In terms of characterizing aggregate packing in stone-based infrastructure materials, such as HMA, the Bailey method is one of the pioneers. It analyzes the combined aggregate blend using three parameters: the coarse aggregate ratio (CA), the coarse portion of fine aggregate ratio (FA_c), and the fine portion of the fine aggregate ratio (FA_f), which are all calculated from the following designated sieves: half sieve, primary control sieve (PCS), secondary control sieve (SCS), and tertiary control sieve (TCS) (2002). Although the Bailey method has been widely used in HMA gradation design and performance evaluation, its application and validity for aggregate base/granular subbase gradation design has not been fully explored yet. Equation C.3 summarizes the essential equations associated with the Bailey method.

$$\text{Half sieve} = 0.5 * \text{NMPS} ;$$

$$\text{PCS} = 0.22 * \text{NMPS}; \text{SCS} = 0.22 * \text{PCS}; \text{TCS} = 0.22 * \text{SCS} ;$$

$$\text{CA ratio} = \frac{\% \text{Passing Half sieve} - \% \text{Passing PCS}}{100\% - \% \text{Passing Half sieve}} ; \quad (\text{C.3})$$

$$\text{FA}_c = \frac{\% \text{Passing SCS}}{\% \text{Passing PCS}} ;$$

$$\text{FA}_f = \frac{\% \text{Passing TCS}}{\% \text{Passing SCS}} .$$

where NMPS is the Nominal Maximum Particle Size, a Superpave® asphalt mix design terminology defined as one sieve larger than the first sieve that retains more than 10%.

Appendix D: List of Symbols and Abbreviations

ω_{opt}	Optimum Moisture Content
γ_{max}	Maximum Dry Density
\square	Achieved Moisture Content
γ_{dry}	Achieved Dry Density
% Fines	Percent Passing #200 sieve (0.075 mm)
ω/ω_{opt}	Moisture Ratio
$\gamma_{dry}/\gamma_{max}$	Density Ratio
d	Particle Size Corresponding to Percent Passing the Sieve Size
a_{ca}	Constant (Intercept) for the Coarse Aggregate Portion
n_{ca}	Slope (Exponent) for the Coarse Aggregate Portion
a_{fa}	Constant (Intercept) for the Fine Aggregate Portion
n_{fa}	Slope (Exponent) for the Fine Aggregate Portion
PCS	Primary Control Sieve Separating Fine and Coarse Aggregate Portions
NMPS	Nominal Maximum Particle Size
M_R	Resilient Modulus
P_a	Atmospheric Pressure Normalization Factor
θ	Bulk Stress (First Stress Invariant)
τ_{oct}	Octahedral Shear Stress
k_1, k_2, k_3	Regression Parameters
R^2	Coefficient of Determination
σ_{df}	Peak Deviator Stress at Failure
$\sigma_{df@4psi}$	Peak Deviator Stress at Failure with 4-psi Confining Pressure
σ_1	Total Axial Stress (or Major Principal Stress)
σ_1 critical	Critical Major Principal Stress Defined by Mohr-Coulomb Criterion
σ_d	Repeated (Cyclic) Deviator Stress
σ_3	Static Confining Pressure (or Minor Principal Stress)
c	Cohesion Angle
\square	Friction Angle
τ_f / τ_{max}	Shear Stress Ratio
SR	Major Principal Stress Ratio Used in MnPAVE Program
F&E Ratio	Flat and Elongated Ratio
AI	Angularity Index
ST	Surface Texture
G/S	The Gravel-to-Sand Ratio based on Definitions of ASTM D2487-11